

COMPOUNDS WITH ANTI-NEUROINFLAMMATORY ACTIVITY FROM *AERIDES FALCATA*



A Thesis Submitted in Partial Fulfillment of the Requirements  
for the Degree of Master of Science in Pharmaceutical Sciences and Technology

FACULTY OF PHARMACEUTICAL SCIENCES

Chulalongkorn University

Academic Year 2022

Copyright of Chulalongkorn University

สารที่มีฤทธิ์ต้านการอักเสบในระบบประสาทจากเอื้องกุหลาบกระเป่าเปิด



วิทยานิพนธ์นี้เป็นส่วนหนึ่งของการศึกษาตามหลักสูตรปริญญาวิทยาศาสตรมหาบัณฑิต  
สาขาวิชาเภสัชศาสตร์และเทคโนโลยี ไม่สังกัดภาควิชา/เทียบเท่า  
คณะเภสัชศาสตร์ จุฬาลงกรณ์มหาวิทยาลัย  
ปีการศึกษา 2565  
ลิขสิทธิ์ของจุฬาลงกรณ์มหาวิทยาลัย

Thesis Title	COMPOUNDS WITH ANTI-NEUROINFLAMMATORY ACTIVITY FROM <i>AERIDES FALCATA</i>
By	Mr. Bachtiar Rivai
Field of Study	Pharmaceutical Sciences and Technology
Thesis Advisor	Associate Professor BOONCHOO SRITULARAK, Ph.D.
Thesis Co Advisor	Professor KITTISAK LIKHITWITAYAWUID, Ph.D.

---

Accepted by the FACULTY OF PHARMACEUTICAL SCIENCES, Chulalongkorn  
University in Partial Fulfillment of the Requirement for the Master of Science

..... Dean of the FACULTY OF  
PHARMACEUTICAL SCIENCES

(Professor PORNANONG ARAMWIT, Ph.D.)

THESIS COMMITTEE

..... Chairman

(Assistant Professor CHAISAK CHANSRINIYOM, Ph.D.)

..... Thesis Advisor

(Associate Professor BOONCHOO SRITULARAK, Ph.D.)

..... Thesis Co-Advisor

(Professor KITTISAK LIKHITWITAYAWUID, Ph.D.)

..... Examiner

(Associate Professor PASARAPA TOWIWAT, Ph.D.)

..... External Examiner

(Associate Professor Veena Satitpatipan, Ph.D.)

บาทเกียรติ์ ริโว : สารที่มีฤทธิ์ต้านการอักเสบในระบบประสาทจากเอื้องกุหลาบกระเป่าเปิด. ( COMPOUNDS WITH ANTI-NEUROINFLAMMATORY ACTIVITY FROM *AERIDES FALCATA*) อ. ที่ปรึกษาหลัก : รศ. ภก. ดร.บุญชู ศรีตุลารักษ์, อ.ที่ปรึกษาร่วม : ศ. ภก. ดร.กิตติศักดิ์ ลิขิตวิฑูมิ

การศึกษาค้นคว้าขององค์ประกอบทางเคมีที่มีฤทธิ์ยับยั้งการอักเสบในเซลล์ประสาทจากกุหลาบกระเป่าเปิด สามารถแยกสารบริสุทธิ์และหาโครงสร้างได้ 10 ชนิด โดยเป็นสารใหม่ 1 ชนิด คือ aerifalcatin และสารที่เคยมีการรายงานไว้แล้วอีก 9 ชนิด ได้แก่ *n*-eicosyl-*trans*-ferulate, denthyrsinin, 2,4-dimethoxy-3,7-dihydroxyphenanthrene, 2,7-dihydroxy-3,4,6-trimethoxyphenanthrene, 3,7-dihydroxy-2,4,6-trimethoxyphenanthrene, agrostinin, syringaresinol, *trans*-*n*-feruloyltyramine, และ *trans*-*n*-coumaroyltyramine สารทุกชนิดถูกนำไปทดสอบฤทธิ์ยับยั้งการอักเสบในเซลล์ประสาท ยกเว้น *trans*-*n*-coumaroyltyramine เนื่องจากมีปริมาณน้อย การทดสอบฤทธิ์ในหลอดทดลองถูกทำในเซลล์ไมโครเกลีย BV2 ที่ถูกกระตุ้นด้วยไลโปพอลิแซคคาไรด์ (LPS) เพื่อประเมินศักยภาพของสารในฤทธิ์ยับยั้งการอักเสบในเซลล์ประสาทโดยใช้แบบจำลองการยับยั้งไนตริกออกไซด์ (NO) ซึ่งมี minocycline เป็นตัวควบคุมเชิงบวก จากการทดสอบพบว่ามีสาร 4 ชนิดที่แสดงความแตกต่างอย่างมีนัยสำคัญทางสถิติในการยับยั้งการสร้าง NO เมื่อเปรียบเทียบกับ minocycline (ค่า  $IC_{50}$   $3.41 \pm 0.30 \mu M$ ) ได้แก่ aerifalcatin (ค่า  $IC_{50}$   $0.87 \pm 0.45$  ไมโครโมลาร์) 2,7-dihydroxy-3,4,6-trimethoxyphenanthrene (ค่า  $IC_{50}$   $2.47 \pm 0.73$  ไมโครโมลาร์) agrostinin (ค่า  $IC_{50}$   $2.55 \pm 0.32$  ไมโครโมลาร์) และ syringaresinol (ค่า  $IC_{50}$   $1.40 \pm 0.17$  ไมโครโมลาร์) นอกจากนี้ ELISA ถูกนำมาใช้ในการวัดระดับไซโตไคน์ (TNF- $\alpha$  and IL-6) สำหรับสารที่มีฤทธิ์ดี โดยผลการทดสอบแสดงการลดลงอย่างมีนัยสำคัญทางสถิติในการแสดงออกของเซลล์ไมโครเกลียที่ถูกกระตุ้นเมื่อเพิ่มความเข้มข้นของสารออกฤทธิ์ ซึ่งบ่งชี้ถึงศักยภาพของสารเหล่านี้ในการยับยั้งการอักเสบในเซลล์ประสาท

จุฬาลงกรณ์มหาวิทยาลัย  
CHULALONGKORN UNIVERSITY

สาขาวิชา      เภสัชศาสตร์และเทคโนโลยี  
ปีการศึกษา      2565

ลายมือชื่อนิสิต .....  
ลายมือชื่อ อ.ที่ปรึกษาหลัก .....  
ลายมือชื่อ อ.ที่ปรึกษาร่วม .....



# # 6470030033 : MAJOR PHARMACEUTICAL SCIENCES AND TECHNOLOGY

KEYWORD: Neuroinflammation, BV-2 cell lines, *Aerides falcata*, aerifalcatin

Bachtiar Rivai : COMPOUNDS WITH ANTI-NEUROINFLAMMATORY ACTIVITY FROM *AERIDES FALCATA*. Advisor: Assoc. Prof. BOONCHOO SRITULARAK, Ph.D. Co-advisor: Prof. KITTISAK LIKHITWITAYAWUID, Ph.D.

In this study, a plant from the Orchidaceae family, *Aerides falcata*, was investigated for its chemical constituents and anti-neuroinflammatory activity. A total of ten compounds were isolated and characterized. The isolated compounds included a new compound which was named aerifalcatin and nine known compounds: *n*-eicosyl-*trans*-ferulate, denthysinin, 2,4-dimethoxy-3,7-dihydroxyphenanthrene, 2,7-dihydroxy-3,4,6-trimethoxyphenanthrene, 3,7-dihydroxy-2,4,6-trimethoxyphenanthrene, agrostinin, syringaresinol, *trans*-*n*-feruloyltyramine, and *trans*-*n*-coumaroyltyramine. All the isolated compounds were evaluated for their anti-neuroinflammatory activity, except for *trans*-*n*-coumaroyltyramine, which was excluded due to its insufficient amount. In vitro testing was conducted on LPS-induced BV2 microglia cells to evaluate their potential anti-neuroinflammatory activity using NO inhibition model. Minocycline, a neuroinflammatory modulator, was used as a positive control. Four compounds demonstrated significant deference to inhibit NO production compared to positive control minocycline (IC<sub>50</sub> value of 3.41 ± 0.30 μM): aerifalcatin (IC<sub>50</sub> value of 0.87 ± 0.45 μM), 2,7-dihydroxy-3,4,6-trimethoxyphenanthrene (IC<sub>50</sub> value of 2.47 ± 0.73 μM), agrostinin (IC<sub>50</sub> value of 2.55 ± 0.32 μM), and syringaresinol (IC<sub>50</sub> value of 1.40 ± 0.17 μM). An ELISA experiment was performed to determine the levels of cytokines (TNF- $\alpha$  and IL-6) for the most potent compounds. The results demonstrated a significant reduction in their expression in activated microglia in a dose-dependent manner, indicating their potential as anti-neuroinflammatory agents.

Field of Study: Pharmaceutical Sciences and Technology Student's Signature .....

Academic Year: 2022 Advisor's Signature .....

Co-advisor's Signature .....

## ACKNOWLEDGEMENTS

First of all, I want to show my great appreciation and respect for my thesis supervisor, Assoc. Prof. Boonchoo Sritularak, Ph.D. and my co-supervisor, Professor Dr. Kitissak Likhitwitaywuid, for their outstanding guidance, helpful advice, motivation, constructive feedback, and unwavering assistance during my research project.

I want to express my deep appreciation to the committee members who evaluated my thesis for their invaluable guidance. I am extremely thankful to the Department of Pharmacognosy and Pharmaceutical Botany staff at the Faculty of Pharmaceutical Sciences at Chulalongkorn University for their generous assistance and support.

My gratitude is also expressed to the senior members and colleagues in Assoc. Prof. Boonchoo's laboratory for their warm and supportive attitude, kind gestures, and valuable assistance. Additionally, I am grateful to my friends and the Pharmaceutical Sciences and Technology program for motivating me and providing me with a fresh perspective on the pharmaceutical field.

I would like to express my sincere gratitude to the Graduate School at Chulalongkorn University for the CU-ASEAN scholarship, which provided me with financial support throughout my academic journey.

Finally, my warmest gratitude toward my parents, my wife, and my son for their love, support, and encouragement whenever I feel weary.

Bachtiar Rivai

## TABLE OF CONTENTS

	Page
ABSTRACT (THAI).....	iii
ABSTRACT (ENGLISH).....	iv
ACKNOWLEDGEMENTS.....	v
TABLE OF CONTENTS.....	vi
LIST OF TABLES.....	x
LIST OF FIGURES.....	xii
ABBREVIATION AND SYMBOLS.....	1
CHAPTER I.....	1
INTRODUCTION.....	1
CHAPTER II.....	12
LITERATURE REVIEW.....	12
1. Traditional uses of Orchids.....	12
1.1. <i>Aerides</i> .....	12
1.1.1. <i>Aerides falcata</i> .....	13
2. Chemical constituents of <i>Aerides</i> species.....	13
3. Biological activities of <i>Aerides</i> species.....	18
CHAPTER III.....	19
EXPERIMENTAL.....	19
1. Materials.....	19
1.1. Plant material.....	19
1.2. Chemical materials.....	19

1.3. Cell culture materials .....	19
2. General Techniques .....	19
2.1. Thin-layer chromatography (TLC) .....	19
2.1.1. Normal phase, thin-layer chromatography .....	19
2.1.2. Preparative thin-layer chromatography (Prep. TLC).....	20
2.2. Column chromatography (CC).....	20
2.2.1. Vacuum liquid chromatography (VLC) .....	20
2.2.2. Normal phase, flash column chromatography (FCC).....	21
2.2.3. Gel filtration chromatography (GFC).....	21
2.3. Semi-preparative, high-pressure liquid chromatography (HPLC) .....	22
2.4. Spectroscopy .....	22
2.4.1. Mass Spectra (MS).....	22
2.4.2. Ultraviolet (UV) spectra .....	22
2.4.3. Infrared (IR) spectra.....	22
2.4.4. Proton and carbon-13 nuclear magnetic resonance ( $^1\text{H}$ and $^{13}\text{C}$ NMR) ....	23
2.4.5. Optical rotation .....	23
3. Extraction and isolation .....	23
3.1. Extraction of <i>A. falcata</i> .....	23
3.2. Separation and isolation .....	24
3.2.1. Isolation of compound AF2 .....	24
3.2.2. Isolation of compound AF3 .....	25
3.2.3. Isolation of compounds AF4 and AF5.....	25
3.2.4. Isolation of compound AF6 .....	25
3.2.5. Isolation of compound AF7 .....	25

3.2.6. Isolation of compound AF1 and AF10 .....	26
3.2.7. Isolation of compound AF8 and AF9 .....	26
4. Physical and spectral data of isolated compounds .....	31
4.1. Compound AF1 (Aerifalcatin).....	31
4.2. Compound AF2 ( <i>n</i> -eicosyl- <i>trans</i> -ferulate) .....	31
4.3. Compound AF3 (Denthyrsinin) .....	31
4.4. Compound AF4 (2,4-Dimethoxy-3,7-dihydroxyphenanthrene) .....	32
4.5. Compound AF5 (2,7-Dihydroxy-3,4,6-trimethoxyphenanthrene).....	32
4.6. Compound AF6 (3,7-Dihydroxy-2,4,6-trimethoxyphenanthrene).....	32
4.7. Compound AF7 (Agrostonin).....	32
4.8. Compound AF8 (Syringaresinol).....	33
4.9. Compound AF9 ( <i>trans-n</i> -feruloyltyramine).....	33
4.10. Compound AF10 ( <i>trans-n</i> -coumaroyltyramine).....	33
5. Evaluation for anti-neuroinflammatory activity <i>in vitro</i> .....	33
5.1. Cell treatment.....	33
5.2. Proinflammatory mediator assay.....	34
CHAPTER IV.....	35
RESULT AND DISCUSSION .....	35
1. Preliminary investigation of anti-neuroinflammatory activity from extracts of <i>Aerides falcata</i> .....	35
2. Chemical investigation.....	37
2.1. Structure elucidation of compound AF1 .....	39
2.2. Identification of compound AF2 .....	42
2.3. Identification of compound AF3 .....	44

2.4. Identification of compound AF4 .....	47
2.5. Identification of compound AF5 .....	49
2.6. Identification of compound AF6 .....	51
2.7. Identification of compound AF7 .....	54
2.8. Identification of compound AF8 .....	56
2.9. Identification of compound AF9 .....	59
2.10. Identification of compound AF10 .....	61
2. Anti-neuroinflammatory activity of compounds from <i>Aerides falcata</i> .....	63
CHAPTER V .....	68
CONCLUSION .....	68
REFERENCES .....	69
APPENDIX .....	81
VITA.....	156

## LIST OF TABLES

	Page
Table 1 Previous reports anti-inflammatory agents from Orchidaceae .....	4
Table 2 Distribution of secondary metabolites in the genus <i>Aerides</i> .....	14
Table 3 NO inhibition of extracts from <i>Aerides falcata</i> .....	35
Table 4 NMR spectral data of compound AF1 .....	40
Table 5 NMR spectral data of compound AF2 and <i>n</i> -eicosyl- <i>trans</i> ferulate.....	43
Table 6 NMR spectral data of compound AF3 and Denthyrsinin.....	46
Table 7 NMR spectral data of compound AF4 and 2,4-dimethoxy-3,7-dihydroxyphenanthrene.....	48
Table 8 NMR spectral data of compound AF5 and 2,7-dihydroxy-3,4,6-trimethoxyphenanthrene.....	50
Table 9 NMR spectral data of compound AF6 and 3,7-dihydroxy-2,4,6-trimethoxyphenanthrene.....	53
Table 10 NMR spectral data of compound AF7 and Agrostonin .....	55
Table 11 NMR spectral data of compound AF8 and Syringaresinol .....	58
Table 12 NMR spectral data of compound AF9 and <i>trans-n</i> -feruloyltyramine.....	60
Table 13 NMR spectral data of compound AF10 and <i>trans-n</i> -coumaroyltyramine....	62
Table 14 Effects of <i>Aerides falcata</i> constituents on LPS-stimulated NO release in BV-2 microglial cells.....	65
Table 15 Effects of compounds of <i>Aerides falcata</i> on the viability of BV-2 microglial cells. ....	133
Table 16 Effects of extracts of <i>Aerides falcata</i> on the viability of BV-2 microglial cells .....	133
Table 17 Effects of compounds of <i>Aerides falcata</i> on the NO inhibition.....	134

Table 18 Effects of extracts of *Aerides falcata* on the NO inhibition ..... 135

Table 19 The IC<sub>50</sub> values of compounds on the NO inhibition..... 135





## LIST OF FIGURES

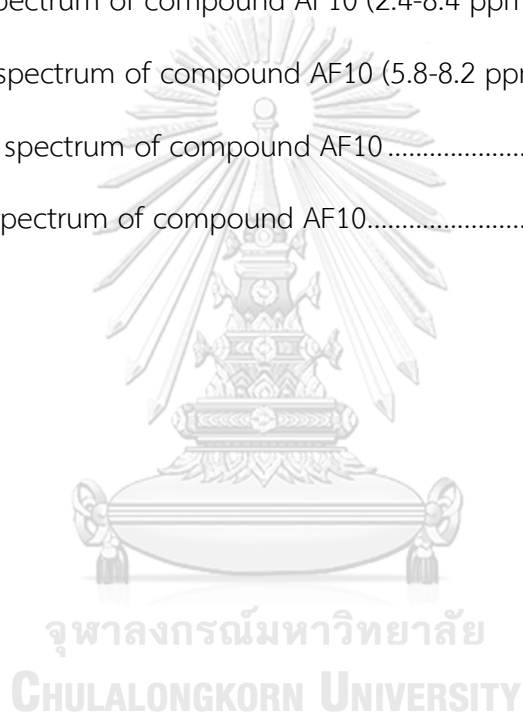
	Page
Figure 1 Anti-inflammatory agents from Orchidaceae family .....	6
Figure 2 <i>Aerides falcata</i> Lindl. & Paxton .....	13
Figure 3 Chemical constituents of <i>Aerides</i> .....	15
Figure 4 Effects of MeOH and EtOAc extract on cytokine release in LPS-stimulated BV-2 microglial cells.....	36
Figure 5 Structures of compounds isolated from <i>Aerides falcata</i> .....	37
Figure 6 Isolated compounds from <i>Aerides falcate</i> .....	64
Figure 7. Effects of active compounds on cytokine release in LPS-stimulated BV-2 microglial cells. ....	66
Figure 8 Mass spectrum of compound AF1 .....	82
Figure 9 UV spectrum of compound AF1 .....	82
Figure 10 FT-IR spectrum of compound AF1 .....	83
Figure 11 <sup>1</sup> H-NMR (400 MHz) spectrum of compound AF1 .....	83
Figure 12 <sup>13</sup> C-NMR (100 MHz) spectrum of compound AF1 .....	84
Figure 13 <sup>13</sup> C-NMR (100 MHz) spectrum of compound AF1 (55-165 ppm).....	84
Figure 14 HSQC spectrum of compound AF1 (3.99-4.30 ppm and 53-58 ppm) .....	85
Figure 15 HSQC spectrum of compound AF1 (6.8-9.3 ppm and 99-129 ppm).....	85
Figure 16 HMBC spectrum of compound AF1 (6.8-9.3 ppm and 108-136 ppm).....	86
Figure 17 HMBC spectrum of compound AF1 (7.24-7.42 ppm and 133-139 ppm )....	86
Figure 18 HMBC spectrum of compound AF1 (4.0-9.1 ppm and 143-162 ppm).....	87
Figure 19 NOESY spectrum of compound AF1 (1-9.5 ppm and 1-9.5 ppm) .....	87
Figure 20 NOESY spectrum of compound AF1 (6.7-9.4 ppm and 3.8-4.6 ppm).....	88

Figure 21 NOESY spectrum of compound AF1 (7.28-7.38 ppm and 7.10-7.28 ppm)..	88
Figure 22 COSY spectrum of compound AF1 .....	89
Figure 23 Mass spectrum of compound AF2.....	89
Figure 24 <sup>1</sup> H-NMR spectrum (400 MHz) of compound AF2 (0 - 10 ppm) .....	90
Figure 25 <sup>1</sup> H-NMR spectrum (400 MHz) of compound AF2 (0 - 2 ppm).....	90
Figure 26 <sup>13</sup> C-NMR spectrum (100 MHz) of compound AF2 .....	91
Figure 27 HSQC spectrum of compound AF2 (0-8 ppm and 0-145 ppm) .....	91
Figure 28 HSQC spectrum of compound AF2 (0-2.3 ppm and 13-40 ppm).....	92
Figure 29 HMBC spectrum of compound AF2 (3.8-8.2 ppm and 20-170 ppm).....	92
Figure 30 HMBC spectrum of compound AF2 (0.6-4.4 ppm and 10-39 ppm).....	93
Figure 31 HMBC spectrum of compound AF2 (4.07-4.28 ppm and 22-37 ppm).....	93
Figure 32 NOESY spectrum of compound AF2.....	94
Figure 33 COSY spectrum of compound AF2 (1-10 ppm and 1-10 ppm).....	94
Figure 34 COSY spectrum of compound AF2 (0.7-4.2 ppm and 0.7-4.2 ppm ).....	95
Figure 35 Mass spectrum of compound AF3.....	95
Figure 36 <sup>1</sup> H-NMR spectrum (400 MHz) of compound AF3 .....	96
Figure 37 <sup>13</sup> C-NMR spectrum (100 MHz) of compound AF3.....	96
Figure 38 HSQC spectrum of compound AF3.....	97
Figure 39 HMBC spectrum of compound AF3 (7-10 ppm and 104-152 ppm).....	97
Figure 40 HMBC spectrum of compound AF3 (4.4-9.6 ppm and 55-155 ppm).....	98
Figure 41 NOESY spectrum of compound AF3.....	98
Figure 42 COSY spectrum of compound AF3.....	99
Figure 43 Mass spectrum of compound AF4.....	99
Figure 44 <sup>1</sup> H-NMR spectrum (400 MHz) of compound AF4 (0.5-10.5 ppm).....	100

Figure 45	$^1\text{H}$ -NMR spectrum (400 MHz) of compound AF4 (2.0-9.5 ppm) .....	100
Figure 46	$^{13}\text{C}$ -NMR spectrum (100 MHz) of compound AF4 .....	101
Figure 47	HSQC spectrum of compound AF4.....	101
Figure 48	HMBC spectrum of compound AF4 (7.0-10 ppm and 104-158 ppm) .....	102
Figure 49	HMBC spectrum of compound AF4 (2.4-10 ppm and 70-160 ppm).....	102
Figure 50	NOESY spectrum of compound AF4 (6.8-9.6 ppm and 6.9-9.6 ppm).....	103
Figure 51	NOESY spectrum of compound AF4 (2.6-10 ppm and 2.9-10 ppm).....	103
Figure 52	COSY spectrum of compound AF4.....	104
Figure 53	Mass spectrum of compound AF5.....	104
Figure 54	$^1\text{H}$ -NMR spectrum (400 MHz) of compound AF5 .....	105
Figure 55	$^{13}\text{C}$ -NMR spectrum (100 MHz) of compound AF5 .....	105
Figure 56	HSQC spectrum of compound AF5.....	106
Figure 57	HMBC spectrum of compound AF5.....	106
Figure 58	COSY spectrum of compound AF5.....	107
Figure 59	Mass spectrum of compound AF6.....	107
Figure 60	$^1\text{H}$ -NMR spectrum (400 MHz) of compound AF6 .....	108
Figure 61	$^{13}\text{C}$ -NMR spectrum (100 MHz) of compound AF6.....	108
Figure 62	HSQC spectrum of compound AF6.....	109
Figure 63	HMBC spectrum of compound AF6.....	109
Figure 64	COSY spectrum of compound AF6.....	110
Figure 65	NOESY spectrum of compound AF6.....	110
Figure 66	Mass spectrum of compound AF7.....	111
Figure 67	$^1\text{H}$ -NMR spectrum (400 MHz) of compound AF7.....	111
Figure 68	$^{13}\text{C}$ -NMR spectrum (100 MHz) of compound AF7 .....	112

Figure 69 HSQC spectrum of compound AF7 (6.8-9.5 ppm and 95-130 ppm ).....	112
Figure 70 HSQC spectrum of compound AF7 (4.04-4.29 ppm and 54.1-56.5 ppm)..	113
Figure 71 HMBC spectrum of compound AF7 (6.8-9.4 ppm and 107-129 ppm).....	113
Figure 72 HMBC spectrum of compound AF7 (4.0-9.6 ppm and 104-162 ppm).....	114
Figure 73 NOESY spectrum of compound AF7.....	114
Figure 74 Mass spectrum of compound AF8.....	115
Figure 75 <sup>1</sup> H-NMR spectrum (400 MHz) of compound AF8.....	115
Figure 76 <sup>13</sup> C-NMR spectrum (100 MHz) of compound AF8.....	116
Figure 77 HSQC spectrum of compound AF8.....	116
Figure 78 HMBC spectrum of compound AF8.....	117
Figure 79 NOESY spectrum of compound AF8.....	117
Figure 80 COSY spectrum of compound AF8.....	118
Figure 81 Mass spectrum of compound AF9.....	118
Figure 82 <sup>1</sup> H-NMR spectrum (400 MHz) of compound AF9.....	119
Figure 83 <sup>13</sup> C-NMR spectrum (100 MHz) of compound AF9.....	119
Figure 84 HSQC spectrum of compound AF9 (1-8 ppm and 30-145 ppm).....	120
Figure 85 HSQC spectrum of compound AF9 (6.3-7.7 ppm and 100-142 ppm).....	120
Figure 86 HMBC spectrum of compound AF9 (1.8-7.8 ppm and 70-150 ppm).....	121
Figure 87 HMBC spectrum of compound AF9 (6.3-7.6 ppm and 114-170 ppm).....	121
Figure 88 HMBC spectrum of compound AF9 (1.9-4.3 ppm and 114-174 ppm).....	122
Figure 89 NOESY spectrum of compound AF9.....	122
Figure 90 COSY spectrum of compound AF9.....	123
Figure 91 Mass spectrum of compound AF10.....	123
Figure 92 <sup>1</sup> H-NMR spectrum (400 MHz) of compound AF10 (0.5-10 ppm).....	124

Figure 93 $^1\text{H}$ -NMR spectrum (400 MHz) of compound AF10 (1-10 ppm).....	124
Figure 94 $^{13}\text{C}$ -NMR spectrum (100 MHz) of compound AF10.....	125
Figure 95 HSQC spectrum of compound AF10 (1.2-7.8 ppm and 20-140 ppm) .....	125
Figure 96 HSQC spectrum of compound AF10 (6.3-7.6 ppm and 108-143 ppm).....	126
Figure 97 HMBC spectrum of compound AF10 (0.6-8 ppm and 5-85 ppm).....	126
Figure 98 HMBC spectrum of compound AF10 (1.1-4.5 ppm and 114-180 ppm).....	127
Figure 99 HMBC spectrum of compound AF10 (2.4-8.4 ppm and 112-122 ppm).....	127
Figure 100 HMBC spectrum of compound AF10 (5.8-8.2 ppm and 95-170 ppm).....	128
Figure 101 NOESY spectrum of compound AF10 .....	128
Figure 102 COSY spectrum of compound AF10.....	129



## ABBREVIATION AND SYMBOLS

Acetone- $d_6$	= Deuterated acetone
BBB	= Blood-brain barrier
$^{\circ}\text{C}$	= Degree Celsius
CC	= Column chromatography
$\text{CDCl}_3$	= Deuterated chloroform
$\text{CH}_2\text{Cl}_2$	= Dichloromethane
cm	= Centimeter
CNS	= Central nervous system
1-D NMR	= One-dimensional nuclear magnetic resonance
2-D NMR	= Two-dimensional nuclear magnetic resonance
d	= Doublet
DAMPs	= Damage-associated molecular patterns
DMEM	= Dulbecco's modified eagle medium
DMSO	= Dimethylsulfoxide
dd	= Double doublet
$\delta$	= Chemical shift
$\epsilon$	= Molar absorptivity
ELISA	= Enzyme-linked immunosorbent assay
EtOAc	= Ethyl acetate
FBS	= Fetal bovine serum

FCC	= Flash column chromatography
g	= Gram
GFC	= Gel filtration chromatography
HMBC	= Heteronuclear multiple bond correlation
$^1\text{H-NMR}$	= Proton nuclear magnetic resonance
HO	= Hydroxyl group
HPLC	= High-pressure liquid chromatography
HRESIMS	= High-resolution electrospray ionization mass spectroscopy
HSQC	= Heteronuclear single quantum coherence
Hz	= Hertz
$\text{IC}_{50}$	= Concentration exhibiting 50% inhibition
IL	= Interleukin
IR	= Infrared
$J$	= Coupling constant
Kg	= Kilogram
L	= Liter
LPS	= lipopolysaccharide
$\lambda_{\text{max}}$	= Wavelength at maximal absorption
$[\text{M-H}]^-$	= Deprotonated molecular ion
m	= multi-plate (for NMR spectra)
MeOH	= Methanol
mg	= Milligram

MHz	= Megahertz
MTT	= Microtetrazolium
$\mu\text{g}$	= Microgram
min	= Minutes
mL	= Mililiter
$\mu\text{L}$	= Microliter
mm	= Mililiter
MS	= Mass spectrum
MW	= Molecule wight
$m/z$	= Mass to charge ratio
NA	= Non-applicable
nm	= Nanometer
NMR	= Nuclear magnetic resonance
NO	= Nitric oxide
NSAIDs	= non-steroidal anti-inflammatory drugs
NOESY	= Nuclear Overhauser effect spectroscopy
COSY	= Correlated spectroscopy
$\mathbf{V}_{\text{max}}$	= Wave number at maximal absorption
OMe	= Methoxy group
PAMPs	= pathogen-associated molecular patterns
%	= Percentage
PGN	= peptidoglycans



ppm	= Part per million
s	= Singlet
SD	= Standard deviation
t	= Triplet
TLC	= Thin layer chromatography
TNF- $\alpha$	= tumor necrosis factor-alpha
UV	= Ultraviolet
VLC	= Vacuum liquid colom chromatography



## CHAPTER I

### INTRODUCTION

Neuroinflammation is a key factor in several diseases of the central nervous system (CNS). These diseases include stroke, Parkinson's disease, multiple sclerosis, and Alzheimer's disease (1). In recent years, neuroinflammation-related diseases have become a significant concern, affecting over 50 million people worldwide. It is predicted that this number will triple by 2050 (2). However, the pathological understanding of these underlying neuroinflammatory diseases is not clear, although several factors are believed to be involved, such as genetic, endogenous, and environmental influences (3).

Brain injuries are the main factor that contributes to the development of CNS inflammation, thereby modulating neuroinflammation (4). Some of these injuries result from the interference of damage-associated molecular patterns (DAMPs) and pathogen-associated molecular patterns (PAMPs). PAMPs are a class of molecules released during microbial invasion of the CNS, such as peptidoglycans (PGN) and lipopolysaccharide (LPS). On the other hand, DAMPs are produced by damaged or dying cells and include molecules such as ATP, biglycan, and uric acid (5, 6).

There are three types of immune cells that respond to injuries in the CNS: CNS-resident glial cells (i.e., microglia, astrocytes, and oligodendrocytes), CNS-resident non-glial cells (i.e., dendritic cells and macrophages), and peripheral immune cells (7). Among the resident glial cells, microglia account for approximately 10% to 15% of the CNS (8). Consequently, they play a central role in phagocytosis and neurodegenerative diseases. Microglia interact with other neuroglial cells, such as astrocytes and oligodendrocytes, both directly and indirectly in neuroinflammation

(9). Additionally, the presence of macrophages and peripheral immune cells in the CNS adds to the complexity of pathological CNS damage (3).

As previously mentioned, neuroinflammation is caused by various factors that activate the immune response in the CNS. Both PAMPs and DAMPs stimuli interact with pattern-recognition receptors (PRRs) on the membranes of glial cells, leading to the activation of the innate immune response (10). Upon the invasion of harmful stimuli, resting microglia arrest their normal signaling from neurons and other glial cells, triggering a transition to the active form. Active microglia can be divided into two phenotypes: M1 and M2 microglia (11). M1 microglia, also known as classical microglia, are considered detrimental as they secrete proinflammatory factors. Conversely, M2 microglia secrete anti-inflammatory factors (12). Activated microglia migrate, carry out phagocytosis and proliferation, and contribute to increased permeability of the blood-brain barrier (BBB). The increased permeability of the BBB disrupts its integrity, allowing peripheral immune cells to infiltrate the CNS (13, 14). In chronic conditions, proinflammatory factors such as interleukin  $1\beta$  (IL- $1\beta$ ), reactive oxygen species (ROS), IL-6, iNOS, tumor necrosis factor  $\alpha$  (TNF- $\alpha$ ), cyclooxygenase (COX)-1, and COX-2 are secreted by M1 microglia or other immune cells (such as astrocytes and peripheral immune cells). These factors contribute to damage and neuronal cell death (15). Neuronal cell disorders associated with these conditions include demyelination, aberrant synaptic pruning, and axonal degeneration (16).

In contrast to immune cells that produce proinflammatory factors, M2 microglia are involved in resolving inflammation and maintaining surrounding homeostasis. M2 microglia secrete anti-inflammatory factors such as IL-4, IL-13, and transforming growth factor  $\beta$  (TGF- $\beta$ ). These anti-inflammatory factors play a role in protecting the extracellular matrix, facilitating phagocytosis of debris, and promoting wound healing. The proinflammatory cytokine IL-4 can induce ARG1, which inhibits the secretion of

iNOS by modulating the amino acid arginine and indirectly converting it into proline and polyamines, which function in wound healing. The presence of M2 microglia is considered crucial for inflammation resolution by maintaining a balance between proinflammatory and anti-inflammatory cytokines. (11).

Currently, neuroinflammatory drugs are classified into several categories, including non-steroidal anti-inflammatory drugs (NSAIDs), antidepressants, muscle relaxants, opioids, antiepileptics, local anesthetics, and NMDA receptor antagonists (such as ketamine) (17). These drugs have various mechanisms for controlling chronic inflammation. For instance, NSAIDs function by inhibiting COX-1, COX-2, and prostaglandin (18). Additionally, ketamine and morphine are known to reduce swelling and inhibit the infiltration of inflammatory cells (19). Despite their effectiveness in treating inflammation, these drugs can have side effects on patients, including cognitive dysfunction, depression, neuropsychiatric disorders, sleep disturbances, and addiction (20, 21).

Recently, several studies have highlighted the potential use of plant derivatives as new drugs for improved inflammatory therapy. One such plant family is Orchidaceae. Orchidaceae plants are known for their colorful flowers and a wide habitat range, allowing them to grow virtually anywhere (22, 23). Plants in this family have long been recognized for the therapeutic potentials of their secondary metabolites in pharmacological medicine (24). These secondary metabolites encompass various chemical classes, including phenanthrenes, bibenzyls, flavonoids, phenylpropanoids, and alkaloids (25, 26). Some of these compounds have been reported to possess anti-inflammatory properties and can be categorized into five major groups: (i) Phenanthrene derivatives, for example 4-methoxy-2,7-phenanthrenediol [1], 1-(4-hydroxybenzyl)-4,8-dimethoxy-2,7-phenanthrenediol [5], 1,5-dimethoxy-2,7-phenanthrenediol [2], 4-methoxy-9,10-dihydro-2,7-

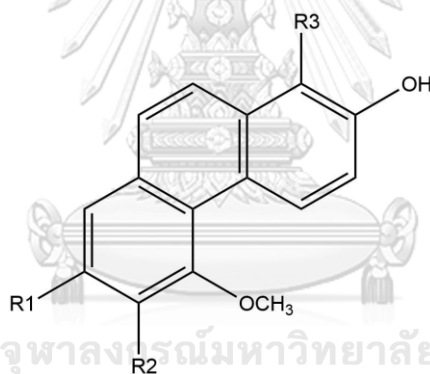
phenanthrenediol [9], 1,5,7-trimethoxy-2,6-phenanthrenediol [3] from the root of *Eulophia macrobulbon*, 5,7-dimethoxyphenanthrene-2,6-diol [4], 1-(4-hydroxybenzyl)-5,7-dimethoxyphenanthrene-2,6-diol [6], 7-(4-hydroxybenzyl)-8-methoxy-9,10-dihydrophenanthrene-2,5-diol [7], shancidin [8], 2-methoxy-9,10-dihydrophenanthrene-4,5-diol [11] from the root of *Cymbidium faberi*, and methoxycoelonin [10] from the stem of *Vanda coerulea* (27, 28, 29); (ii) phenanthropyrans, for example, imbricatin [12] and flavidin [13] from the stem of *Vanda coerulea* (29); (iii) bibenzyl derivatives, for example, batastasin III [14] from the whole plant of *Dendrobium scabrilingue* and *Liparis odorata* and gigantol [15] from stem of *Vanda coerulea* (29, 30, 31); (iv) flavones, for example luteolin [16] from the whole plant of *Liparis odorata*; and (v) phenolic glycosides, for example, liparisglycoside A [17], liparisglycoside B [18], liparisglycoside C [19] and anodendrosin A [20] from the whole plant of *Liparis odorata* (31) (Table 1 and Figure 1).

**Table 1** Previous reports anti-inflammatory agents from Orchidaceae

compounds	source	part of plant	References
<b>(i) Phenenthrane</b>			
4-Methoxy-2,7-Phenanthrenediol [1]	<i>Eulophia macrobulbon</i>	root	(28)
1,5-Dimethoxy-2,7-phenanthrenediol [2]	<i>Eulophia macrobulbon</i>	root	(28)
1,5,7-Trimethoxy-2,6-phenanthrenediol [3]	<i>Eulophia macrobulbon</i>	root	(28)
5,7-Dimethoxyphenanthrene-2,6-diol [4]	<i>Cymbidium faberi</i>	root	(27)

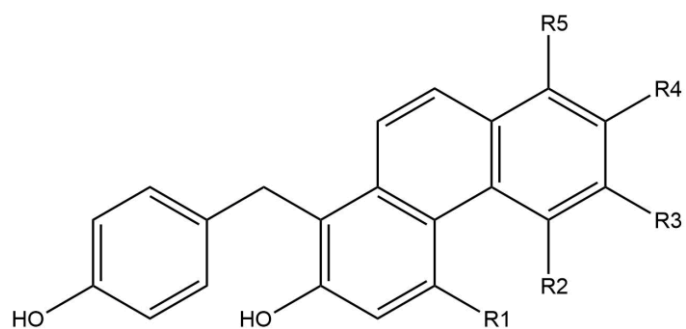
compounds	source	part of plant	References
1-(4-Hydroxybenzyl)-4,8-dimethoxy-2,7-phenanthrenediol [5]	<i>Eulophia macrobulbon</i>	root	(28)
1-(4-Hydroxybenzyl)-5,7-dimethoxy-phenanthrene-2,6-diol [6]	<i>Cymbidium faberi</i>	root	(27)
7-(4-Hydroxybenzyl)-8-methoxy-9,10-dihydrophenanthrene-2,5-diol [7]	<i>Cymbidium faberi</i>	root	(27)
Shancidin [8]	<i>Cymbidium faberi</i>	root	(27)
4-Methoxy-9,10-dihydro-2,7-phenanthrenediol [9]	<i>Eulophia macrobulbon</i>	root	(27, 28, 29)
Methoxycoelonin [10]	<i>Vanda coerulea</i>	stem	(27, 29)
2-Methoxy-9,10-dihydro-phenanthrene-4,5-diol [11]	<i>Cymbidium faberi</i>	root	(27)
<b>(ii) Phenentropyrans</b>			
Imbricatin [12]	<i>Vanda coerulea</i>	stem	(29)
Flavidin [13]	<i>Vanda coerulea</i>	stem	(29)
<b>(iii) Bibenzyl</b>			
Batatasin III [14]	<i>Dendrobium scabrilingue</i>	whole	(30)

compounds	source	part of plant	References
Gigantol [15]	<i>Vanda coerulea</i>	stem	(29)
<b>(iv) Flavone</b>			
Luteolin [16]	<i>Liparis odorata</i>	whole	(31)
<b>(v) Phenolic glycoside</b>			
Liparisglycoside A [17]	<i>Liparis odorata</i>	whole	(31)
Liparisglycoside B [18]	<i>Liparis odorata</i>	whole	(31)
Liparisglycoside C [19]	<i>Liparis odorata</i>	whole	(31)
Anodendrosin A [20]	<i>Liparis odorata</i>	whole	(31)

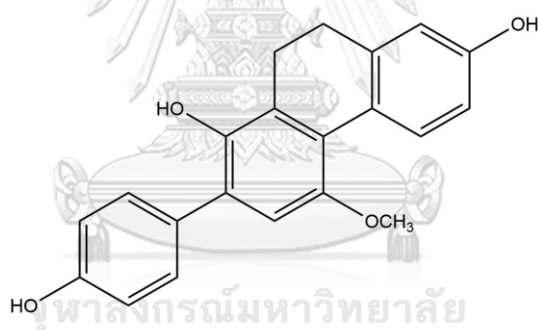


	R1	R2	R3
4-Methoxy-2,7-phenanthrenediol [1]	OH	H	H
1,5-Dimethoxy-2,7-phenanthrenediol [2]	OH	H	OCH <sub>3</sub>
1,5,7-Trimethoxy-2,6-phenanthrenediol [3]	OCH <sub>3</sub>	OH	OCH <sub>3</sub>
5,7- Dimethoxyphenanthrene-2,6-diol [4]	OCH <sub>3</sub>	OH	H

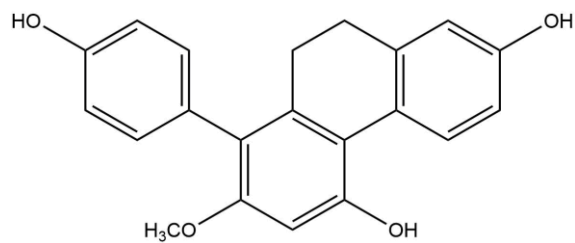
**Figure 1** Anti-inflammatory agents from Orchidaceae family



	R1	R2	R3	R4	R5
1-(4-Hydroxybenzyl)- 4,8-dimethoxy-2,7-phenanthrenediol [5]	OCH <sub>3</sub>	H	H	OH	OCH <sub>3</sub>
1-(4-Hydroxybenzyl)-5,7-dimethoxy- phenanthrene-2,6-diol [6]	H	OCH <sub>3</sub>	OH	OCH <sub>3</sub>	H



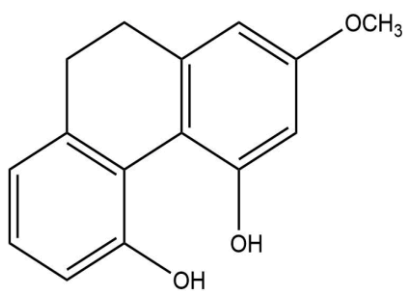
4-Methoxy-9,10-dihydro-2,7 phenanthrenediol [9]



Methoxycoelonin [10]

Figure 1 continue





2-Methoxy-9,10-dihydro-phenanthrene-4,5-diol [11]

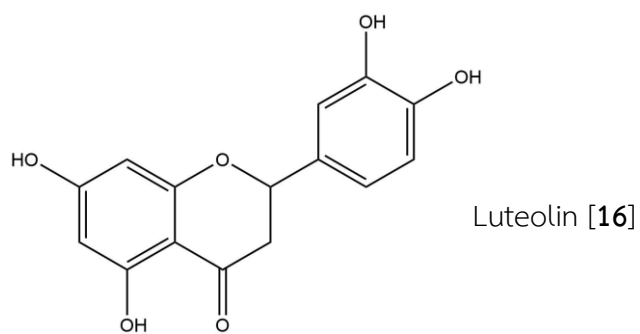
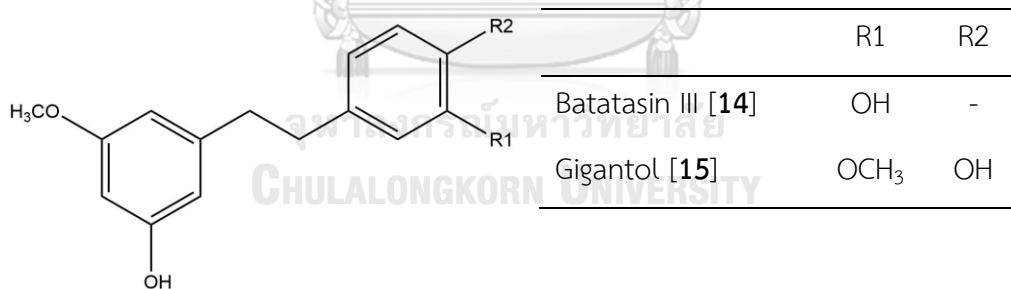
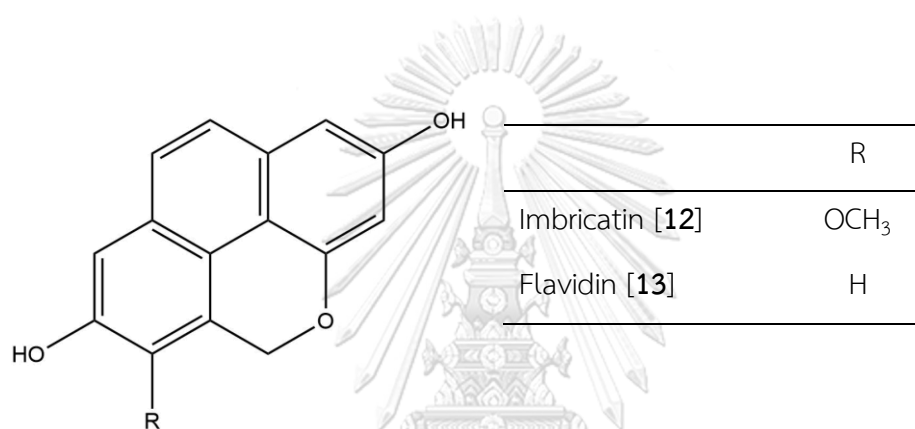
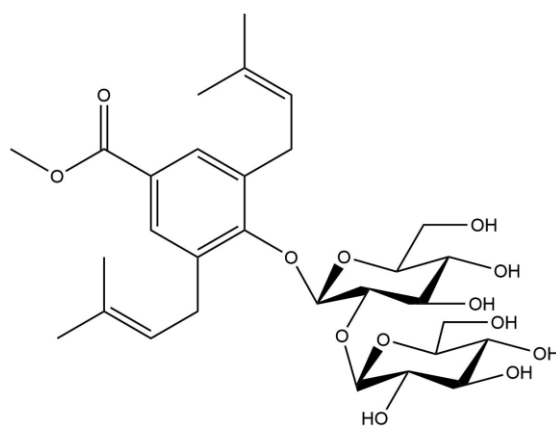
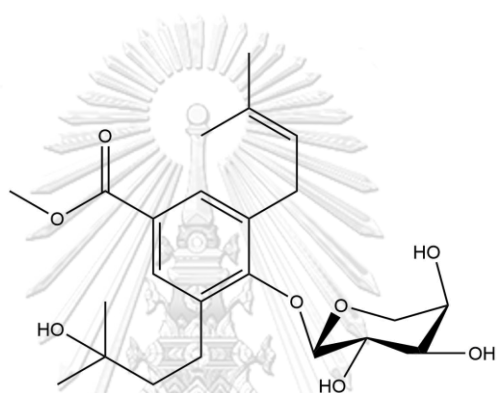


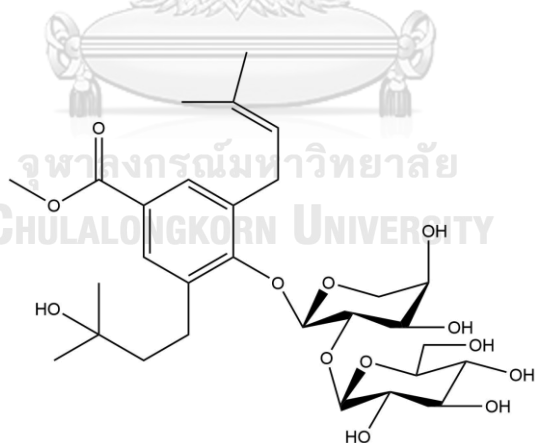
Figure 1 (continued)



Liparisglycoside A [17]

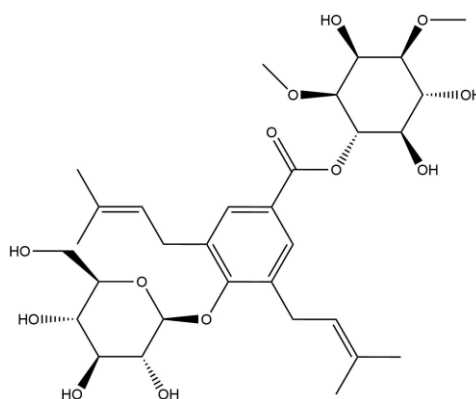


Liparisglycoside B [18]



Liparisglycoside C [19]

Figure 1 (continued)



Anodendrosin A [20]

Figure 1 (continued)

The preliminary study evaluated the anti-neuroinflammatory activity of the methanolic and ethyl acetate extracts of *Aerides falcata* using LPS-induced BV-2 cells. The study found no significant difference in the NO production between the extracts and the positive control (minocycline). However, both extracts significantly reduced the levels of the proinflammatory cytokines TNF- $\alpha$  and IL-6 compared to the LPS-induced group that was not treated with the extracts, as determined by ELISA assay. Interestingly, the ethyl acetate extract showed higher activity than the methanolic extract (experimental details can be found in the study). BV-2 cells are mouse microglia cell lines that express macrophage markers and do not express markers for astrocytes and oligodendrocytes (32). BV-2 cells have been widely used in in vitro studies of neuroinflammation and neurodegenerative diseases for many years (33).

Based on the above-mentioned preliminary results, the ethyl acetate extract of *Aerides falcata* was subjected to further studies to identify the active principles. In this study the following objectives have been put forwards:

1. To isolate and determine the structures of the chemical constituents of *Aerides falcata*
2. To evaluate the anti-neuroinflammatory activity of isolated compounds from *Aerides falcata*



## CHAPTER II

### LITERATURE REVIEW

#### 1. Traditional uses of Orchids

Some orchid plants have been recognized as sources of herbal remedies in China and India (24), such as *Dendrobium nobile*, *Pholidota articulata*, *Bulbophyllum odoratissimum*, *Flickingeria fugax*, and *Aerides odoratum* (34). Additionally, *Aerides falcata* has traditionally been used as a tonic for infants and for wound healing in the treatment of various skin diseases (35). The efficacies of these orchids are attributed to their bioactive constituents, which have shown benefits for several diseases. However, there are limited reports on the bioactive components of these plants (36). This study will discuss the chemical constituents and their bioactivities of *Aerides falcata*.

##### 1.1. *Aerides*

*Aerides* spp. are monopodial epiphytic plants, forming a small genus within the Orchidaceae family. This genus *Aerides* comprises 21 species (37) that are found in various regions of Asia, including South Asia (Sri Lanka, India, Nepal, Bangladesh, and Bhutan), Southeast Asia (Malaysia, Laos, Indonesia, Vietnam, Myanmar, Thailand, Philippines, and Cambodia), China, and Papua New Guinea (38). Previous studies have demonstrated the biological activities of certain *Aerides* species. For instance, *Aerides odorata* is known for its anticancer activity (39), while *Aerides multiflora* exhibits  $\alpha$ -glucosidase inhibitory activity (39). *Aerides multiflora* has  $\alpha$ -glucosidase inhibitory activity (26) and *Aerides falcata* has been studied for its cellulolytic activity through the production of endophytic fungi (40).

### 1.1.1. *Aerides falcata*

*Aerides falcata* Lindl. & Paxton (Figure 2), also known as "Ueng Kulaab Krapao Perd" in Thai, is found in Vietnam, Thailand, Laos, Myanmar, and South-Central China. The specific epithet "*falcata*" is derived from "falcate," which means "sickle-shaped" (41). *Aerides falcata* has several heterotypic synonyms, including *A. larpentae*, *A. mendelii*, *A. retrofracta*, and *A. siamensis* (38). It typically flowers from April to June. The flower exhibits a broadly falcate shape at the lip lobe and a broadly ovate shape at the middle lobe. The spur is angled at 45 degrees and upright, while the petals measure approximately 12.5 mm in length and 9 mm in width. The leaves of *Aerides falcata* are distichous, sessile, oblong, glabrous, flattened, and thick, reaching up to 48 cm in length and 4.8 cm in width (42, 43).



Figure 2 *Aerides falcata* Lindl. & Paxton

## 2. Chemical constituents of *Aerides* species

According to previous reports, the chemical constituents of *Aerides* species can be categorized into 4 major classes, including phenanthropyrans, phenanthrenes, phenylpropanoid esters, and bibenzyls. The phenanthrene derivatives are the largest group in this genus. The distribution of these chemical constituents is shown in Table 2 and Figure 3.

**Table 2** Distribution of secondary metabolites in the genus *Aerides*

Category/Compound	Source	Part of Plant	Reference
Phenanthropyrans			
Aeridin [21]	<i>A. crispum</i>	tubers	(44)
Imbricatin [12]	<i>A. rosea</i>	Stem	(26, 45)
	<i>A. multiflora</i>	Whole plant	
Phenanthrenes			
5-Methoxyphenanthrene-2,3,7-triol (Aerosanthrene) [22]	<i>A. rosea</i>	Stem	(45)
3-Methoxy-9,10-dihydro-2,5,7-phenanthrenetriol (aerosin) [23]	<i>A. rosea</i>	Stem	(26, 45)
	<i>A. multiflora</i>	Whole plant	
5-Methoxy-9,10-dihydro-2,3,7-phenanthrenetriol [24]	<i>A. rosea</i>	Stem	(45)
3,5-Dimethoxyphenanthrene-2,7-diol [25]	<i>A. rosea</i>	Stem	(45)
Coelonin [26]	<i>A. rosea</i>	Stem	(45)
Methoxycoelonin [10]	<i>A. rosea</i>	Stem	(26, 45)
	<i>A. multiflora</i>	Whole plant	
6-Methoxycoelonin [27]	<i>A. multiflora</i>	Whole plant	(26)
Aerimultin A [29]	<i>A. multiflora</i>	Whole plant	(26)
Aerimultin B [30]	<i>A. multiflora</i>	Whole plant	(26)
Aerimultin C [31]	<i>A. multiflora</i>	Whole plant	(26)
Agrostonin [32]	<i>A. multiflora</i>	Whole plant	(26)

Phenylpropanoid esters			
Dihydrosinapyl dihydroferulate [33]	<i>A. multiflora</i>	Whole plant	(26)
Dihydroconiferyl dihydro- <i>p</i> -coumarate [34]	<i>A. multiflora</i>	Whole plant	(26)
Bibenzyls			
Gigantol [15]	<i>A. rosea</i>	Stem	(26, 45)
	<i>A. multiflora</i>	Whole plant	

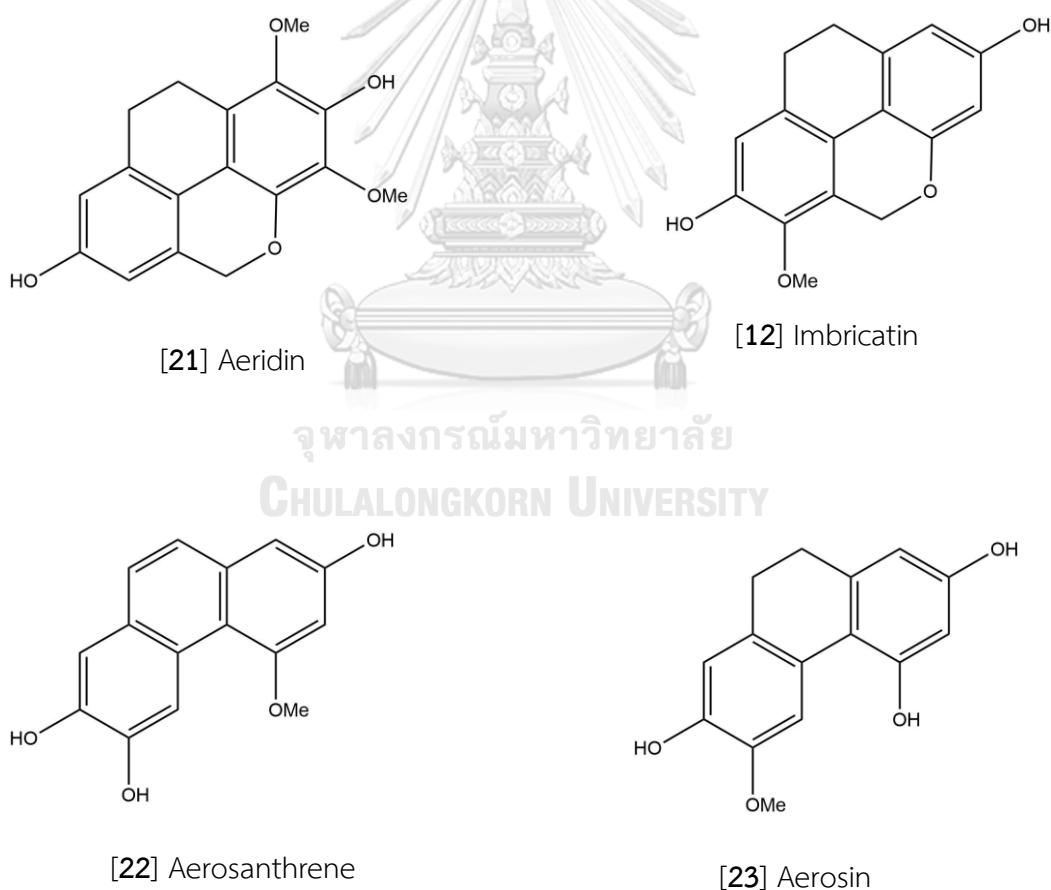
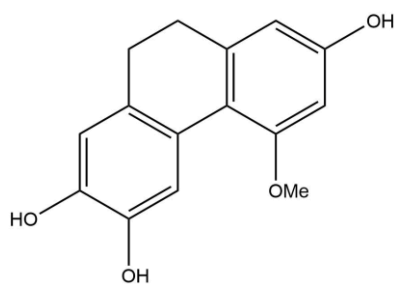
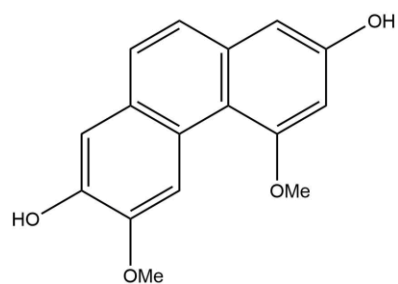


Figure 3 Chemical constituents of *Aerides*

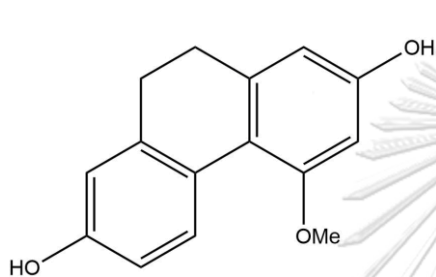




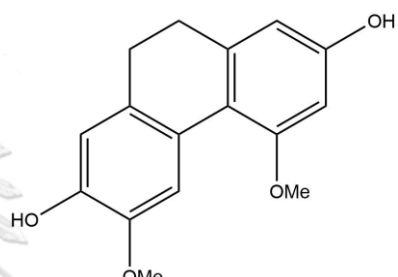
[24] 5-Methoxy-9,10-dihydro-2,3,7



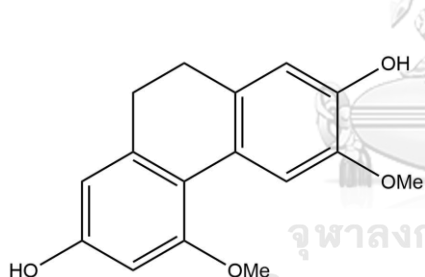
[25] 3,5-Dimethoxy phenanthrene-2,7-diol



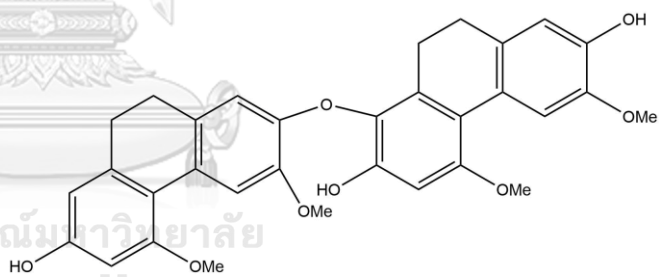
[26] Coelonin



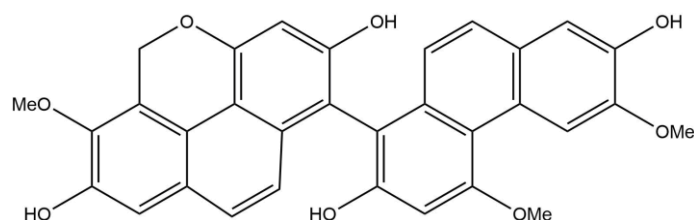
[10] Methoxycoelonin



[27] 6-Methoxycoelonin

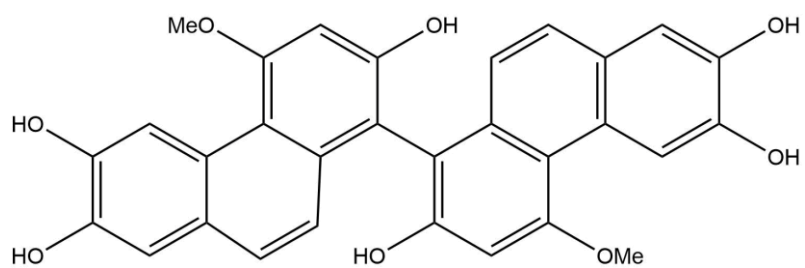


[29] Aerimultin A

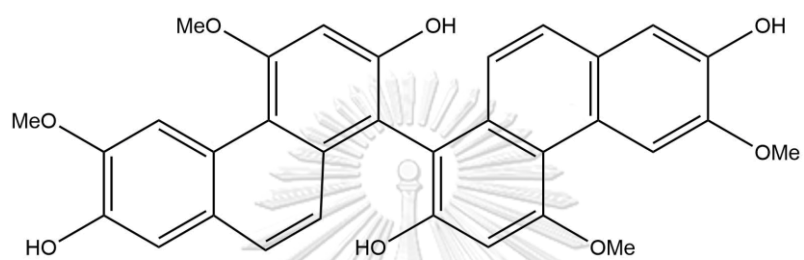


[30] Aerimultin B

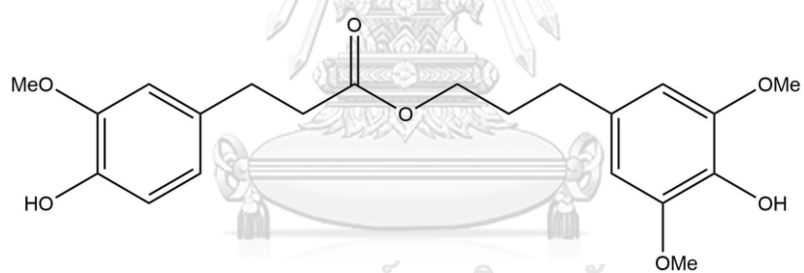
Figure 3 (continued)



[31] Aerimultin C



[32] Agrostonin



[33] Dihydrosinapyl dihydroferulate

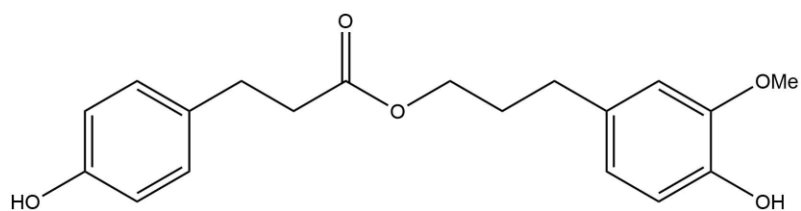
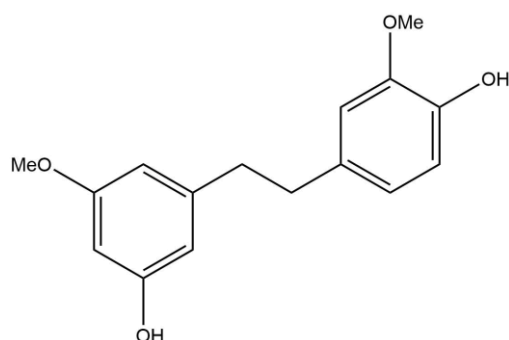
[34] Dihydroconiferyl dihydro-*p*-coumarate

Figure 3 (continued)



[15] Gigantol

Figure 3 (continued)

### 3. Biological activities of *Aerides* species

As previously described, *Aerides* species have already been used in traditional medicine. For example, *Aerides falcata* has been used for wound healing in several skin diseases (35), while *Aerides odorata* has been recognized for its antibacterial properties (34). Recently, the methanolic and ethyl acetate extracts of *Aerides odorata* were reported to exhibit cytotoxicity against MCF-7 cancer cells (39). Furthermore, several compounds isolated from *Aerides multiflora* were investigated for their ability to inhibit  $\alpha$ -glucosidase activity (26).

## CHAPTER III

### EXPERIMENTAL

#### 1. Materials

##### 1.1. Plant material

The whole plants of *Aerides falcata* were procured from the Chatuchak market in June 2021. Mr. Yanyong Punpreuk, a senior botanist at the Department of Agriculture, Bangkok, Thailand, identified the plant materials, and a voucher specimen (BS-AF-022564) was deposited at the Department of Pharmacognosy and Pharmaceutical Botany, Chulalongkorn University.

##### 1.2. Chemical materials

Organic solvents such as methanol (MeOH), acetone (CH<sub>3</sub>COCH<sub>3</sub>), ethyl acetate (EtOAc), dichloromethane (CH<sub>2</sub>Cl<sub>2</sub>), hexane, water, and *n*-butanol in this study are of commercial grade and were redistilled before use.

##### 1.3. Cell culture materials

BV-2 microglial cells were procured from Accigen. Fetal Bovine Serum (FBS) and Dulbecco's Modified Eagle Medium (DMEM), two components used in cell culture, were purchased from (PAN Biotech, Aidenbach, Germany). Lipopolysaccharide (LPS), an inducer of inflammatory responses, and minocycline, a reference compound for anti-neuroinflammatory activity, were obtained from Sigma-Aldrich, St. Louis, MO, USA.

#### 2. General Techniques

##### 2.1. Thin-layer chromatography (TLC)

##### 2.1.1. Normal phase, thin-layer chromatography

Technique : One-dimension ascending

Stationary phase	: Silica gel 60 F <sub>254</sub> precoated plates (E. Merck)
Mobile phase	: Organic Solvents
Temperature	: Room temperature (30-35°C)
Detection	: 1. Visualized under UV light at 254nm and 365nm. 2. Sprayed with anisaldehyde reagent in a fume hood and followed by heating at 105°C for 10 minutes.

### 2.1.2. Preparative thin-layer chromatography (Prep. TLC)

Technique	: One-dimension ascending
Stationary phase	: Silica gel 60 F <sub>254</sub> precoated plates (E. Merck), size 20x20 cm
Mobile phase	: Organic solvents
Temperature	: Room temperature (30-35°C)
Sample loading	:The sample was applied onto a TLC plate using capillary tube. The spots are dried, and the plate is then placed in a developing chamber with organic solvent as mobile phase
Detection	: Visualized under UV light at wavelengths of 254nm and 365nm

## 2.2. Column chromatography (CC)

### 2.2.1. Vacuum liquid chromatography (VLC)

Stationary phase	: Silica gel 60 (No. 1.07734.2500), size 0.063-0.200 mm (E. Merck)
Mobile Phase	: Organic solvents
Packing method	: Dry packing
Sample loading	:The sample was dissolved in a small volume of organic solvent, adsorbed by a small quantity of the

adsorbent, dried and then gradually placed on top of the column

Detection : Each fraction was visualized under UV light at wavelengths 254nm and 365nm on a TLC plate.

### 2.2.2. Normal phase, flash column chromatography (FCC)

Stationary phase : Silica gel 60 (No. 1.07734.2500), size 0.063-0.200 mm (E. Merck)

Mobile phase : Organic solvents

Packing method : Dry packing

Sample loading : The sample was dissolved in small volume of organic solvent, adsorbed by small quantities of the adsorbent, dried, and then gradually placed on the column

Detection : Fractions were visualized under UV light at wavelengths 254nm and 365nm on a TLC plate

### 2.2.3. Gel filtration chromatography (GFC)

Stationary phase : Sephadex LH-20 particle size 25-100  $\mu\text{m}$  (GE Healthcare)

Mobile phase : Organic solvent

Packing method : Wet packing

Sample loading : The sample was dissolved in a small volume of an organic solvent, and this mixture was then applied onto the top of the column.

Detection : Fractions were visualized under UV light at wavelengths 254nm and 365nm on a TLC plate

### 2.3. Semi-preparative, high-pressure liquid chromatography (HPLC)

Column	: COSMOSIL 5C <sub>18</sub> – AR-II (10ID × 250 mm)
Mobile phase	: Organic solvent and water
Sample preparation	: The sample was dissolved with a small eluent and filtered through Millipore filter paper before injection
Injection volume	: 2 mL
Temperature	: Room temperature
Pump	: LC-8A (Shimadzu)
Detector	: SPD-10A UV-Vis Detector (Shimadzu)
Recorder	: C-R6A Chromatopac (Shimadzu)

### 2.4. Spectroscopy

#### 2.4.1. Mass Spectra (MS)

Mass spectra were recorded on a Bruker micro TOF mass spectrometer (ESI-MS) at the Department of Chemistry, Faculty of Science, Naresuan University.

#### 2.4.2. Ultraviolet (UV) spectra

UV spectra were measured with a Milton Roy Spectronic 3000 Array spectrophotometer (Pharmaceutical Research Instrument Center, Faculty of Pharmaceutical Sciences, Chulalongkorn University).

#### 2.4.3. Infrared (IR) spectra

IR Spectra were recorded on a Perkin-Elmer FT-IR 1760X spectrophotometer (Scientific and Technology Research Equipment Center, Chulalongkorn University).

#### 2.4.4. Proton and carbon-13 nuclear magnetic resonance ( $^1\text{H}$ and $^{13}\text{C}$ NMR)

$^1\text{H}$  NMR (400 MHz) and  $^{13}\text{C}$  NMR (100 MHz) spectra were recorded on a Bruker Advance Neo 400 MHz spectrometer (Faculty of Pharmaceutical Sciences, Chulalongkorn University).

The solvent for NMR spectra was deuterated acetone (acetone- $d_6$ ). Chemical shifts were reported in the ppm scale using the chemical shift of the solvent as the reference signal.

#### 2.4.5. Optical rotation

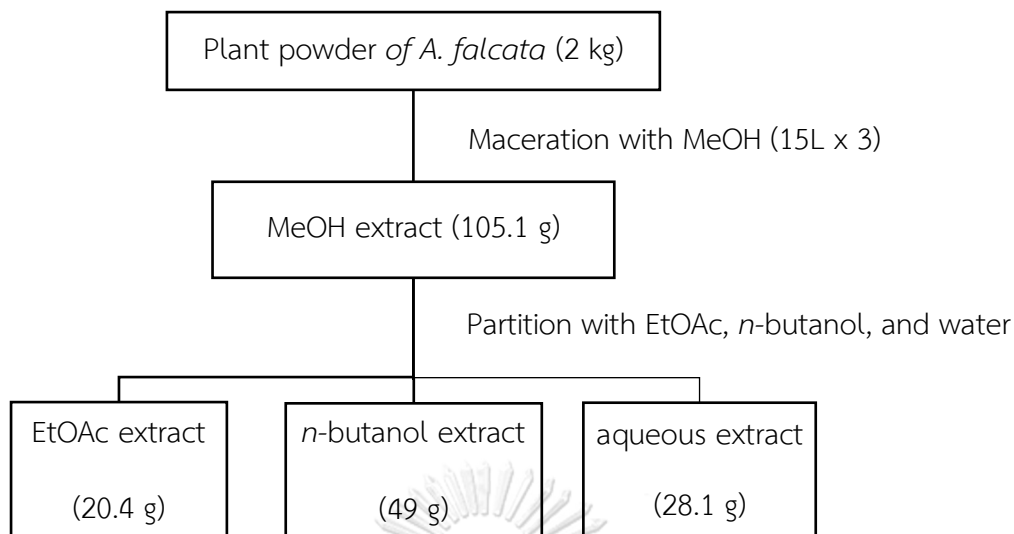
Optical rotation was measured on a Jasco P-2000 polarimeter (Pharmaceutical Research Instrument Center, Faculty of Pharmaceutical Sciences, Chulalongkorn University).

### 3. Extraction and isolation

#### 3.1. Extraction of *A. falcata*

The dried whole plant of *A. falcata* (2 kg) was ground to produce a dried powder. The powder (2 kg) was macerated with MeOH (3 x 15 L), soaked for 72 hours for each maceration, and a dried MeOH extract was obtained after removal of the organic solvent. This extract was treated with EtOAc, *n*-butanol, and aqueous to produce an EtOAc extract, *n*-butanol extract, and aqueous extract, respectively, after evaporation of the solvent.





**Scheme 1** Extraction steps of *Aerides falcata*

### 3.2. Separation and isolation

The EtOAc extract (20.4 g) was separated by vacuum liquid chromatography (silica gel, hexane – EtOAc, gradient) to give 7 fractions (A –G). Fraction C (7.2 g), fraction D (3.9 g), fraction E (2.2 g), fraction F (6.7 g), and fraction G (10.8 g) were isolated using several chromatographic techniques as described in section 2.2.

#### 3.2.1. Isolation of compound AF2

Fraction C (7.2 g) was separated by Sephadex LH-20 (acetone) chromatography to give 5 fractions (CA – CE). Fraction CB (612 mg) was re-separated by column chromatography (CC) (silica gel, hexane – CH<sub>2</sub>Cl<sub>2</sub>, gradient elution) to give CBA – CBH. CBE (108 mg) was subjected to CC (silica gel, hexane – EtOAc 10%, isocratic elution) to yield AF2 (36.3 mg) which was identified as *n*-eicosyl-*trans*-ferulate.

### 3.2.2. Isolation of compound AF3

Fraction D (3.9 g) was fractionated on Sephadex LH-20 (acetone) to give 6 fractions (DA – DF). Fraction DB (1.2 g) was separated by CC (silica gel, hexane – CH<sub>2</sub>Cl<sub>2</sub>, gradient elution) to AF3 (7 mg), identified as denthyrsinin.

### 3.2.3. Isolation of compounds AF4 and AF5

Fraction DB (1.2 g) was re-separated by CC (silica gel, hexane – CH<sub>2</sub>Cl<sub>2</sub>, gradient elution) by give 9 fractions (DBA – DBI). DBH (23.5 mg) and DBI (21 mg) were purified with CC (silica gel, hexane – EtOAc, gradient elution) to yield AF4 and AF5, respectively. AF4 (10 mg) was identified as 2,4-dimethoxy-3,7-dihydroxyphenanthrene, and AF5 (7 mg) was identified as 2,7-dihydroxy-3,4,6-trimethoxyphenanthrene.

### 3.2.4. Isolation of compound AF6

Fraction E (2.2 g) was fractionated on Sephadex LH-20 (MeOH) to give 6 fractions (EA – EF). Fraction EC (60.2 mg) was separated by CC (silica gel, hexane – EtOAc, gradient elution) to give fractions ECA – ECH. Fraction ECA (15.2 mg) was re-separated by CC (silica gel, hexane – EtOAc, gradient elution) to yield 4 fractions (ECAA, ECAB, ECAC, and ECAD). Fraction ECAD (5.1 mg) was purified with CC (silica gel, CH<sub>2</sub>Cl<sub>2</sub>, isocratic elution) to furnish AF6 (2.2 mg) which was identified as 3,7-dihydroxy-2,4,6-trimethoxyphenanthrene.

### 3.2.5. Isolation of compound AF7

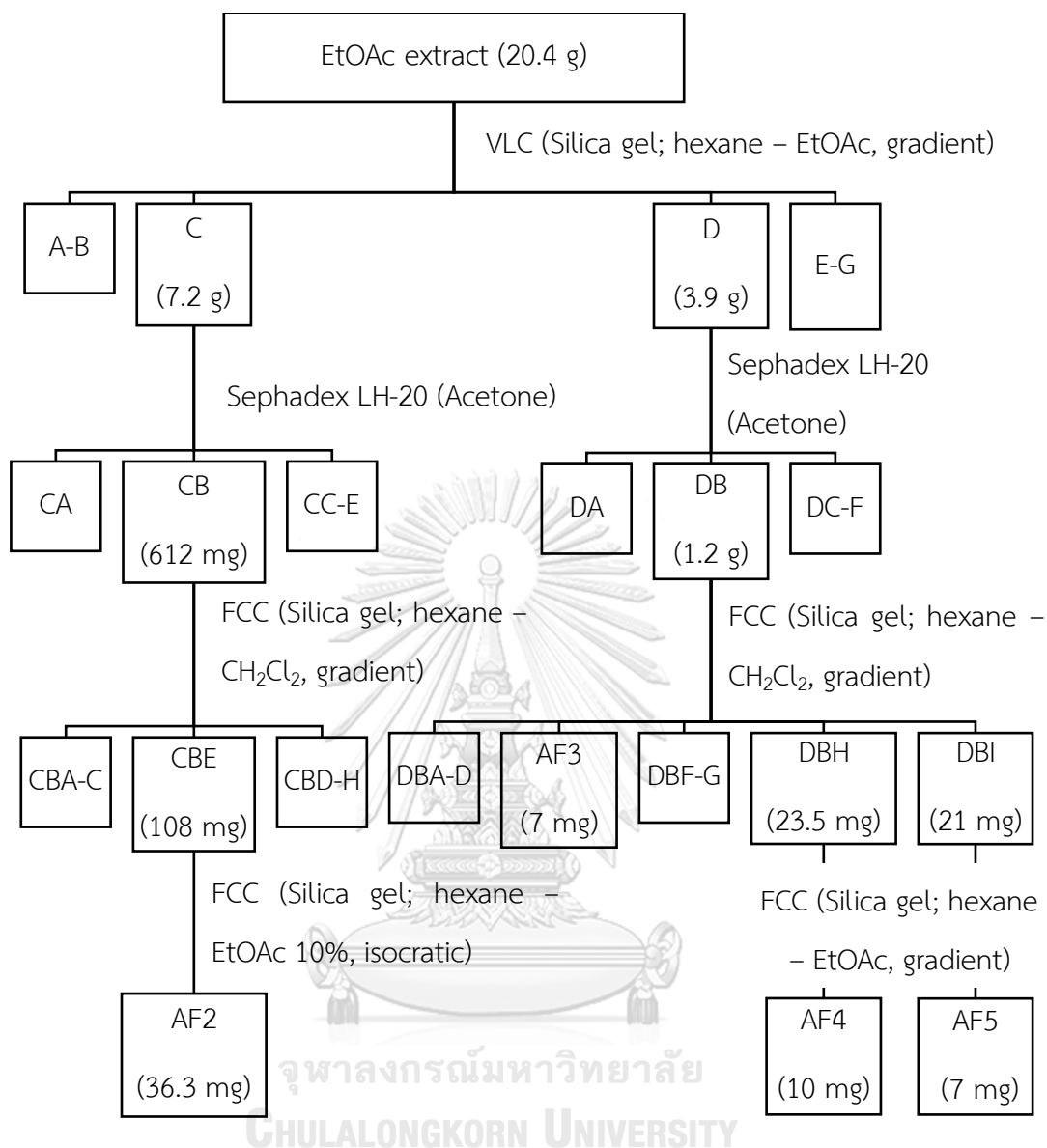
Fraction F (6.7 g) was fractionated on Sephadex LH-20 (MeOH) to give 7 fractions (FA – FG). Fraction FD (87.3 mg) was purified by CC (silica gel, hexane-acetone 50%, gradient elution) to furnish AF7 (58 mg) which was identified as agrostonin.

### 3.2.6. Isolation of compound AF1 and AF10

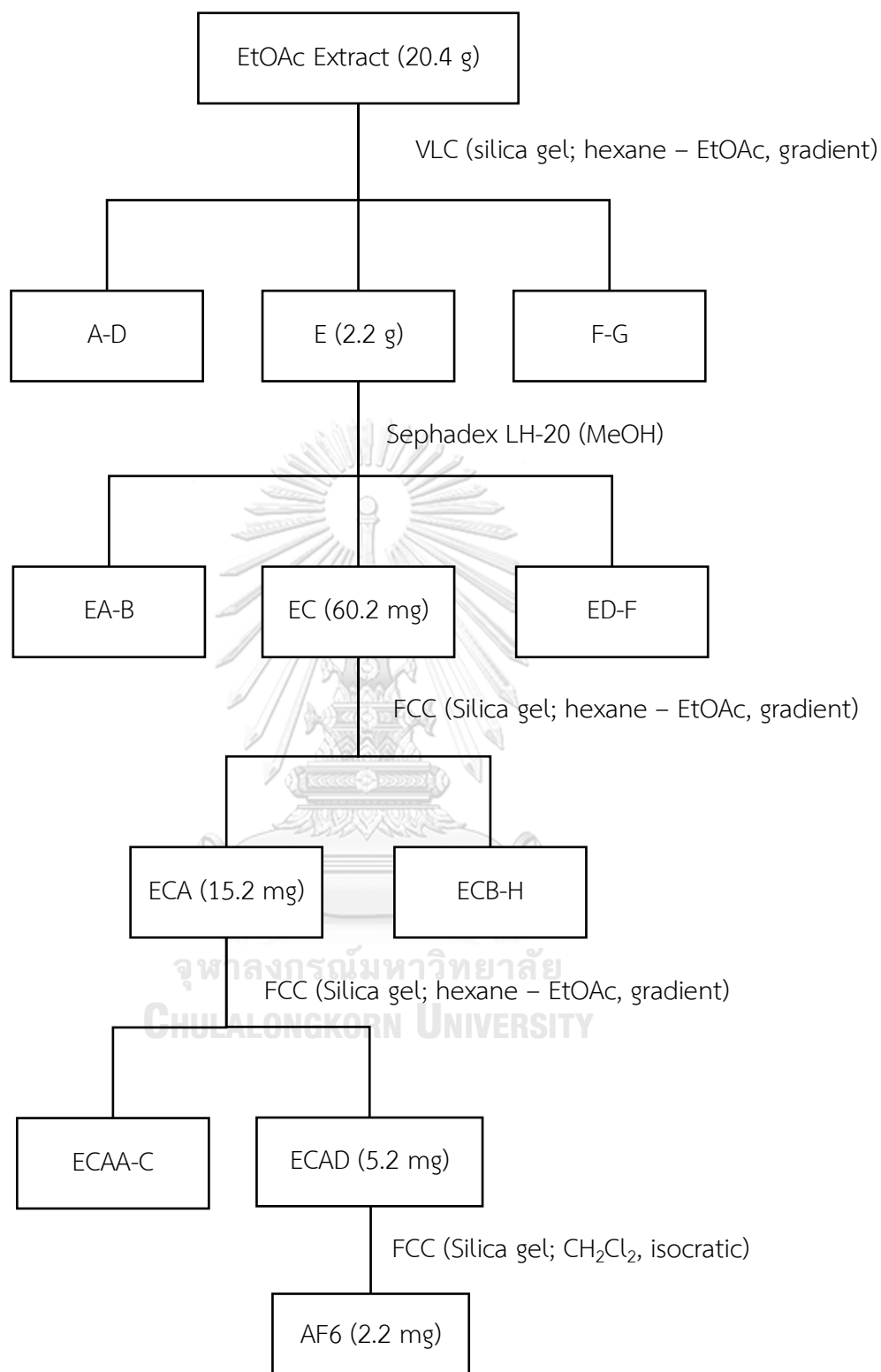
Fraction FE (98.2 mg) was re-separated by CC (silica gel, CH<sub>2</sub>Cl<sub>2</sub> – MeOH 5%, gradient) to give 10 fractions (FEA – FEJ). Fraction FEC (15.1 mg) was purified by preparative TLC (hexane: EtOAc 20%, thrice developments) to yield AF1 (11.8 mg) which was identified as aerifalcatin. Fraction FED (20.3 mg) was purified with HPLC (semi-prep, CH<sub>2</sub>Cl<sub>2</sub> – MeOH 5%, flow rate 0.8 ml/min) to yield AF10 (1.5 mg) which was identified as *trans-n*-coumaroyltyramine.

### 3.2.7. Isolation of compound AF8 and AF9

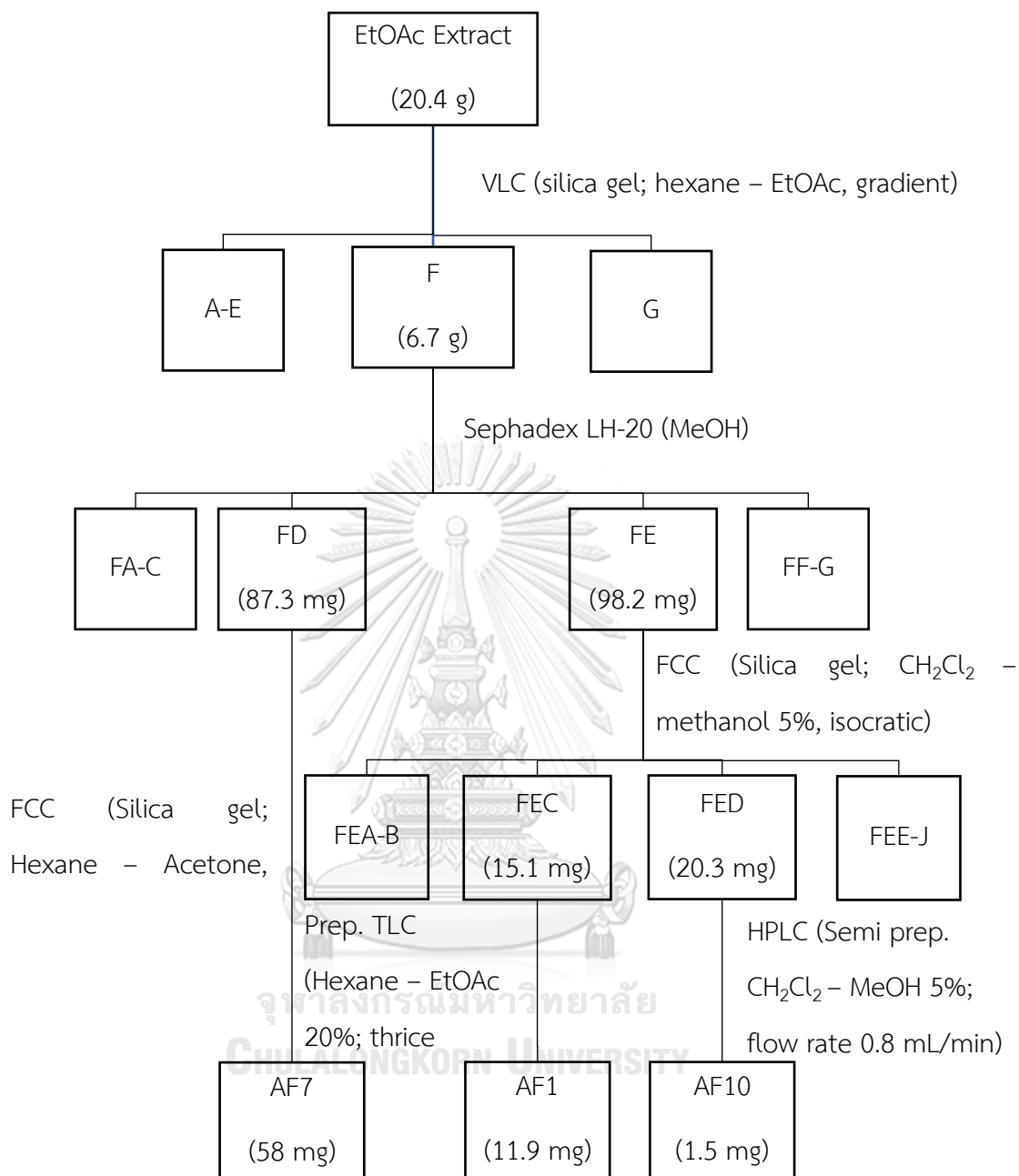
Fraction G (10.8 g) was fractionated by CC (silica gel, CH<sub>2</sub>Cl<sub>2</sub> – EtOAc 30%, gradient) to give 5 fractions (GA – GE). Fraction GA (93 mg) was separated by CC (silica gel, CH<sub>2</sub>Cl<sub>2</sub>, isocratic elution) to yield 12 fractions (GAA – GAL). GAL (40 mg) was re-separated by CC (CH<sub>2</sub>Cl<sub>2</sub> – MeOH 3%, gradient elution) to yield 9 fractions (GALA – GALI). Fraction GALC (18.3 mg) was purified by CC (silica gel, CH<sub>2</sub>Cl<sub>2</sub> – EtOAc 20%, gradient elution) to furnish 2 pure compounds, AF8 (7.4 mg) and AF9 (2.6 mg) that were identified as syringaresinol and *trans-n*-feruloyltyramine, respectively.



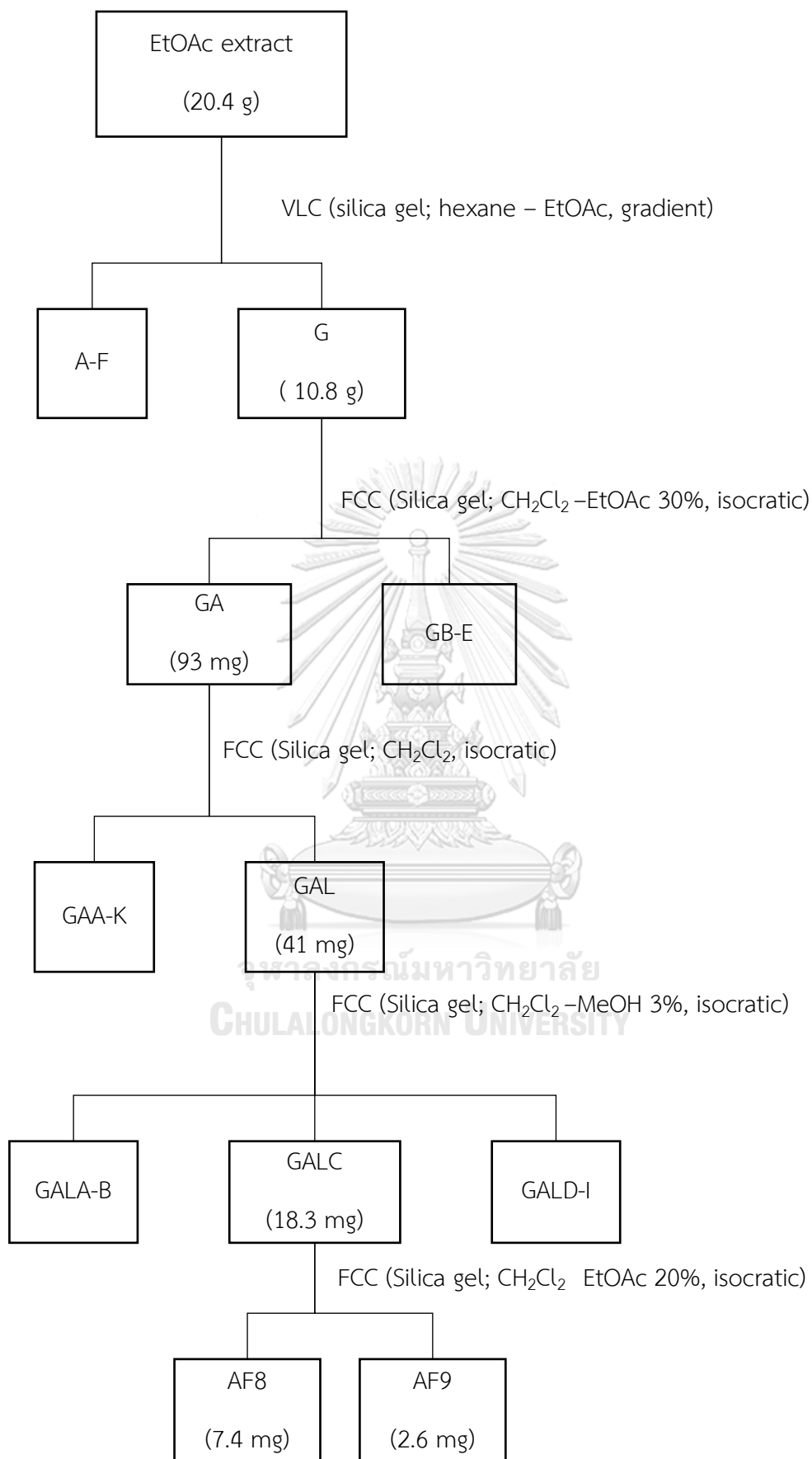
**Scheme 2** Separation and isolation of compounds from *Aerides*



Scheme 2 (Continued)



Scheme 2 (Continued)



Scheme 2 (Continued)

#### 4. Physical and spectral data of isolated compounds

##### 4.1. Compound AF1 (Aerifalcatin)

Compound AF1 was obtained as a brown amorphous solid (11.9 mg, 0.00059% of the dry weight of the plant). It was soluble in acetone.

HR-ESIMS : [M-H]<sup>-</sup> ion at  $m/z$  523.1387 (C<sub>31</sub>H<sub>23</sub>O<sub>8</sub>) (calcd. 523.1392)

UV :  $\lambda_{\max}$  nm (log  $\epsilon$ ), in methanol: 265 (4.33), 313 (3.50), 353 (3.30), 371 (3.44)

FT-IR :  $\nu$ : 3384, 2935, 2850, 1589, 1475, 1371, 1266 cm<sup>-1</sup>

Optical rotation :  $[\alpha]_D^{20}$ : -20.0 (c 0.5, MeOH)

<sup>1</sup>H NMR :  $\delta$  ppm, 400 MHz, in acetone-*d*<sub>6</sub>; Table 4

<sup>13</sup>C NMR :  $\delta$  ppm, 100 MHz, in acetone-*d*<sub>6</sub>; Table 4

##### 4.2. Compound AF2 (*n*-eicosyl-*trans*-ferulate)

Compound AF2 was obtained as a yellow powder (36.1 mg, 0.0018% of the dry weight of the plant). It was soluble in acetone.

HR-ESIMS : [M-H]<sup>-</sup> ion at  $m/z$  473.3562 (C<sub>30</sub>H<sub>49</sub>O<sub>4</sub>) (calcd. 473.3630)

<sup>1</sup>H NMR :  $\delta$  ppm, 400 MHz, in acetone-*d*<sub>6</sub>; Table 5

<sup>13</sup>C NMR :  $\delta$  ppm, 100 MHz, in acetone-*d*<sub>6</sub>; Table 5

##### 4.3. Compound AF3 (Denthyrsinin)

Compound AF3 was obtained as a brown amorphous solid (7 mg, 0.00035% of the dry weight of the plant). It was soluble in acetone.

HR-ESIMS : [M-H]<sup>-</sup> ion at  $m/z$  299.0929 (C<sub>17</sub>H<sub>15</sub>O<sub>5</sub>) (calcd. 299.0919)

<sup>1</sup>H NMR :  $\delta$  ppm, 400 MHz, in acetone-*d*<sub>6</sub>; Table 6

<sup>13</sup>C NMR :  $\delta$  ppm, 100 MHz, in acetone-*d*<sub>6</sub>; Table 6



#### 4.4. Compound AF4 (2,4-Dimethoxy-3,7-dihydroxyphenanthrene)

Compound AF4 was obtained as a brown amorphous solid (10 mg, 0.0005% of the dry weight of the plant). It was soluble in acetone.

HR-ESIMS : [M-H]<sup>-</sup> ion at  $m/z$  269.0816 (C<sub>16</sub>H<sub>13</sub>O<sub>4</sub>) (calcd. 269.0813)

<sup>1</sup>H NMR :  $\delta$  ppm, 400 MHz, in acetone-*d*<sub>6</sub>; Table 7

<sup>13</sup>C NMR :  $\delta$  ppm, 100 MHz, in acetone-*d*<sub>6</sub>; Table 7

#### 4.5. Compound AF5 (2,7-Dihydroxy-3,4,6-trimethoxyphenanthrene)

Compound AF5 was obtained as a brown amorphous solid (7 mg, 0.00035% of the dry weight of the plant). It was soluble in acetone.

HR-ESIMS : [M-H]<sup>-</sup> ion at  $m/z$  299.0922 (C<sub>17</sub>H<sub>15</sub>O<sub>5</sub>) (calcd. 299.0919)

<sup>1</sup>H NMR :  $\delta$  ppm, 400 MHz, in acetone-*d*<sub>6</sub>; Table 8

<sup>13</sup>C NMR :  $\delta$  ppm, 100 MHz, in acetone-*d*<sub>6</sub>; Table 8

#### 4.6. Compound AF6 (3,7-Dihydroxy-2,4,6-trimethoxyphenanthrene)

Compound AF6 was obtained as a brown amorphous solid (2.2 mg, 0.00011% of the dry weight of the plant). It was soluble in acetone.

HR-ESIMS : [M-H]<sup>-</sup> ion at  $m/z$  299.0926 (C<sub>17</sub>H<sub>15</sub>O<sub>5</sub>) (calcd. 299.0919)

<sup>1</sup>H NMR :  $\delta$  ppm, 400 MHz, in acetone-*d*<sub>6</sub>; Table 9

<sup>13</sup>C NMR :  $\delta$  ppm, 100 MHz, in acetone-*d*<sub>6</sub>; Table 9

#### 4.7. Compound AF7 (Agrostonin)

Compound AF7 was obtained as a brown amorphous solid (58 mg, 0.0029% of the dry weight of the plant). It was soluble in acetone.

HR-ESIMS : [M-H]<sup>-</sup> ion at  $m/z$  537.1543 (C<sub>32</sub>H<sub>25</sub>O<sub>8</sub>) (calcd. 537.1549)

<sup>1</sup>H NMR :  $\delta$  ppm, 400 MHz, in acetone-*d*<sub>6</sub>; Table 10

<sup>13</sup>C NMR :  $\delta$  ppm, 100 MHz, in acetone-*d*<sub>6</sub>; Table 10

#### 4.8. Compound AF8 (Syringaresinol)

Compound AF8 was obtained as a white amorphous solid (7.4 mg, 0.00037% of the dry weight of the plant). It was soluble in acetone.

HR-ESIMS : [M-H]<sup>-</sup> ion at  $m/z$  417.1558 (C<sub>22</sub>H<sub>25</sub>O<sub>8</sub>) (calcd. 417.1549)

<sup>1</sup>H NMR :  $\delta$  ppm, 400 MHz, in acetone-*d*<sub>6</sub>; Table 11

<sup>13</sup>C NMR :  $\delta$  ppm, 100 MHz, in acetone-*d*<sub>6</sub>; Table 11

#### 4.9. Compound AF9 (*trans-n-feruloyltyramine*)

Compound AF9 was obtained as a brown amorphous solid (2.6 mg, 0.00012% of the dry weight of the plant). It was soluble in acetone.

HR-ESIMS : [M-H]<sup>-</sup> ion at  $m/z$  312.1232 (C<sub>18</sub>H<sub>18</sub>NO<sub>4</sub>) (calcd. 312.1235)

<sup>1</sup>H NMR :  $\delta$  ppm, 400 MHz, in acetone-*d*<sub>6</sub>; Table 12

<sup>13</sup>C NMR :  $\delta$  ppm, 100 MHz, in acetone-*d*<sub>6</sub>; Table 12

#### 4.10. Compound AF10 (*trans-n-coumaroyltyramine*)

Compound AF10 was obtained as a white amorphous solid (1.5 mg, 0.00012% of the dry weight of the plant). It was soluble in acetone.

HR-ESIMS : [M-H]<sup>-</sup> ion at  $m/z$  282.1124 (C<sub>17</sub>H<sub>17</sub>NO<sub>4</sub>) (calcd. 282.1130)

<sup>1</sup>H NMR :  $\delta$  ppm, 400 MHz, in acetone-*d*<sub>6</sub>; Table 13

<sup>13</sup>C NMR :  $\delta$  ppm, 100 MHz, in acetone-*d*<sub>6</sub>; Table 13

### 5. Evaluation for anti-neuroinflammatory activity *in vitro*

#### 5.1. Cell treatment

LPS-induced BV-2 microglial cells were used as a model of neuroinflammation. Firstly, the cells were seeded at 96-well plates at a density of  $2 \times 10^4$  cells/well for 24 hours, followed by various compound concentrations to perform cell viability. Cell viability was determined using the MTT test (Sigma-

Aldrich, St. Louis, MO, USA) to obtain a safe (non-toxic) concentration. First, the media in multi-well plates were removed and cleaned after the cell treatment. Next, MTT solution (0.5 mg/mL) was added. The formazan crystals were dissolved in DMSO after three hours (Sigma-Aldrich, St. Louis, MO, USA). At a maximum wavelength of 570 nm, the absorbance was measured using a microplate reader (BMG Labtech, Ortenberg, Germany).

After that, the safe concentrations were used to perform NO and ELISA assays. Briefly, 48-well plates with  $7.5 \times 10^4$  cells per well were used to seed the cells for 24 hours. Following a 2-hour test chemical treatment, the cells were co-incubated with LPS for a further 22 hours. The media were gathered for use in cytokine and NO tests in the future.

## 5.2. Proinflammatory mediator assay

The manufacturer's instructions were followed in preparing the NO assay reagents (Sigma-Aldrich, St. Louis, MO, USA). After cell treatment, 100  $\mu$ L of culture media was collected and placed into 96-well plates. Griess reagent was added to the collected media in 100  $\mu$ L, and the mixture was then incubated for 20 minutes in the dark. The absorbance was measured in the microplate reader at 520 nm. The cytokine levels (IL-6 and TNF- $\alpha$ ) were measured using the ELISA assay (BioLegend, San Diego, CA, USA) for the most potent compounds obtained in the NO assay.

## CHAPTER IV

## RESULT AND DISCUSSION

### 1. Preliminary investigation of anti-neuroinflammatory activity from extracts of *Aerides falcata*

In this research, the dried powder of *Aerides falcata* (2 kg) was extracted with methanol, yielding the methanolic extract (105.08 g). The methanolic extract was then partitioned with water, ethyl acetate, and *n*-butanol, resulting in the aqueous extract (28.13 g), ethyl acetate extract (20.4 g), and *n*-butanol extract (48.98 g). During the preliminary study, the methanolic and ethyl acetate extracts were investigated for their anti-neuroinflammatory activity in LPS-induced BV-2 microglial cells. The ethyl acetate extract exhibited a higher NO inhibitory activity than the methanolic extract and the positive control (minocycline) (Table 3). Furthermore, both extracts showed a reduction in cytokine levels in a dose-dependent manner (Figure 4). Based on this evidence, the ethyl acetate extract was selected for further investigation to identify the active principles.

**Table 3** NO inhibition of extracts from *Aerides falcata*

Extracts	IC <sub>50</sub> (µg/mL)
Methanol	14.01 ± 2.0
Ethyl acetate	5.06 ± 3.5
Minocycline	8.63 ± 2.4

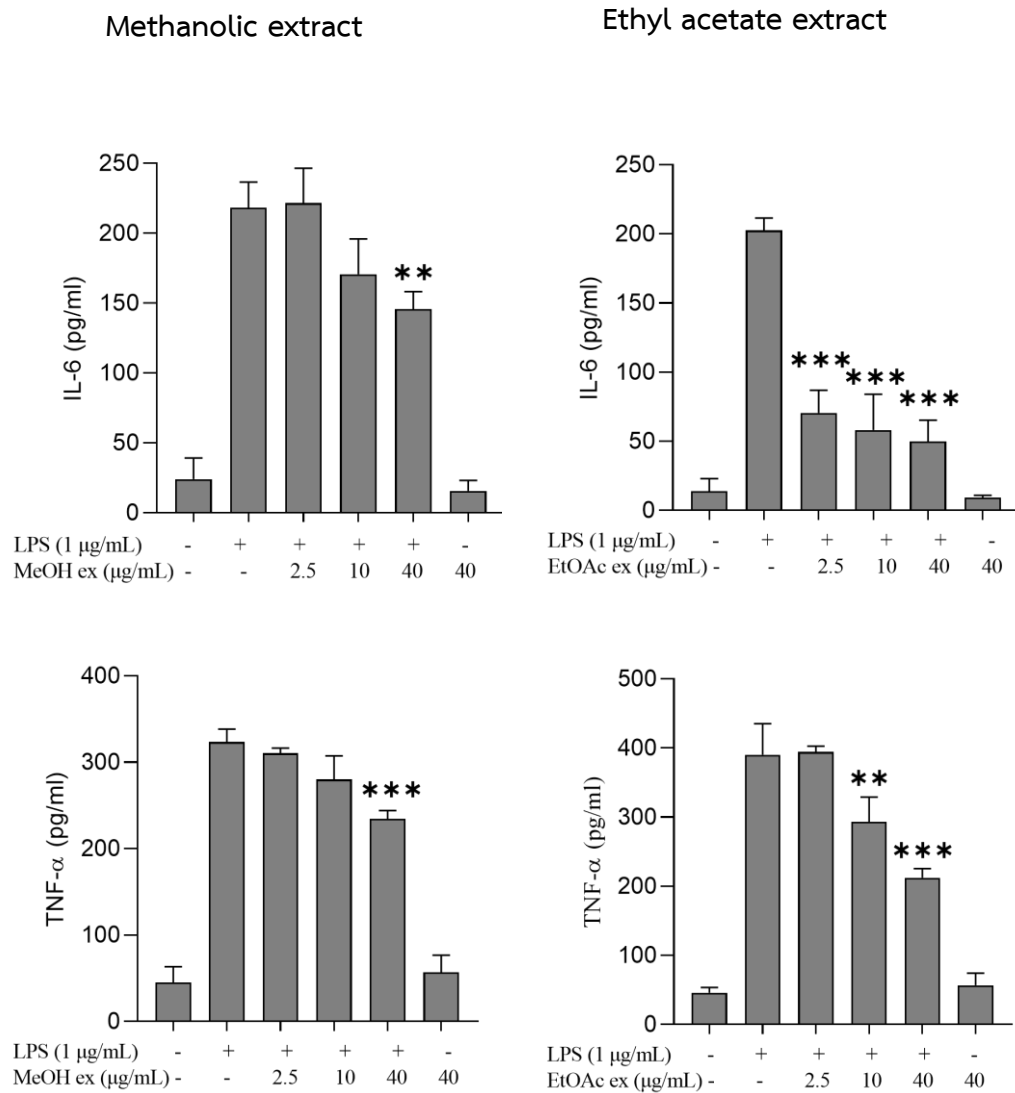
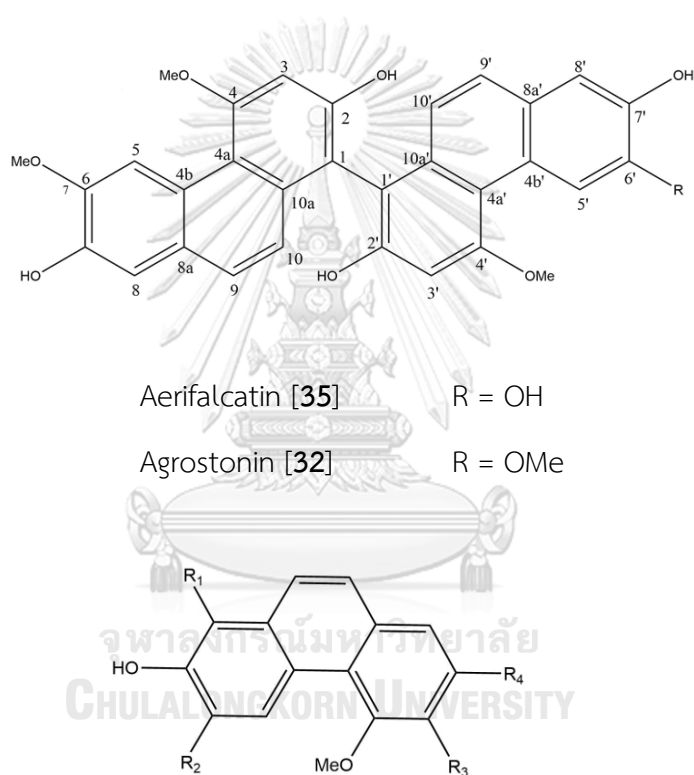


**Figure 4** Effects of MeOH and EtOAc extract on cytokine release in LPS-stimulated BV-2 microglial cells.

Data was presented as mean  $\pm$  SD, n = 3. n = 3. \*\*p < 0.01, \*\*\*p < 0.001, LPS vs extract-treated groups. Statistical difference between extracts was analyzed using one-way ANOVA followed by Tukey's multiple comparisons test.

## 2. Chemical investigation

From the ethyl acetate extract, a new compound named aerifalcatin [35] was isolated, along with nine known compounds, namely *n*-eicosyl-*trans*-ferulate [38], dentyrsinin [3], 2,4-dimethoxy-3,7-dihydroxyphenanthrene [4], 2,7-dihydroxy-3,4,6-trimethoxyphenanthrene [36], 3,7-dihydroxy-2,4,6-trimethoxyphenanthrene [37], agrostonin [32], syringaresinol [39], *trans*-*n*-feruloyltyramine [40], and *trans*-*n*-coumaroyltyramine [41] (Figure 5).



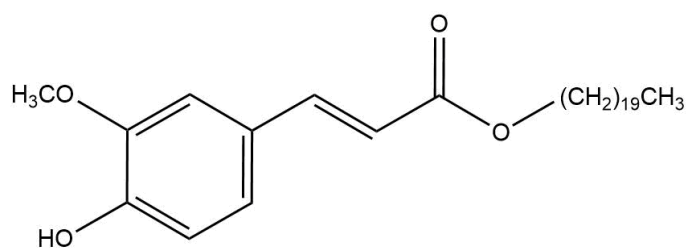
Dentyrsinin [3];  $R_1 = R_4 = \text{OMe}$ ,  $R_2 = \text{H}$ ,  $R_3 = \text{OH}$

2,4-Dimethoxy-3,7-dihydroxyphenanthrene [4];  $R_1 = R_2 = \text{H}$ ,  $R_3 = \text{OH}$ ,  $R_4 = \text{OMe}$

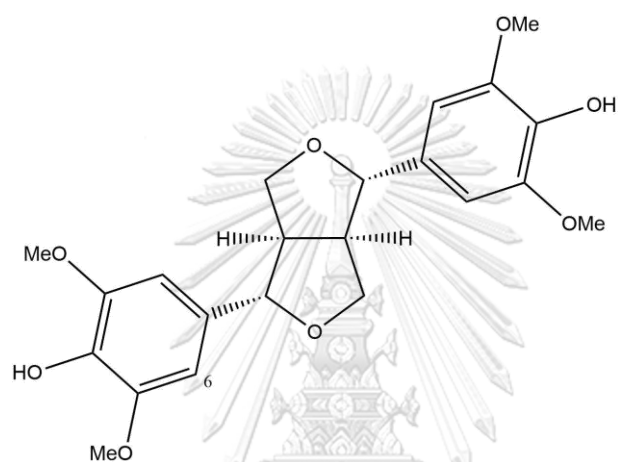
2,7-Dihydroxy-3,4,6-trimethoxyphenanthrene [36];  $R_1 = \text{H}$ ,  $R_2 = R_3 = \text{OMe}$ ,  $R_4 = \text{OH}$

3,7-Dihydroxy-2,4,6-trimethoxyphenanthrene [37];  $R_1 = \text{H}$ ,  $R_2 = R_4 = \text{OMe}$ ,  $R_3 = \text{OH}$

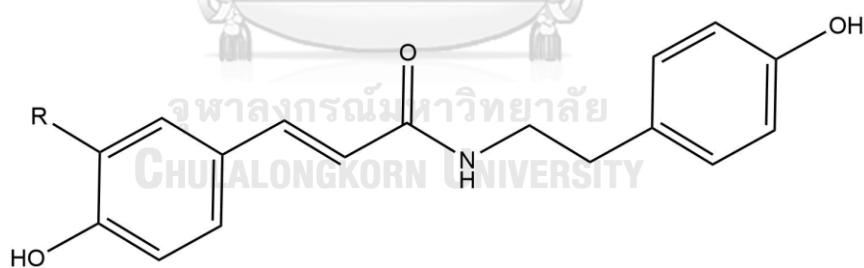
**Figure 5** Structures of compounds isolated from *Aerides falcata*



*n*-eicosyl-*trans*-ferulate [38]



Syringaresinol [39]



*trans*-*n*-feruloyltyramine [40]; R = OMe

*trans*-*n*-coumaroyltyramine [41]; R = H

Figure 5. (Continued)

## 2.1. Structure elucidation of compound AF1

AF1 was isolated as a brown amorphous solid. It was given the molecular formula  $C_{31}H_{24}O_8$  according to the negative HRESIMS spectrum which displayed a pseudo molecular ion peak  $[M-H]^-$  at  $m/z$  523.1387 (calcd. 523.1392) (Figure 8). The UV absorption at 265, 313, 353, and 371 nm (Figure 9) suggested a phenanthrene skeleton (46). The IR spectrum exhibited absorption bands for the hydroxyl groups (3384), and aromatic rings (2935, 1589) (Figure 10).

The  $^1H$  NMR spectrum presented signals in the aromatic area ( $\delta$  6.87-9.25) (Figure 11 and Table 4). It showed two pairs of coupled doublets at H-9 ( $\delta$  7.36, d,  $J$  = 8.8 Hz), H-10 ( $\delta$  6.94, d,  $J$  = 9.2 Hz), H-9' ( $\delta$  7.32, d,  $J$  = 8.8 Hz), and H-10' ( $\delta$  6.87, d,  $J$  = 9.2 Hz). Six one-proton singlets representing H-3 ( $\delta$  6.99), H-5 ( $\delta$  9.25), H-8 ( $\delta$  7.20), H-3' ( $\delta$  6.96), H-5' ( $\delta$  9.19) and H-8' ( $\delta$  7.19) indicated that this structure was a dimeric phenanthrene derivative. Furthermore, the presence of twenty-nine  $^{13}C$  NMR signals signified an asymmetrical structure (Figure 12 and Table 4). The first unit phenanthrene of AF1 (rings A, B, and C) displayed HMBC correlation between C-8 ( $\delta$  112.1) and H-9, and between C-9 ( $\delta$  127.9) and H-8. This unit showed two methoxy groups at  $\delta$  4.23 (MeO-4) and  $\delta$  4.07 (MeO-6). Their NOESY correlations with H-3 and H-5 confirmed the positions of these methoxy groups at C-4 ( $\delta$  160.2) and C-6 ( $\delta$  148.4). From the NMR data of the first unit, three quaternary carbons at C-2 ( $\delta$  155.0) and C-7 ( $\delta$  146.0) should be occupied by two hydroxy groups, and C-1 ( $\delta$  109.9) provided a bridge linking to another monomer of phenanthrene. The position of C-1 was supported by its HMBC correlation with H-3 and H-10 (Figures 16, 17, and 18). The second unit of AF1 was almost identical to the first unit. C-8' ( $\delta$  112.4) showed correlation with H-9', and C-9' ( $\delta$  128.1) also showed correlation with H-8' in the HMBC spectrum. However, there was only one methoxy group at MeO-4' ( $\delta$  4.17,



s). The position of this methoxy group at C-4' ( $\delta$  160.3) was supported by its cross-peak with H-3' in the NOESY spectrum (Figures 19, 20, and 21). The hydroxyl groups were attached to three quaternary carbons, C-2' ( $\delta$  155.0), C-6' ( $\delta$  146.2), and C-7' ( $\delta$  145.0) while C-1' ( $\delta$  109.6) was assigned as the bridging point based on its HMBC correlation to H-3' and H-10'. The bridge C-1 ( $\delta$  109.9) and C-1' ( $\delta$  109.6) was also supported by their chemical shift values, typical for non-oxygenated quaternary carbons (47). From all of the above spectral evidence, it was concluded that 1 had the structure 4,4',6-trimethoxy(1,1'-biphenanthrene)-2,2',6',7,7'-pentol and was given the trivial name aerifalcatin.

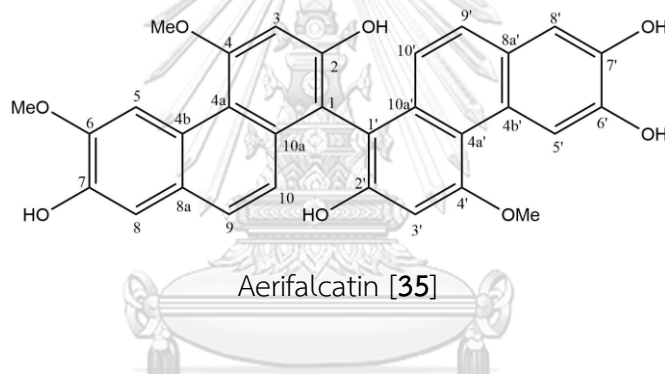


**Table 4** NMR spectral data of compound AF1

Position	AF1 (acetone- $d_6$ )		
	$^1\text{H}$	$^{13}\text{C}$	HMBC (correlation with $^1\text{H}$ )
1	-	109.9	3, 10
2	-	155.0	3*
3	6.99 (s)	100.0	-
4	-	160.2	3*, MeO-4
4a	-	116.3	3, 5, 10
4b	-	125.8	8, 9
5	9.25 (s)	109.7	-

6	-	148.4	5*, 8, MeO-6
7	-	146.0	5, 8*
8	7.20 (s)	112.1	9
8a	-	128.0	5, 10
9	7.36 (d, $J = 8.8$ Hz)	127.9	8
10	6.94 (d, $J = 8.8$ Hz)	123.3	-
10a	-	135.4	9
1'	-	109.6	3', 10'
2'	-	155.0	3'*
3'	6.96 (s)	99.7	-
4'	-	160.3	3'*, MeO-4'
4a'	-	116.0	3', 5', 10'
4b'	-	126.2	8', 9'
5'	9.19 (s)	113.5	-
6'	-	146.2	5'*, 8'
7'	-	145.0	5', 8'*
8'	7.19 (s)	112.4	9'
8a'	-	127.6	5', 10'
9'	7.32 (d, $J = 9.2$ Hz)	128.1	8'
10'	6.87 (d, $J = 9.2$ Hz)	122.6	-
10a'	-	135.5	9'
MeO-4	4.23 (s)	56.1	
MeO-6	4.07 (s)	56.0	
MeO-4'	4.17 (s)	55.8	

\*Two-bond coupling

## 2.2. Identification of compound AF2

Compound AF2 was isolated as a yellow powder. It presented the molecular formula  $C_{30}H_{50}O_4$  based on the negative HRESIMS spectrum which displayed a pseudo molecular ion peak  $[M-H]^-$  at  $m/z$  473.3562 (calcd. 473.3630). The  $^1H$  NMR signals (Figure 24 and Table 5) in the aromatic region showed meta-coupling proton at  $\delta_H$  7.34 (1H, d,  $J = 2.0$  Hz, H-6), a double doublet proton signals at  $\delta_H$  7.14 (1H, dd,  $J = 2.0, 8.0$  Hz, H-2), an ortho-coupling at  $\delta_H$  6.87 (1H, d,  $J = 8.4$  Hz, H-3), and uncoupled of a methoxy group at  $\delta_H$  3.92 (3H, s, MeO-5). Two olefinic protons showed at  $\delta_H$  7.59 (1H, d,  $J = 16.0$  Hz, H-7) and  $\delta_H$  6.39 (1H, d,  $J = 16.0$  Hz, H-8), a methylene proton at  $\delta_H$  4.15 (2H, t,  $J = 6.8$  Hz, H-1'), a methyl proton at  $\delta_H$  0.87 (3H, t,  $J = 4.0$  Hz, H-Me). The  $^1H$  NMR signals (Figure 25 and Table 5) showed a strong signal at the methylene region at  $\delta_H$  1.28 (m, H-methylene, H-n-2, H-n-1), the methylene aliphatic chain was suggested as  $-(CH_2)_{14}-$  based on calculating between HRESIMS and known NMR structure. The  $^{13}C$  NMR and HSQC spectra (Figures 25, 26, and 27) of AF2 revealed seventeen signals, including one carbonyl of ester form at  $\delta_C$  167.57 (C-9), one methoxy group at  $\delta_C$  56.42 (OMe-5), one methyl group, five methine carbons, three quaternary carbons, and six methylene carbons. The above NMR data of AF2 suggested a ferulic acid ester skeleton (48).

The HMBC spectrum of AF2 (Figures 29, 30, and 31) confirmed H-7 was correlated with C-6 ( $\delta_C$  111.3), C-9 ( $\delta_C$  167.5), and C-2 ( $\delta_C$  124.0). the ester group was supported with HMBC correlation C-9 ( $\delta_C$  167.5) with H-1' and the long chain of aliphatic was continued with connection H-1' to H-2' and H-3' supported by HMBC, NOESY (Figure 32), COSY (Figures 33 and 34) data, where there were presented their connection. the primary carbon of methyl ( $\delta_C$  14.4) at the end of this chain was correlated with the proton methylene group  $\delta_H$  1.28 (4H, m, H<sub>2</sub>-n-1, H<sub>2</sub>-n-2), based on

the HMBC correlation. The position of the methoxy group of MeO-5 was determined by HMBC correlation with C-5 ( $\delta_c$  149.0) and supported by NOESY correlation between OMe-5 and H-6.

Based on the above spectroscopy data evidence, AF2 was identified as *n*-eicosyl *trans*-ferulate. This known compound was previously reported in *Synadenium glaucescens* (49) and several *Dendrobiums* such as *Dendrobium christyanum* and *Dendrobium clavatum* (50, 51).

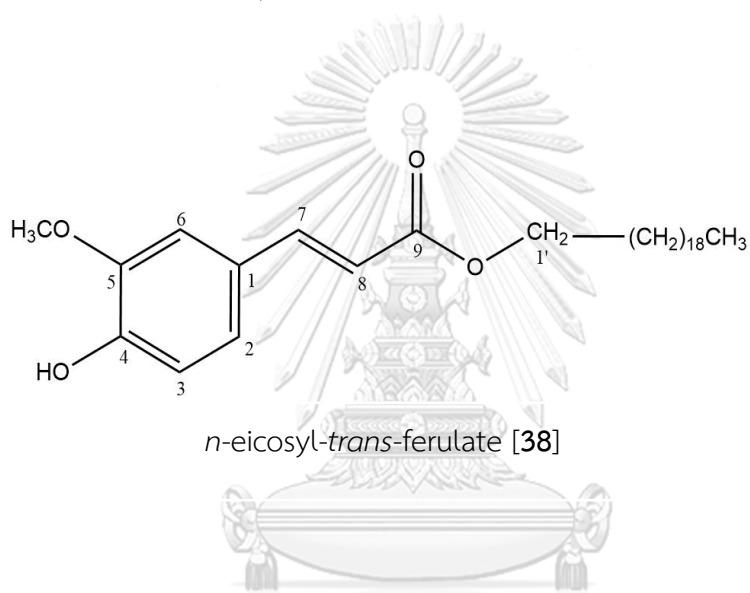


**Table 5** NMR spectral data of compound AF2 and *n*-eicosyl-*trans* ferulate

Position	AF2 (acetone- $d_6$ )		<i>n</i> -eicosyl- <i>trans</i> ferulate (CDCl <sub>3</sub> ) (48)	
	$\delta_H$ (mult., $J$ in Hz)	$\delta_C$	$\delta_H$ (mult., $J$ in Hz)	$\delta_C$
1	-	127.9	s-	127.1
2	7.14 (dd, $J = 2.0, 8.0$ Hz)	124.0	7.07 (dd, $J = 2.0, 8.0$ Hz)	122.9
3	6.87 (d, $J = 8.4$ Hz)	116.1	6.91 (d, $J = 8.0$ Hz)	114.6
4	-	150.3	-	146.7
5	-	149.0	-	147.8
6	7.34 (d, $J = 2.0$ Hz)	111.3	7.03 (d, $J = 2.0$ Hz)	109.3

7	7.59 (d, $J = 16.0$ Hz)	145.6	7.61 (d, $J = 16.0$ Hz)	144.6
8	6.39 (d, $J = 16.0$ Hz)	116.0	6.29 (d, $J = 16.0$ Hz)	115.6
9	-	167.5	-	167.3
1'	4.15 (t, $J = 6.8$ Hz)	64.7	4.18 (t)	64.6
2'	1.58 (m)	29.6	1.64 (m)	31.8
3'	1.42 (m)	26.8	1.64 (m)	25.9
-(CH <sub>2</sub> ) <sub>14</sub>	1.28 (m)	23.4 - 29.6	1.25 (m)	25.9- 29.6
n-2	1.28 (m)	32.7	1.25 (m)	31.9
n-1	1.28 (m)	23.4	1.25 (m)	22.7
Me	0.87 (t, $J = 4.0$ Hz)	14.4	0.86 (t)	14.1
MeO-5	3.92 (s)	56.42	3.92 (s)	55.9

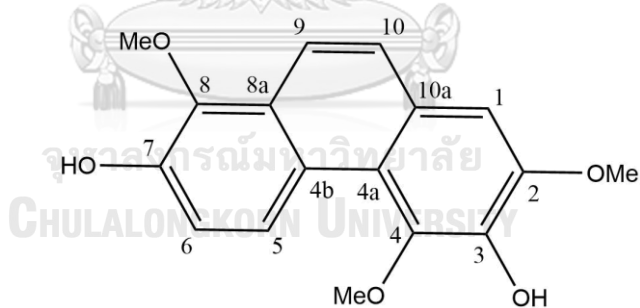
### 2.3. Identification of compound AF3

Compound AF3 was isolated as a brown amorphous solid. The pseudo molecular ion showed a negative HRESIMS spectrum (Figure 35)  $[M-H]^-$  at  $m/z$  299.0929 (calcd. 299.0919) suggesting molecular formula C<sub>17</sub>H<sub>16</sub>O<sub>5</sub>. The <sup>1</sup>H-NMR spectra of AF3 (Figure 36 and Table 6) presented aromatic region in four ortho-coupling proton signals at  $\delta_H$  9.10 (1H, d,  $J = 9.2$  Hz, H-5),  $\delta_H$  7.24 (1H, d,  $J = 9.2$  Hz, H-6),  $\delta_H$  7.85 (1H, d,  $J = 9.2$  Hz, H-9),  $\delta_H$  7.67 (1H, d,  $J = 8.8$  Hz, H-10) and one singlet signal at  $\delta_H$  7.25 (1H, s, H-1). Three singlet signals were provided at  $\delta_H$  3.99 (3H, MeO-2),  $\delta_H$  3.91 (3H, MeO-4), and  $\delta_H$  3.92 (3H, MeO-8), suggested as three methoxy groups. Additional remaining two singlet signals at  $\delta_H$  7.96 and  $\delta_H$  8.31 represent HO-3 and HO-7 respectively. The <sup>13</sup>C-NMR and HSQC correlation of AF3 (Figure 37, 38 and Table

6), showed seventeen signals including nine quaternary carbon, five methine carbon, and three methoxy groups. These data confirmed a monomeric phenanthrene skeleton.

This monomeric phenanthrene was equipped with a correlation between H-9 and H-10 at COSY of AF3 (Figure 42). It was supported by HMBC correlation (Figure 39), H-9 has a correlation with C-4b ( $\delta_c$  124.8), C-10a ( $\delta_c$  126.4), and C-8 ( $\delta_c$  142.2), whereas H-10 was correlated with C-1 ( $\delta_c$  105.9) and C-4a ( $\delta_c$  120.4). Positions of methoxy groups were supported by NOESY correlation (Figure 41), MeO-2, MeO-4, and MeO-8, showed correlations with H-1, H-5 and H-9, respectively.

Based on the above NMR spectral data, AF3 was identified as denthyrsinin. This compound was confirmed by comparison with NMR spectral data that was previously reported as 3,7-dihydroxy-2,4,8-trimethoxyphenanthrene, which was earlier isolated from *Bletilla striata* (52).



Denthyrsinin [3]

**Table 6** NMR spectral data of compound AF3 and Denthyrsinin

Position	AF3 (acetone- <i>d</i> <sub>6</sub> )		Denthyrsinin (CDCl <sub>3</sub> ) (53)	
	$\delta_{\text{H}}$ (mult., <i>J</i> in Hz)	$\delta_{\text{C}}$	$\delta_{\text{H}}$ (mult., <i>J</i> in Hz)	$\delta_{\text{C}}$
1	7.25 (s)	105.9	7.09 (s)	104.9
2	-	148.7	-	146.8
3	-	141.2	-	139.4
4	-	145.4	-	144.0
4a	-	120.4	-	119.2
4b	-	124.8	-	124.2
5	9.15 (d, <i>J</i> = 9.2 Hz)	124.2	9.16 (d, <i>J</i> = 9.2 Hz)	124.0
6	7.24 (d, <i>J</i> = 9.2 Hz)	117.9	7.30 (d, <i>J</i> = 9.2 Hz)	116.1
7	-	147.3	-	145.6
8	-	142.2	-	140.8
8a	-	128.5	-	125.7
9	7.85 (d, <i>J</i> = 9.2 Hz)	118.6	7.82 (d, <i>J</i> = 9.2 Hz)	117.9
10	7.67 (d, <i>J</i> = 8.8 Hz)	128.7	7.63 (d, <i>J</i> = 9.2 Hz)	127.5
10a	-	126.4	-	126.6
MeO-2	3.99 (s)	56.3	4.05 (s)	56.1
MeO-4	3.91 (s)	59.6	3.94 (s)	59.8
MeO-8	3.92 (s)	61.3	3.98 (s)	61.9
HO-3	7.96 (s)	-	5.79 (s)	-
HO-7	8.31 (s)	-	6.01 (s)	-

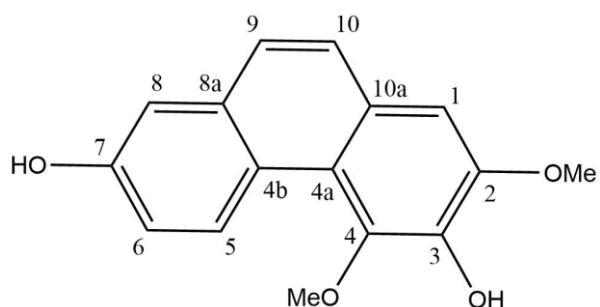
#### 2.4. Identification of compound AF4

Compound AF4 was determined as a brown amorphous solid. The HRESIMS spectrum (Figure 43) showed a negative molecular ion  $[M-H]^-$  at  $m/z$  269.0816 (calcd. 269.0813) suggesting the molecular formula as  $C_{16}H_{14}O_4$ . The  $^1H$ -NMR spectra of AF4 (Figures 44, 45 and Table 7) served doublet protons of ortho-coupling at  $\delta_H$  9.34 (1H, d,  $J = 9.2$  Hz, H-5),  $\delta_H$  7.45 (1H, d,  $J = 8.8$  Hz, H-9), and  $\delta_H$  7.59 (1H, d,  $J = 8.8$  Hz, H-10). The  $^1H$  NMR also exhibited a double doublet proton at  $\delta_H$  7.18 (1H, dd,  $J = 9.2, 2.8$  Hz H-6), one uncoupled proton at  $\delta_H$  7.22 (1H, s, H-1), and two singlet signals of methoxy groups at  $\delta_H$  3.98 (3H, MeO-2) and  $\delta_H$  3.92 (3H, MeO-4). The  $^{13}C$ -NMR spectra and HSQC correlation (Figures 46, 47, and Table 7), presented sixteen signals, including eight quaternary carbons, six methine carbons, and two methoxy groups. These  $^1H$  and  $^{13}C$ -NMR offered data that was similar to AF3, presenting a monomeric phenanthrene skeleton.

The assignment of H-9 and H-10 positions supported by its correlation with C-8 ( $\delta_C$  112.2) and C-1 ( $\delta_C$  105.9), respectively, in HMBC spectrum (Figure 48). The methoxy group positions of AF4 were determined by the HMBC correlation (Figure 49) where the proton of MeO-2 connected to C-2 ( $\delta_C$  148.4) and the proton of MeO-4 connected to C-4 ( $\delta_C$  145.3). These positions strengthened with NOESY correlation of AF4 (Figure 51), MeO-2 and MeO-4 linked to H-1 and H-5, respectively.

From the above data spectroscopy evidence, AF4 was identified as 2,4-dimethoxy-3,7-dihydroxyphenanthrene. It was reported previously as Epheranthol B isolated from the stems of *Flickingria fimbriata* (54) and *Dendrobium chrysotoxum* (55).





2,4-dimethoxy-3,7-dihydroxyphenanthrene [4]

**Table 7** NMR spectral data of compound AF4 and 2,4-dimethoxy-3,7-dihydroxyphenanthrene

Position	AF4 (acetone- $d_6$ )		2,4-dimethoxy-3,7-dihydroxyphenanthrene (CDCl <sub>3</sub> ) (52)	
	$\delta_{\text{H}}$ (mult., $J$ in Hz)	$\delta_{\text{C}}$	$\delta_{\text{H}}$ (mult., $J$ in Hz)	$\delta_{\text{C}}$
1	7.22 (s)	105.9	7.12 (s)	105.0
2	-	148.4	-	147.7
3	-	141.1	-	139.9
4	-	145.3	-	144.5
4a	-	120.0	-	119.1
4b	-	123.9	-	123.0
5	9.34 (d, $J = 9.2$ Hz)	129.1	9.27 (d, $J = 9.0$ Hz)	128.0
6	7.18 (dd, $J = 9.2, 2.8$ Hz)	117.4	7.09 (dd, $J = 9.0, 2.5$ Hz)	116.1
7	-	155.9	-	154.8
8	7.24 (d, $J = 2.8$ Hz)	112.2	7.14 (d, $J = 2.5$ Hz)	111.1
8a	-	135.0	-	134.2

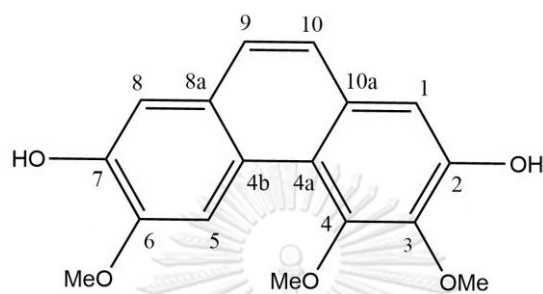
9	7.45 (d, $J = 8.8$ Hz)	125.3	7.52 (d, $J = 9.0$ Hz)	124.3
10	7.59 (d, $J = 8.8$ Hz)	128.1	7.39 (d, $J = 9.0$ Hz)	127.0
10a	-	126.4	-	125.8
MeO-2	3.98 (s)	56.3	3.87 (s)	55.2
MeO-4	3.92 (s)	59.6	3.97 (s)	58.6

## 2.5. Identification of compound AF5

Compound AF5 was obtained as a brown amorphous solid. It was suggested the molecular formula for  $C_{17}H_{16}O_5$  based on its HRESIMS spectrum (Figure 53) in a negative molecular ion  $[M-H]^-$  at  $m/z$  299.0922 (calcd. 299.0919).  $^1H$ -NMR spectra of AF5 (Figure 54 and Table 8) showed seven signals at the aromatic region including two pairs ortho-coupling at  $\delta_H$  7.48 (1H, d,  $J = 8.8$  Hz, H-9) and  $\delta_H$  7.43 (1H, d,  $J = 8.8$  Hz, H-10). Three uncoupled protons at  $\delta_H$  7.14 (1H, s, H-1),  $\delta_H$  9.04 (1H, s, H-5),  $\delta_H$  7.25 (1H, s, H-8), and two phenolic hydroxyl group at  $\delta_H$  7.29 (1H, s, HO-2), and  $\delta_H$  8.28 (1H, s, HO-7). The presence of a monomeric phenanthrene skeleton was indicated by  $^{13}C$ -NMR spectra and HSQC correlation of AF5 (Figures 55, 56 and Table 8) which showed seventeen signals including the presence of nine quaternary carbons, five methine carbon, and three methoxy groups.

The position of three methoxy groups was confirmed by HMBC correlation of AF5 (Figures 59), which was MeO-3 was correlated with C-3 ( $\delta_C$  142.6), MeO-4 was correlated with C-4 ( $\delta_C$  152.1), and MeO-6 was correlated with C-6 ( $\delta_C$  148.7). HMBC correlations also presented the relation of C-6 to HO-7 proton and C-1 to HO-2 proton, suggesting the position of hydroxyl groups.

Based on the above evidence, the structure of AF5 was suggested as 2,7-dihydroxy-3,4,6-trimethoxyphenanthrene. This compound was earlier reported from *Appendicula reflexa* with the synonym 3,4,6-trimethoxyphenanthrene-2,7-diol (56) and isolated from the heartwood of *Combretum psidioides* (57)



2,7-dihydroxy-3,4,6-trimethoxyphenanthrene [36]

**Table 8** NMR spectral data of compound AF5 and 2,7-dihydroxy-3,4,6-trimethoxyphenanthrene

Position	AF5 (acetone- $d_6$ )		
	$\delta_{\text{H}}$ (mult., $J$ in Hz)	$\delta_{\text{C}}$	HMBC Correlation with $^1\text{H}$
1	7.14 (s)	109.7	10, OH-2
2	-	150.0	1*, OH-2*
3	-	142.6	1, MeO-3
4	-	152.1	MeO-4
4a	-	118.8	1, 5, 10
4b	-	124.7	8, 9
5	9.04 (s)	108.2	-
6	-	148.7	8, MeO-6, OH-7

7	-	146.5	5, 8*, OH-7*
8	7.25 (s)	112.7	9, OH-7
8a	-	128.4	5, 10
9	7.48 (d, $J = 8.8$ Hz)	126.7	8
10	7.43 (d, $J = 8.8$ Hz)	125.4	1
10a	-	130.7	9, 10*
MeO-3	4.01 (s)	61.3	-
MeO-4	4.02 (s)	60.4	-
MeO-6	4.04 (s)	56.1	-
HO-2	7.29 (s)	-	-
HO-7	8.28 (s)	-	-

\*Two-bond coupling

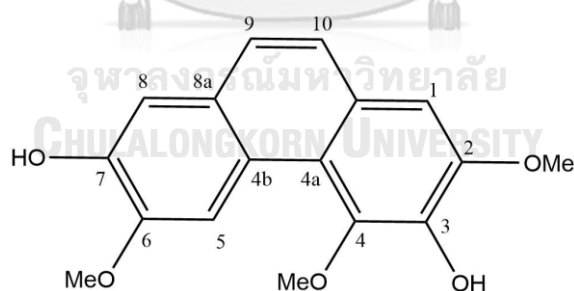
## 2.6. Identification of compound AF6

Compound AF6 was obtained as a brown amorphous solid. The molecular formula was identified as  $C_{17}H_{16}O_5$  based on HRESIMS spectrum (Figure 59) in a negative molecular ion  $[M-H]^-$  at  $m/z$  299.0926 (calcd. 299.0919). The  $^1H$ -NMR spectrum of AF6 (Figure 60 and Table 9) showed three uncoupled protons of methoxy group at  $\delta_H$  4.04 (3H, s, MeO-2),  $\delta_H$  3.99 (3H, s, MeO-4), and  $\delta_H$  3.98 (3H, s, MeO-6). Three singlet proton signals at  $\delta_H$  7.22 (1H, s, H-1),  $\delta_H$  9.06 (1H, s, H-5), and  $\delta_H$  7.25 (1H, s, H-8). Two pairs of ortho-coupling at  $\delta_H$  7.45 (1H, d,  $J = 8.8$  Hz, H-9), and  $\delta_H$  7.51 (1H, d,  $J = 8.8$  Hz, H-10). Two singlet signals of hydroxyl groups at  $\delta_H$  7.85 (1H, s, HO-3) and  $\delta_H$  7.91 (1H, s, HO-7). The  $^{13}C$ -NMR spectrum and HSQC correlation of AF6 (Figures 61, 62, and Table 9) showed seventeen signals including, nine quaternary carbons, five methine carbon, and three methoxy groups. Based on

the presence of spectrum  $^1\text{H-NMR}$  and  $^{13}\text{C-NMR}$ , it showed similar data with AF3 and AF5, which suggested a monomeric phenanthrene skeleton.

The HMBC correlation of AF6 (Figure 63) suggested the position of hydroxyl groups with the presence of their correlation of C-2 ( $\delta_{\text{C}}$  144.9) and C-4 ( $\delta_{\text{C}}$  148.3) with HO-3 and C-6 ( $\delta_{\text{C}}$  148.4) and C-8 ( $\delta_{\text{C}}$  105.9) with HO-7. The HMBC correlation also obtained the position of methoxy groups that were correlated between carbon aromatic rings and proton methoxy groups including proton MeO-2 to C-2 ( $\delta_{\text{C}}$  144.9), MeO-4 to C-4 ( $\delta_{\text{C}}$  148.3), and MeO-6 to C-6 ( $\delta_{\text{C}}$  148.4). These positions were completed with the other evidence from the NOESY and COSY correlations of AF6 (Figures 64 and 65), where the proton of MeO-2 was correlated with H-1, and the proton of MeO-6 was correlated with H-5.

The above data NMR spectroscopy suggested AF6 was 3,7-dihydroxy-2,4,6-trimethoxyphenanthrene. This compound was the first isolated from the whole plant of *Bulbophyllum odoratissimum* (49).



3,7-dihydroxy-2,4,6-trimethoxyphenanthrene [37]

**Table 9** NMR spectral data of compound AF6 and 3,7-dihydroxy-2,4,6-trimethoxyphenanthrene

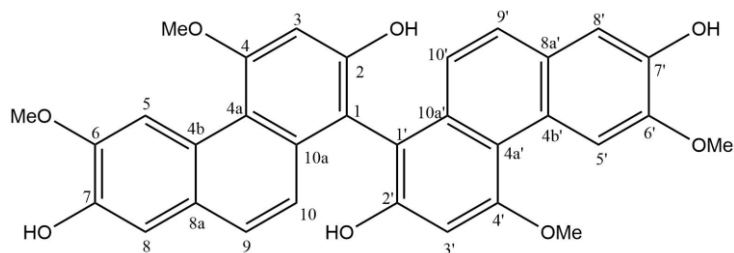
Position	AF6 (acetone- $d_6$ )		3,7-dihydroxy-2,4,6-trimethoxyphenanthrene (CDCl <sub>3</sub> ) (49)	
	$\delta_{\text{H}}$ (mult., $J$ in Hz)	$\delta_{\text{C}}$	$\delta_{\text{H}}$ (mult., $J$ in Hz)	$\delta_{\text{C}}$
1	7.22 (s)	105.6	6.97 (s)	103.6
2	-	144.9	-	146.5
3	-	140.6	-	138.3
4	-	148.3	-	143.0
4a	-	126.7	-	117.4
4b	-	124.2	-	122.2
5	9.06 (s)	108.1	8.95 (s)	106.1
6	-	148.4	-	146.6
7	-	146.5	-	144.3
8	7.25 (s)	105.9	7.19 (s)	110.4
8a	-	128.8	-	126.9
9	7.45 (d, $J = 8.8$ Hz)	124.9	7.31(s)	122.8
10	7.51 (d, $J = 8.8$ Hz)	125.7	7.31(s)	123.7
10a	-	119.5	-	124.9
MeO-2	4.04 (s)	59.8	3.88 (s)	54.0
MeO-4	3.99 (s)	56.2	3.85 (s)	57.8
MeO-6	3.98 (s)	56.0	3.97 (s)	53.8

## 2.7. Identification of compound AF7

AF7 was identified as a brown amorphous solid. HRESIMS mass spectrum of AF7 (Figure 66) showed a negative molecular ion  $[M-H]^-$  at  $m/z$  537.1543 (calcd. 537.1549), suggesting the molecular formula  $C_{32}H_{26}O_8$ . The  $^1H$ -NMR spectra of AF7 (Figure 67 and Table 10) showed the presence of the presence of a pair of two-proton doublets with ortho-coupling at  $\delta_H$  7.37 (2H, d,  $J = 9.2$  Hz, H-9/H-9') and 6.92 (2H, d,  $J = 9.2$  Hz, H-10/H-10'). Three sharp singlets at  $\delta_H$  7.02 (2H, s, H-3/H-3'),  $\delta_H$  9.27 (2H, s, H-5/H-5'), and  $\delta_H$  7.21 (2H, s, H-8/H-8'). Two methoxy groups with singlet signals at  $\delta_H$  4.25 (6H, s, MeO-4/MeO-4') and  $\delta_H$  4.09 (6H, s, MeO-6/MeO-6'). The  $^{13}C$ -NMR and HSQC spectra (Figures 68, 69, 70, and Table 10) revealed sixteen carbon signals, suggesting that AF8 was a symmetrical dimeric phenanthrene. Moreover, the two phenanthrene units were symmetrically linked to each other through a C-C' bond between C-1-C1' as supported by the HMBC correlation of AF7 (Figure 71), where C-1/1' at  $\delta_C$  (109.1) connected to H-3/3' and H-10/10' (47).

The positioning of methoxy groups was suggested by the HMBC correlation of AF7 (Figure 72), proved by correlation C-4/4' ( $\delta_C$  159.3) to the proton of MeO-4/4' and C-6/6' ( $\delta_C$  147.7) to the proton of MeO-6/6'. This condition was supported by the NOESY correlation of AF7 (Figure 73), which showed the proton of MeO-4/4' correlated to H-3 and MeO-6/6' correlated to H-5.

Through the comparison of the above evidence NMR spectra data with previously reported compound (47), which identified that AF7 is agrostinin. AF7 is a known compound that was first found in *Agrostophyllum khasiyanum* (58) and was isolated from *Aerides multiflora* (26).



Agrostinin [32]

**Table 10** NMR spectral data of compound AF7 and Agrostinin

Position	AF7 (acetone- $d_6$ )		Agrostinin (acetone- $d_6$ ) (49)	
	$\delta_{\text{H}}$ (mult., $J$ in Hz)	$\delta_{\text{C}}$	$\delta_{\text{H}}$ (mult., $J$ in Hz)	$\delta_{\text{C}}$
1	-	109.1	-	109.8
2	-	154.1	-	155.1
3	7.02 (s)	99.1	7.00 (s)	100.0
4	-	159.3	-	160.2
4a	-	115.4	-	116.3
4b	-	125.0	-	125.8
5	9.27 (s)	159.0	9.25 (s)	109.7
6	-	147.7	-	148.5
7	-	145.2	-	146.0
8	7.21 (s)	111.3	7.19 (s)	112.2
8a	-	127.1	-	128.1
9	7.37 (d, $J = 9.2$ Hz)	127.0	7.36 (d, $J = 9.2$ Hz)	127.9
10	6.92 (d, $J = 9.2$ Hz)	122.5	6.93 (d, $J = 9.2$ Hz)	123.3
10a	-	134.6	-	135.4
1'	-	109.1	-	109.8
2'	-	154.1	-	155.1
3'	7.02 (s)	99.1	7.00 (s)	100.0



4'	-	159.3	-	160.2
4a'	-	115.4	-	116.3
4b'	-	125.0	-	125.8
5'	9.27 (s)	159.0	9.25 (s)	109.7
6'	-	147.7	-	148.5
7'	-	145.2	-	146.0
8'	7.21 (s)	111.3	7.19 (s)	112.2
8a'	-	127.1	-	128.1
9'	7.37 (d, $J = 9.2$ Hz)	127.0	7.36 (d, $J = 9.2$ Hz)	127.9
10'	6.92 (d, $J = 9.2$ Hz)	122.5	6.93 (d, $J = 9.2$ Hz)	123.3
10a'	-	134.6	-	135.4
MeO-4	4.25 (s)	55.3	4.23 (s)	55.6
MeO-6	4.09 (s)	55.2	4.07 (s)	56.0
MeO-4'	4.25 (s)	55.3	4.23 (s)	56.1
MeO-6'	4.09 (s)	55.2	4.07 (s)	56.0

จุฬาลงกรณ์มหาวิทยาลัย  
CHULALONGKORN UNIVERSITY

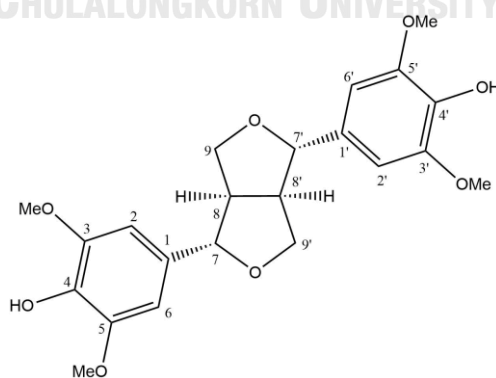
## 2.8. Identification of compound AF8

Compound AF8 was obtained as a white amorphous solid. The molecular formula was determined as  $C_{22}H_{26}O_8$  suggested by negative molecular ion  $[M-H]^-$  at  $m/z$  417.1558 (calcd. 417.1549) in the HRESIMS (Figure 74). The  $^1H$ -NMR spectrum of AF8 (Figure 75 and Table 11) showed 1 sharp single proton in aromatic region at  $\delta_H$  6.68 (4H, s, H-2, H-2', H-6, H-6'). two pairs of methine proton at  $\delta_H$  6.68 (2H, m, H-8, H-8') and  $\delta_H$  4.67 (2H, d,  $J = 4.0$  Hz, H-7, H-7'). two pairs of methylene proton at  $\delta_H$

4.22 (2H, dd,  $J = 9.2, 6.8$  Hz, Ha-9, Ha-9') and  $\delta_{\text{H}}$  3.84 (2H, Hb-9, Hb-9'). Four methoxy groups were suggested by a sharp singlet at  $\delta_{\text{H}}$  3.83 (12H, d, MeO-3, MeO-3', MeO-5, and MeO-5'). The  $^{13}\text{C}$ -NMR spectra and HSQC correlation of AF8 (Figures 76, 77 and Table 11) showed eight resonances including one signal methoxy groups, two methine carbon, three quaternary carbon and two signals oxygenated carbon at C-7/7' ( $\delta_{\text{C}}$  86.8) and C-9/9' ( $\delta_{\text{C}}$  72.3) that indicated the presence of a diepoxylignan skeleton (59) with two pairs of methoxy groups symmetrically in each ring.

The HMBC correlation of AF8 (Figure 78) revealed a correlation of C-7/7' ( $\delta_{\text{C}}$  86.8) to Ha-9/9', Hb-9/9', H-2/2' and H-6/6'. The positioning of the methoxy group was identified with correlation proton MeO-3/3' and MeO-5/5' to C-3/3' ( $\delta_{\text{C}}$  148.6) and C-5/5' ( $\delta_{\text{C}}$  146.8), respectively. This positioning was supported by the NOESY correlation of AF8 (Figure 79) which showed a correlation between H-2 to proton MeO-3 and H-6 to proton MeO-5.

From the above data NMR spectra identified that AF8 was syringaresinol. This compound was previously isolated from *Magnolia thailandica* (60) and in several *Dendrobium* such as *D. nobile*, *D. scundum*, and *D. heterocarpum* (53, 61, 62)



Syringaresinol [39]

**Table 11** NMR spectral data of compound AF8 and Syringaresinol

Position	AF8 (acetone- $d_6$ )		Syringaresinol (CDCl <sub>3</sub> ) (53)	
	$\delta_{\text{H}}$ (mult., $J$ in Hz)	$\delta_{\text{C}}$	$\delta_{\text{H}}$ (mult., $J$ in Hz)	$\delta_{\text{C}}$
1	-	113.2	-	132.1
2	6.68 (s)	104.4	6.59 (s)	102.8
3	-	148.6	-	147.2
4	-	136.2	-	134.4
5	-	148.6	-	147.2
6	6.68 (s)	104.4	6.59 (s)	102.8
7	4.67 (d, $J = 4.0$ Hz)	86.8	4.73 (d, $J = 4.3$ Hz)	86.0
8	3.09 (m)	55.3	3.10 (m)	54.3
9a	4.22 (dd, $J = 9.2, 6.8$ Hz)	72.3	4.28 (dd, $J = 8.8, 6.4$ Hz)	71.8
9b	3.84	72.3	3.92	71.8
1'	-	113.2	-	132.1
2'	6.68 (s)	104.4	6.59 (s)	102.8
3'	-	148.6	-	147.2
4'	-	136.2	-	134.4
5'	-	148.6	-	147.2
6'	6.68 (s)	104.4	6.59 (s)	102.8
7'	4.67 (d, $J = 4.0$ Hz)	86.8	4.73 (d, $J = 4.3$ Hz)	86.0
8'	3.09 (m)	55.3	3.10 (m)	54.3
9'a	4.22 (dd, $J = 9.2, 6.8$ Hz)	72.3	4.28 (dd, $J = 8.8, 6.4$ Hz)	71.8
9'b	3.84	72.3	3.92	71.8
MeO-3	3.83 (s)	56.6	3.89 (s)	56.4
MeO-5	3.82 (s)	56.6	3.89 (s)	56.4

MeO-3'	3.83 (s)	56.6	3.89 (s)	56.4
MeO-5'	3.82 (s)	56.6	3.89 (s)	56.4

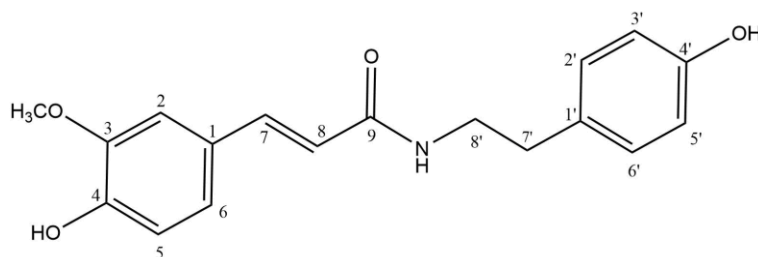
## 2.9. Identification of compound AF9

Compound AF9 was obtained as a brown amorphous solid. Molecular formula  $C_{18}H_{19}NO_4$  was suggested by HRESIMS of AF9 (Figure 81) in negative molecular ion  $[M-H]^-$  at  $m/z$  312.1232 (calcd. 312.1235). The  $^1H$ -NMR spectra of AF9 (Figure 82 and Table 12) showed five aromatic proton signals at  $\delta_H$  7.15 (d,  $J = 2.0$  Hz, H-2), 6.83 (d,  $J = 8.0$  Hz, H-5), 7.03 (dd,  $J = 8.0$  Hz, 2.0 Hz, H-6), 7.06 (d,  $J = 8.4$  Hz, H-2', H-6'), 6.75 (d,  $J = 8.4$  Hz, H-3', H-5'), Proton vicinal coupling trans position at  $\delta_H$  7.44 (d,  $J = 15.6$  Hz, H-7) and 6.50 (d,  $J = 15.6$  Hz, H-8), one proton methoxy group  $\delta_H$  3.88 (s), two proton methylene at  $\delta_H$  2.74 (t,  $J = 7.6$  Hz, H-7') and 3.48 (t,  $J = 7.6$  Hz, H-8'). The  $^{13}C$ -NMR spectra and HSQC correlation of AF9 (Figures 83, 84, 85, and Table 12) indicated sixteen signals including one signal methoxy group, two signals aliphatic methylene groups, five aromatic signals methine group, five signals aromatic quaternary carbon, two signals double carbon (trans), and a secondary amide.

The HMBC correlation (Figures 86, 87, and 88) showed the correlation of carbon from secondary amide C-9 ( $\delta_C$  166.3) with H-7, H-8 and H-8' that indicated the presence of phenylpropanoid amide skeleton. The positioning of the methoxy group was obtained from the correlation of C-3 ( $\delta_C$  149) with proton MeO-3. It was supported by the NOESY correlation (Figure 90) between H-2 and OMe-3.

Through the comparison from the above data spectroscopy, AF9 was known as *trans-n-feruloytyramine* (63). This compound was first isolated from *Cannabis*

*sativa* (64). *Trans-n-feruloytyramine* has a synonym as moupinamide and was reported as an anti-inflammatory in vitro study (65).



*trans-n-feruloytyramine* [40]

**Table 12** NMR spectral data of compound AF9 and *trans-n-feruloytyramine*

Position	AF9 (acetone- $d_6$ )		<i>trans-n-feruloytyramine</i> (CD <sub>3</sub> OD) (63)	
	$\delta_{\text{H}}$ (mult., $J$ in Hz)	$\delta_{\text{C}}$	$\delta_{\text{H}}$ (mult., $J$ in Hz)	$\delta_{\text{C}}$
1	-	128.3	-	128.2
2	7.15 (d, $J = 2.0$ Hz)	111.2	7.13 (d, $J = 1.2$ Hz)	111.5
3	-	149.0	-	149.3
4	-	148.6	-	149.8
5	6.83 (d, $J = 8.0$ Hz)	116.0	6.81 (d, $J = 8.5$ Hz)	116.4
6	7.03 (dd, $J = 8.0, 2.0$ Hz)	122.5	7.04 (dd, $J = 8.5, 1.2$ Hz)	123.2
7	7.44 (d, $J = 15.6$ Hz)	140.2	7.44 (d, $J = 15.6$ Hz)	142.0
8	6.50 (d, $J = 15.6$ Hz)	120.0	6.41 (d, $J = 15.5$ Hz)	118.7
9	-	166.3	-	169.2
1'	-	131.2	-	131.3
2'	7.06 (d, $J = 8.4$ Hz)	130.5	7.07 (d, $J = 8.4$ Hz)	130.7
3'	6.75 (d, $J = 8.4$ Hz)	116.0	6.73 (d, $J = 8.4$ Hz)	116.2

4'	-	156.7	-	156.9
5'	6.75 (d, $J = 8.4$ Hz)	116.0	6.73 (d, $J = 8.4$ Hz)	116.2
6'	7.06 (d, $J = 8.4$ Hz)	130.5	7.07 (d, $J = 8.4$ Hz)	130.7
7'	2.74 (t, $J = 7.6$ Hz)	35.0	2.76 (t, $J = 7.5$ Hz)	35.8
8'	3.48 (t, $J = 7.6$ Hz)	41.9	3.47 (t, $J = 7.5$ Hz)	42.5
MeO-3	3.88 (s)	56.2	3.85 (s)	56.4

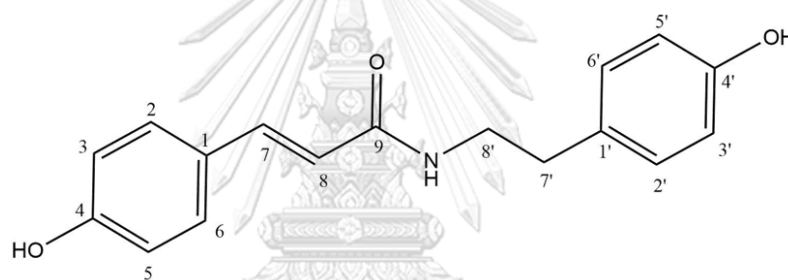
### 2.10. Identification of compound AF10

Compound AF10 was obtained as a white amorphous solid. Molecular formula  $C_{17}H_{17}NO_3$  was suggested by HRESIMS of AF9 (Figure 91) in negative molecular ion  $[M-H]^-$  at  $m/z$  282.1124 (calcd. 282.1130). The  $^1H$ -NMR spectra of AF10 (Figure 92, 93 and Table 13) showed the presence of four signals aromatic proton at  $\delta_H$  7.41 (d,  $J = 8.0$  Hz, H-2, H-6), 6.84 (d,  $J = 8.4$  Hz, H-3, H-5), 7.05 (d,  $J = 8.4$  Hz, H-2', H-6'), 6.75 (d,  $J = 8.4$  Hz, H-3', H-5'), Proton vicinal coupling trans position at  $\delta_H$  7.45 (d,  $J = 15.6$  Hz, H-7) and 6.47 (d,  $J = 15.6$  Hz, H-8), and two proton methylene at  $\delta_H$  2.74 (t,  $J = 7.2$  Hz, H-7') and 3.45 (t,  $J = 7.2$  Hz H-8'). The  $^{13}C$ -NMR spectra and HSQC correlation of AF9 (Figures 94, 95, 96, and Table 13) indicated thirteen signals including, two signals for aliphatic methylene groups, four aromatic signals for methine group, four signals for aromatic quaternary carbon, two signals for double carbon (trans), and a secondary amide. The data  $^1H$  and  $^{13}C$ -NMR indicated that AF10 is the same skeleton as AF9 without the methoxy group.

The HMBC correlation (Figures 98 and 100) revealed the correlation between carbon secondary amides C-9 ( $\delta_H$  166.4) with proton H-7, H-8, and H-8'. The

correlation of C-7' (35.7) to proton aromatic H-6' and H-2' (Figure 99) and the correlation C-7 (140.0) to another proton aromatic H-2 and H-6 was supported the phenylpropanoid amides skeleton.

Based on the above data NMR suggested that AF10 is *trans-n*-coumaroyl tyramine (63). It is a known compound and was isolated from *Capsicum annum*, *Dendrobium devonianum* and *Dendrobium moliniforme* (66, 67, 68). *Trans-n*-coumaroyl tyramine has the trivial name as paprazine and this constituent was reported as  $\alpha$ -glucosidase inhibitory activity and acetylcholinesterase (AChE) inhibitory activity (69, 70).



*trans-n*-coumaroyltyramine [41]

**Table 13** NMR spectral data of compound AF10 and *trans-n*-coumaroyltyramine

Position	AF10 (acetone- $d_6$ )		<i>trans-n</i> -coumaroyltyramine (CD <sub>3</sub> OD) (63)	
	$\delta_H$ (mult., $J$ in Hz)	$\delta_C$	$\delta_H$ (mult., $J$ in Hz)	$\delta_C$
1	-	127.8	-	127.7
2	7.41 (d, $J$ = 8.0 Hz)	130.1	7.41 (d, $J$ = 8.4 Hz)	130.5
3	6.84 (d, $J$ = 8.4 Hz)	116.5	6.80 (d, $J$ = 8.4 Hz)	116.2
4	-	160.0	-	160.5
5	6.84 (d, $J$ = 8.4 Hz)	116.5	6.80 (d, $J$ = 8.4 Hz)	116.2

6	7.41 (d, $J = 8.0$ Hz)	130.1	7.41 (d, $J = 8.4$ Hz)	130.5
7	7.45 (d, $J = 15.6$ Hz)	140.0	6.38 (d, $J = 15.5$ Hz)	141.8
8	6.47 (d, $J = 15.6$ Hz)	119.7	7.44 (d, $J = 15.5$ Hz)	118.4
9	-	166.4	-	169.2
1'	-	131.1	-	131.3
2'	7.05 (d, $J = 8.4$ Hz)	130.5	7.06 (d, $J = 8.6$ Hz)	130.7
3'	6.75 (d, $J = 8.4$ Hz)	116.0	6.73 (d, $J = 8.6$ Hz)	116.7
4'	-	156.7	-	156.9
5'	6.75 (d, $J = 8.4$ Hz)	116.0	6.73 (d, $J = 8.6$ Hz)	116.7
6'	7.05 (d, $J = 8.4$ Hz)	130.5	7.06 (d, $J = 8.6$ Hz)	130.7
7'	2.74 (t, $J = 7.2$ Hz)	35.7	2.75 (t, $J = 7.5$ Hz)	35.8
8'	3.45 (t, $J = 7.2$ Hz)	41.9	3.46 (t, $J = 7.5$ Hz)	42.5

## 2. Anti-neuroinflammatory activity of compounds from *Aerides falcata*

The isolated compounds that have sufficient weight (more than 1 mg) were evaluated for anti-neuroinflammatory activity following LPS-induced BV-2 microglia cells. the inhibition of NO from aerifalcatin [35] ( $IC_{50}$  value of  $0.87 \pm 0.45 \mu\text{M}$ ), 2,7-dihydroxy-3,4,6-trimethoxyphenanthrene [36] ( $IC_{50}$  value of  $2.47 \pm 0.73 \mu\text{M}$ ), agrostonin [32] ( $IC_{50}$  value of  $2.55 \pm 0.32 \mu\text{M}$ ), and syringaresinol [39] ( $IC_{50}$  value of  $1.40 \pm 0.17 \mu\text{M}$ ) showed strong activity when compared with positive control minocycline ( $IC_{50}$  value of  $3.41 \pm 0.30 \mu\text{M}$ ). the  $IC_{50}$  values were higher than the positive control shown from phenanthrene denthysinin [3] ( $IC_{50}$  value of  $8.99 \pm 0.91 \mu\text{M}$ ); 2,4-dimethoxy-3,7-dihydroxyphenanthrene [4] ( $IC_{50}$  value of  $12.56 \pm 1.30 \mu\text{M}$ ); 3,7-dihydroxy-2,4,6-trimethoxyphenanthrene [37] ( $IC_{50}$  value of  $21.92 \pm 3.70 \mu\text{M}$ ), *n*-



icosyl-*trans*-ferulate [38] ( $IC_{50}$  value of  $19.76 \pm 1.36 \mu M$ ), and *n-trans*-feruloytyramine [40] ( $IC_{50}$  value of  $18.62 \pm 9.56 \mu M$ ). (Table 14).

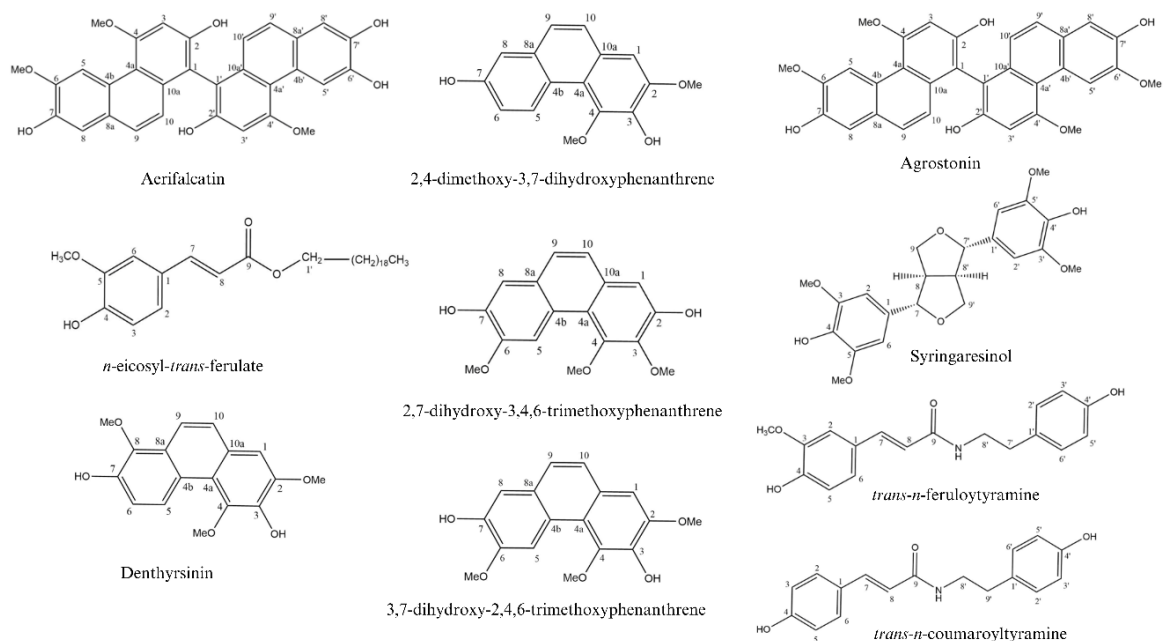


Figure 6 Isolated compounds from *Aerides falcate*

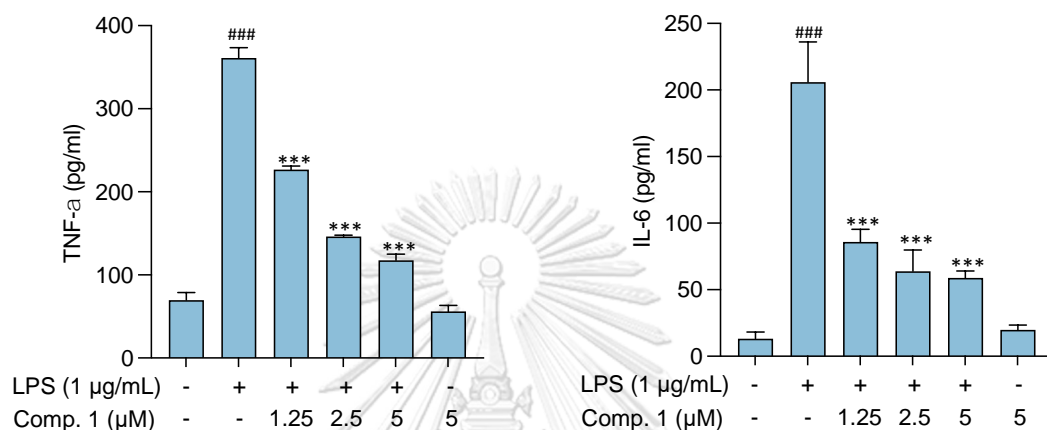
**Table 14** Effects of *Aerides falcata* constituents on LPS-stimulated NO release in BV-2 microglial cells.

Compound	IC <sub>50</sub> (mean $\pm$ SD) ( $\mu$ M)
Aerifalcatin [35]	0.87 $\pm$ 0.45
<i>n</i> -eicosyl- <i>trans</i> -ferulate [38]	19.76 $\pm$ 1.36
Denthyrsinin [3]	8.99 $\pm$ 0.91
2,4-dimethoxy-3,7-dihydroxyphenanthrene [4]	12.56 $\pm$ 1.30
2,7-dihydroxy-3,4,6-trimethoxyphenanthrene [36]	2.47 $\pm$ 0.73
3,7-dihydroxy-2,4,6-trimethoxyphenanthrene [37]	21.92 $\pm$ 3.70
Agrostonin [32]	2.55 $\pm$ 0.32
Syringaresinol [39]	1.40 $\pm$ 0.17
<i>trans-n</i> -feruloytyramine [40]	18.62 $\pm$ 9.56
Minocycline	3.41 $\pm$ 0.30

The cytokine levels were obtained for the active compounds that showed lower inhibition of NO compared to positive control minocycline. Aerifalcatin [35], 2,7-dihydroxy-3,4,6-trimethoxyphenanthrene [36], agrostonin [32], and syringaresinol [39] significantly reduce the expression of proinflammatory cytokines, TNF- $\alpha$ , and IL-6 in activated microglia, suggesting their potential as anti-neuroinflammatory agents (Figure 6). These active compounds can reduce cytokine levels along with increasing the concentration. Aerifalcatin [35] was performed as the most potent compound because it reduced significantly ( $p > 0.001$ , LPS vs low concentration) at both TNF- $\alpha$ , and IL-6. Whereas 2,7-dihydroxy-3,4,6-trimethoxyphenanthrene [36] reduces significantly both cytokine levels ( $p > 0.001$ , at LPS vs middle concentration), agrostonin [32] reduces significantly TNF- $\alpha$  levels ( $p > 0.05$ , at LPS vs middle

concentration) and IL-6 levels ( $p > 0.001$ , at LPS vs low concentration), and syringaresinol [39] reduces significantly TNF- $\alpha$  levels ( $p > 0.01$ , at LPS vs middle concentration) and IL-6 levels ( $p > 0.01$ , at LPS vs low concentration)

#### Aerifalcatin [35]



#### 2,7-dihydroxy-3,4,6-trimethoxyphenanthrene [36]

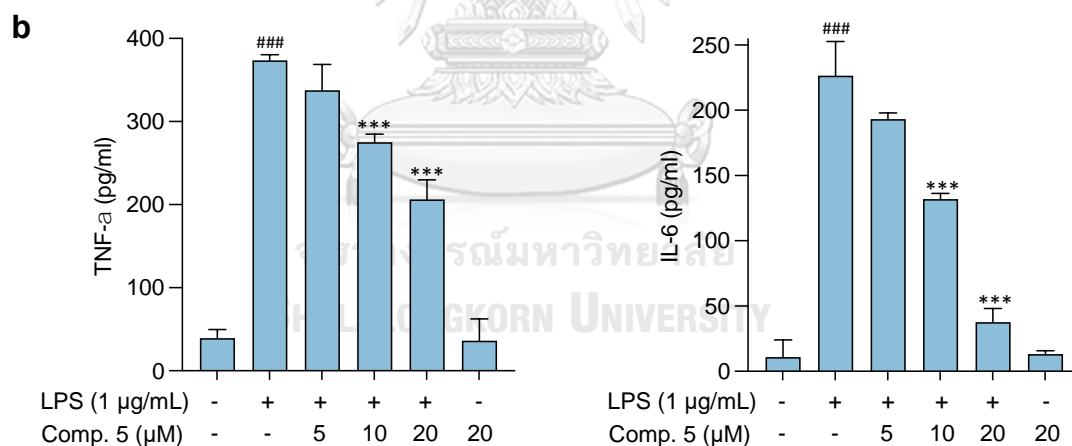
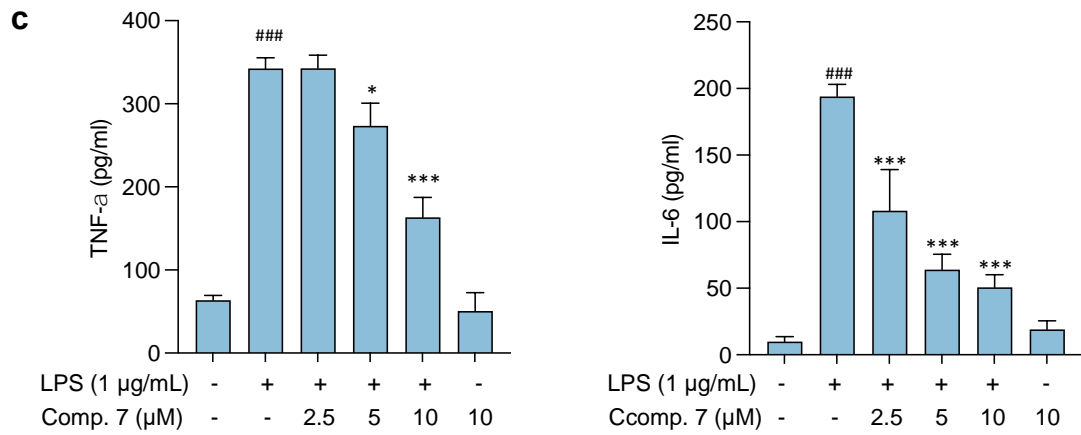


**Figure 7.** Effects of active compounds on cytokine release in LPS-stimulated BV-2 microglial cells.

Data are presented as mean  $\pm$  SD,  $n = 3$ . <sup>###</sup>  $p < 0.01$ , control (0.5% DMSO) vs. LPS groups. \* $p < 0.05$ , \*\* $p < 0.01$ , \*\*\* $p < 0.01$ , LPS vs compound-treated groups. Statistical difference between groups was analyzed using one-way ANOVA followed by Bonferroni post hoc test.

## Agrostonin [32]



## Syringaresinol [39]

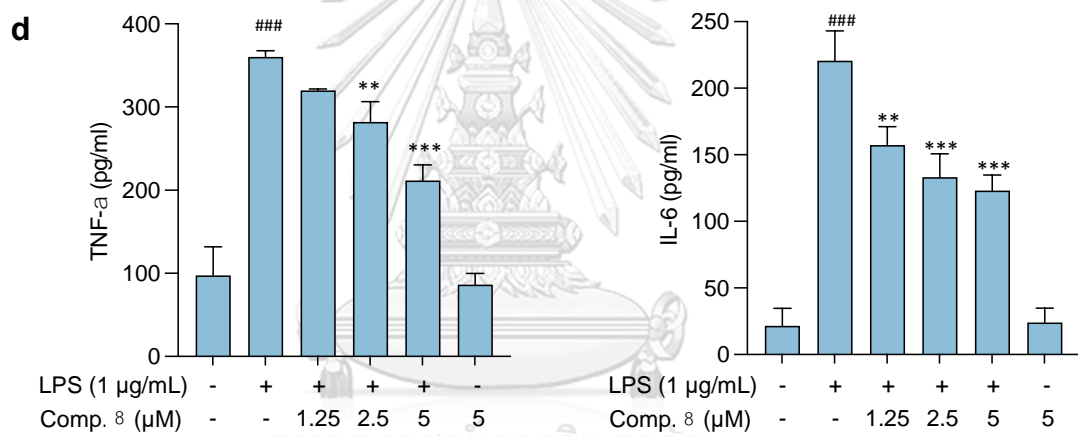


Figure 7 (Continued)

## CHAPTER V

### CONCLUSION

In this study, ten compounds were isolated from *Aerides falcata*, including a new compound called aerifalcatin [35] and nine known compounds, namely *n*-eicosyl-*trans*-ferulate [39], denthysinin [3], 2,4-dimethoxy-3,7-dihydroxyphenanthrene [4], 2,7-dihydroxy-3,4,6-trimethoxyphenanthrene [36], 3,7-dihydroxy-2,4,6-trimethoxyphenanthrene [37], agrostonin [32], syringaresinol [38], *trans*-*n*-feruloyltyramine [40], and *trans*-*n*-coumaroyltyramine [41]. All these isolated compounds were evaluated for anti-neuroinflammatory activity except *trans*-*n*-coumaroyltyramine due to lack of weight. The neuroinflammatory modulator, Minocycline, was performed for comparison as a positive control. *In vitro* testing on LPS-induced BV2 microglia cells was performed to evaluate their potential as anti-neuroinflammatory agents. Four compounds, including aerifalcatin [35], 2,7-dihydroxy-3,4,6-trimethoxyphenanthrene [36], agrostonin [32], and syringaresinol [39], showed strong activity in inhibiting the production of NO, although their potency was lower than that of minocycline, the positive control. These active compounds were further tested for their ability to inhibit proinflammatory cytokines TNF- $\alpha$  and IL-6 and were found to significantly reduce their expression in activated microglia, indicating their potential as anti-neuroinflammatory agents. Additionally, these active compounds were found to reduce cytokine levels while increasing their concentration.

In summary, this study investigated the chemical and biological properties of secondary metabolites found in *Aerides falcata*. The findings on the compounds' effects on neuroinflammatory activity can be beneficial in developing new anti-neuroinflammatory drugs from natural sources in the future

## REFERENCES



จุฬาลงกรณ์มหาวิทยาลัย  
**CHULALONGKORN UNIVERSITY**

1. Barcelos IP, and Troxell RM, Graves JS. Mitochondrial dysfunction and multiple sclerosis. *Biology (Basel)*. 2019;8(2):37
2. Li T, Lu L, Pember E, Li, X, Zhang B, and Zhu Z. New insights into neuroinflammation involved in pathogenic mechanism of Alzheimer's disease and its potential for therapeutic intervention. *Cells*. 2022; 11(12):1925
3. Kwon HS, and Koh SH. Neuroinflammation in neurodegenerative disorders: the roles of microglia and astrocytes. *Translational Neurodegeneration*. 2020;9(1):42.
4. Gao P, Tang S, Chen H, Zhou X, Ou Y, Shen R, and He Y. Preconditioning increases brain resistance against acute brain injury via neuroinflammation modulation. *Experimental Neurology*. 2021;341:113712
5. Serna-Rodriguez MF, Bernal-Vega S, de la Barquera JAO, Camacho-Morales A, and Perez-Maya AA. The role of damage associated molecular pattern molecules (DAMPs) and permeability of the blood-brain barrier in depression and neuroinflammation. *Journal of Neuroimmunology*. 2022;371:577951.
6. Zhu X, Huang HH, and Zhao L. PAMPs and DAMPs as the bridge between periodontitis and atherosclerosis: the potential therapeutic targets. *Frontiers in Cell Development Biology*. 2022;10:856118.

7. Jäkel S, and Dimou, L. Glial cells and their function in the adult brain: a journey through the history of their ablation. *Frontiers in Cellular Neuroscience* 2017;11:24.
8. Cho IKH. Microglia and macrophages in central nervous systems. *Recent Advancements in Microbial Diversity Academic press*; 2022. p. 185-208.
9. Szepesi Z, Manouchehrian O, Bachiller S, and Deierborg T. Bidirectional Microglia-Neuron communication in health and disease. *Frontier in Cellular Neuroscience*. 2018;12:323.
10. Donnelly C, Chen O, and Ji R. How do sensory neurons sense danger signals? *Trends in Neurosciences*. 2020;43(10):822-838.
11. Jurga AM, Paleczna M, and Kuter KZ. Overview of general and discriminating markers of differential microglia phenotypes. *Frontiers in Cellular Neuroscience*. 2020;14:198.
12. Cai Z, Hussain MD, and Yan LJ. Microglia, neuroinflammation, and beta-amyloid protein in Alzheimer's disease. *International Journal of Neuroscience*. 2014;124(5):307-321.
13. Harukawa K, Ikegami A, Tachibana Y, Ohno N, Konishi H, Hashimoto A, Matsumoto M, Kato D, Ono R, Kiyama H, Moorhouse AJ, Nabekura J, and Wake H. Dual microglia effects on blood-brain barrier permeability induced by systemic inflammation. *Nature Communications*. 2019;10:5816.



14. Kaur N, Chugh H, Sakharkar MK, Dhawan U, Chidambaram SB, and Chandra R. Neuroinflammation mechanisms and phytotherapeutic intervention: a systematic review. *ACS Chemical Neuroscience*. 2020;11(22):3707-31.
15. Kolliker-Frers R, Udovin L, Otero-Losada M, Kobiec T, Herrera MI, Palacios J, et al. Neuroinflammation: an integrating overview of reactive-neuroimmune cell interactions in health and disease. *Mediators of Inflammation*. 2021;2021:9999146.
16. Werneburg S, Jung J, Kunjamma RB, Ha S, Luciano NJ, Willis CM, Gao G, Biscola NP, Havton LA, Crocker SJ, Popko B, Reich DS, and Schafer DP. targeted complement inhibition at synapses prevents microglial synaptic engulfment and synapse loss in demyelinating disease. *Immunity*. 2019;52(1):167-182.
17. Mathew E, Kim E, and Zempsky W. Pharmacologic treatment of pain. *Seminars in Pediatric Neurology*. 2016;23(3):209-219.
18. Ajmone-Cat MA, Bernardo A, Greco A, and Minghetti L. Non-steroidal anti-inflammatory drugs and brain inflammation: effects on microglial functions. *Pharmaceuticals (Basel)*. 2010;3(6):1949-1965.
19. Boettger MK, Weber K, Gajda M, Bräuer R, and Schaible H. Spinally applied ketamine or morphine attenuates peripheral inflammation and hyperalgesia in acute and chronic phases of experimental arthritis. *Brain, Behavior, immunity*. 2010;24(3):474-485.

20. Auriel E, Regev K, and Korczyn AD. Nonsteroidal anti-inflammatory drugs exposure and the central nervous system. *Handbook of Clinical Neurology*. 2014;119:577-584.
21. Mohamed HM, and Mahmoud AM. Chronic exposure to the opioid tramadol induces oxidative damage, inflammation and apoptosis, and alters cerebral monoamine neurotransmitters in rats. *Biomedicine & Pharmacotherapy*. 2019;110:239-247.
22. Djordjević V, and Tsiftsis, S. The Role of ecological factors in distribution and abundance of terrestrial orchids. In: Merillon J, Kodja, H, editor. *Orchids Phytochemistry, Biology and Horticulture*: Springer; 2019. p. 1-71.
23. Kirillova IA, Dubrovskiy YA, and Novakovskiy AB. Ecological and habitat ranges of orchids in the northernmost regions of their distribution areas: A case study from Ural Mountains, Russia. *Plant Diversity*. 2022;4(2):211-218.
24. Hossain MM. Therapeutic orchids: traditional uses and recent advances--an overview. *Fitoterapia*. 2011;82(2):102-140.
25. Gantait S, Das A, Mitra M, and Chen J. Secondary metabolites in orchid: Biosynthesis, medicinal uses, and biotechnology. *South African Journal of Botany*. 2021;139:338-351.
26. Thant MT, Sritularak B, Chatsumpun N, Mekboonsonglarp W, Punpreuk Y, and Likhitwitayawuid K. Three novel biphenanthrene derivatives and a new

- phenylpropanoid ester from *Aerides multiflora* and their  $\alpha$ -glucosidase inhibitory activity. *Plants*. 2021;10:385-399.
27. Lv S, Fu Y, Chen J, and Chen S. Six phenanthrenes from the roots of *Cymbidium faberi* Rolfe. and their biological activities. *Natural Product Research*. 2020;5(36):1170-1181.
28. Schuster R, Zeindl L, Holzer W, Khumpirapang N, Okonogi S, Viernstein H, and Mueller M. *Eulophia macrobulbon* is an orchid with significant anti-inflammatory and antioxidant effects and anticancerogenic potential exerted by its root extract. *Phytomedicine*. 2016; 24(2017):157-165.
29. Simmler C, Antheaume C, and Lobstein A. Antioxidant biomarkers from *Vanda coerulea* stems reduce irradiated HaCaT PGE-2 production as a result of COX-2 inhibition. *PLoS One*. 2010;5(10):1-9.
30. Hasriadi, Wasana PWD, Sritularak B, Vajragupta O, Rojsitthisak P, and Towiwat P. Batatasin III, a Constituent of *Dendrobium scabrilingue*, Improves Murine Pain-like Behaviors with a Favorable CNS Safety Profile. *Journal of Natural Product*. 2022;85(7):1816-1825.
31. Li B, Liu H, Zhang D, Lai X, Liu B, Xu X, et al. Three new bioactive phenolic glycosides from *Liparis odorata*. *Natural Product Research*. 2014;28(8):522-529.
32. Timmerman R, Burm SM, and Bajramovic JJ An overview of in vitro method to study microglia. *Frontiers in Cellular Neuroscience*. 2018;12:242.

33. Stansley B, Post J, and Hensley K. A comparative review of cell culture systems for the study of microglial biology in Alzheimer's disease. *Journal of Neuroinflammation*. 2012;9:115.
34. Pant B. Medicinal orchids and their uses: Tissue culture a potential alternative for conservation. *African Journal of Plant Science* 2013;7(10):448-467.
35. Lawler LJ. *Ethnobotany of the Orchidaceae*. Arditti J, editor. Ithaca: Cornell University Press; 1984.
36. Gutiérrez RMP. Orchids: A review of uses in traditional medicine, its phytochemistry and pharmacology. *Journal of Medicinal Plants Research*. 2010;4(8):592-638.
37. Kocyan A, Vogel EF, Conti E, and Gravendeel B. Molecular phylogeny of *Aerides* (Orchidaceae) based on one nuclear and two plastid markers: a step forward in understanding the evolution of the Aeridinae. *Molecular Phylogenetics and Evolution*. 2008;48(2):422-443.
38. Smith MJ, Brodie C, Kowalczyk J, Michnowicz S, McGough HL, and Roberts JA. Cites orchid checklist, for the genera: *Aerides*, *Coelogyne*, *Comparettia* and *Masdevallia*. Kew: Royal Botanic Gardens; 2006.
39. Katta J, Rampilla V, and Khasim SM. A study on phytochemical and anticancer activities of epiphytic orchid *Aerides odorata* Lour. *European Journal of Medicinal Plant*. 2019; 28(23):1-21.

40. Sopalun K, and Lamtham S. Isolation and screening of extracellular enzymatic activity endophytic fungi isolated from thai orchids. *South African Journal of Botany*. 2020;134:273-279.
41. Teoh ES. *Medicinal orchid in Asia*: Springer; 2016.
42. Averyanov LV, Truong BV, Nguyen VC, Nguyen KS, and Maisak TV. New orchids (Orchidaceae) in the flora of Vietnam II. *Vandaeae*. *Taiwania*. 2019;64(3):285-98.
43. Motes M, Leon MDL, Cootes J, and Cabactulan D. A spectacular new species of *Aerides* (Orchidaceae) from the Philippines. *Orchideen Journal*. 2020;8(1):1-6.
44. Anuradha V, and Rao NP. Aeridin: A phenanthopyran from *Aerides crispum*. *Phytochemistry*. 1998;48(1):602-606.
45. Cakova V, Urbain A, Antheaume C, Rimlinger N, Wehrung P, Bonté F, and Lobstein A. Identification of phenanthrene derivatives in *Aerides rosea* (Orchidaceae) using the combined system HPLC-ESI-RMS/MS and HPLC-DAD-MS-SPE-UV-NMR. *Phytochemical Analysis*. 2015;26(1):34-39.
46. Thant MT, Chatsumpun N, Mekboonsonglarp W, Sritularak B, and Likhitwitayawuid K. New fluorene derivatives from *Dendrobium gibsonii* and their  $\alpha$ -glucosidase inhibitory activity. *Molecules*. 2020;25(21):4931.

47. Liu L, Yin QM, Zhang XW, Wang W, Dong XY, Yan X, and Hu R. Bioactivity-guided isolation of biphenanthrenes from *Liparis nervosa*. *Fitoterapia*. 2016;115:15-18.
48. Baldé AM, Claeys M, Pieters LA, Wray V, and Vlietinck AJ. Ferulic acid esters from stem bark of *Pavetta owariensis*. *Phytochemistry*. 1991;30(3):1024–1026.
49. Rwegoshora F, Mabiki F, Machumi F, Chacha M, Styryshave B, and Cornett C. Isolation and toxicity evaluation of feruloyl ester and other triterpenoids from *Synadenium glaucescens* Pax. *The Journal of Phytopharmacology*. 2022;11(5):347–352.
50. San HT, Boonsongcheep P, Putalun W, Mekboonsonglarp W, Sritularak B, and Likhitwitayawuid K.  $\alpha$ -Glucosidase inhibitory and glucose uptake stimulatory effects of phenolic compounds from *Dendrobium christyanum*. *Natural Product Communications*. 2020;15(3).
51. Chang SJ, Lin TH, and Chen CC. Constituents from the stems of *Dendrobium clavatum* var. *aurantiacum*. *Journal Chinese Medicine*. 2001;12(3):211–218.
52. Woo KW, Park JE, Choi SU, Kim KH, and Lee KR. Phytochemical constituents of *Bletilla striata* and their cytotoxic activity. *Natural Product Sciences*. 2014;20(2):91–94.
53. Ono M, Ito Y, Masuoka C, Koga H, and Nohara T. Antioxidative constituents from *Dendrobii Herba* (Stems of *Dendrobium* spp.). *Food Science and Technology*. 1995;1(2):15-20.

54. Wu YP, Liu WJ, Zhong WJ, Chen YJ, Chen DN, He F, and Jiang L. Phenolic compounds from the stems of *Flickingeria fimbriata*. *Natural Product Research*. 2017 31(13):1518–1522.
55. Jiangmiao Hu WF, Fawu Dong, Zehong Miao, Jun Zhou. Chemical components of *Dendrobium chrysotoxum*. *Chinese Journal of Chemistry*. 2012;30(6):1327–1330.
56. Apel C, Dumontet V, Lozach O, Meijer L, Guéritte F, and Litaudon M. Phenanthrene derivatives from *Appendicula reflexa* as new CDK1/cyclin B inhibitors. *Phytochemistry Letters*. 2012;5(4):814–818.
57. Letcher RM, and Nhamo LRM. Chemical constituents of the combretaceae. Part III. Substituted phenanthrenes, 9,10-dihydrophenanthrenes, and bibenzyls from the heartwood of *Combretum psidioides*. *Journal of the Chemical Society, Perkin Transactions 1*. 1972: 2941-2946
58. Majumder PL, Banerjee S, Lahiri S, Mukhoti N, and Sen S. Dimeric phenathrenes from two *Agrostophyllum* species. *Phytochemistry*. 1998;47(5):855–860.
59. Susilawati S, Matsjeh S, Pranowo HD, and Anwar C. Macronone, a novel diepoxylican from bark of mahkota dewa (*Phaleria macrocarpa* (Scheff.) Boerl.) and its antioxidant activity. *Indonesian Journal of Chemistry*. 2012;12(1):62-69.

60. Monthong W, Pitchuanom S, Nuntasen N and Pompimon W. (+)-Syringaresinol lignan from new species *Magnolia Thailandica*. *American Journal of Applied Sciences*. 2011;8(12):1268–1271.
61. Sritularak B, Duangrak N, and Likhitwitayawuid K. A New Bibenzyl from *Dendrobium secundum*. *Zeitschrift fur Naturforschung*. 2011;66(5-6):205-208.
62. Warinhomhoun S, Khine HEE, Sritularak B, Likhitwitayawuid K, Miyamoto T, Tanaka C, Punsawad C, Punpreuk Y, Sungthong R, and Chaotham C. Secondary metabolites in the *Dendrobium heterocarpum* methanolic extract and their impacts on viability and lipid storage of 3t3-l1 pre-adipocytes. *Nutrients*. 2022;14(14):2886.
63. Al-Taweel AM, Perveen S, El-Shafae AM, Fawzy GA, Malik A, Afza N, and Iqbal L, Latif M. Bioactive phenolic amides from *Celtis africana*. *Molecules*. 2012;17(3):2675–2682.
64. Yamamoto I, Matsunaga T, Kobayashi H, Watanabe K, and Yoshimura H. Analysis and pharmacotoxicity of feruloyltyramine as a new constituent and p-coumaroyltyramine in *Cannabis sativa* L. *Pharmacology Biochemistry and Behavior*. 1991;40(3):465–469.
65. Aswad M, Rayan M, Abu-Lafi S, Falah M, Raiyn J, Abdallah Z, and Rayan A. Nature is the best source of anti-inflammatory drugs: indexing natural products for their anti-inflammatory bioactivity. *Inflammation Research*. 2018;67(1):67–75.



66. Chen CY, Yeh YT, and Yang WL. Amides from the Stem of *Capsicum annuum*. *Natural Product Communications* 2011;6(2):227-226.
67. Sun J, Zhang F, Yang M, Zhang J, Chen L, Zhan R, Li L, and Chen Y. Isolation of  $\alpha$ -glucosidase inhibitors including a new flavonol glycoside from *Dendrobium devonianum*. *Natural Product Research*. 2014;28(21):1900–1905.
68. Zhao N, Yang G, Zhang Y, Chen L, and Chen Y. A new 9,10-dihydrophenanthrene from *Dendrobium moniliforme*. *Natural Product Research*. 2016;30(2):174–179.
69. Kim DK, and Lee K. Inhibitory effect of *trans-n-p*-coumaroyl tryamine from the twigs of *Celtis chinensis* on the acetylcholinesterase. *Archives of Pharmacal Research* 2003;26(9):735–738.
70. Nishioka T, Watanabe J, Kawabata J, and Niki R. Isolation and Activity of *n-p*-coumaroyltyramine, an  $\alpha$ -glucosidase inhibitor in welsh onion (*Allium fistulosum*). *Bioscience, Biotechnology, and Biochemistry*. 1997;61(7):1138–



● Data compound AF1

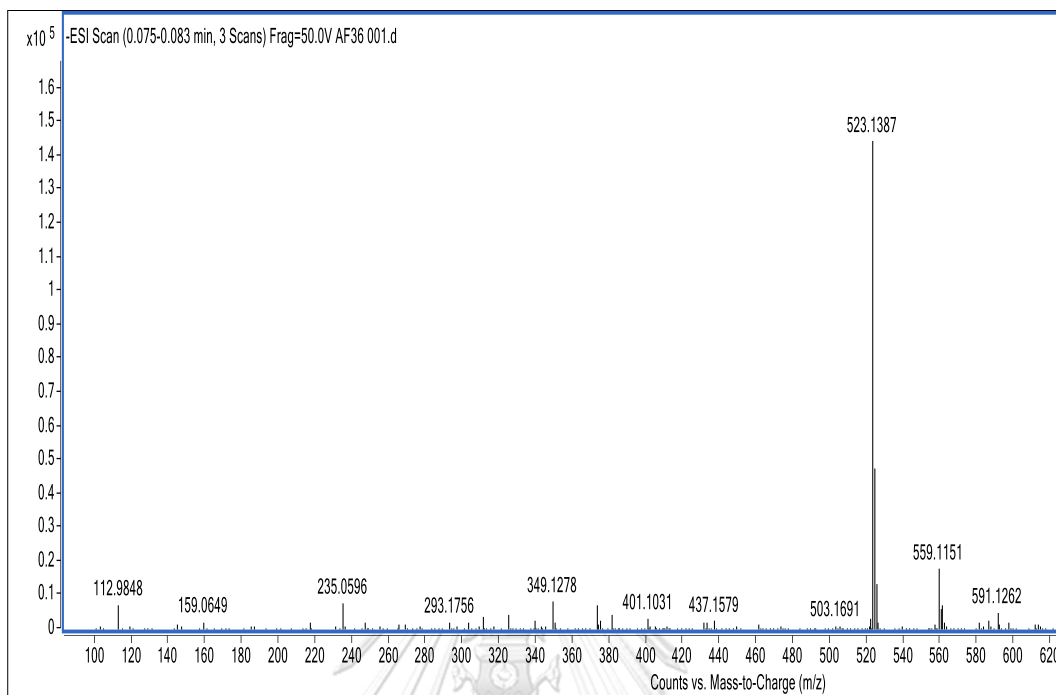


Figure 8 Mass spectrum of compound AF1

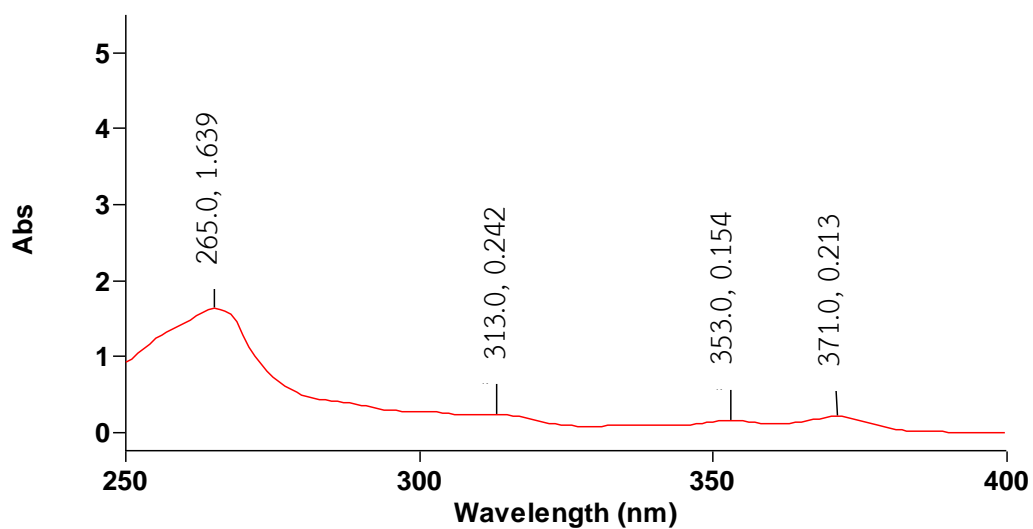


Figure 9 UV spectrum of compound AF1

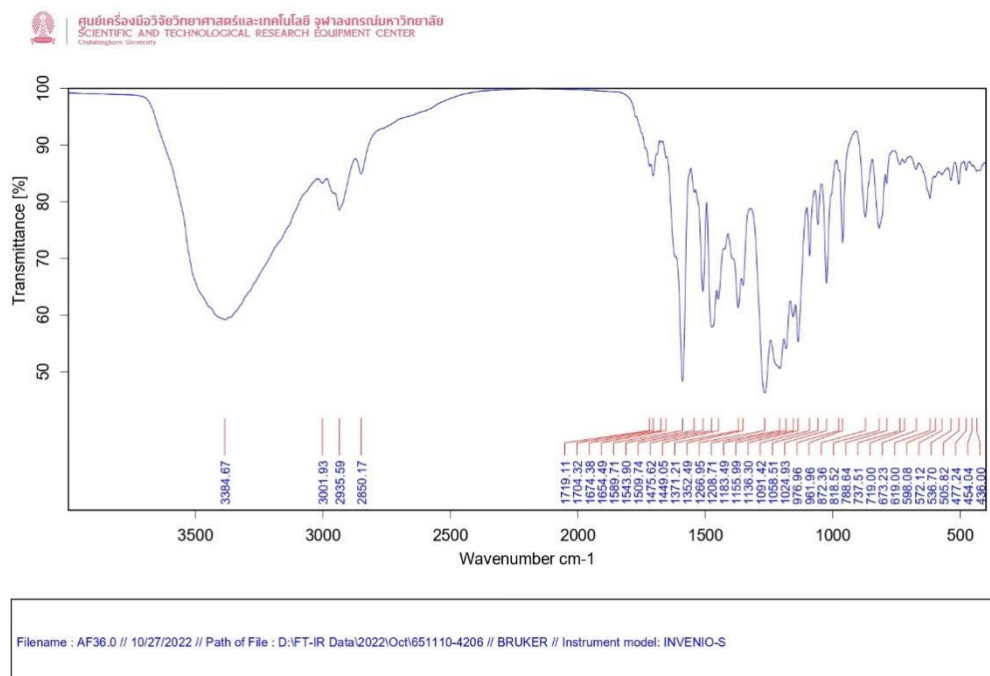


Figure 10 FT-IR spectrum of compound AF1

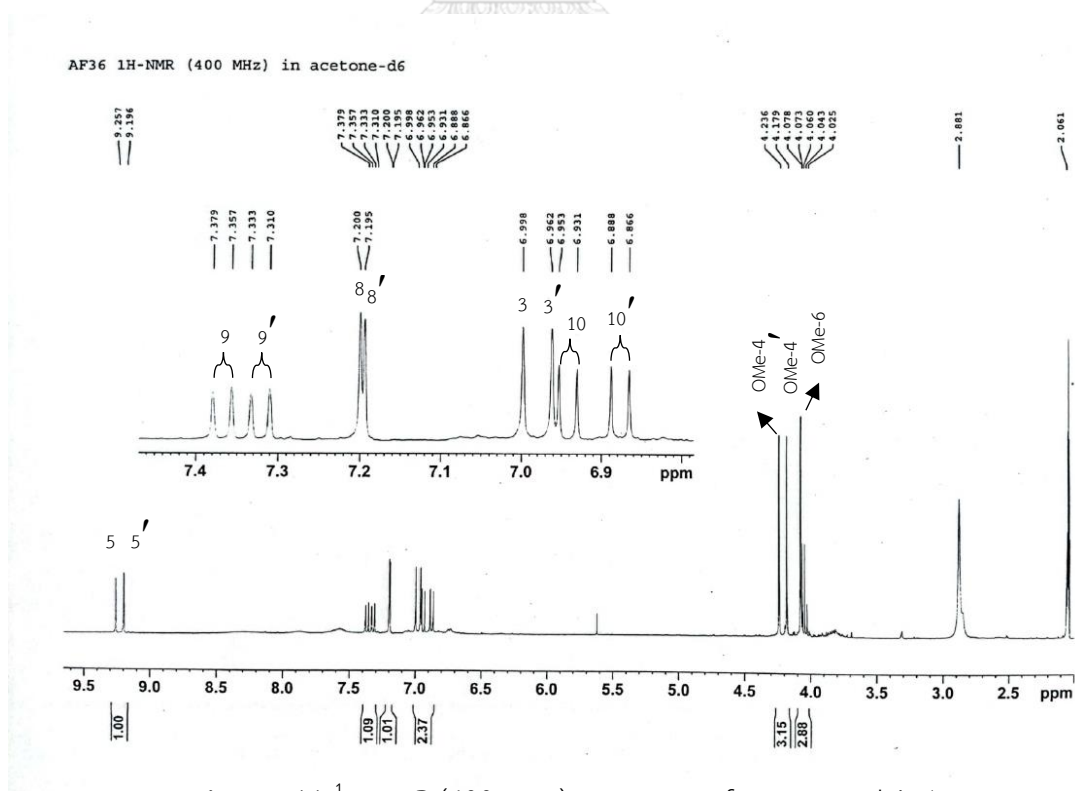


Figure 11 <sup>1</sup>H-NMR (400 MHz) spectrum of compound AF1

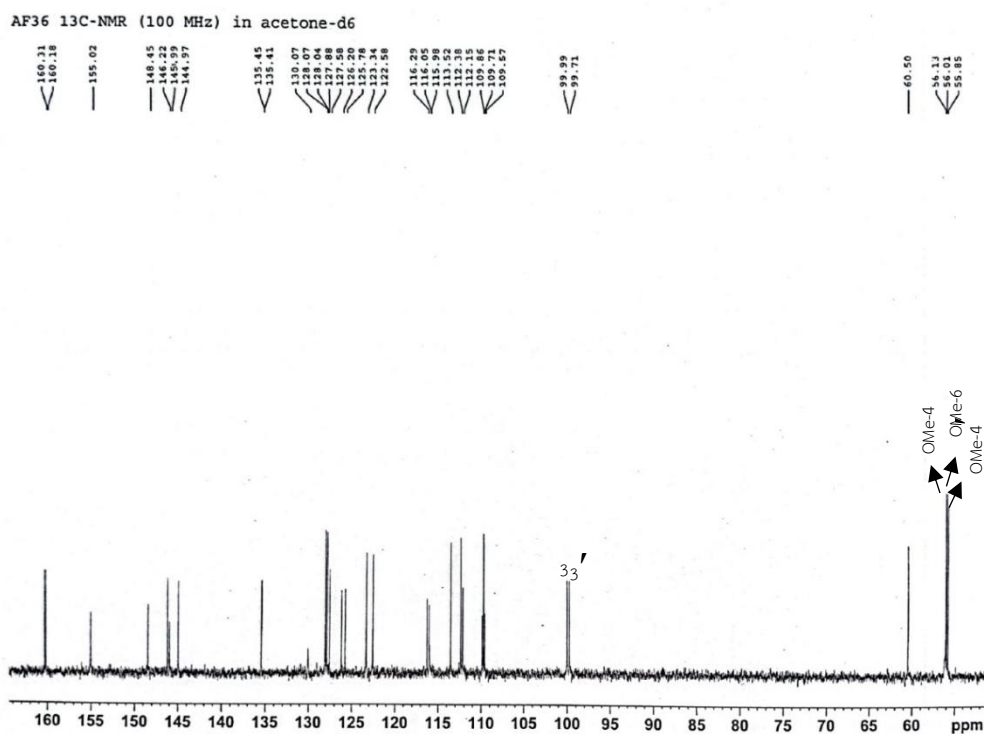


Figure 12  $^{13}\text{C-NMR}$  (100 MHz) spectrum of compound AF1

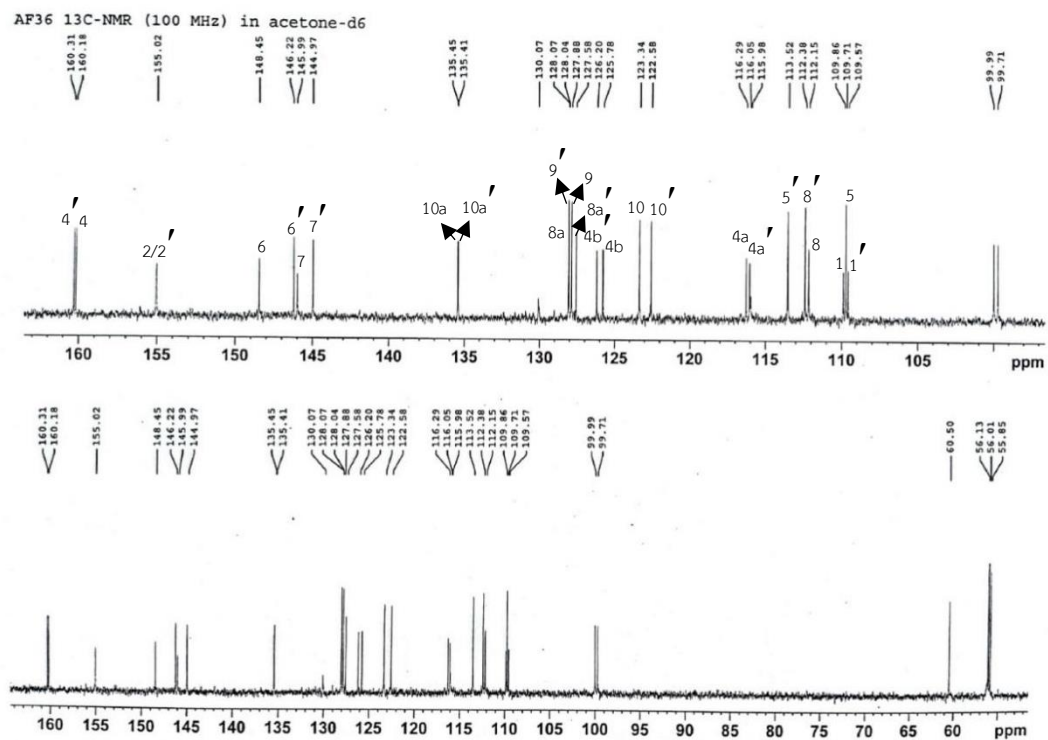


Figure 13  $^{13}\text{C-NMR}$  (100 MHz) spectrum of compound AF1 (55-165 ppm)

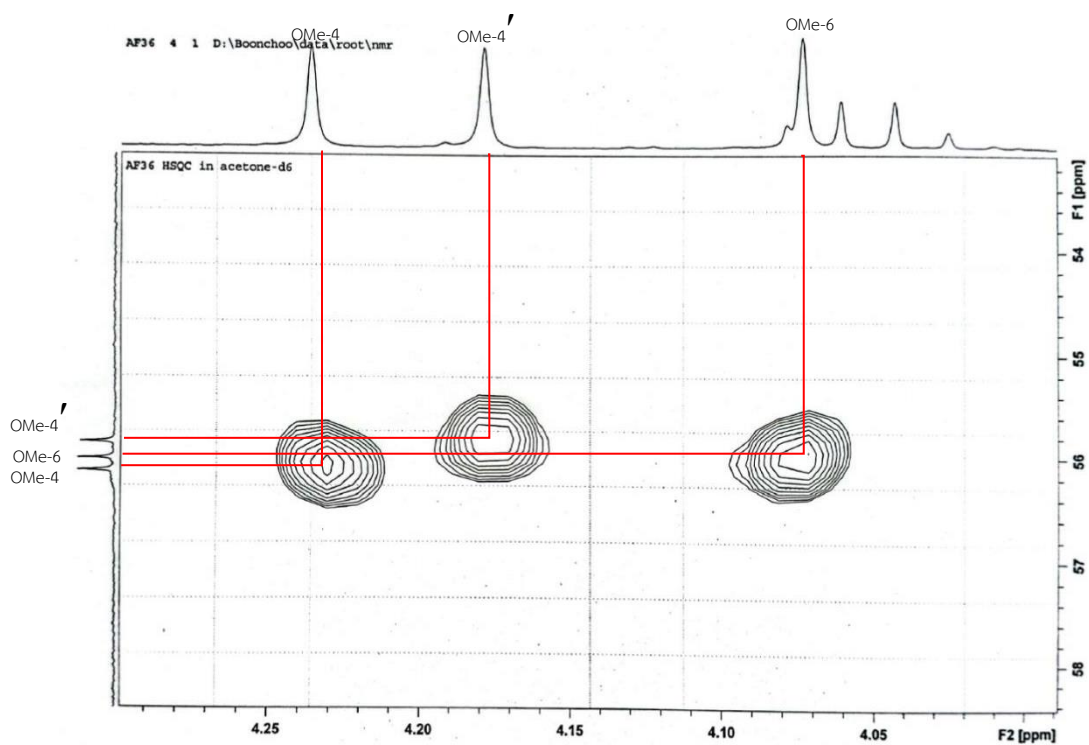


Figure 14 HSQC spectrum of compound AF1 (3.99-4.30 ppm and 53-58 ppm)

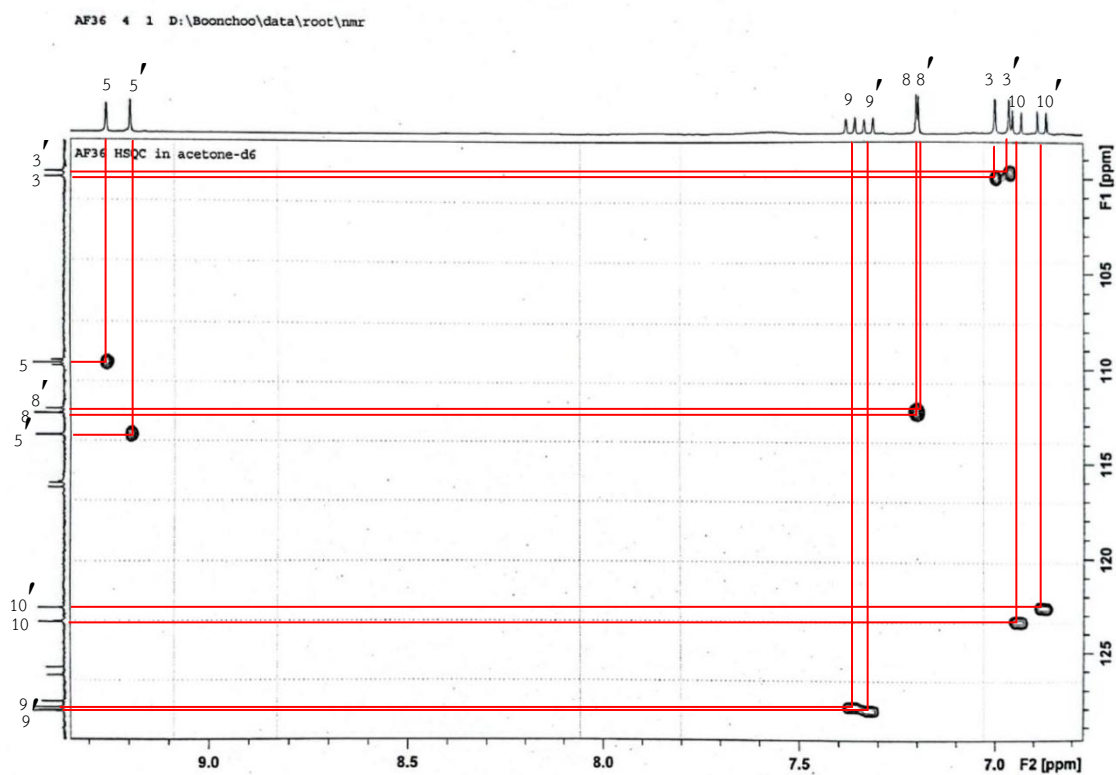


Figure 15 HSQC spectrum of compound AF1 (6.8-9.3 ppm and 99-129 ppm)

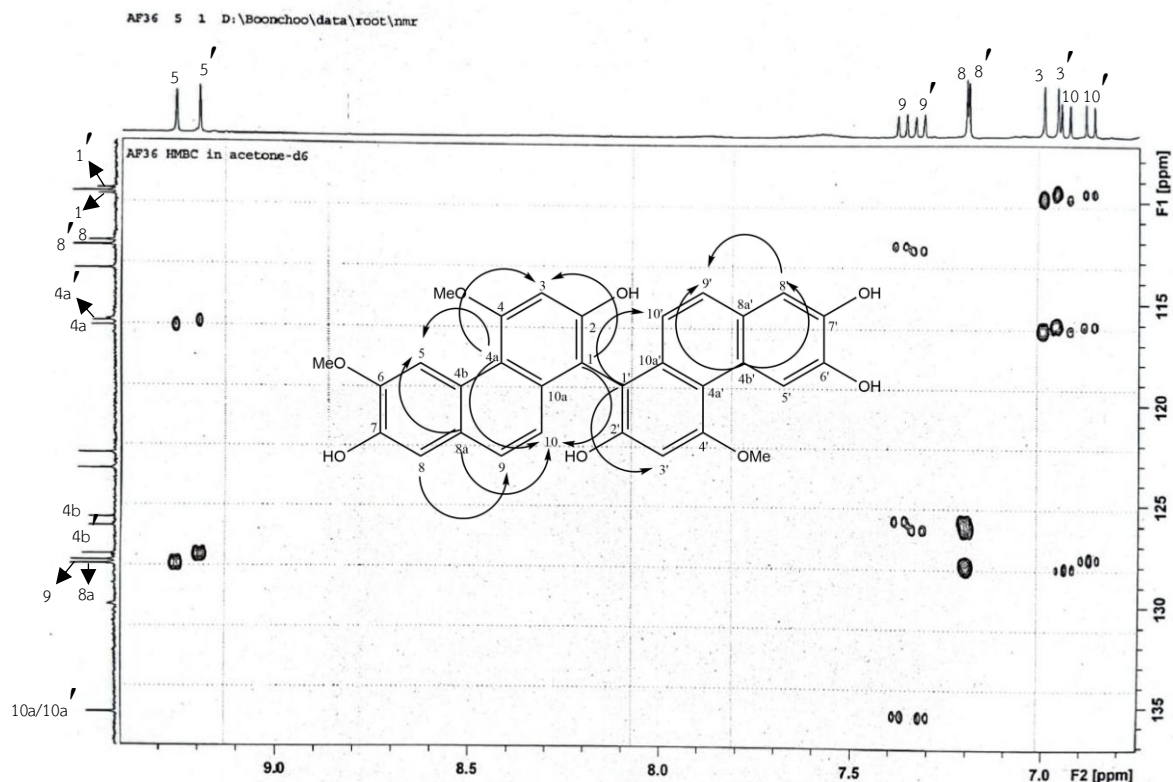


Figure 16 HMBC spectrum of compound AF1 (6.8-9.3 ppm and 108-136 ppm)

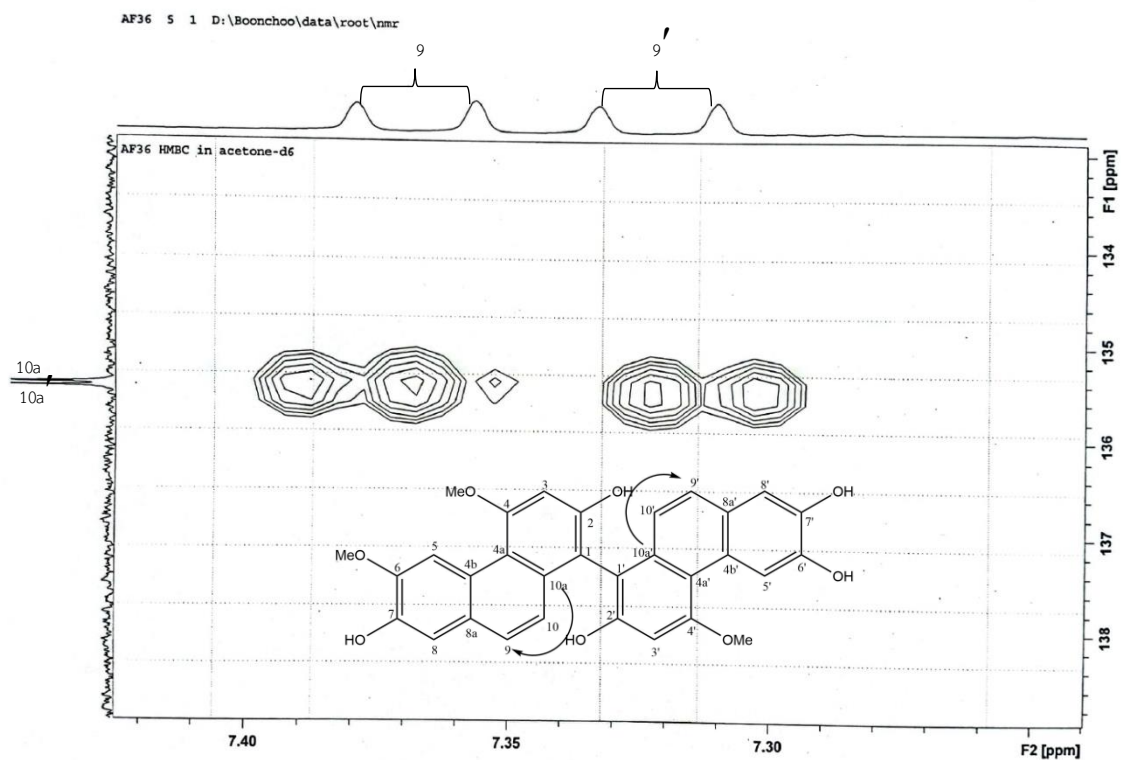


Figure 17 HMBC spectrum of compound AF1 (7.24-7.42 ppm and 133-139 ppm )



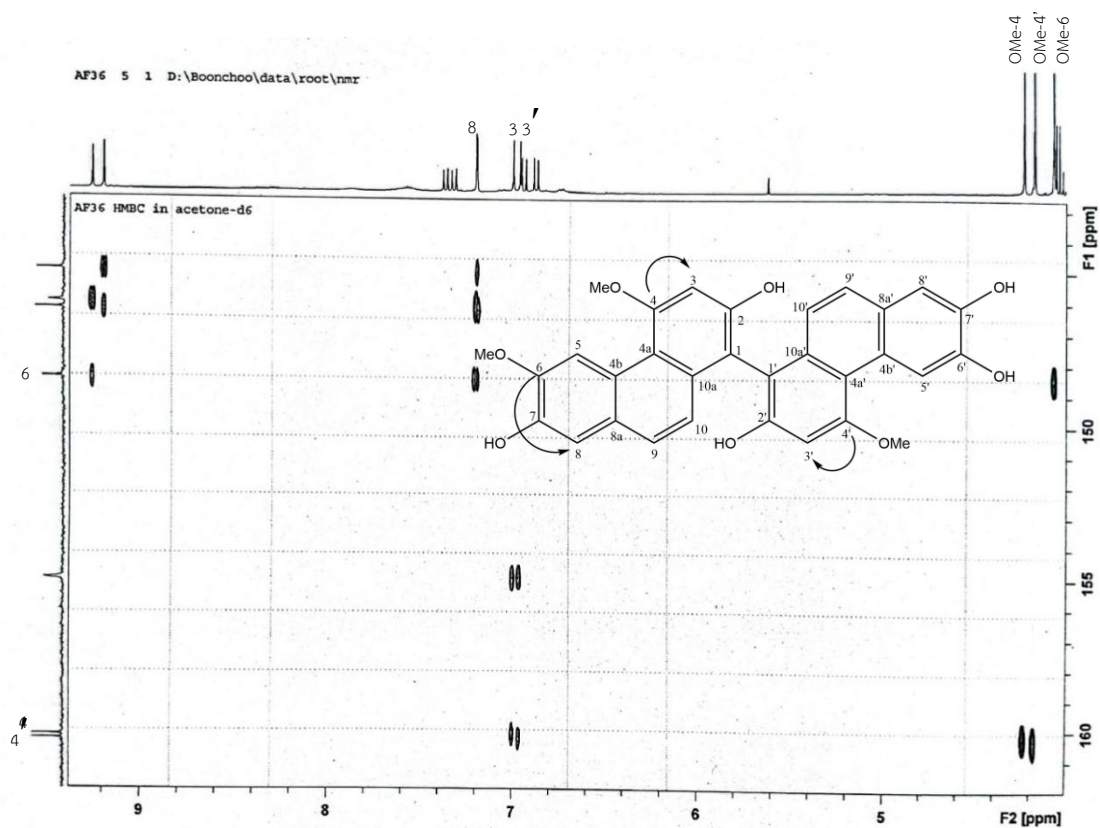


Figure 18 HMBC spectrum of compound AF1 (4.0-9.1 ppm and 143-162 ppm)

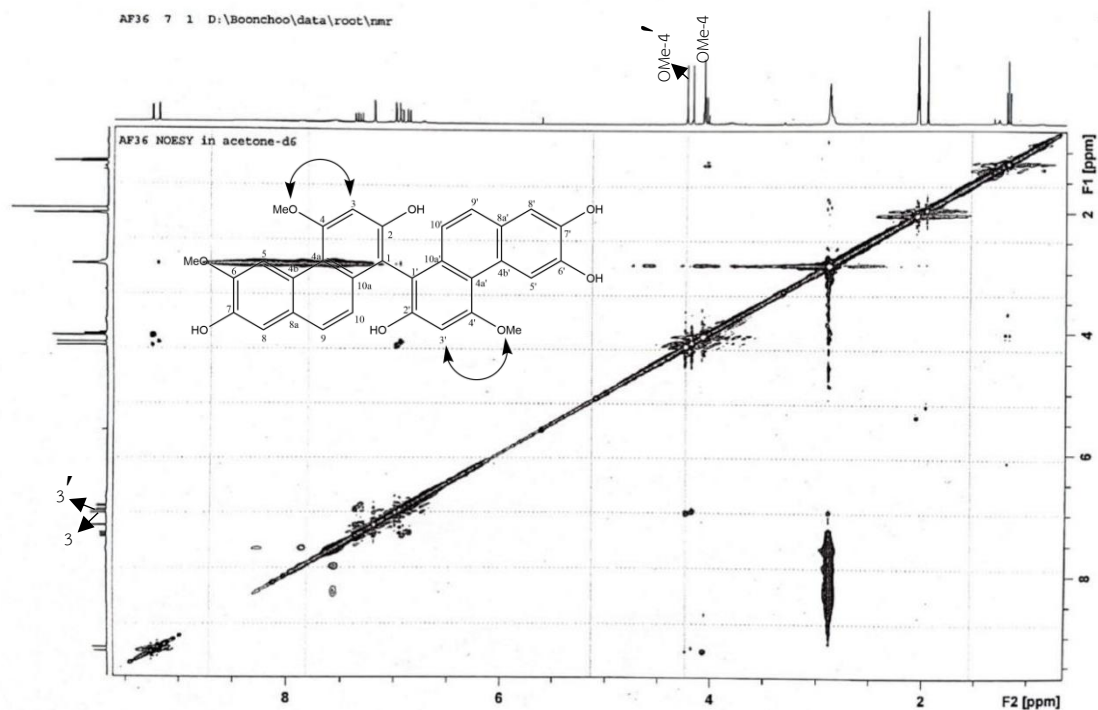


Figure 19 NOESY spectrum of compound AF1 (1-9.5 ppm and 1-9.5 ppm)



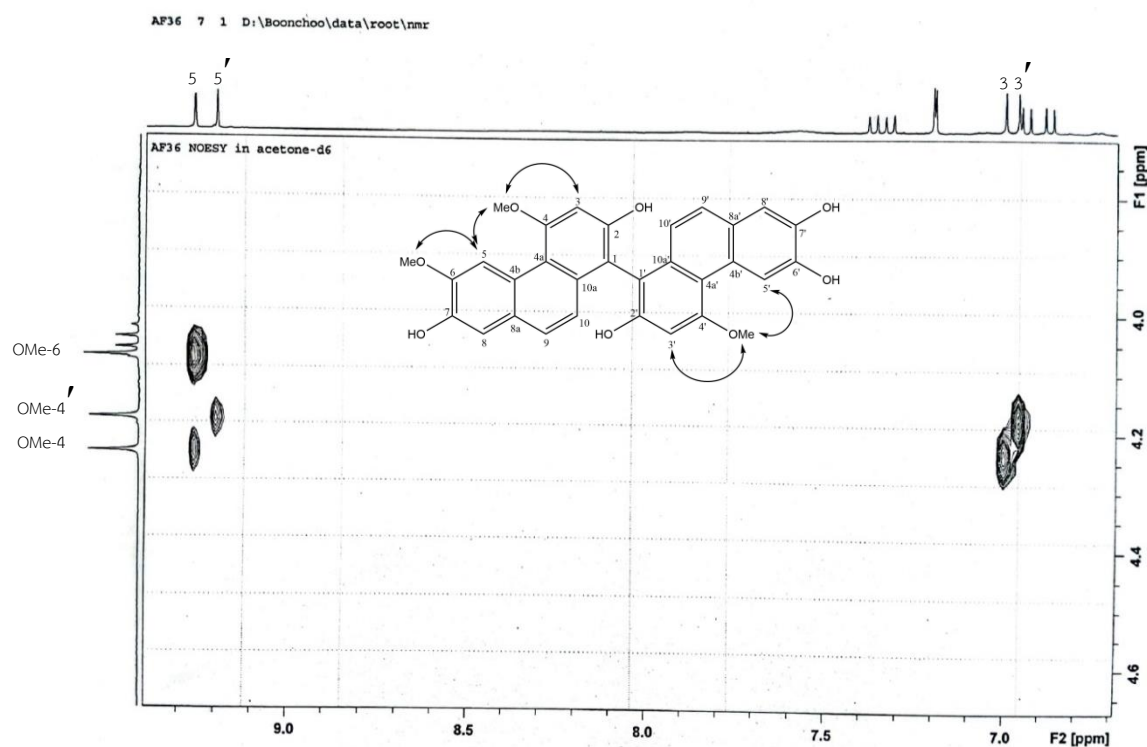


Figure 20 NOESY spectrum of compound AF1 (6.7-9.4 ppm and 3.8-4.6 ppm)

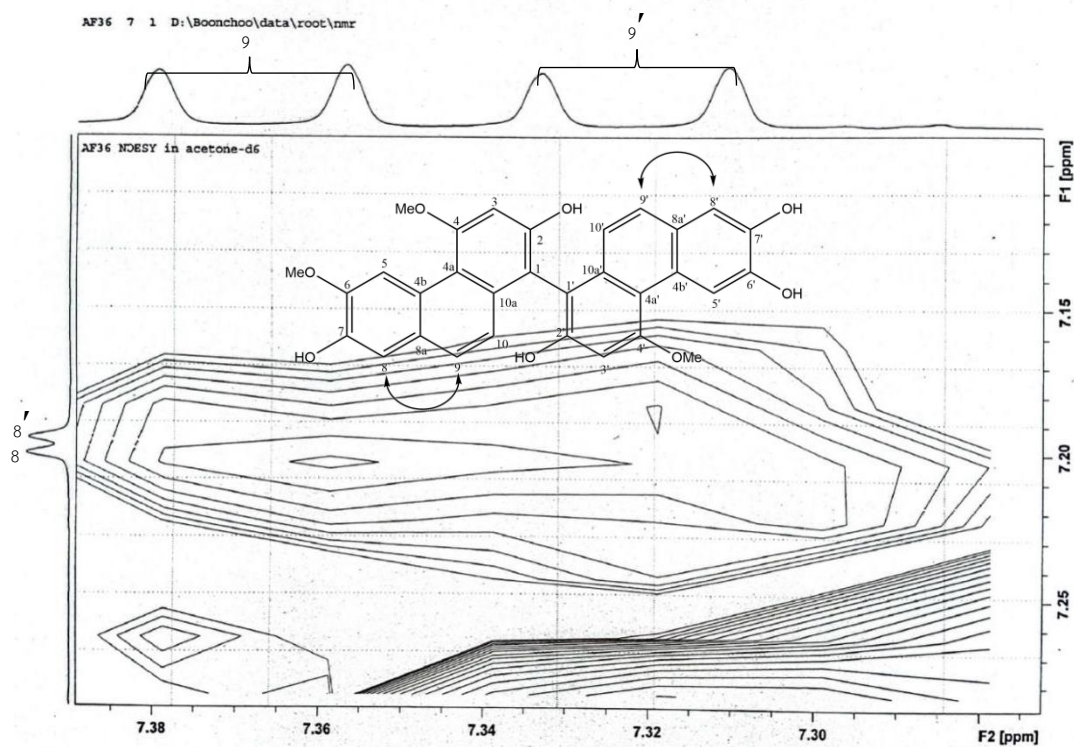


Figure 21 NOESY spectrum of compound AF1 (7.28-7.38 ppm and 7.10-7.28 ppm)

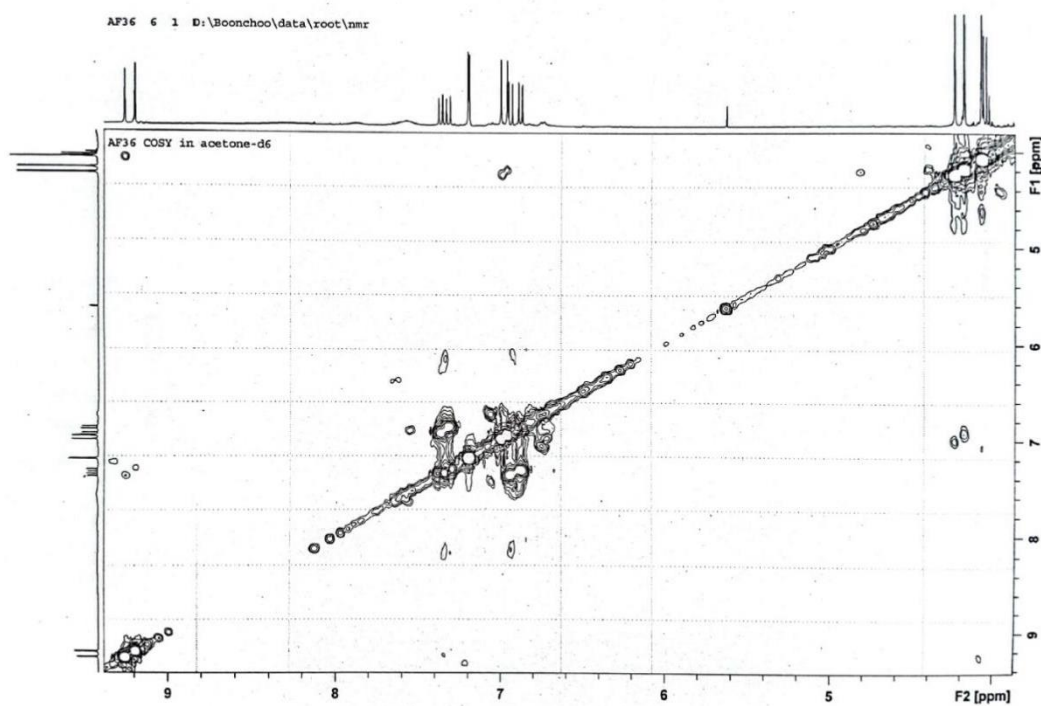


Figure 22 COSY spectrum of compound AF1

- Data Compound AF2

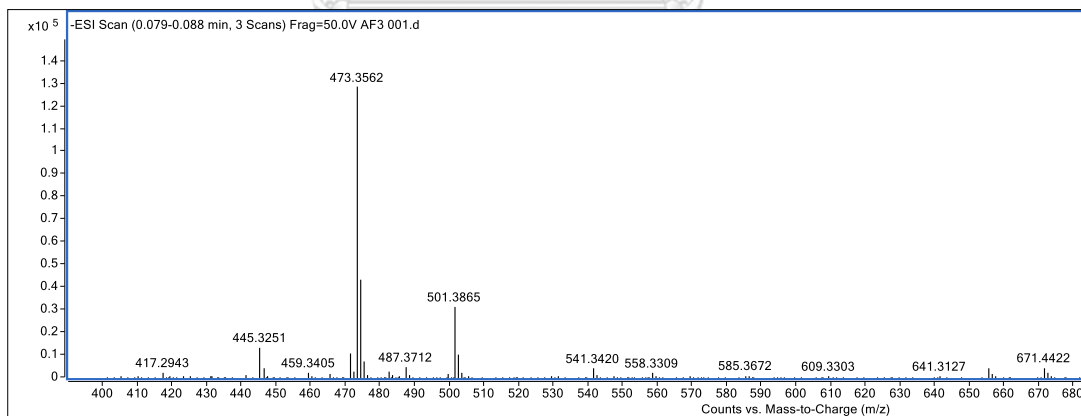


Figure 23 Mass spectrum of compound AF2

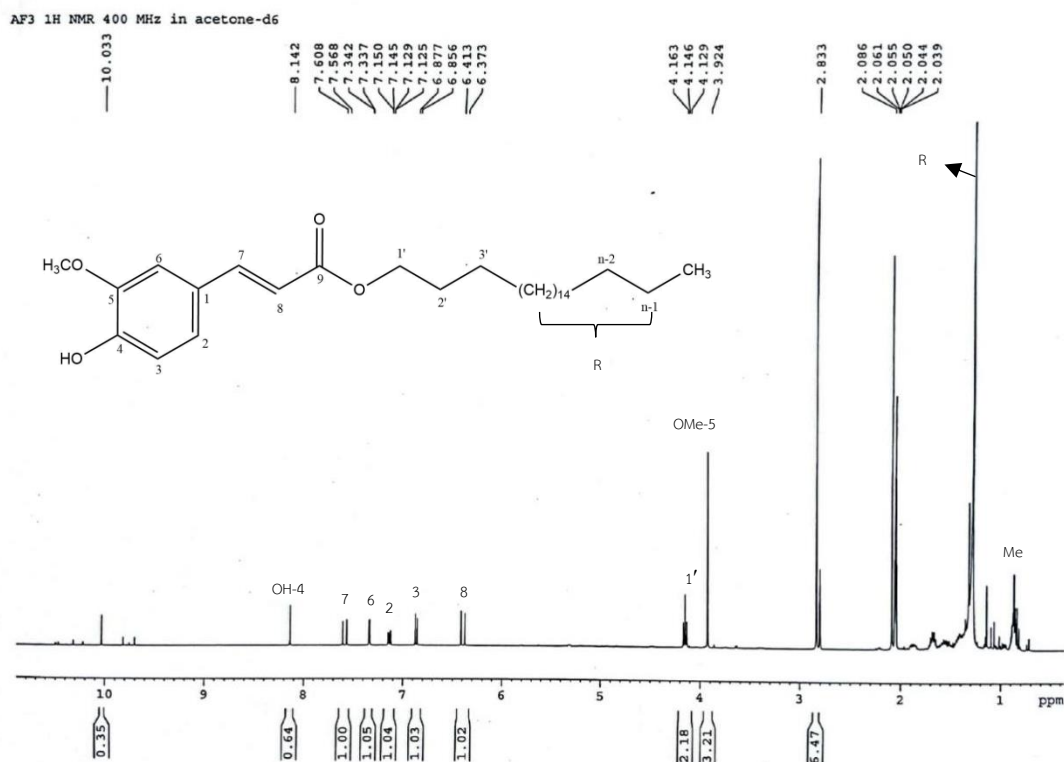


Figure 24 <sup>1</sup>H-NMR spectrum (400 MHz) of compound AF2 (0 - 10 ppm)

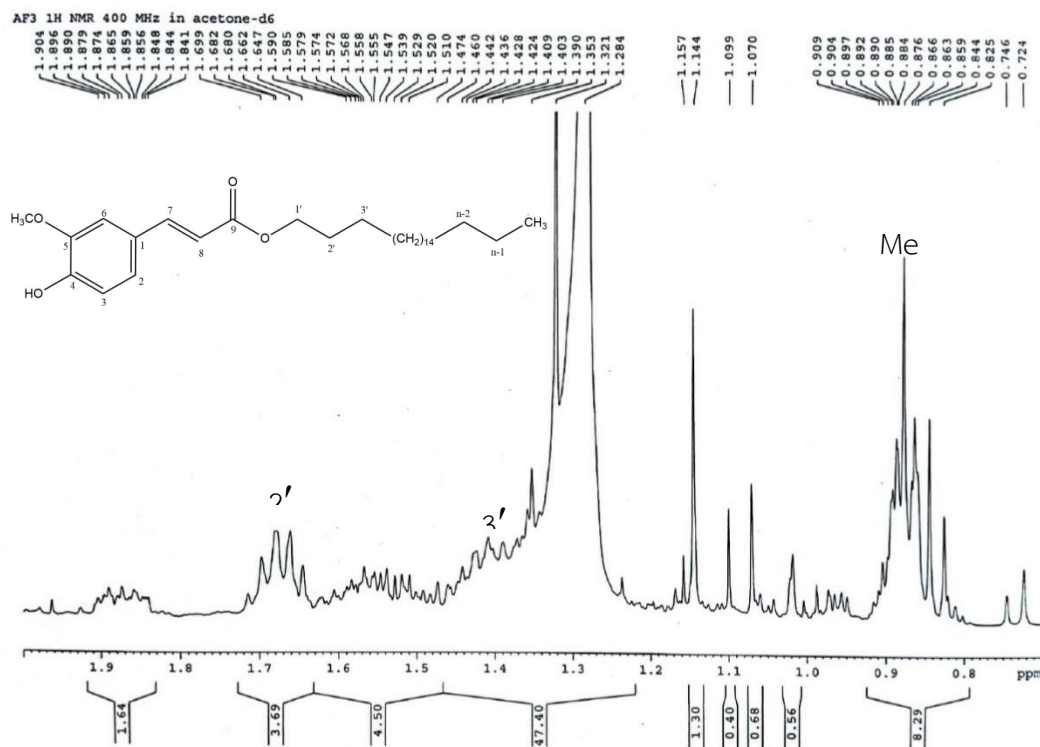


Figure 25 <sup>1</sup>H-NMR spectrum (400 MHz) of compound AF2 (0 - 2 ppm)

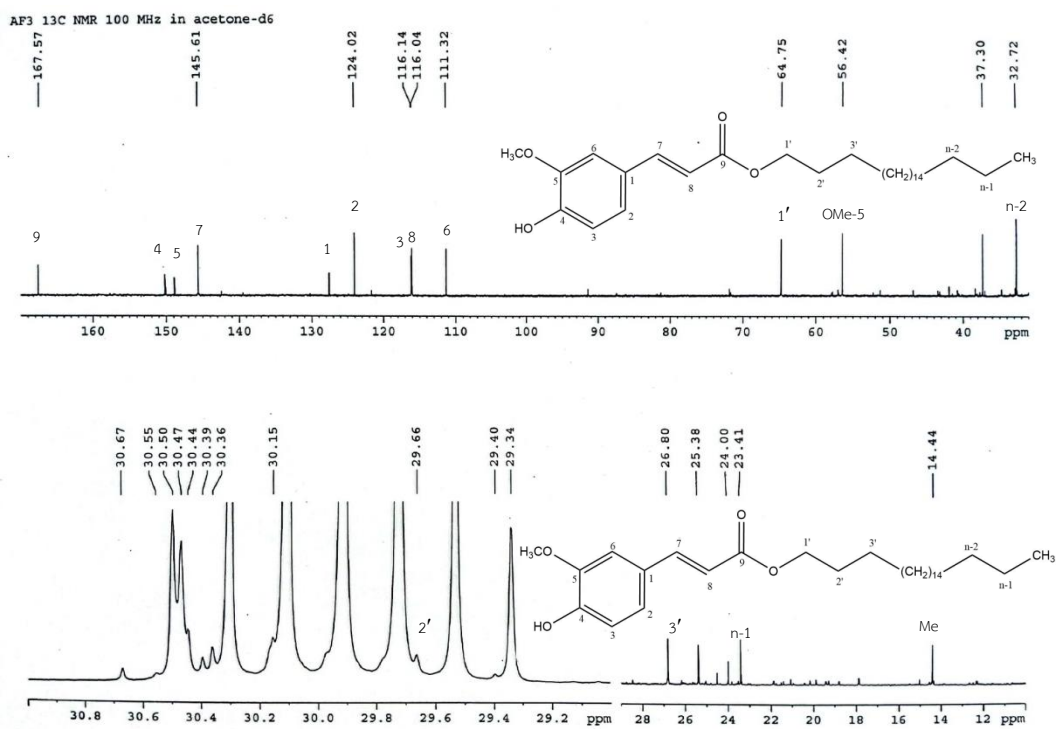


Figure 26  $^{13}\text{C}$ -NMR spectrum (100 MHz) of compound AF2

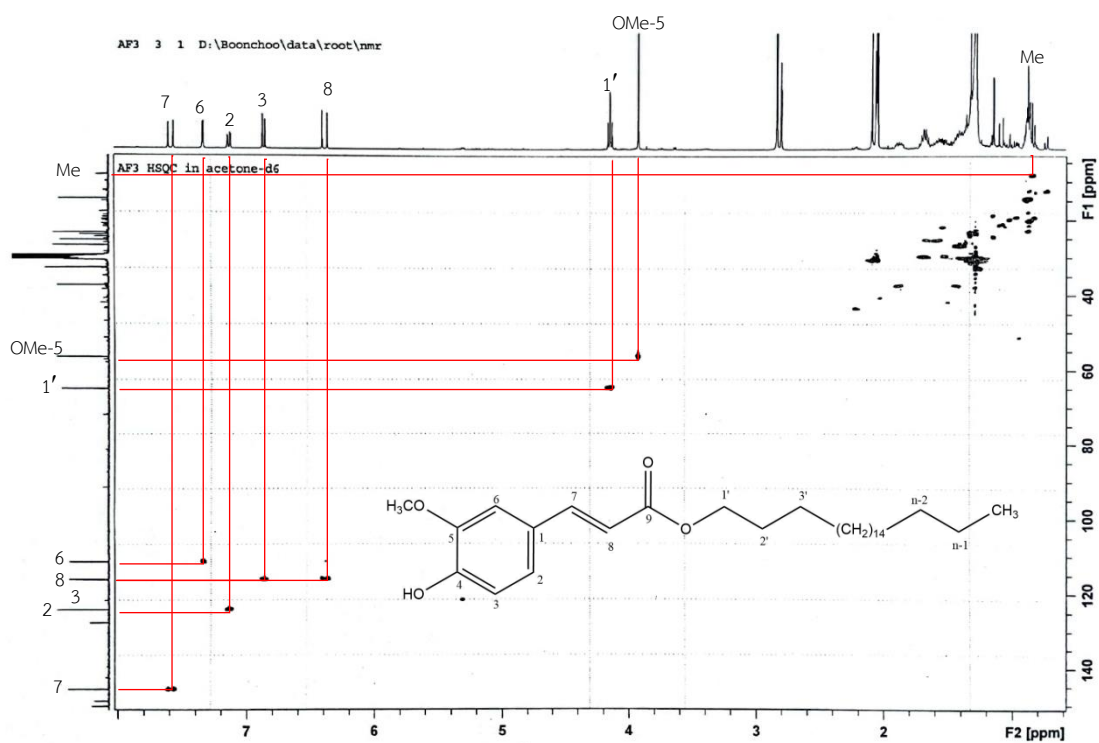


Figure 27 HSQC spectrum of compound AF2 (0-8 ppm and 0-145 ppm)

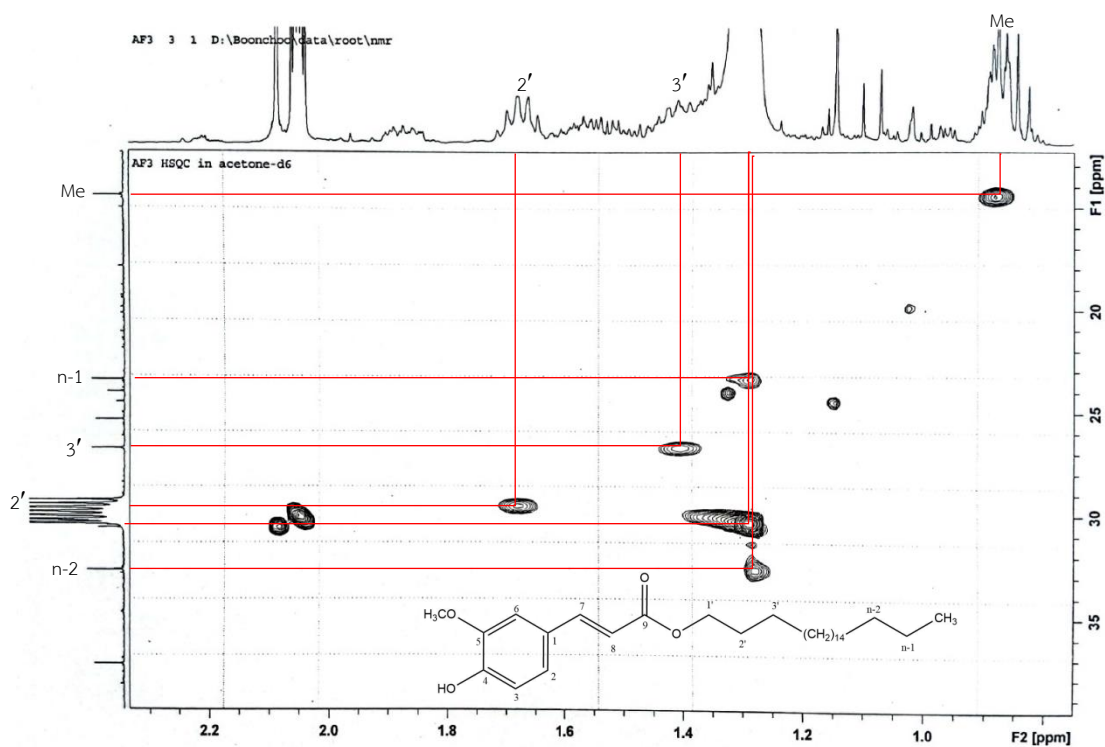


Figure 28 HSQC spectrum of compound AF2 (0-2.3 ppm and 13-40 ppm)

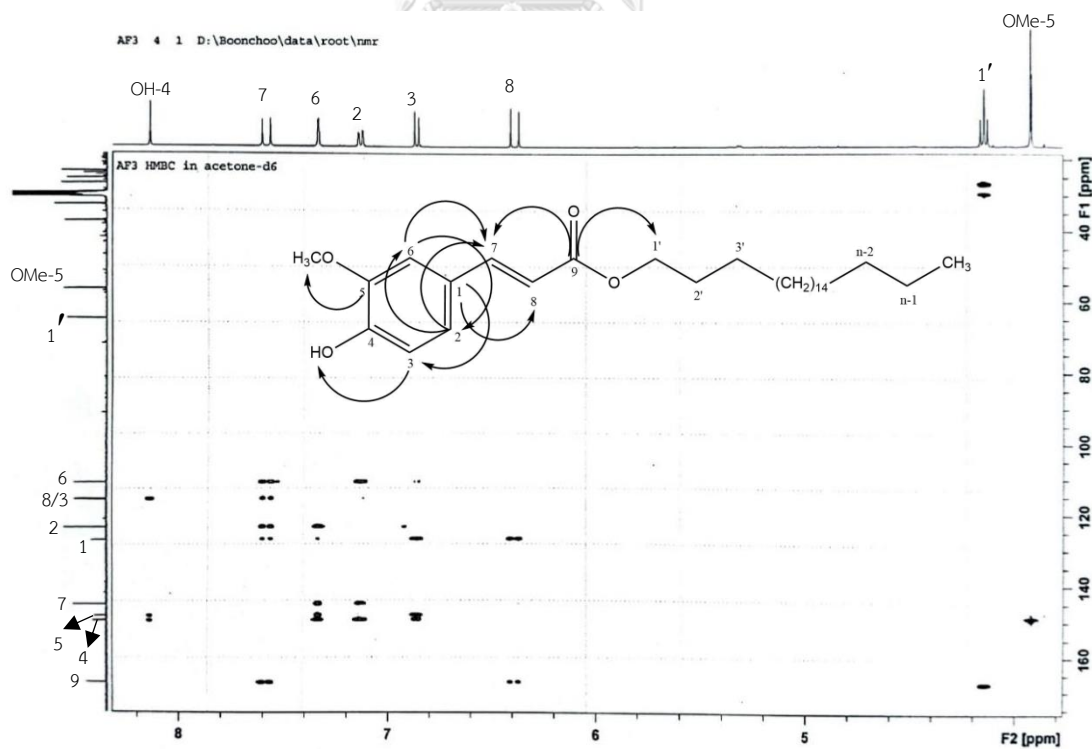


Figure 29 HMBC spectrum of compound AF2 (3.8-8.2 ppm and 20-170 ppm)



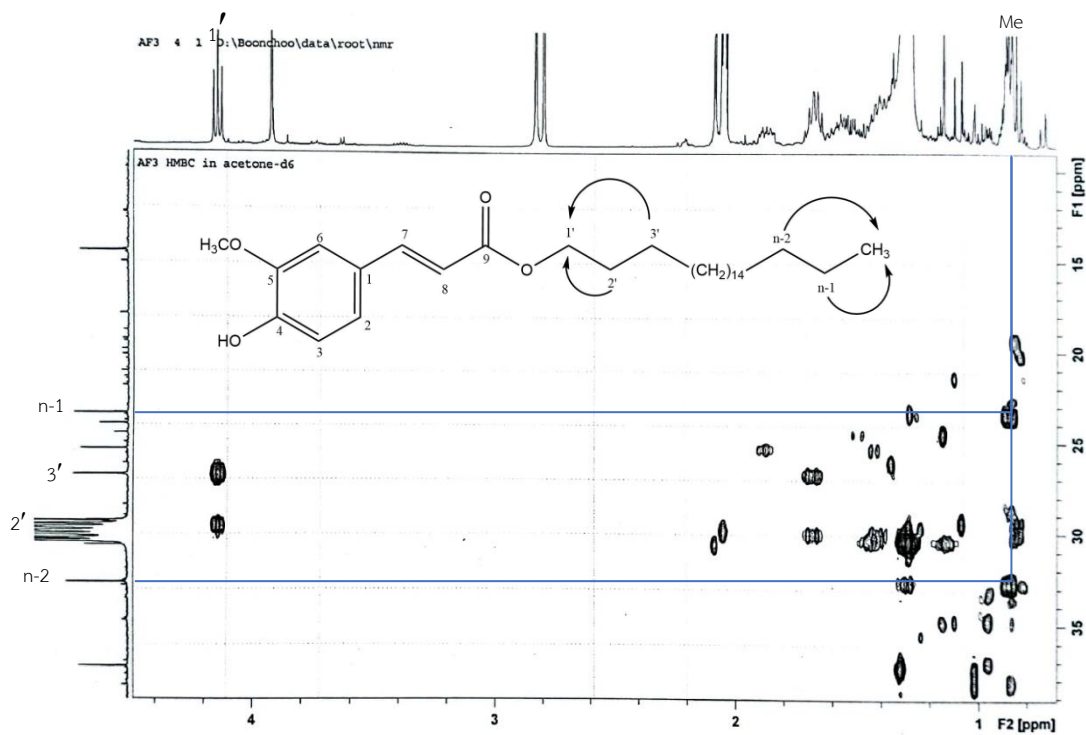


Figure 30 HMBC spectrum of compound AF2 (0.6-4.4 ppm and 10-39 ppm)

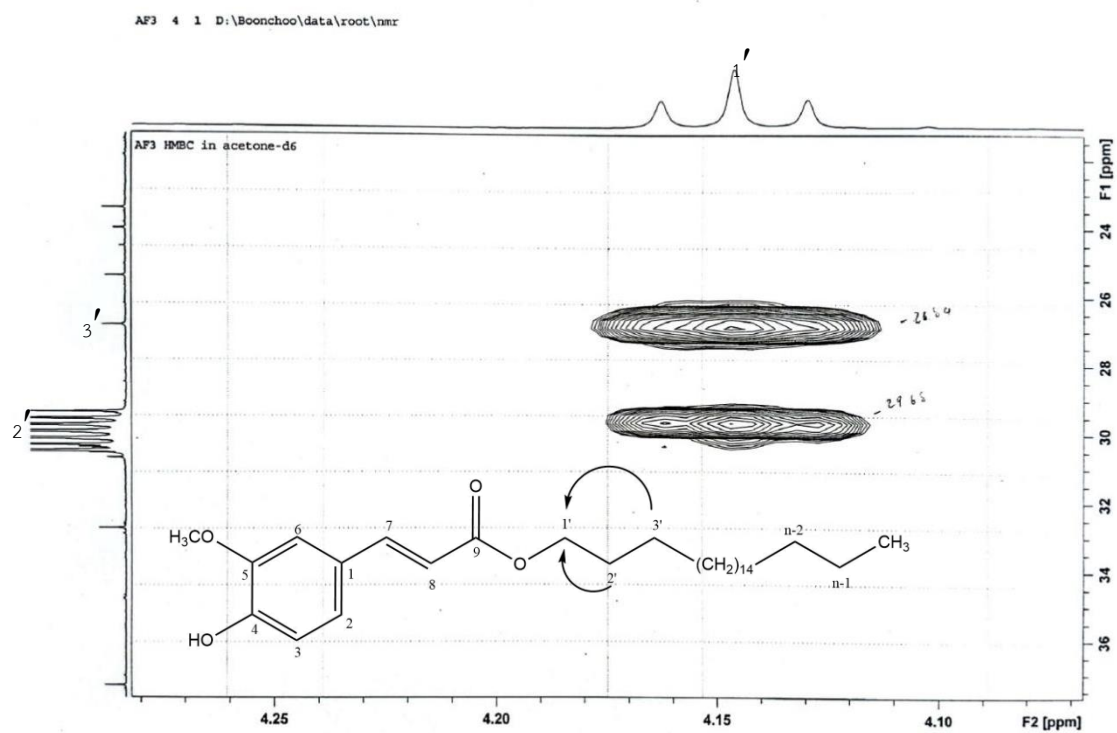


Figure 31 HMBC spectrum of compound AF2 (4.07-4.28 ppm and 22-37 ppm)

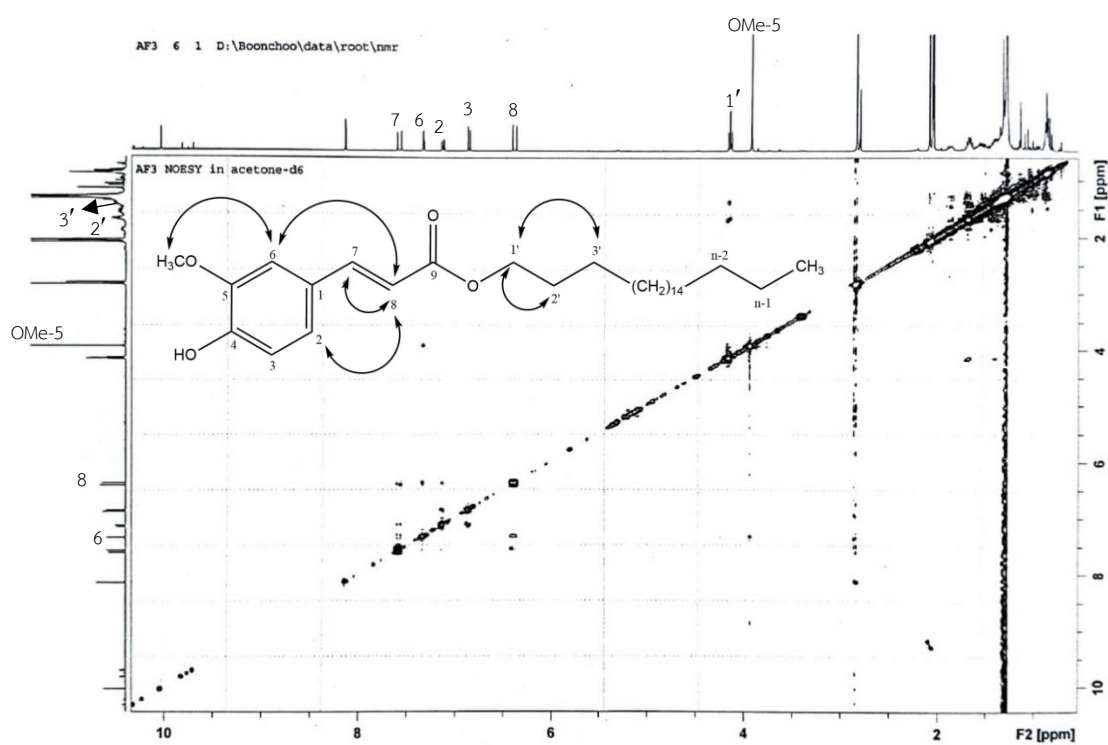


Figure 32 NOESY spectrum of compound AF2

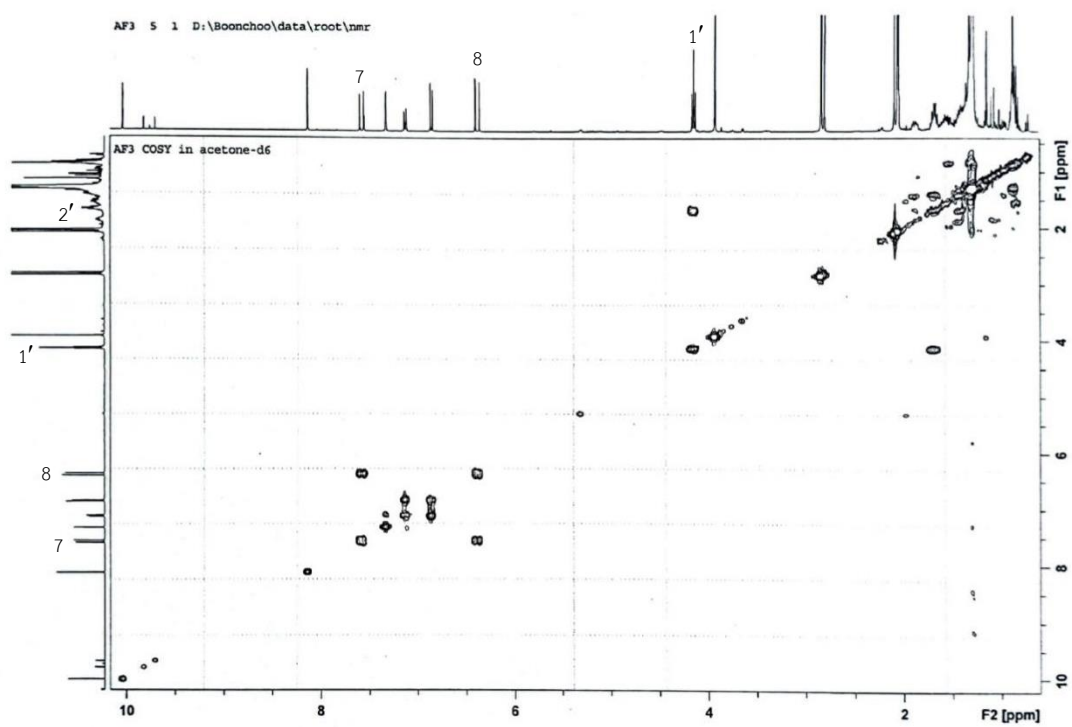


Figure 33 COSY spectrum of compound AF2 (1-10 ppm and 1-10 ppm)

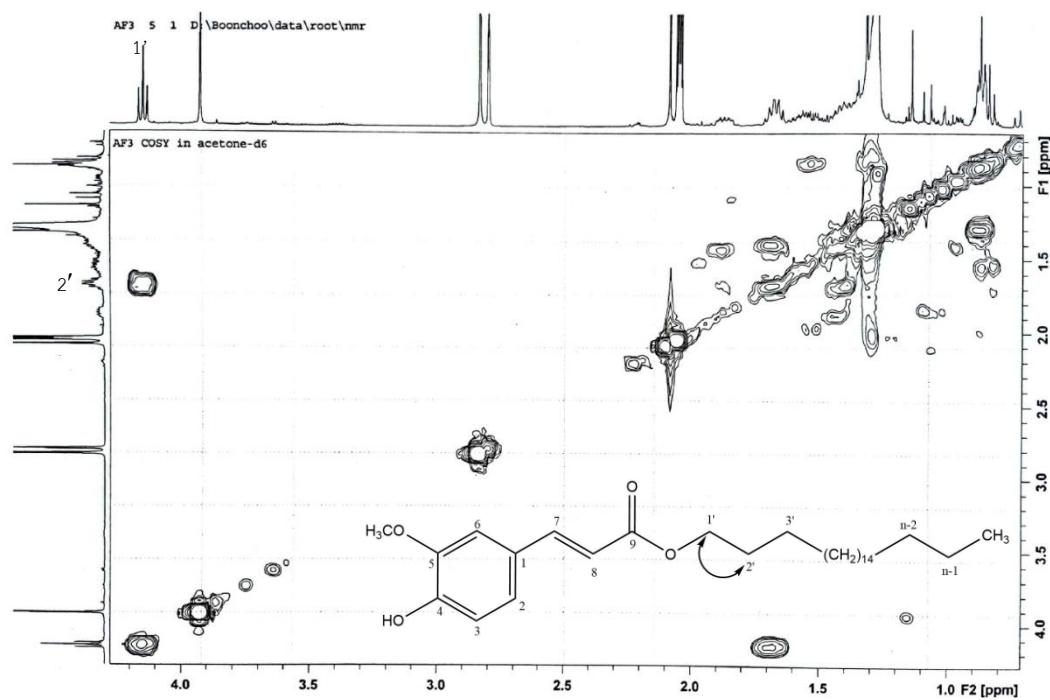


Figure 34 COSY spectrum of compound AF2 (0.7-4.2 ppm and 0.7-4.2 ppm )

● Data Compound AF3

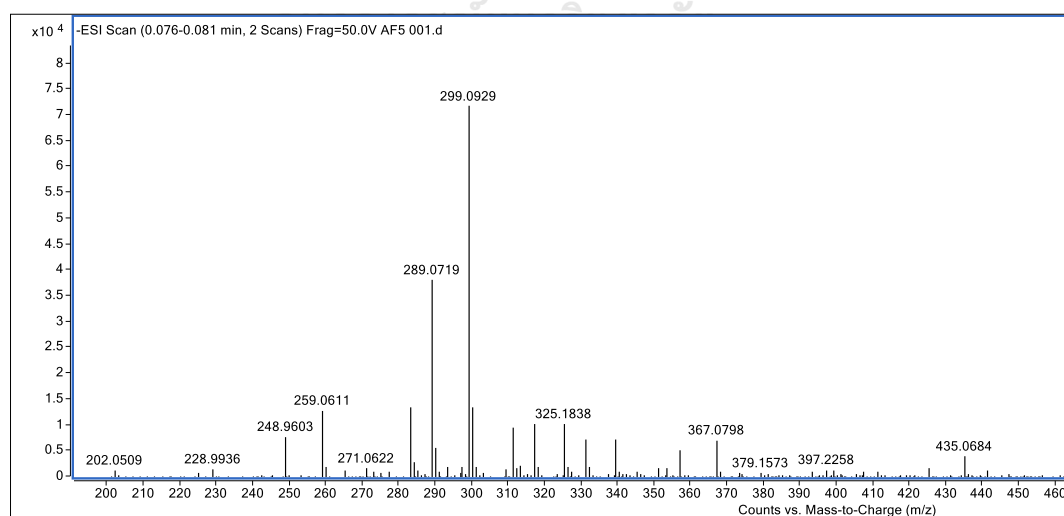


Figure 35 Mass spectrum of compound AF3



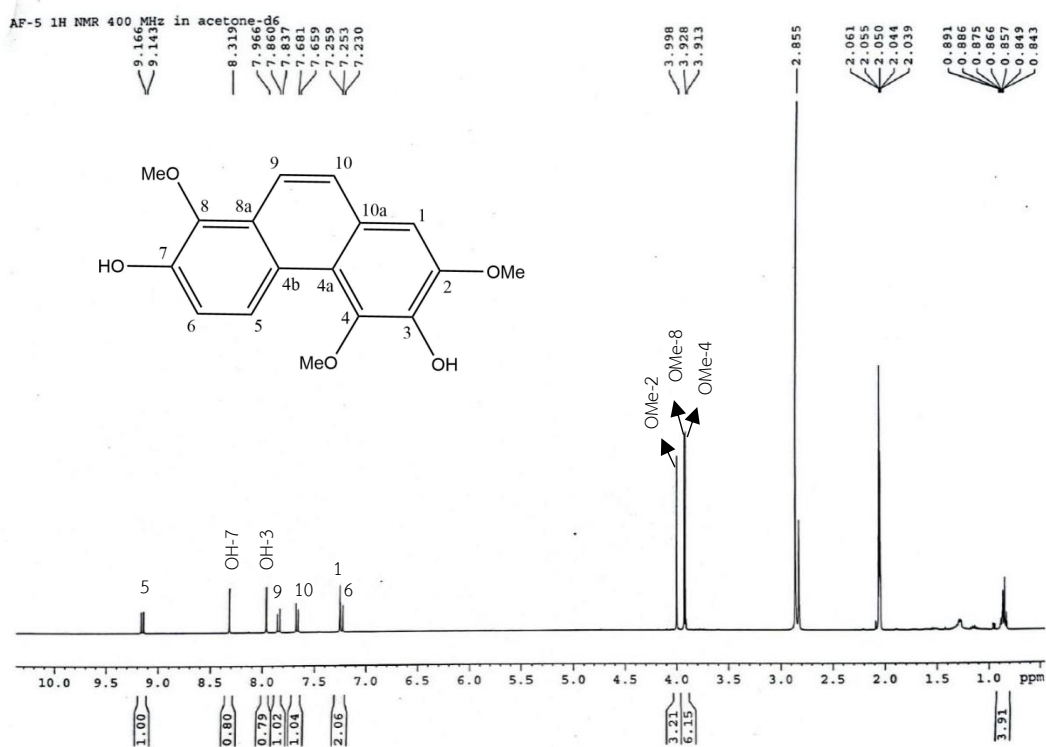


Figure 36  $^1\text{H-NMR}$  spectrum (400 MHz) of compound AF3

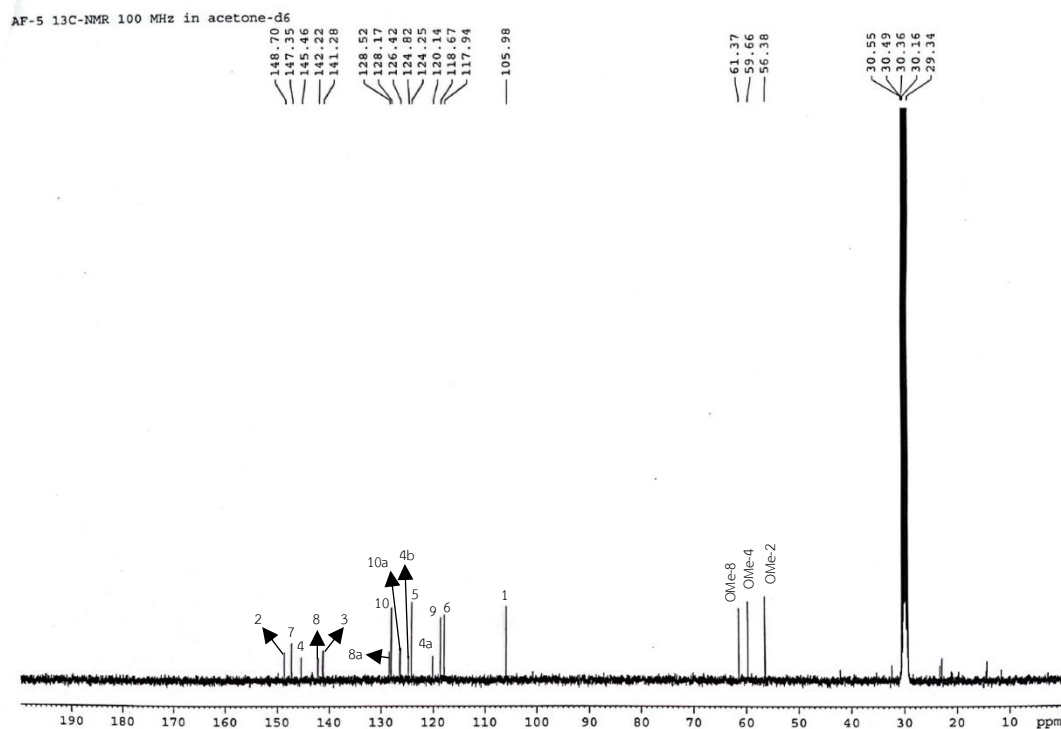


Figure 37  $^{13}\text{C-NMR}$  spectrum (100 MHz) of compound AF3

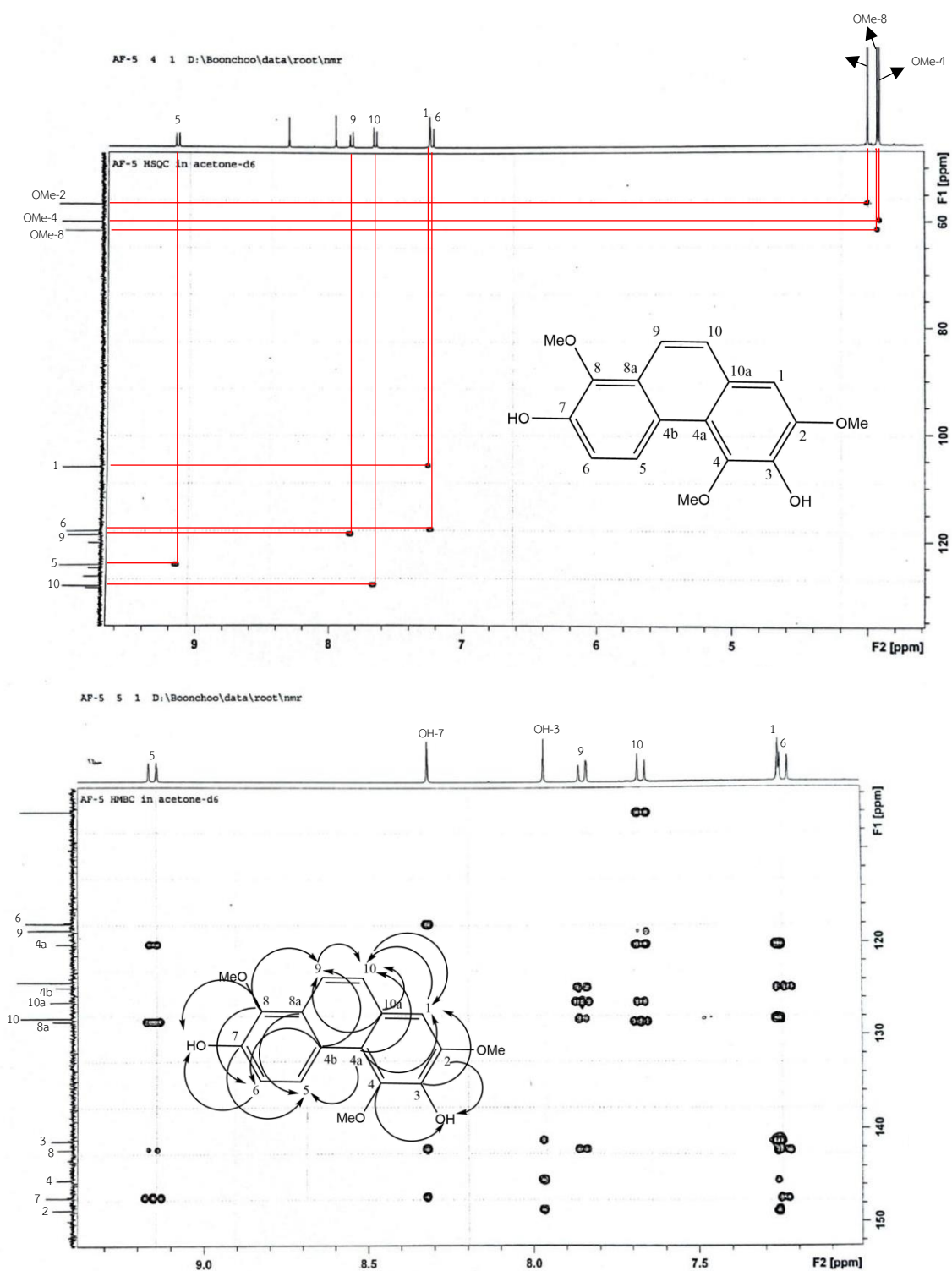


Figure 39 HMBC spectrum of compound AF3 (7-10 ppm and 104-152 ppm)

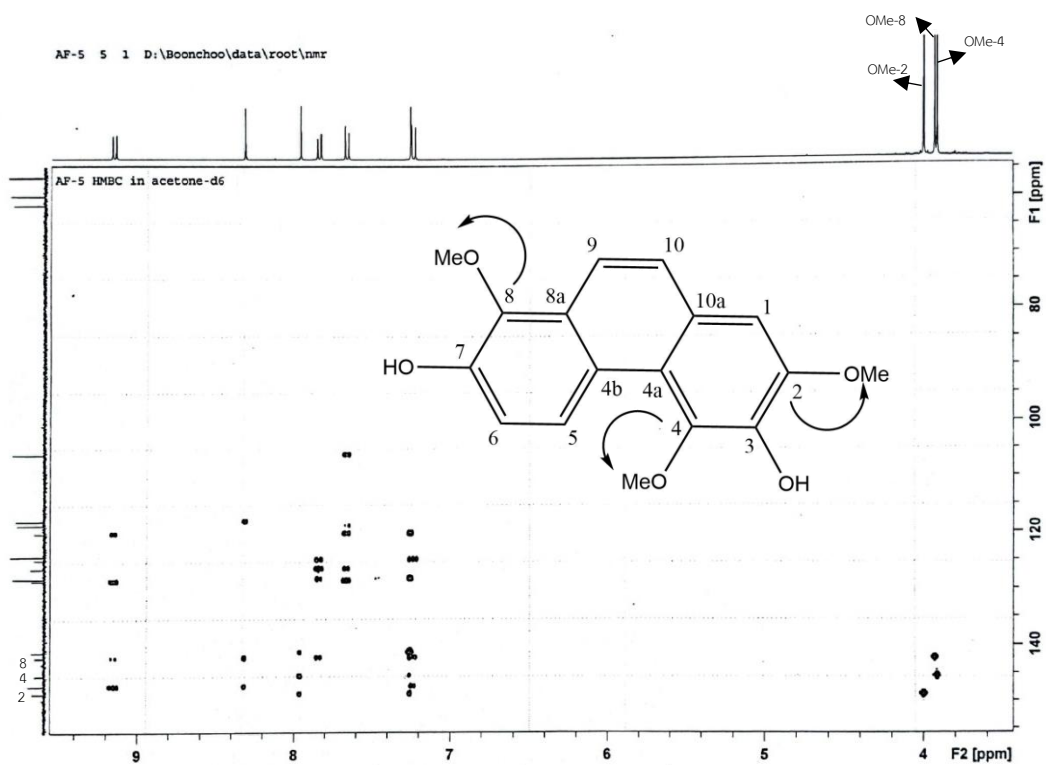


Figure 40 HMBC spectrum of compound AF3 (4.4-9.6 ppm and 55-155 ppm)

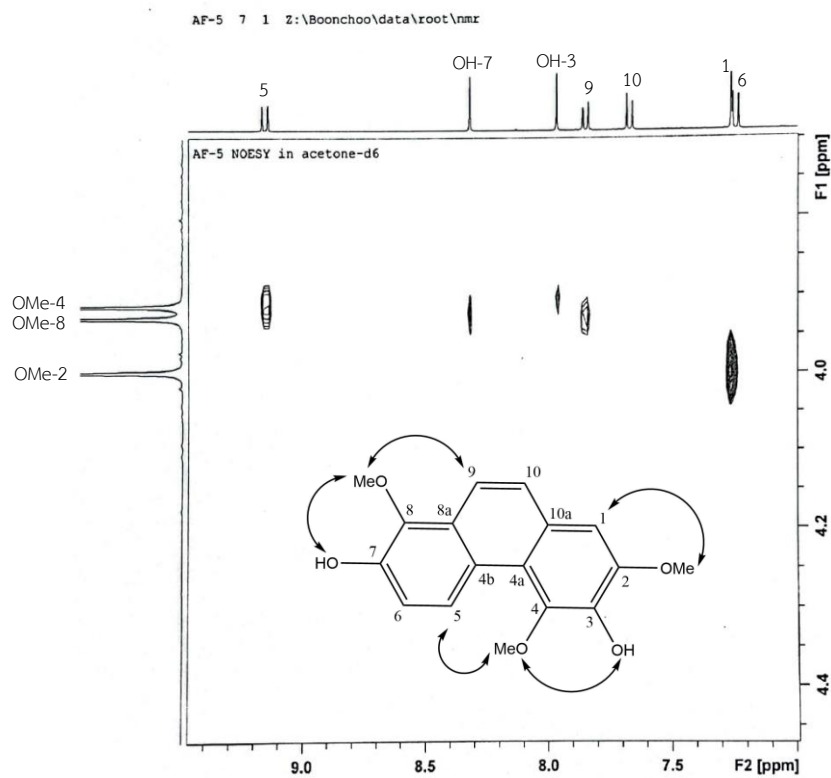


Figure 41 NOESY spectrum of compound AF3

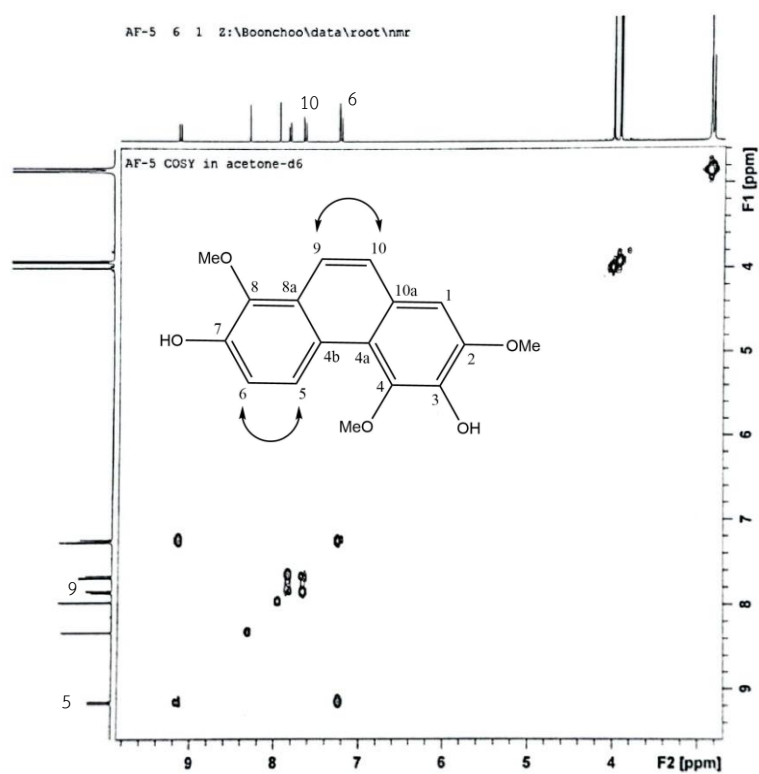


Figure 42 COSY spectrum of compound AF3

- Data compound AF4

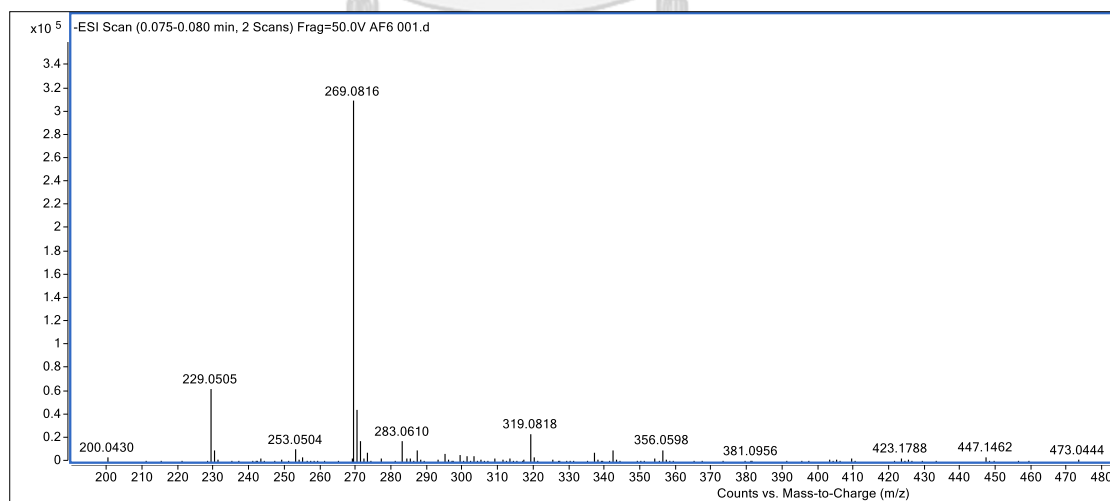


Figure 43 Mass spectrum of compound AF4

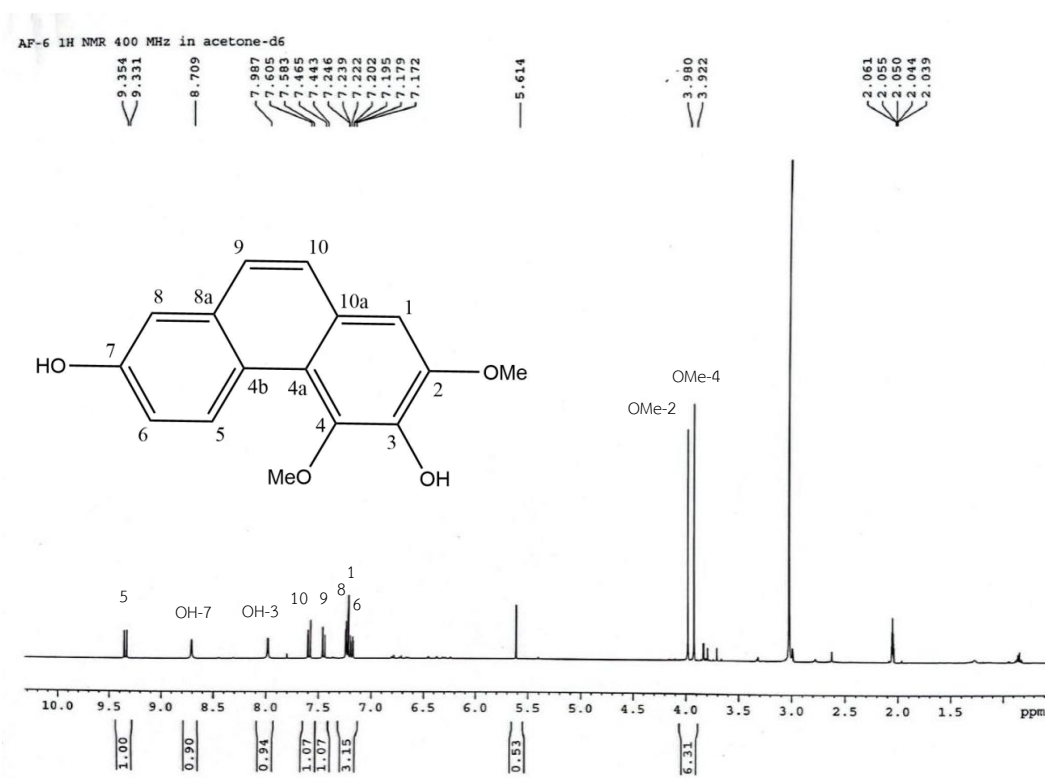


Figure 44  $^1\text{H}$ -NMR spectrum (400 MHz) of compound AF4 (0.5-10.5 ppm)

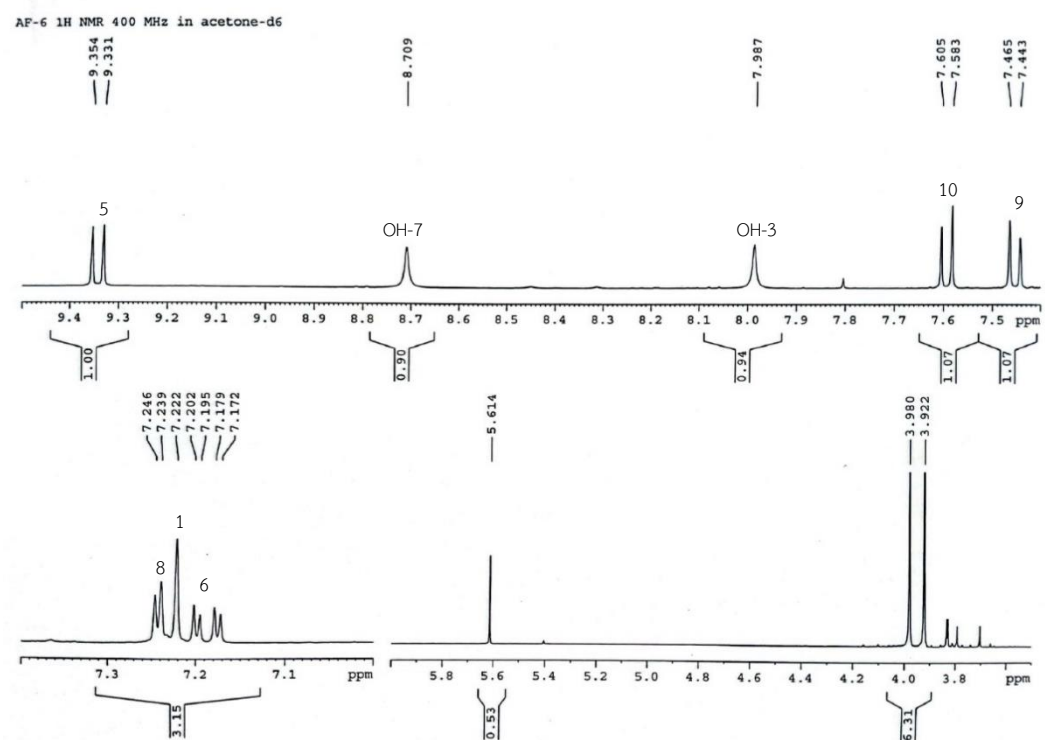


Figure 45  $^1\text{H}$ -NMR spectrum (400 MHz) of compound AF4 (2.0-9.5 ppm)

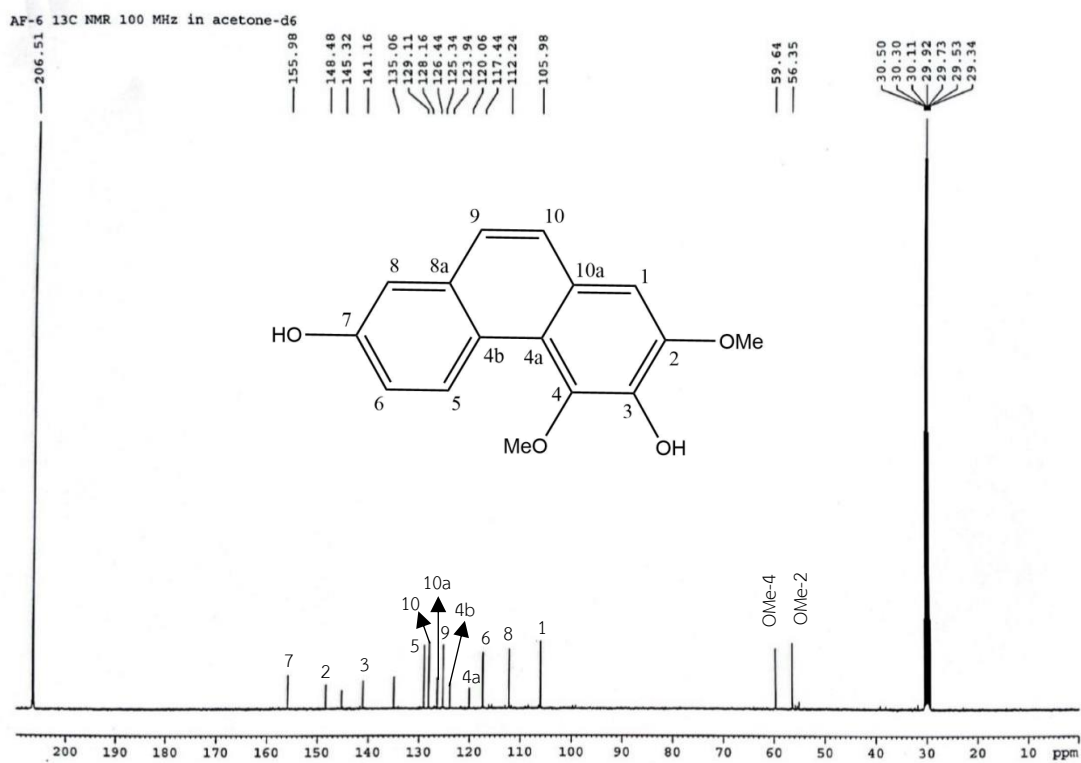


Figure 46  $^{13}\text{C}$ -NMR spectrum (100 MHz) of compound AF4

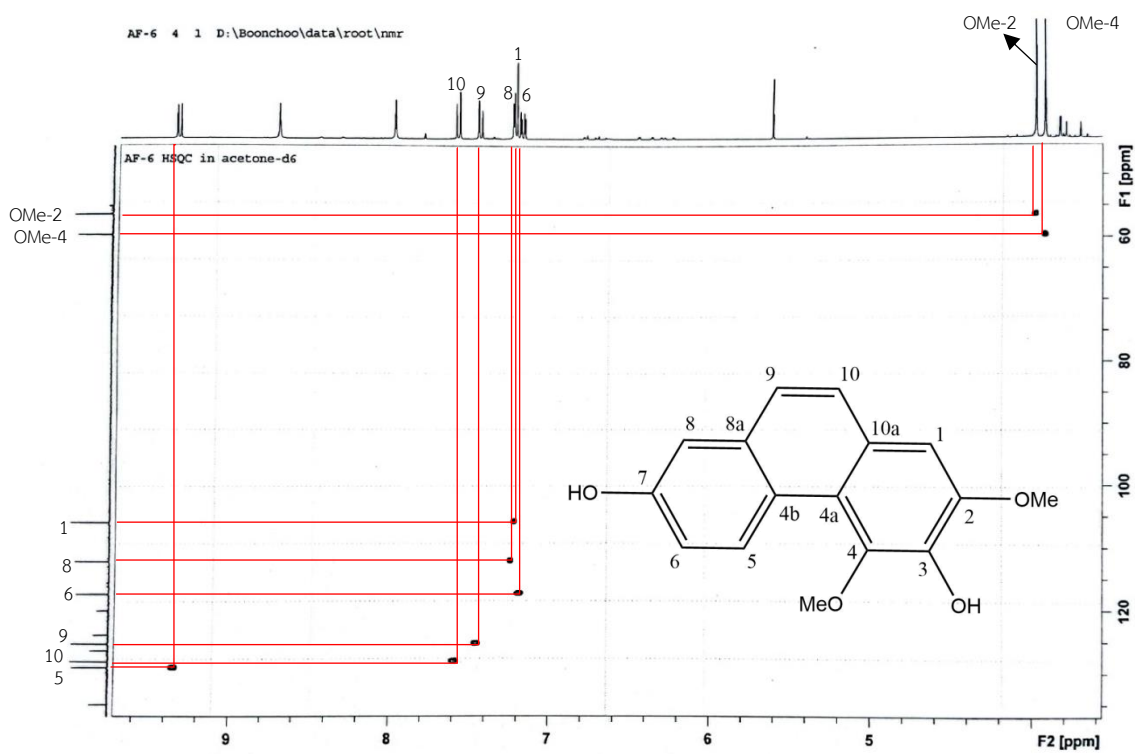


Figure 47 HSQC spectrum of compound AF4

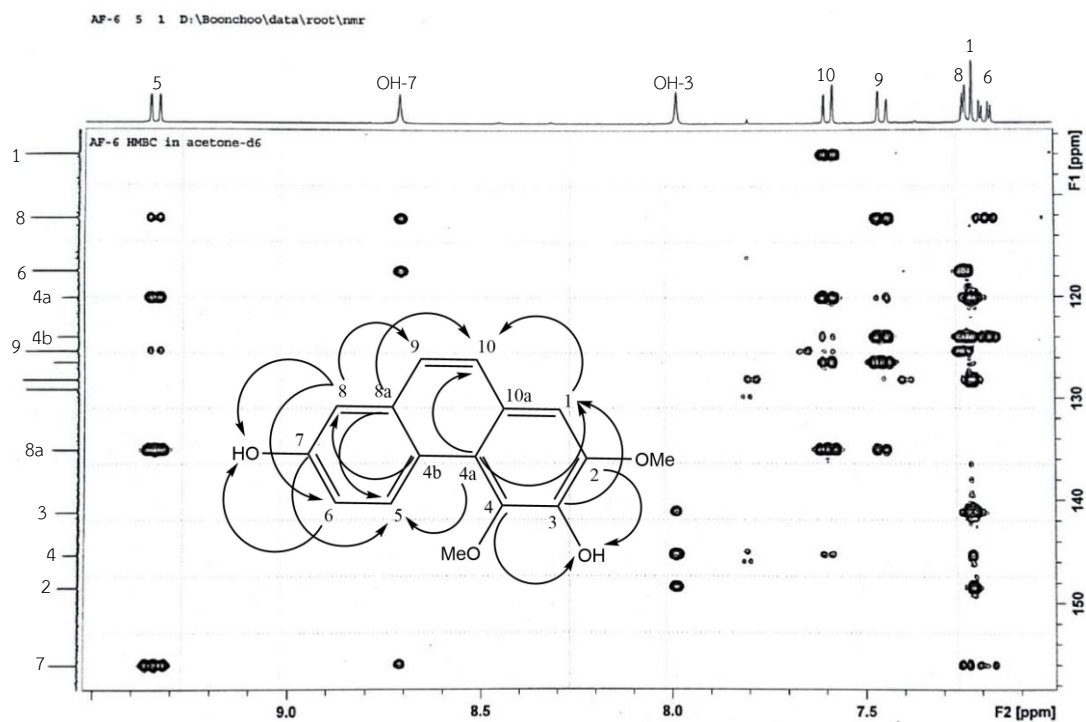


Figure 48 HMBC spectrum of compound AF4 (7.0-10 ppm and 104-158 ppm)

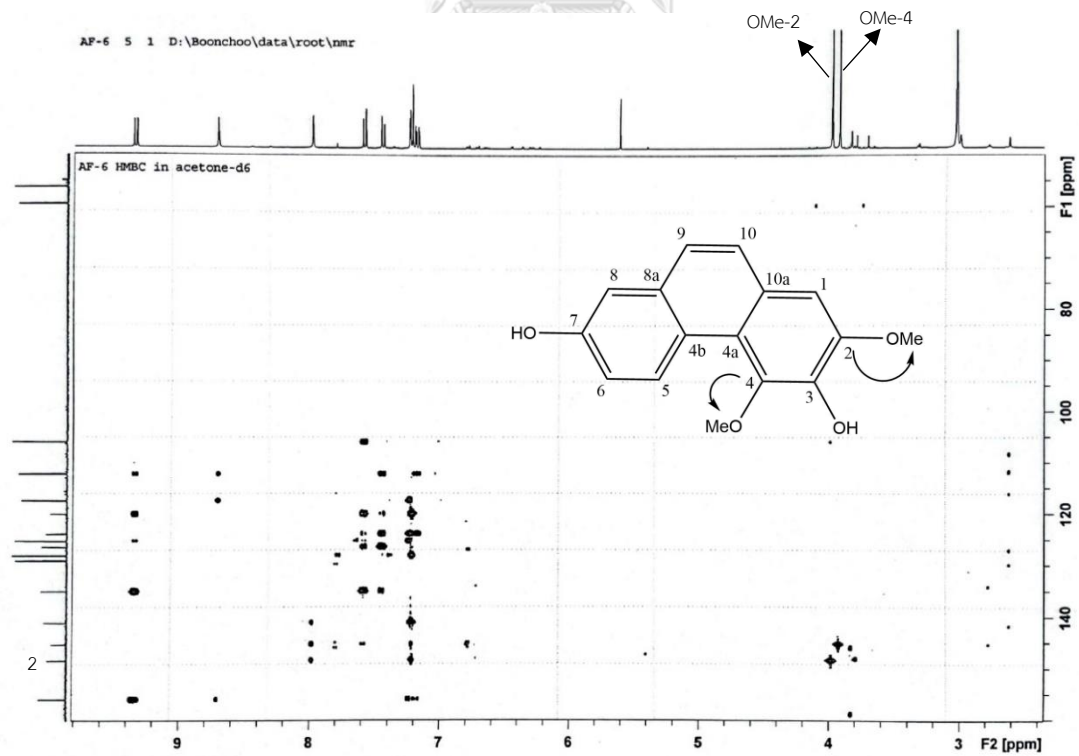


Figure 49 HMBC spectrum of compound AF4 (2.4-10 ppm and 70-160 ppm)

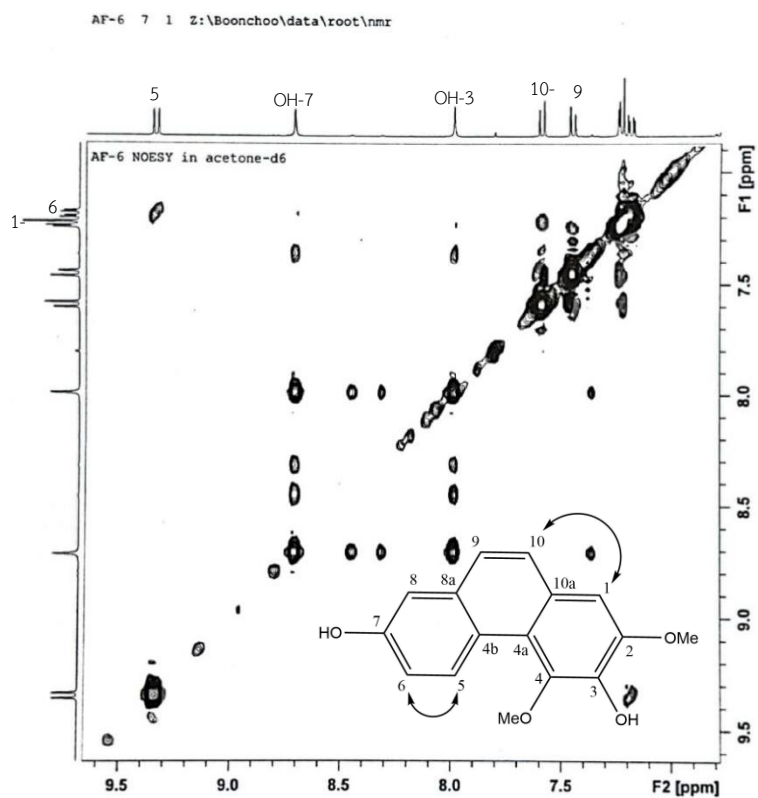


Figure 50 NOESY spectrum of compound AF4 (6.8-9.6 ppm and 6.9-9.6 ppm)

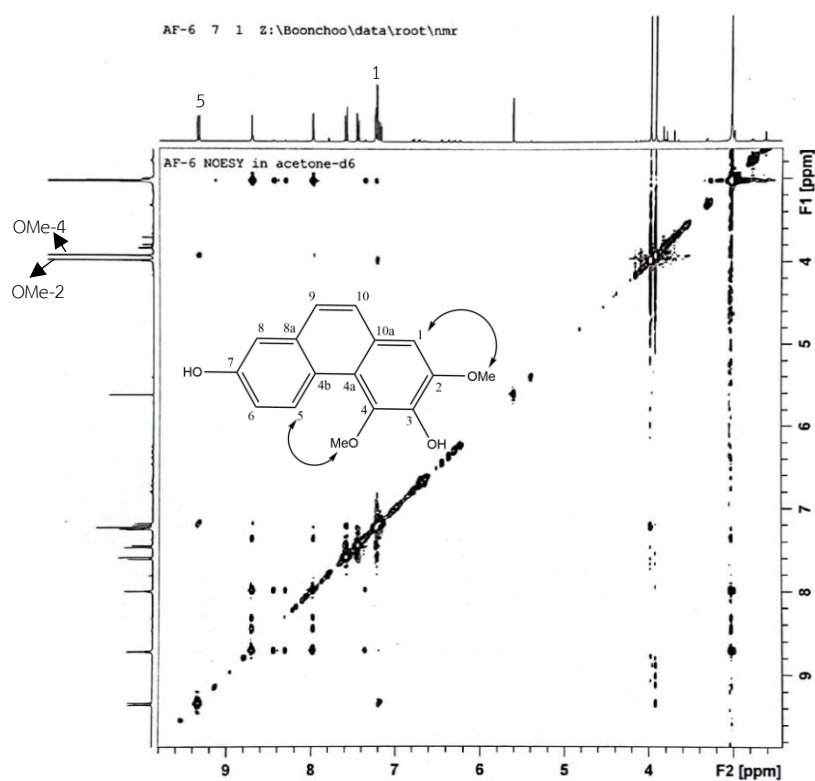
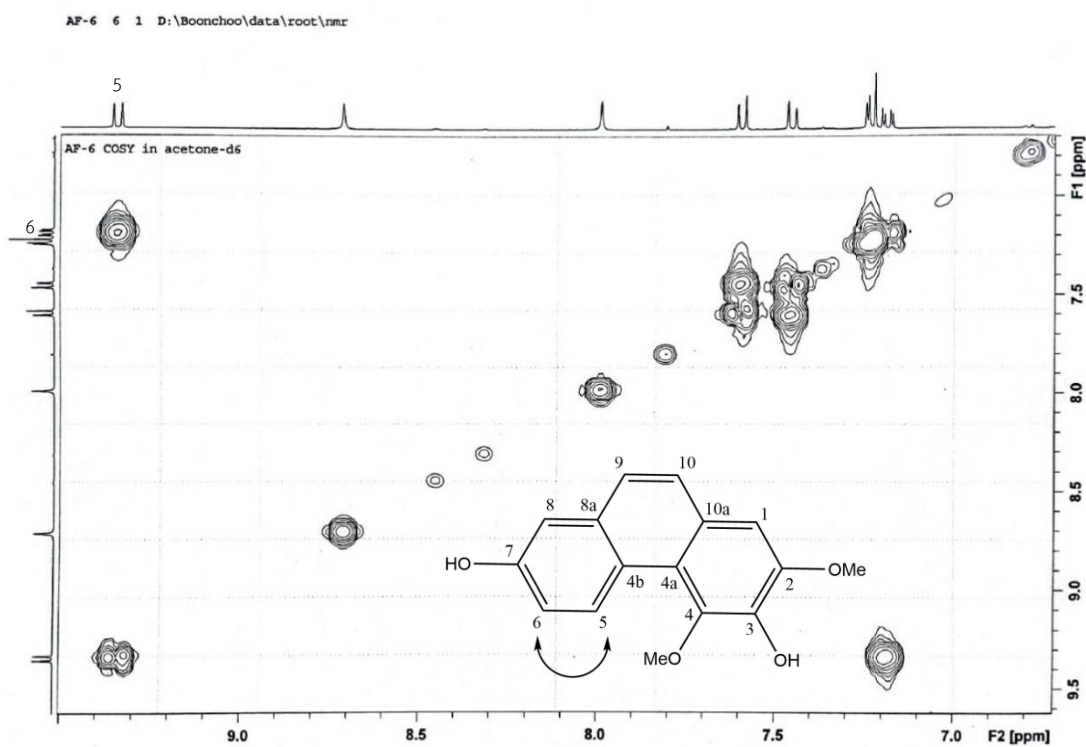
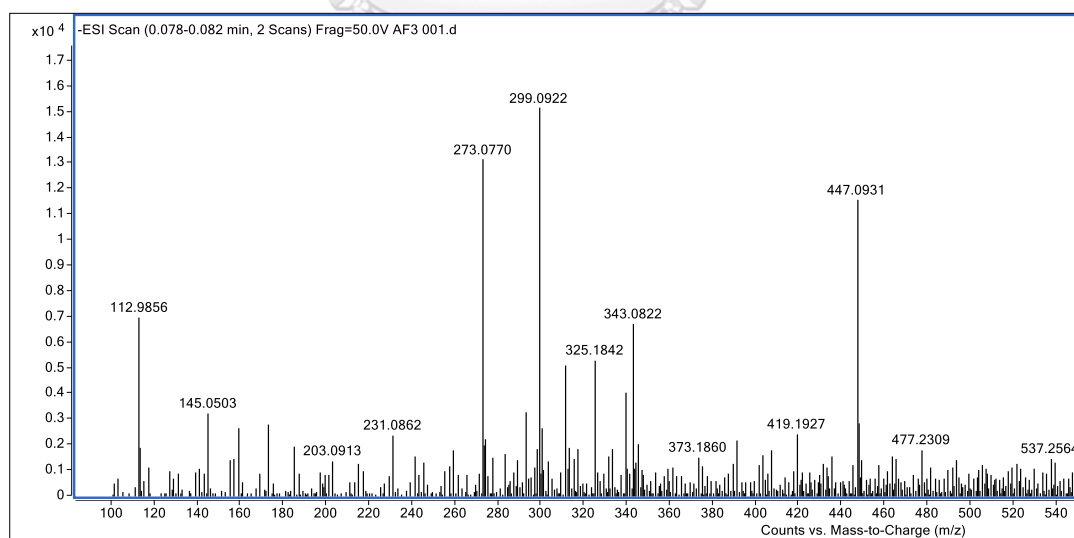


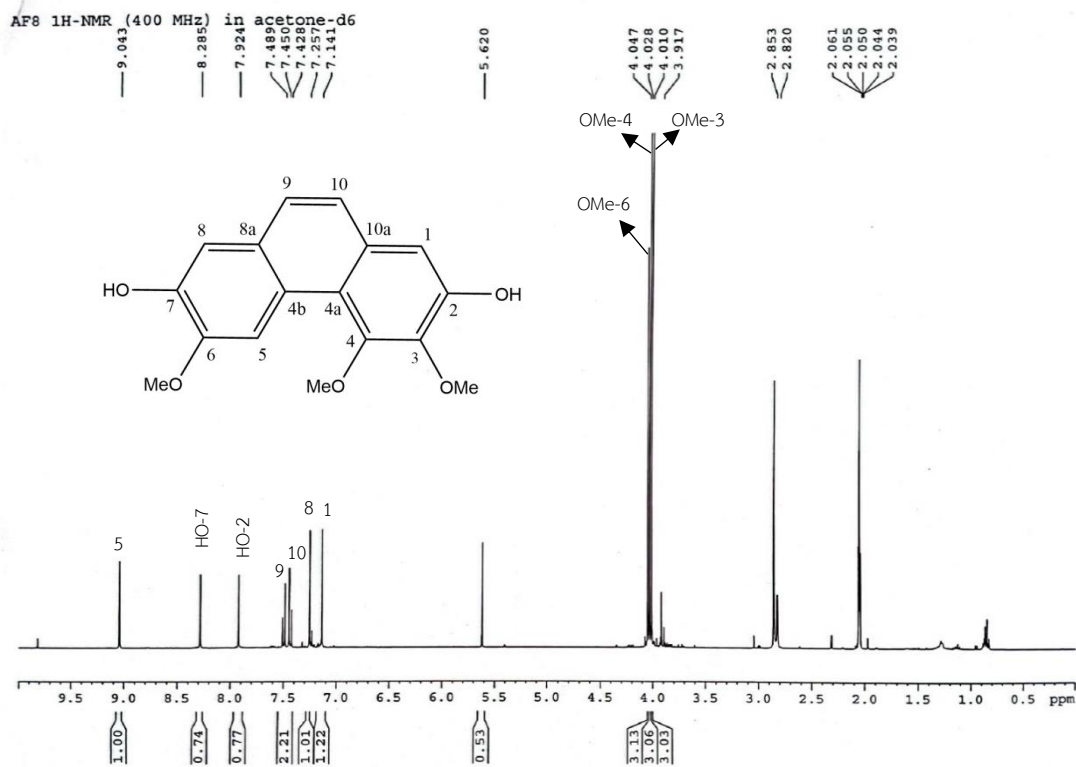
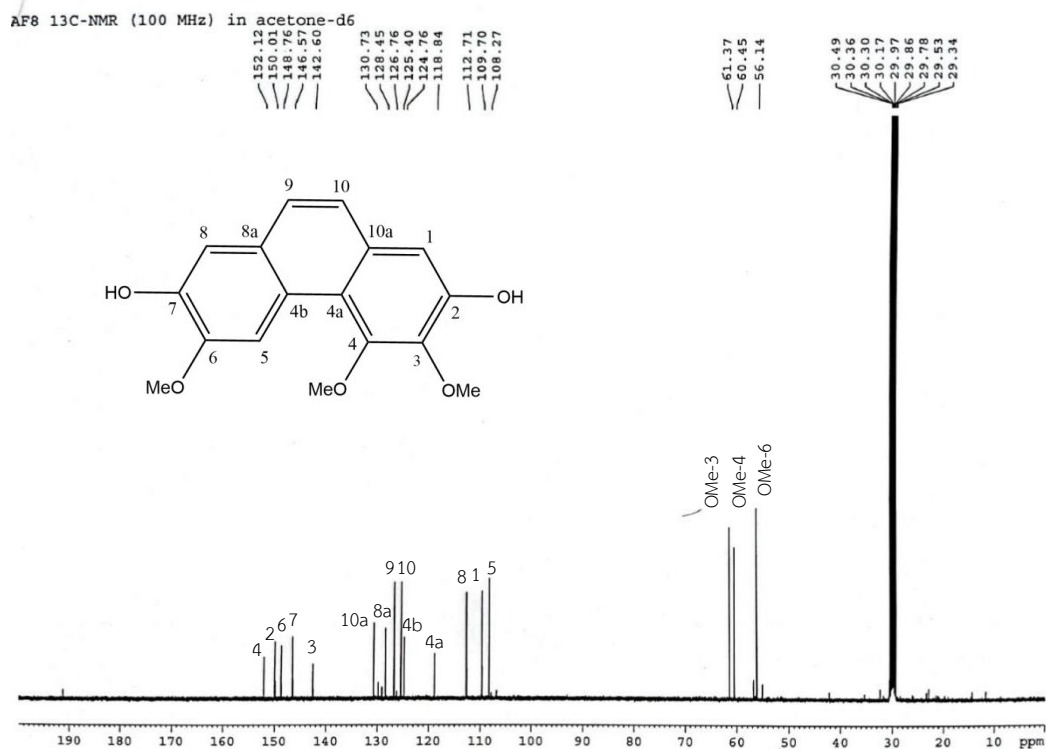
Figure 51 NOESY spectrum of compound AF4 (2.6-10 ppm and 2.9-10 ppm)





- Data compound AF5



Figure 54  $^1\text{H-NMR}$  spectrum (400 MHz) of compound AF5Figure 55  $^{13}\text{C-NMR}$  spectrum (100 MHz) of compound AF5

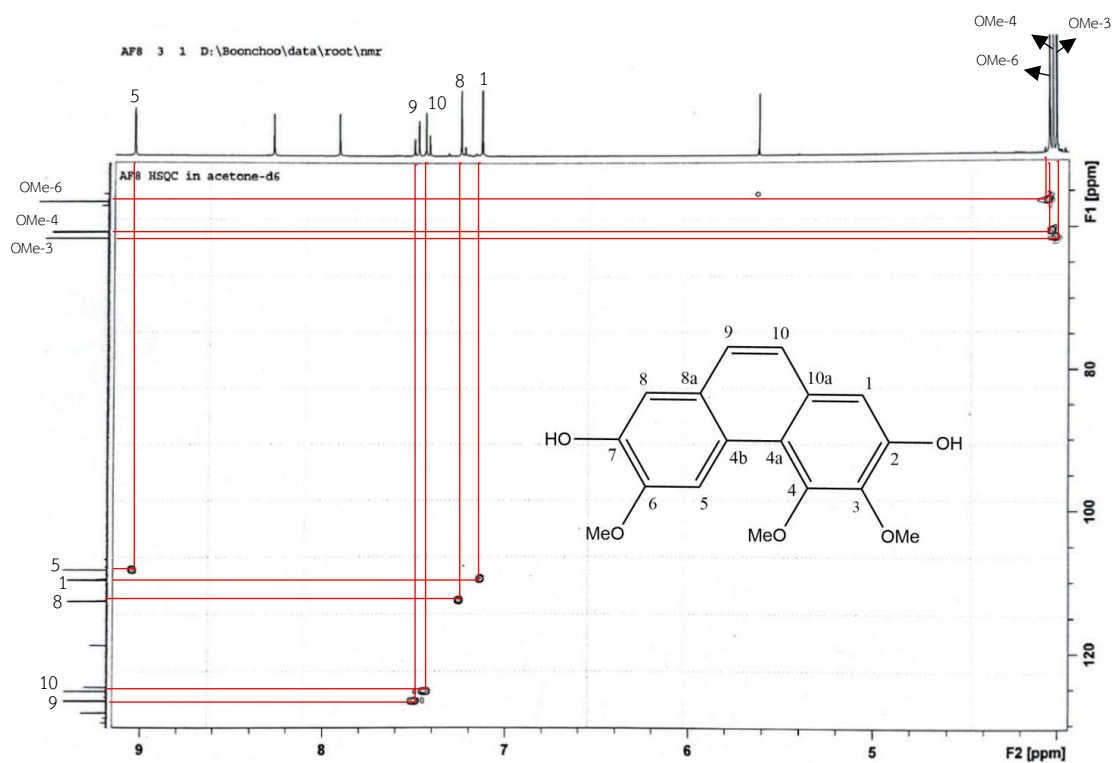


Figure 56 HSQC spectrum of compound AF5

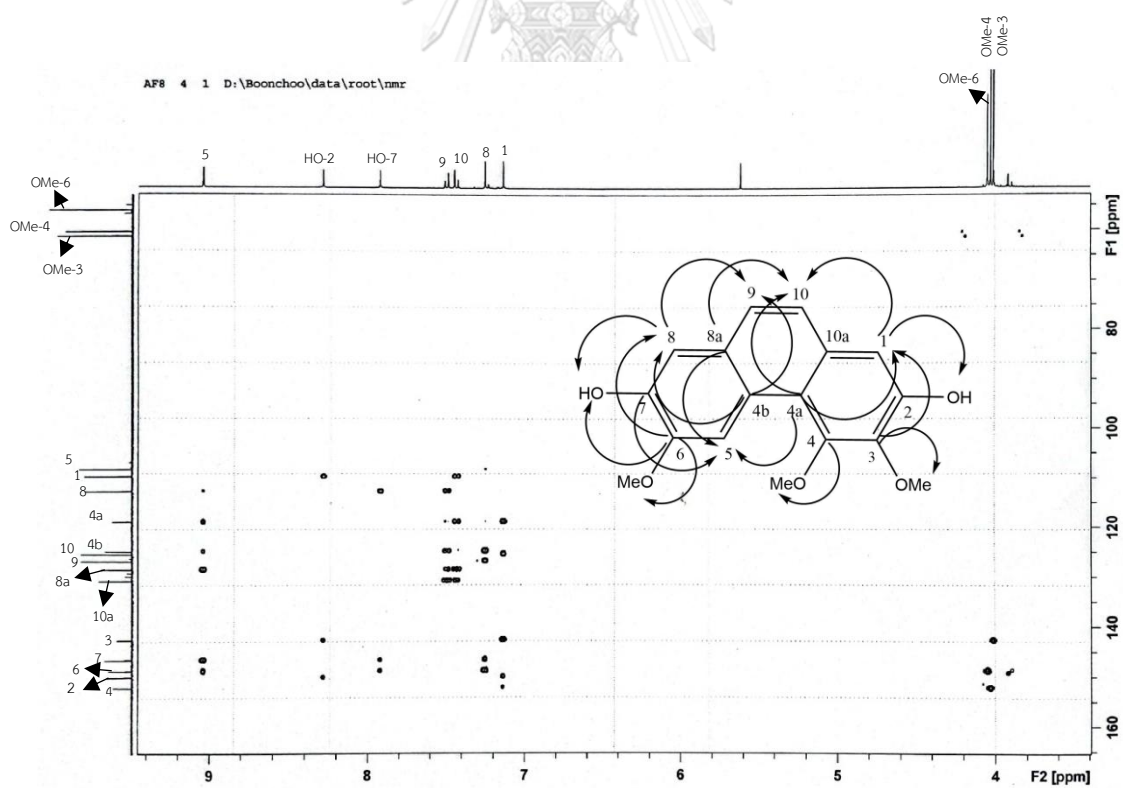


Figure 57 HMBC spectrum of compound AF5

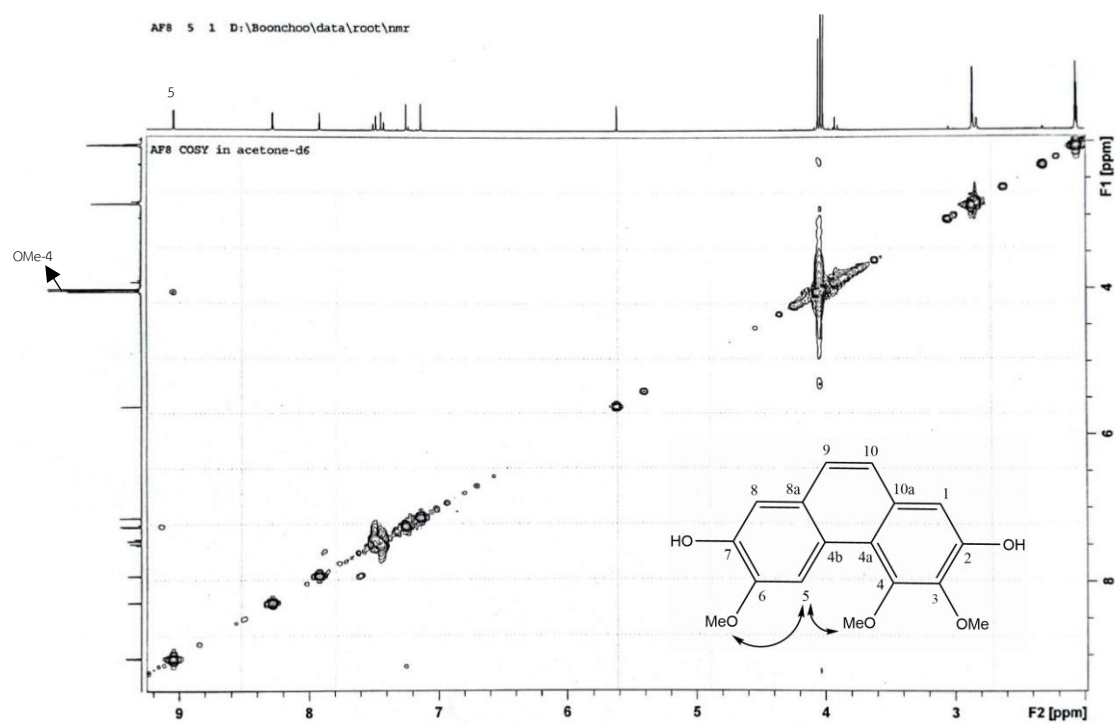


Figure 58 COSY spectrum of compound AF5

- Data compound AF6

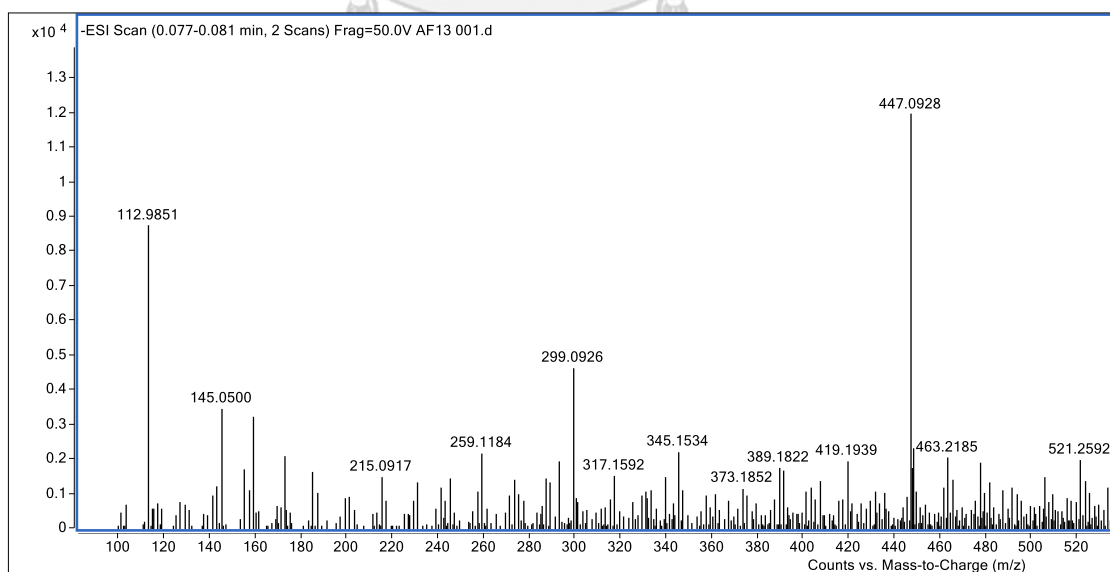
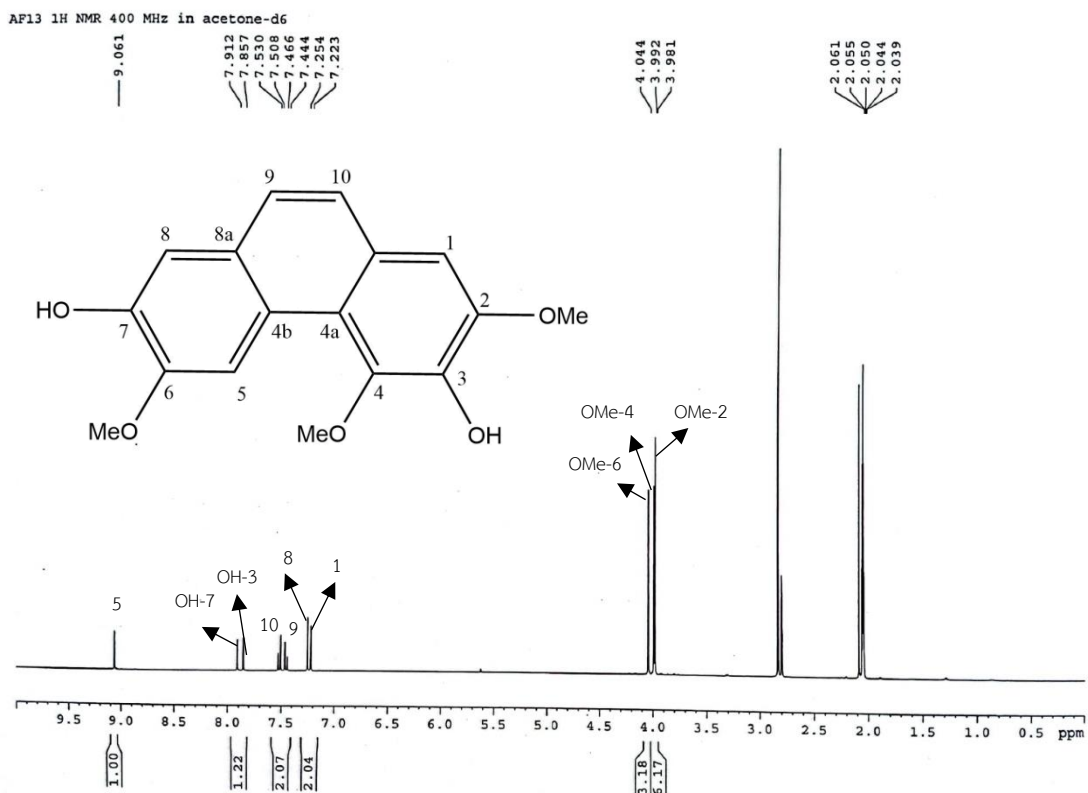
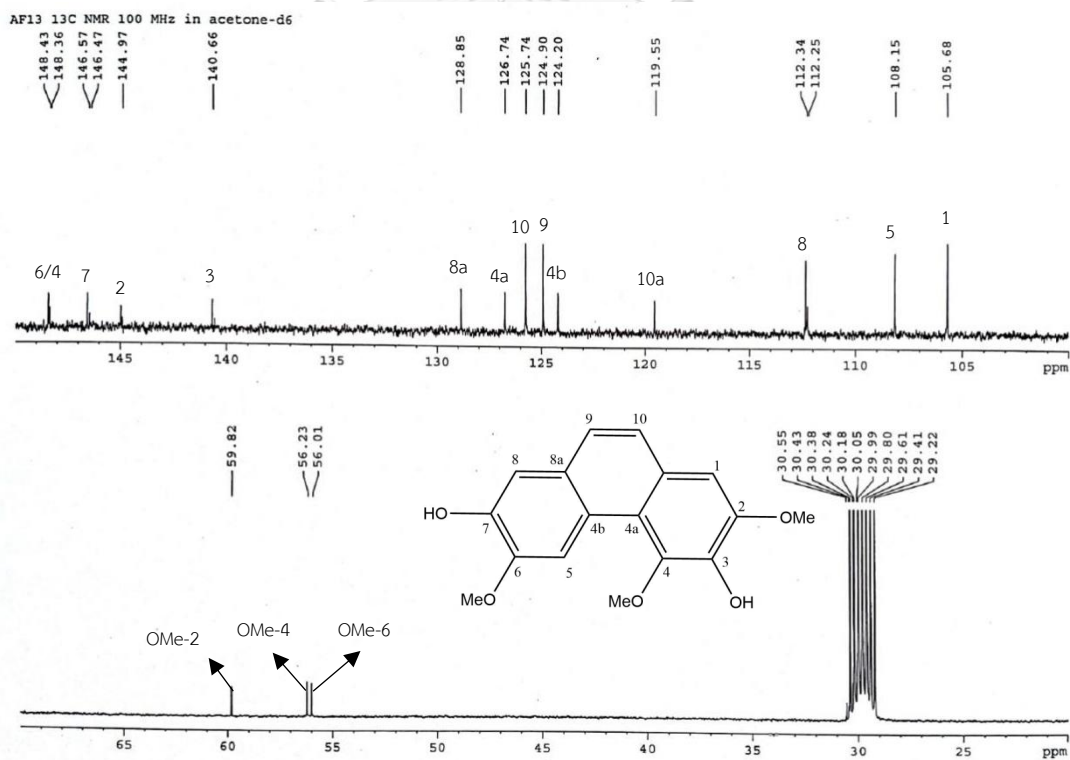


Figure 59 Mass spectrum of compound AF6

Figure 60  $^1\text{H}$ -NMR spectrum (400 MHz) of compound AF6Figure 61  $^{13}\text{C}$ -NMR spectrum (100 MHz) of compound AF6

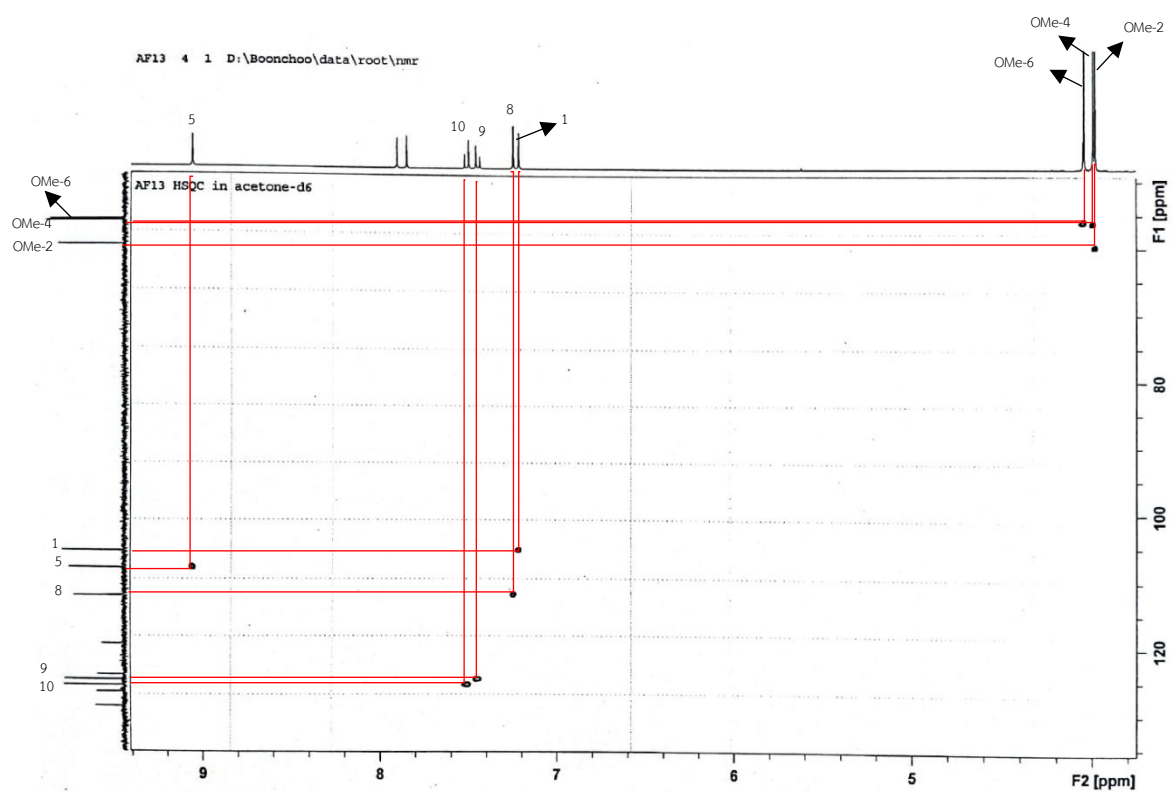


Figure 62 HSQC spectrum of compound AF6

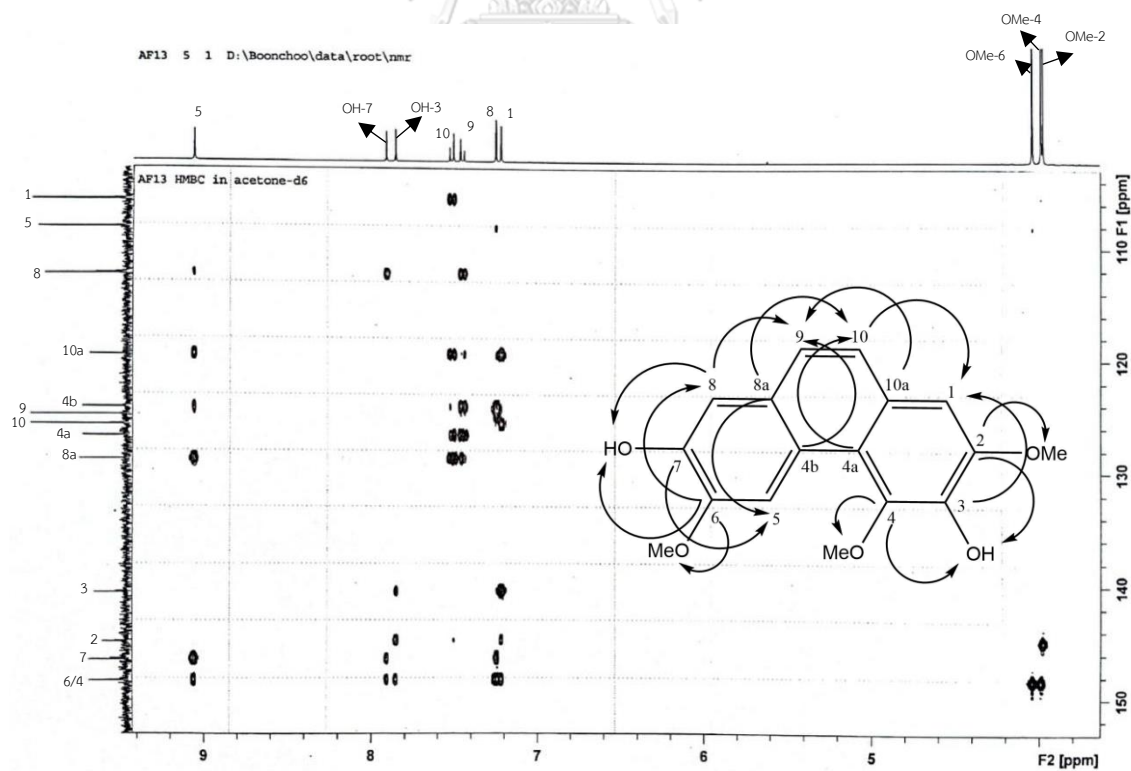


Figure 63 HMBC spectrum of compound AF6

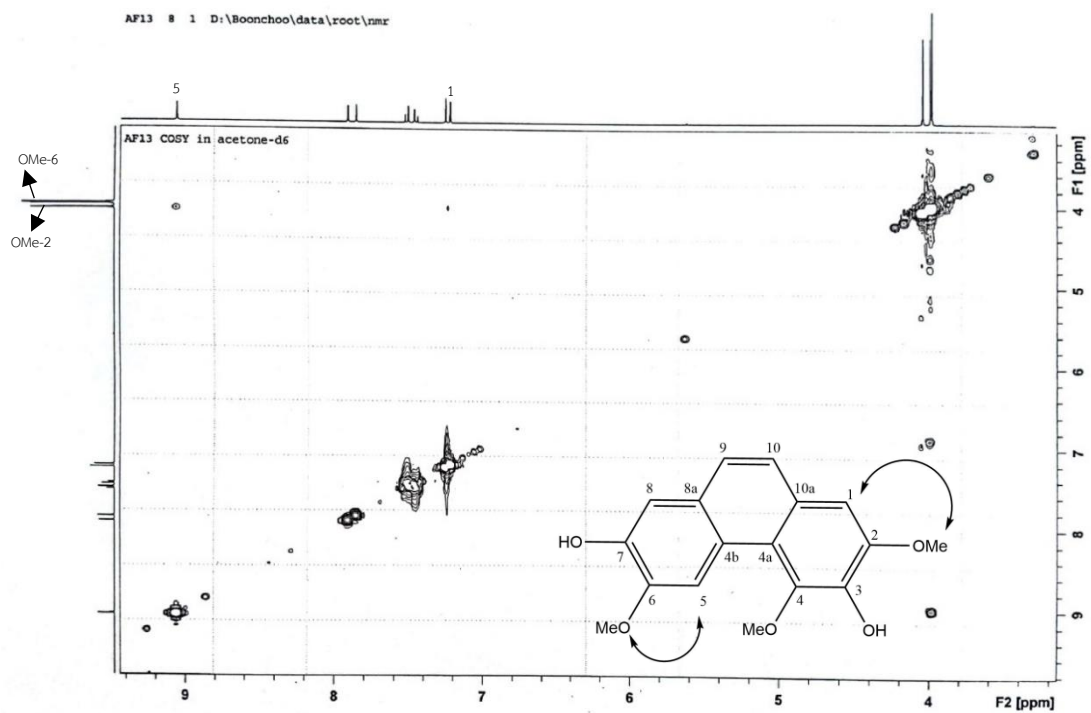


Figure 64 COSY spectrum of compound AF6

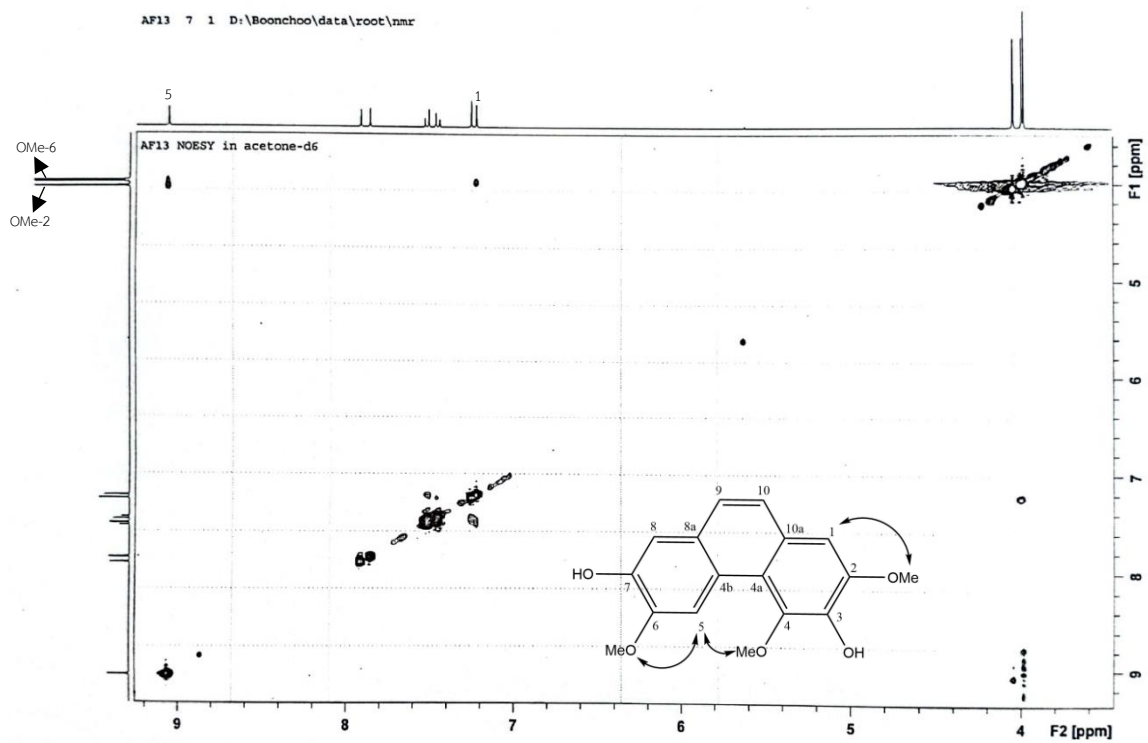


Figure 65 NOESY spectrum of compound AF6



● Data compound AF7

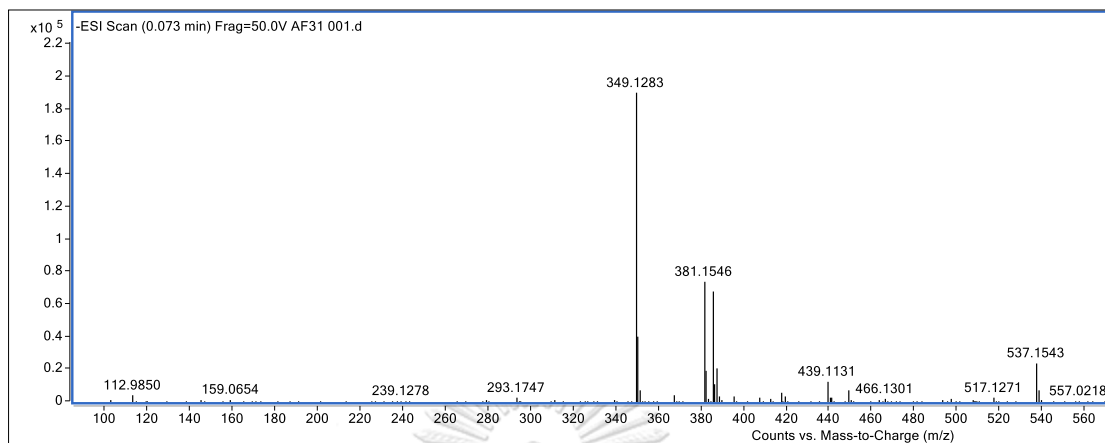


Figure 66 Mass spectrum of compound AF7

AF35 <sup>1</sup>H-NMR (400 MHz) in acetone-d<sub>6</sub>

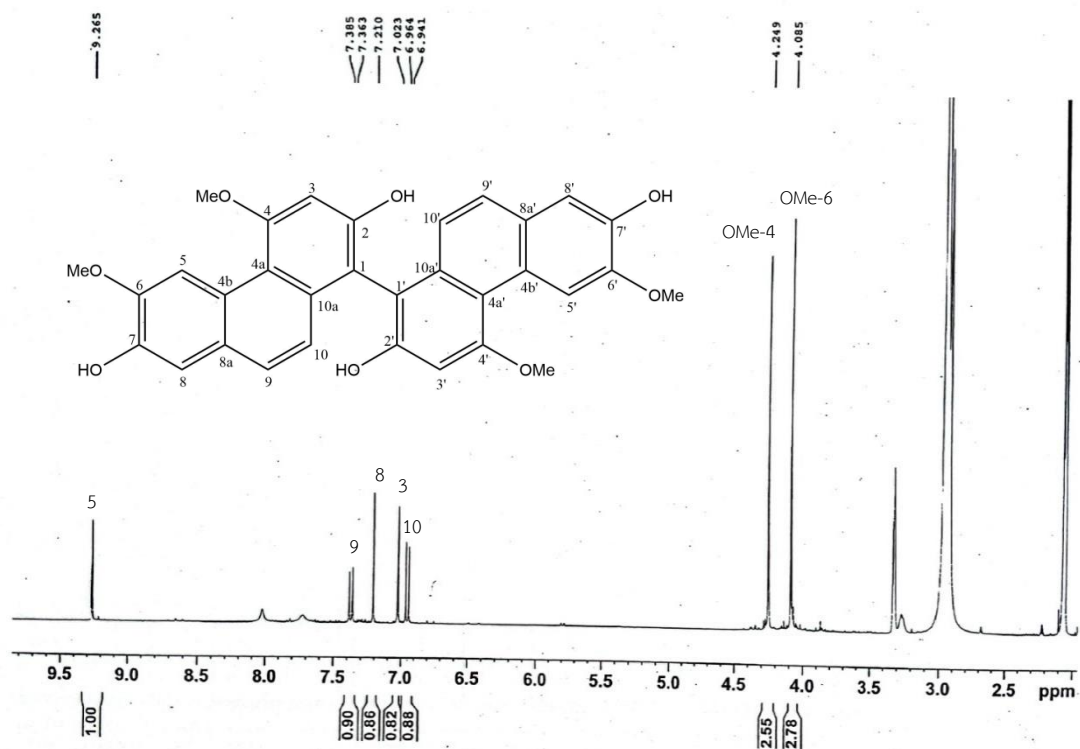


Figure 67 <sup>1</sup>H-NMR spectrum (400 MHz) of compound AF7



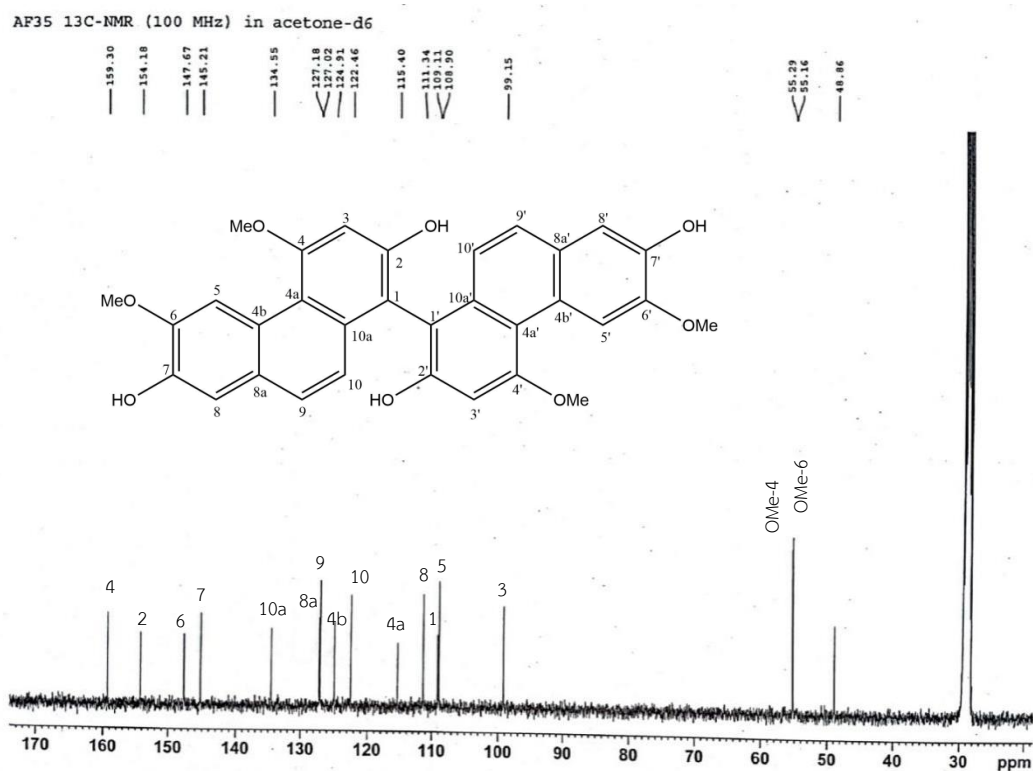


Figure 68  $^{13}\text{C-NMR}$  spectrum (100 MHz) of compound AF7

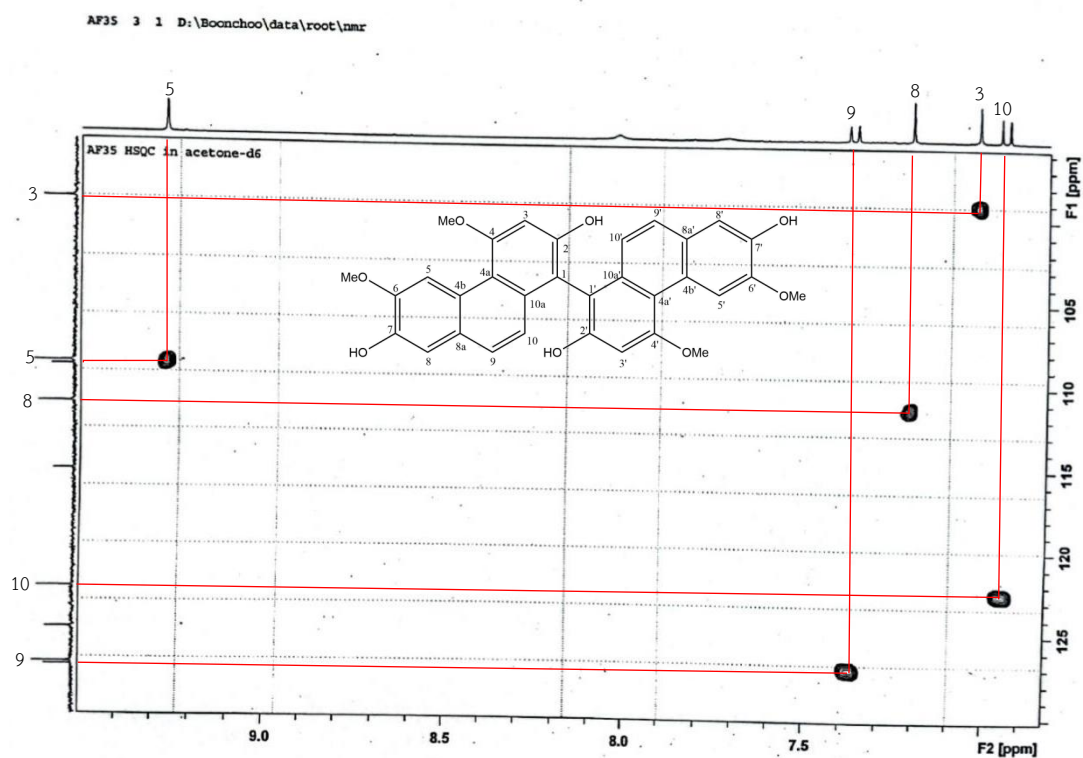


Figure 69 HSQC spectrum of compound AF7 (6.8-9.5 ppm and 95-130 ppm)

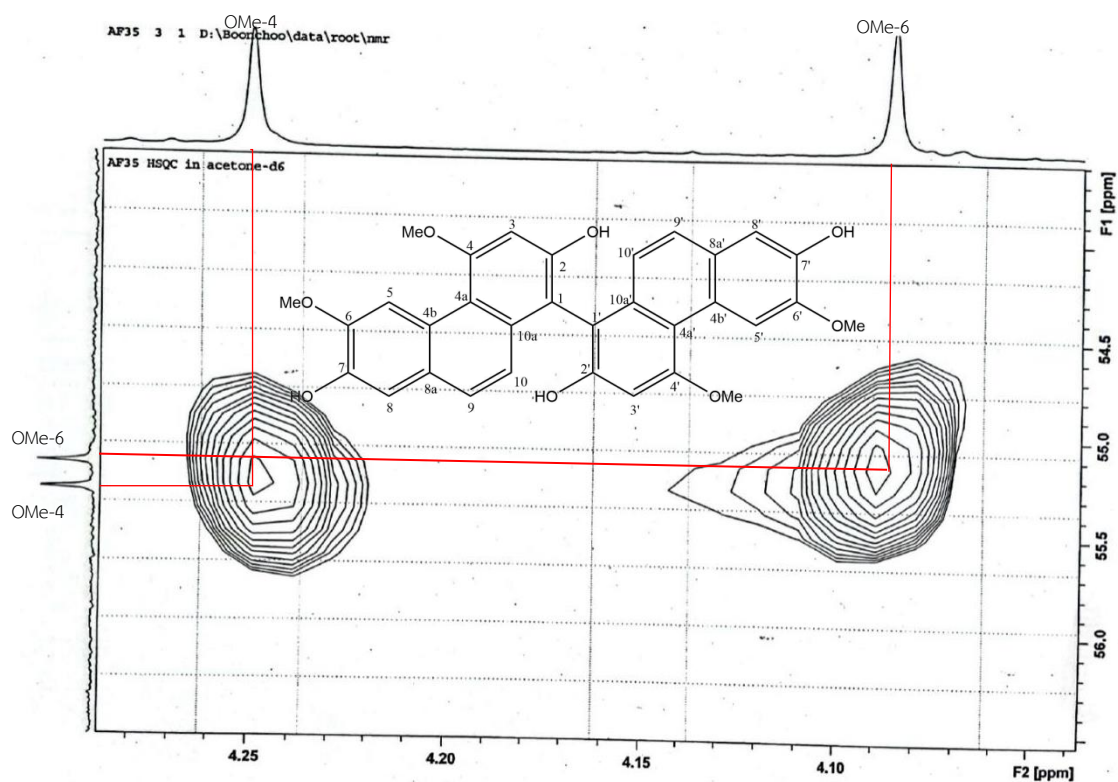


Figure 70 HSQC spectrum of compound AF7 (4.04-4.29 ppm and 54.1-56.5 ppm)

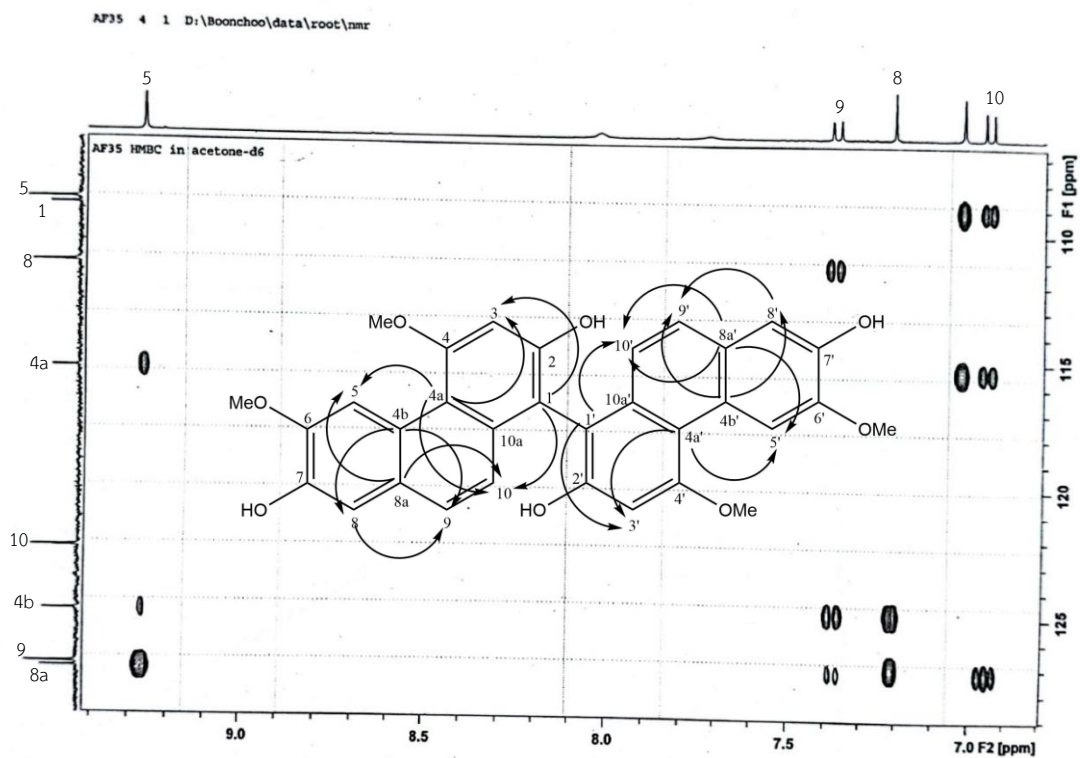


Figure 71 HMBC spectrum of compound AF7 (6.8-9.4 ppm and 107-129 ppm)



- Data compound AF8

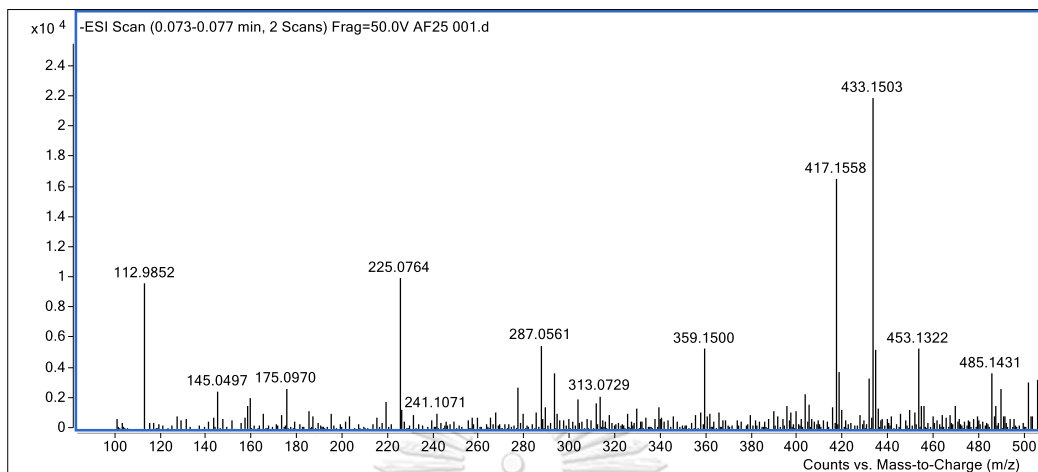


Figure 74 Mass spectrum of compound AF8

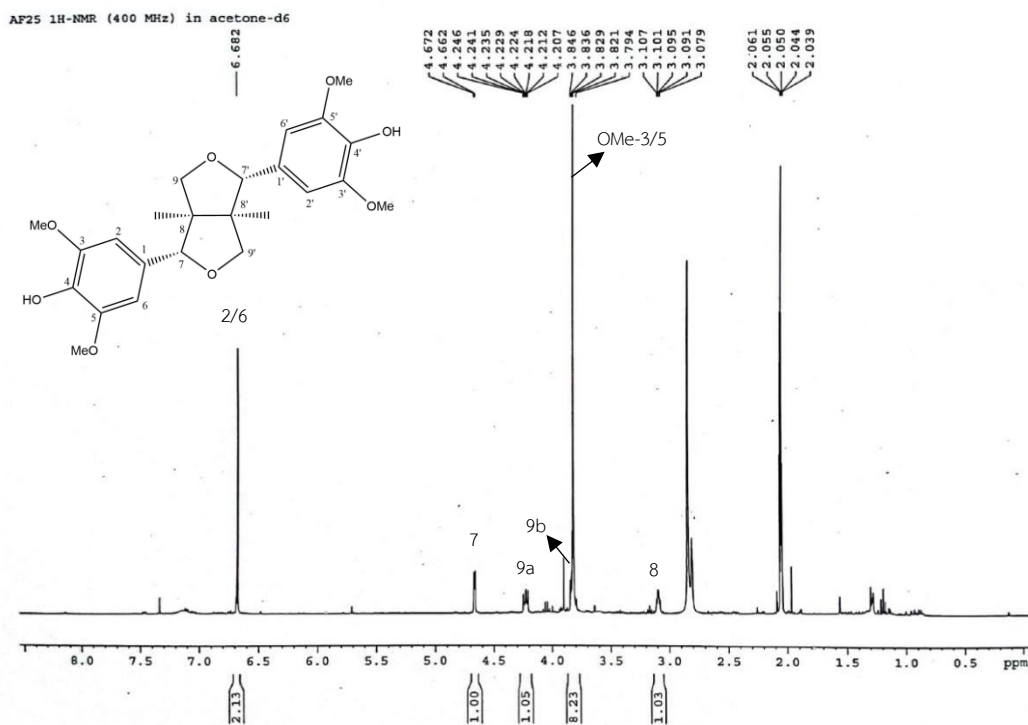


Figure 75 <sup>1</sup>H-NMR spectrum (400 MHz) of compound AF8

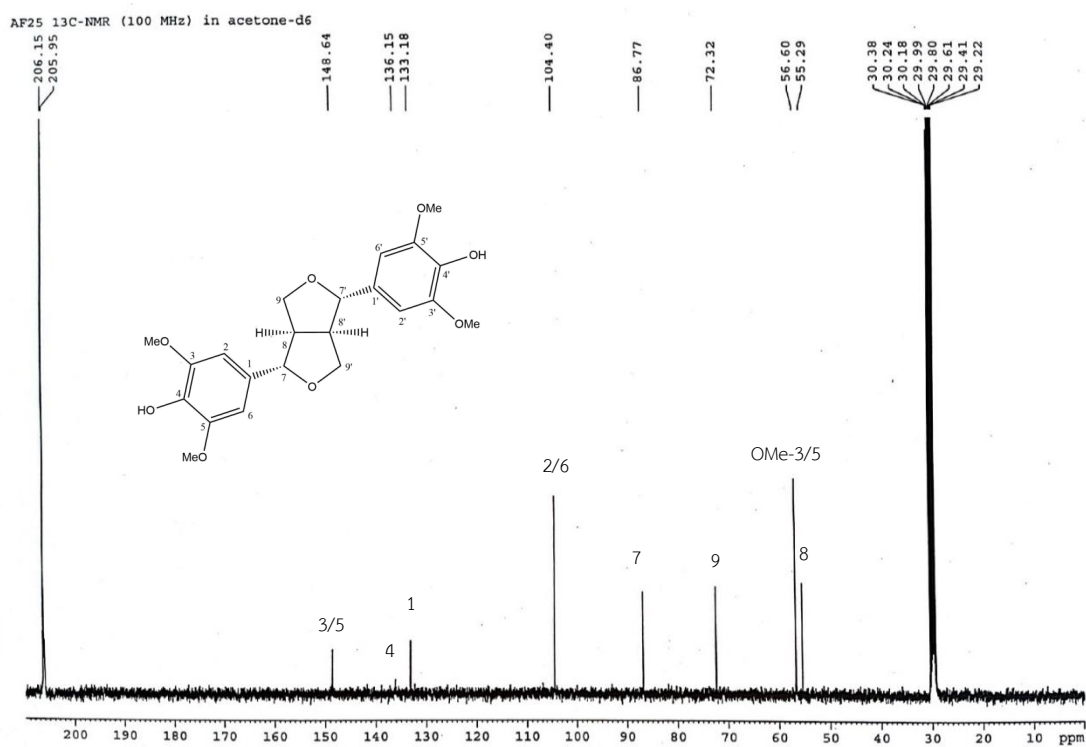


Figure 76  $^{13}\text{C}$ -NMR spectrum (100 MHz) of compound AF8

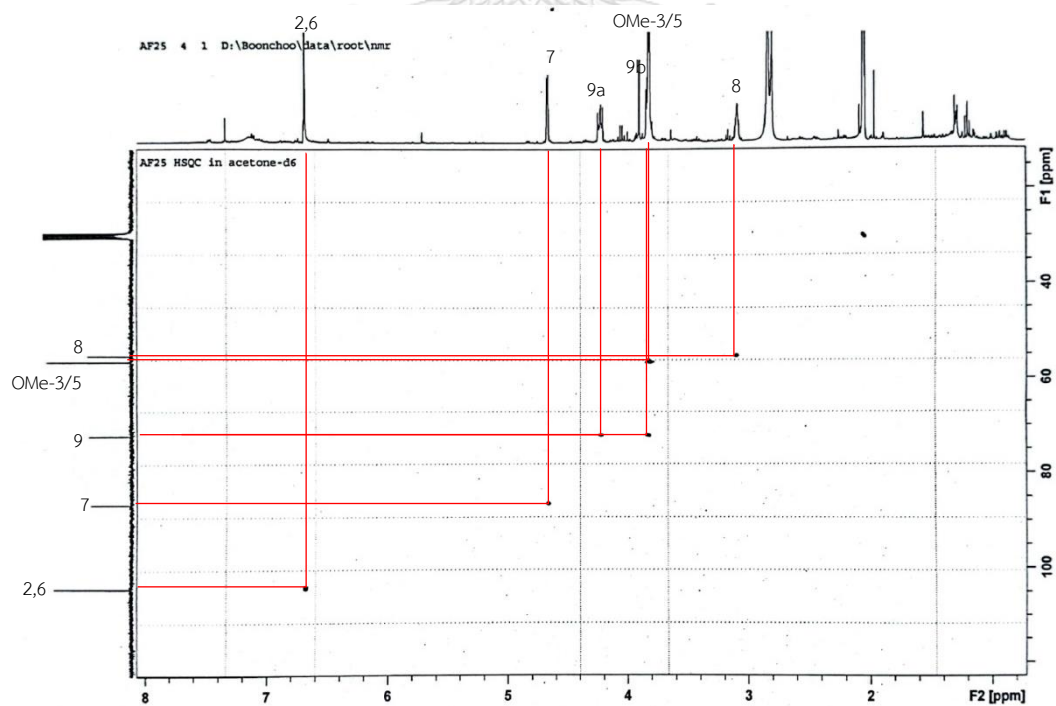


Figure 77 HSQC spectrum of compound AF8



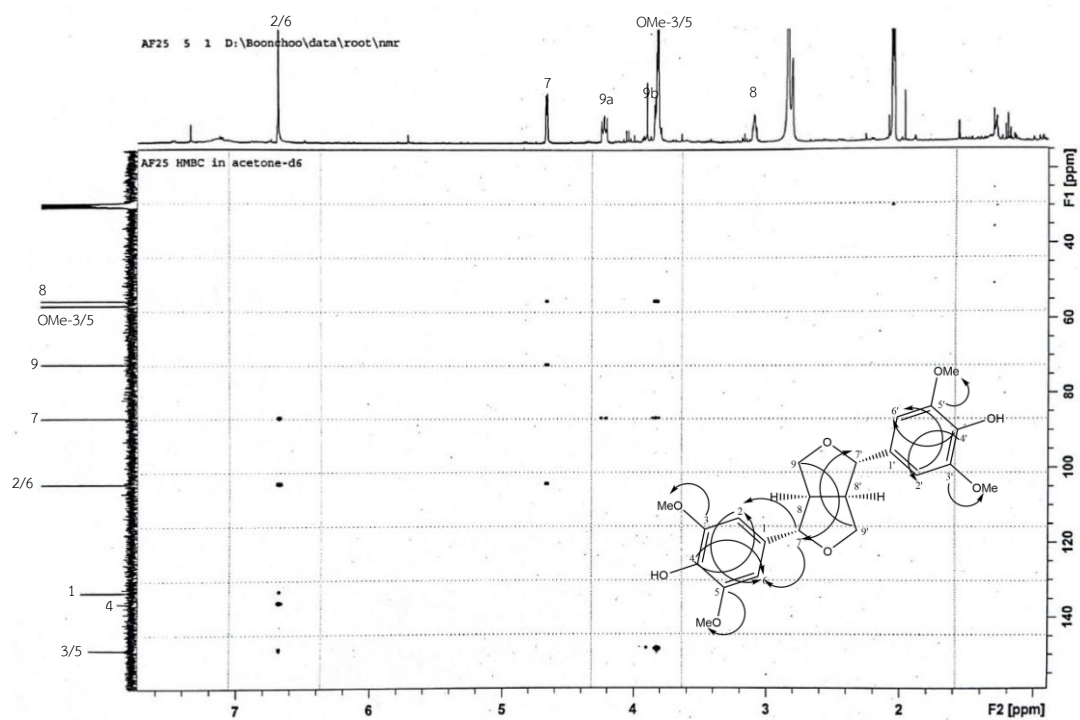


Figure 78 HMBC spectrum of compound AF8

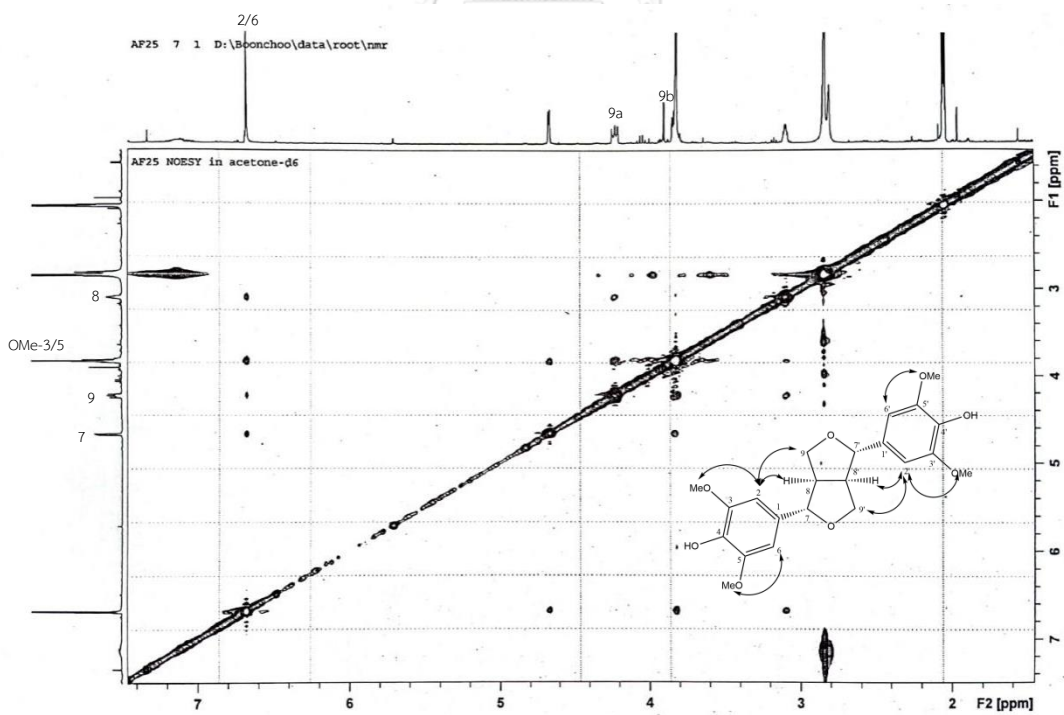


Figure 79 NOESY spectrum of compound AF8

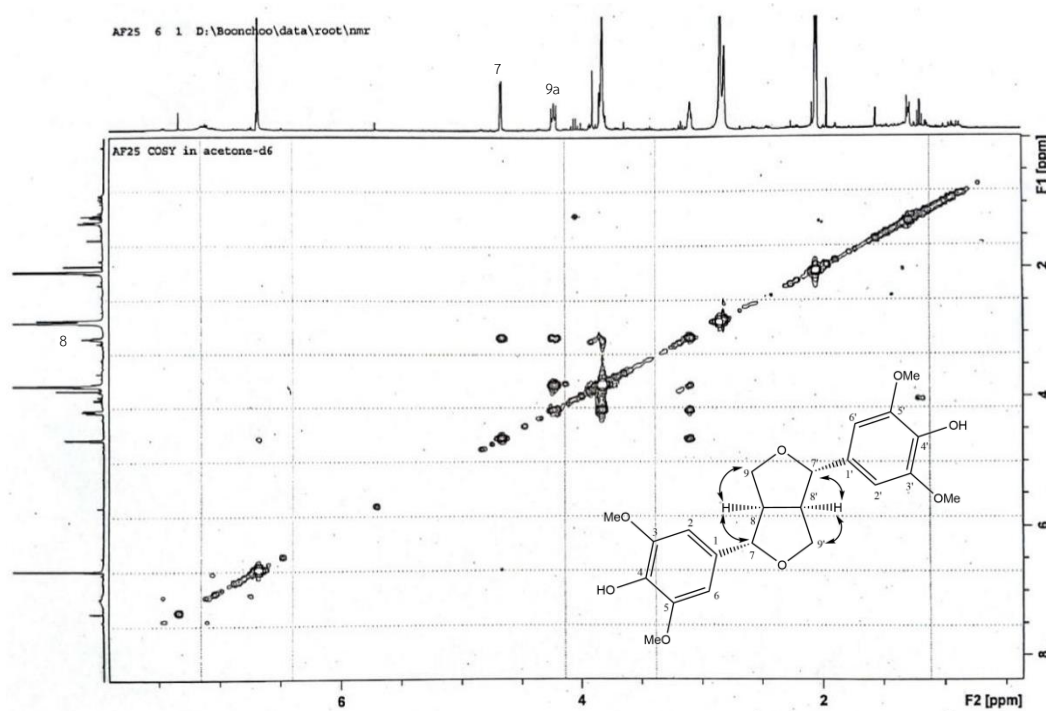


Figure 80 COSY spectrum of compound AF8

- Data compound AF9

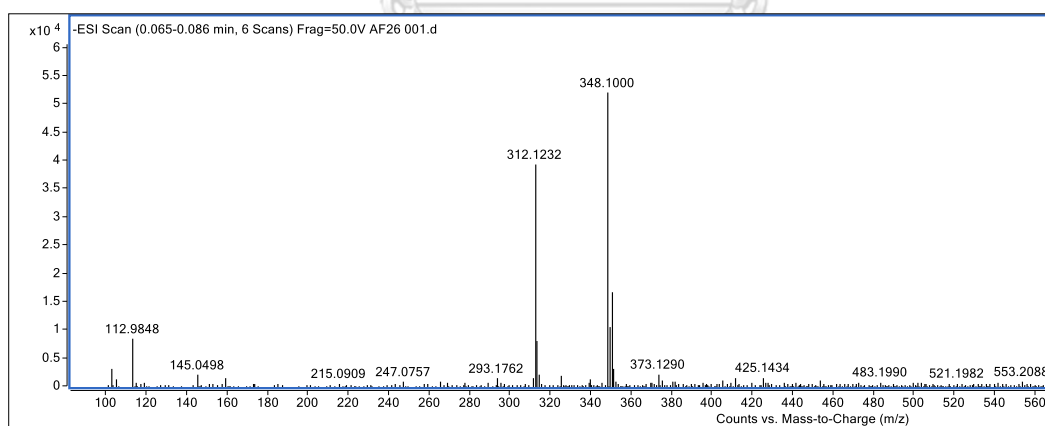


Figure 81 Mass spectrum of compound AF9

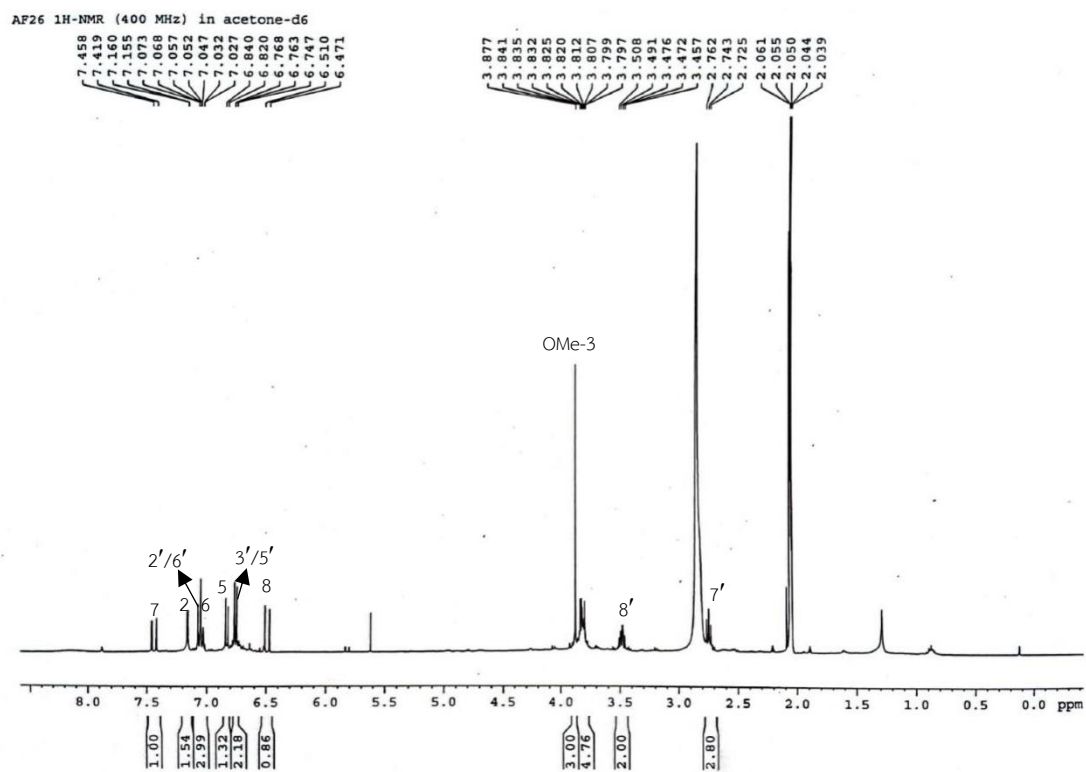


Figure 82  $^1\text{H-NMR}$  spectrum (400 MHz) of compound AF9

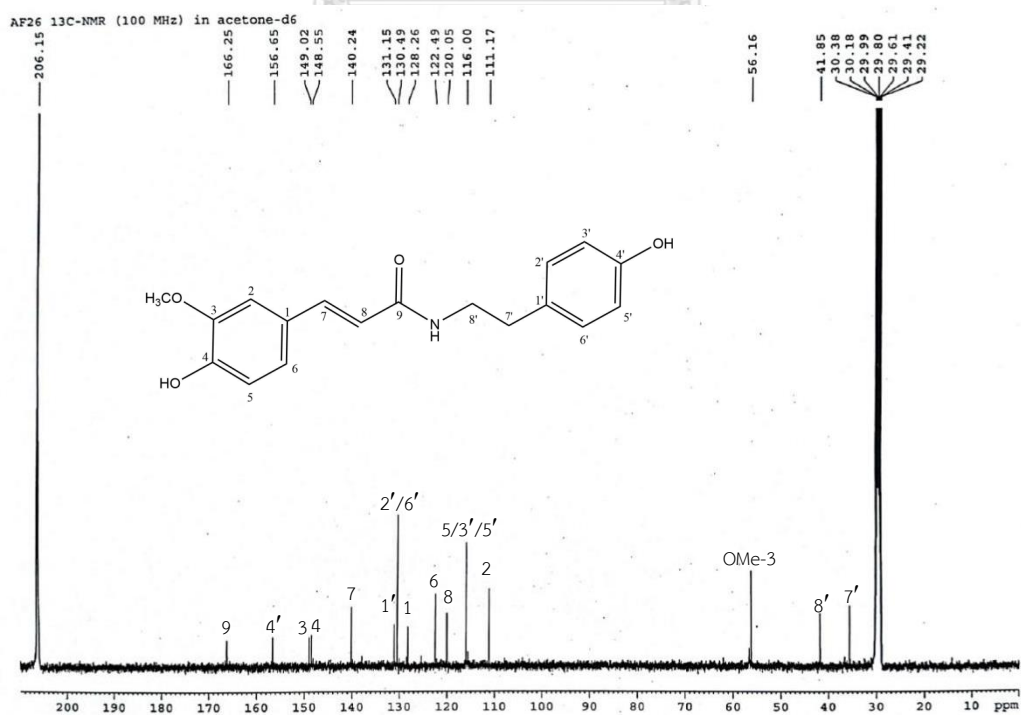


Figure 83  $^{13}\text{C-NMR}$  spectrum (100 MHz) of compound AF9



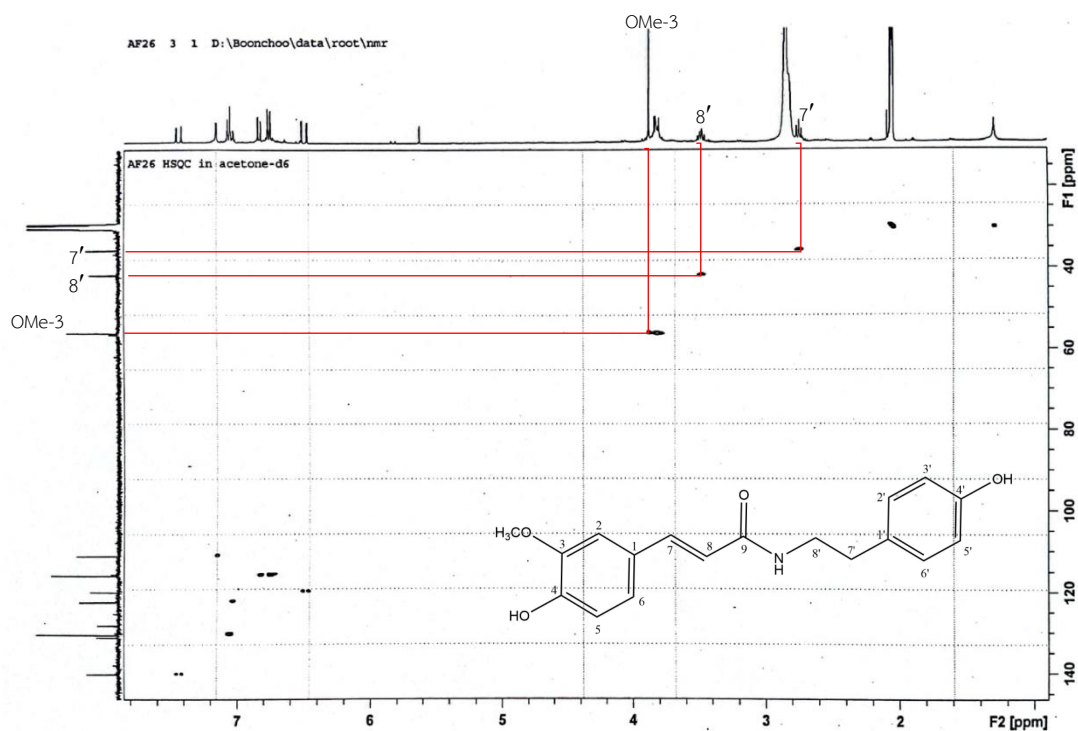


Figure 84 HSQC spectrum of compound AF9 (1-8 ppm and 30-145 ppm)

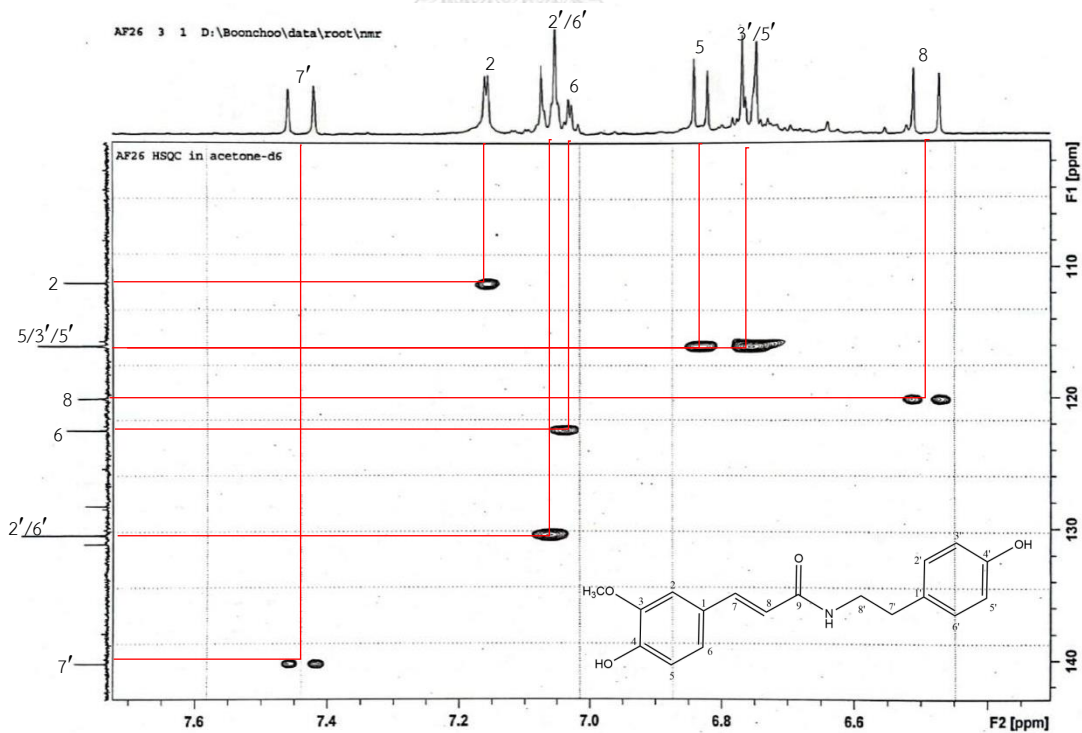


Figure 85 HSQC spectrum of compound AF9 (6.3-7.7 ppm and 100-142 ppm)

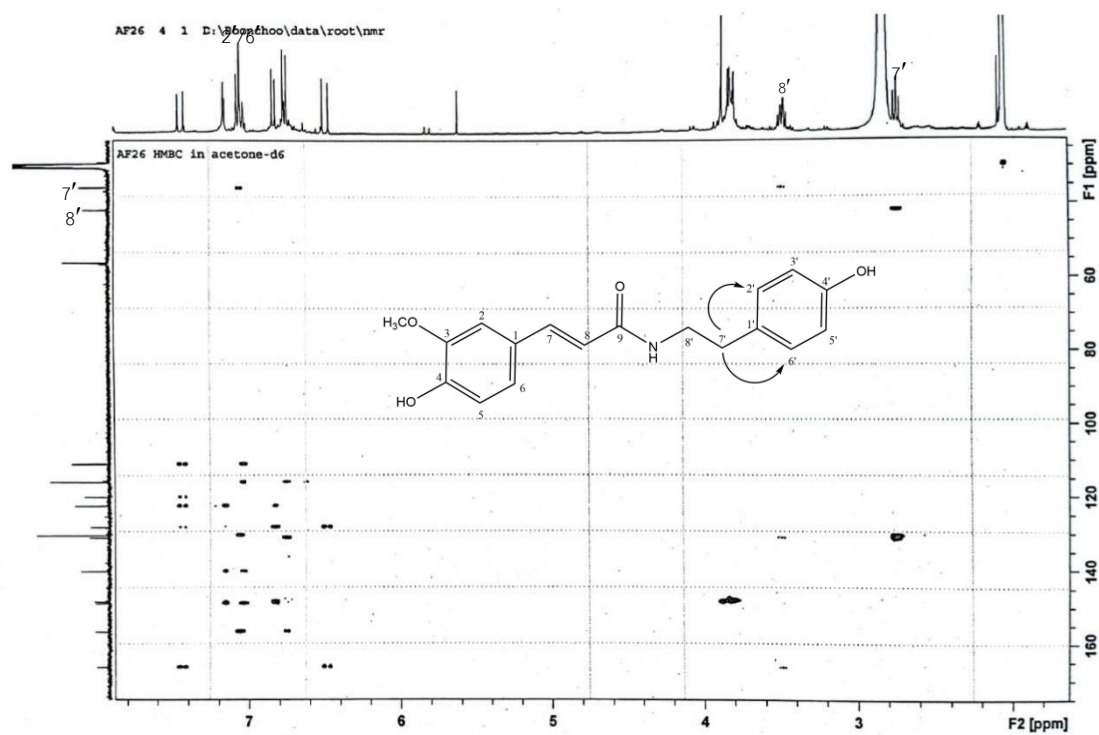


Figure 86 HMBC spectrum of compound AF9 (1.8-7.8 ppm and 70-150 ppm)

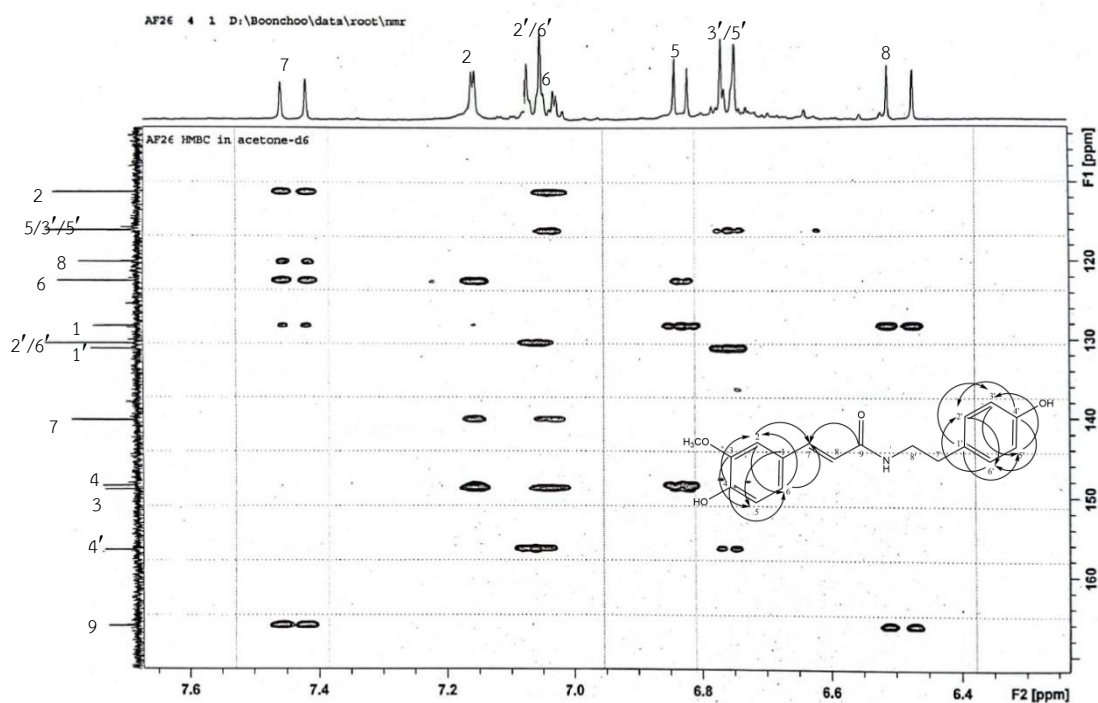


Figure 87 HMBC spectrum of compound AF9 (6.3-7.6 ppm and 114-170 ppm)

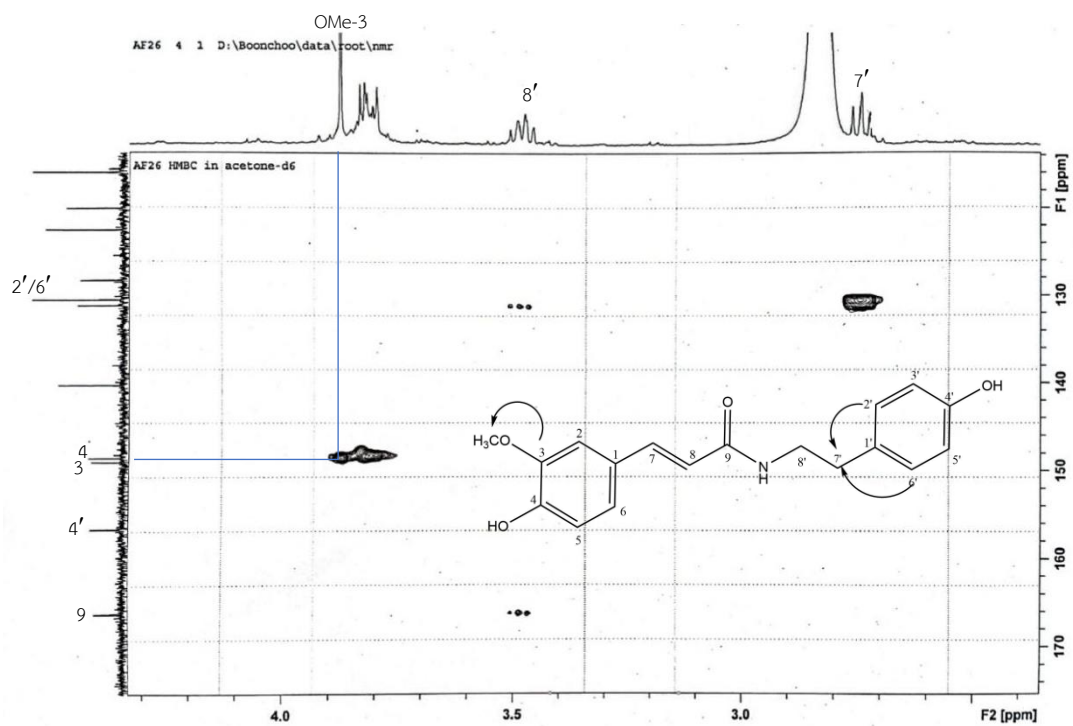


Figure 88 HMBC spectrum of compound AF9 (1.9-4.3 ppm and 114-174 ppm)

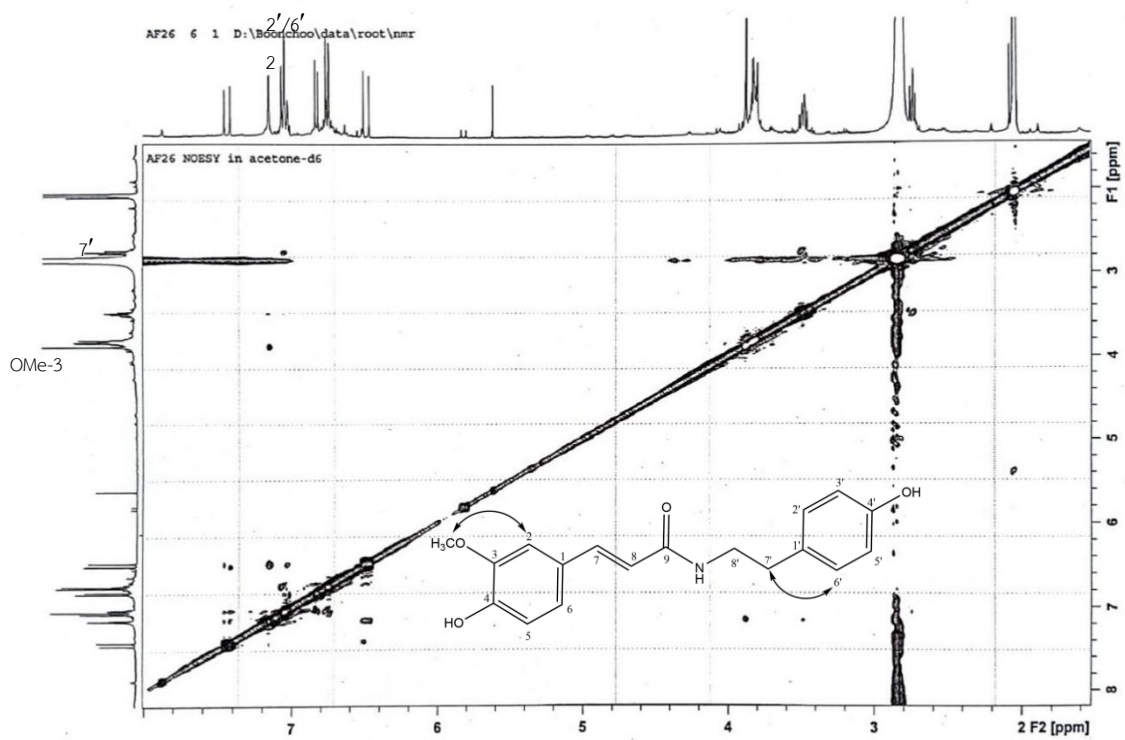
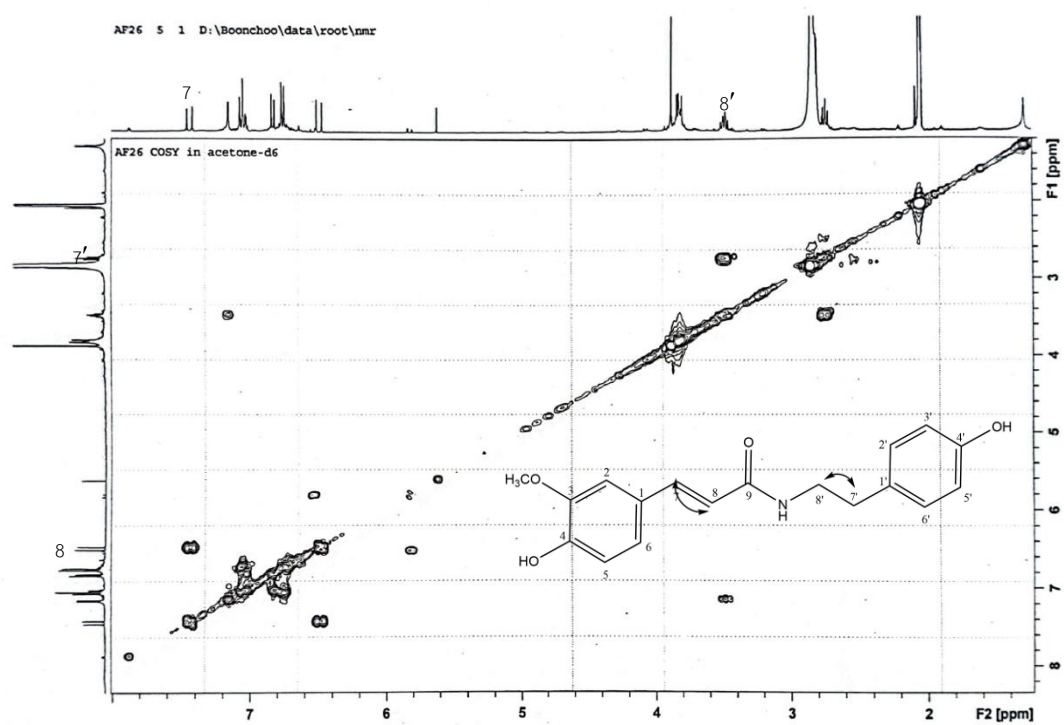


Figure 89 NOESY spectrum of compound AF9



- Data compound AF10

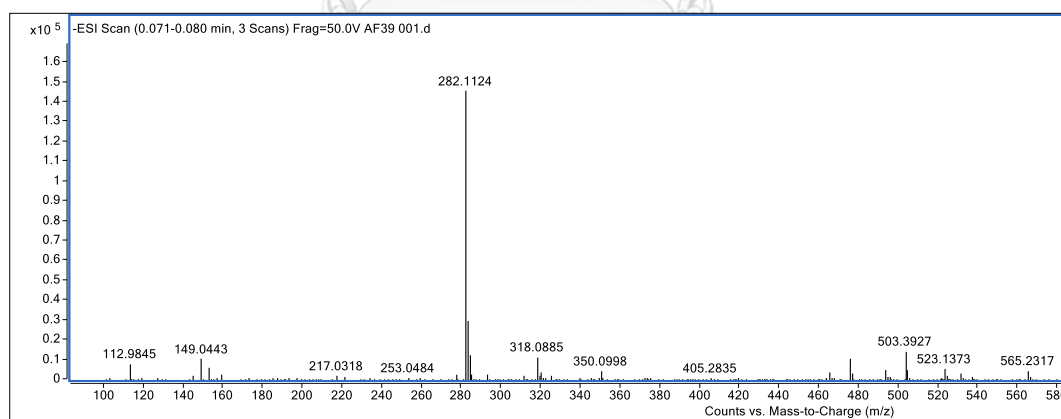


Figure 91 Mass spectrum of compound AF10

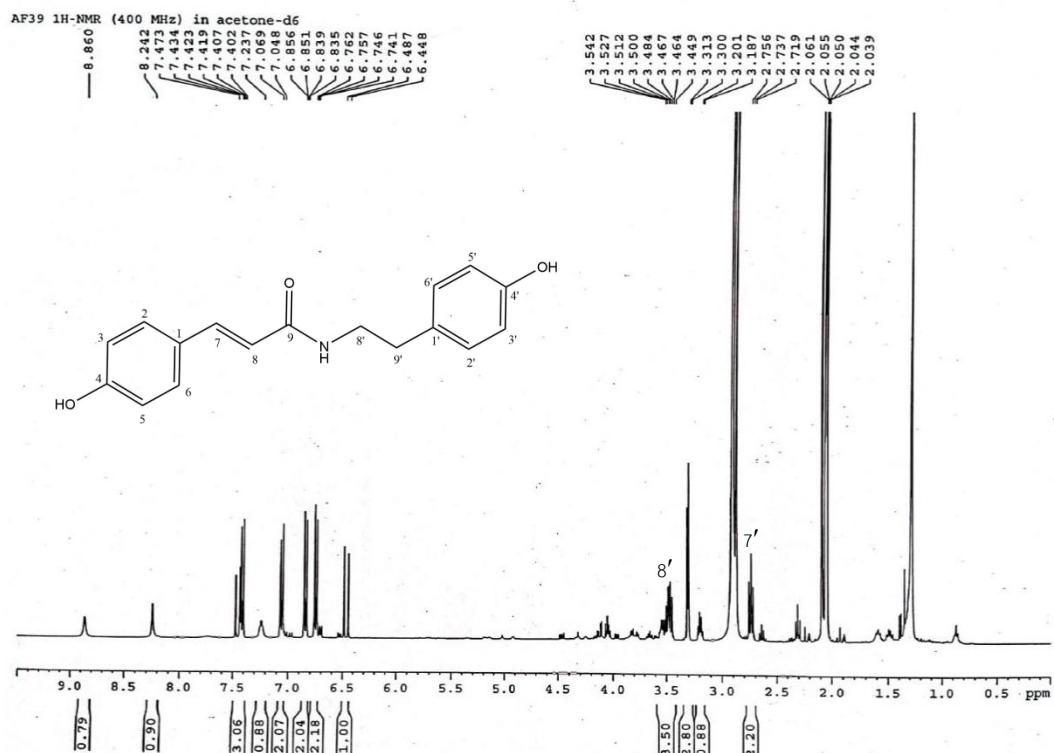


Figure 92 <sup>1</sup>H-NMR spectrum (400 MHz) of compound AF10 (0.5-10 ppm)

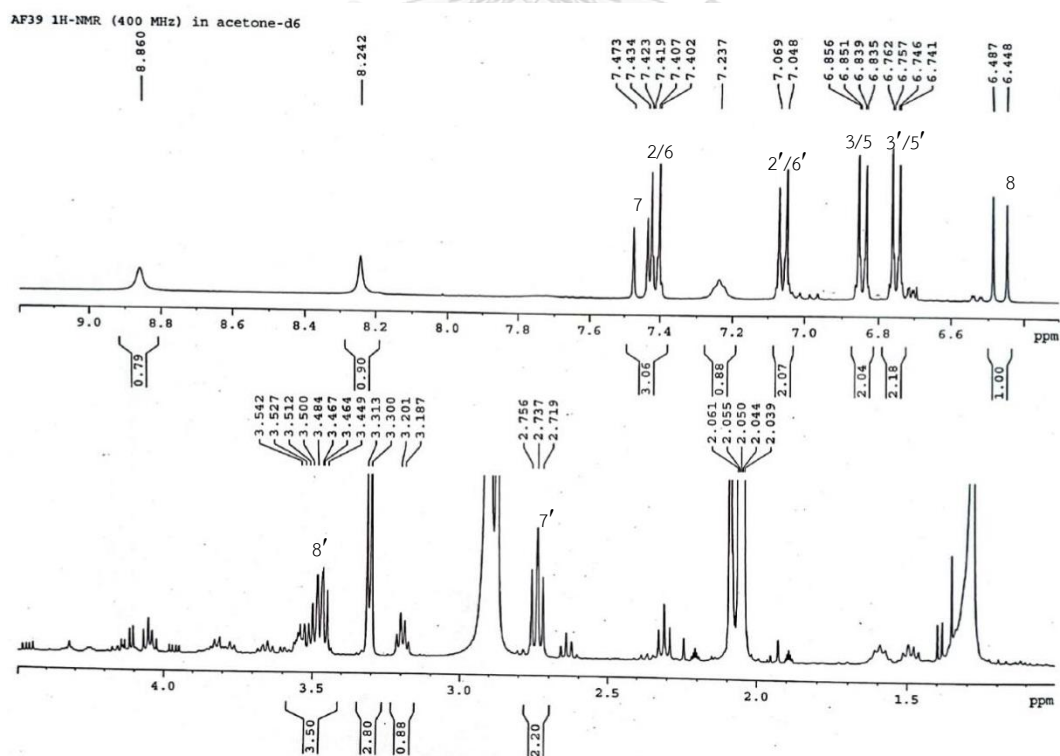
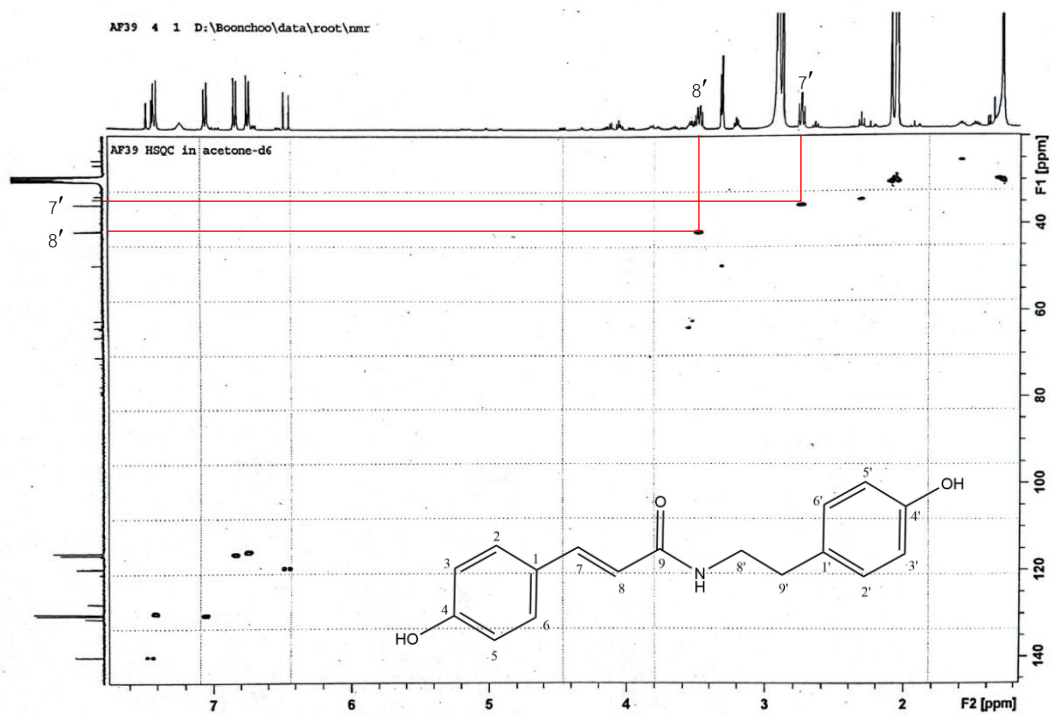
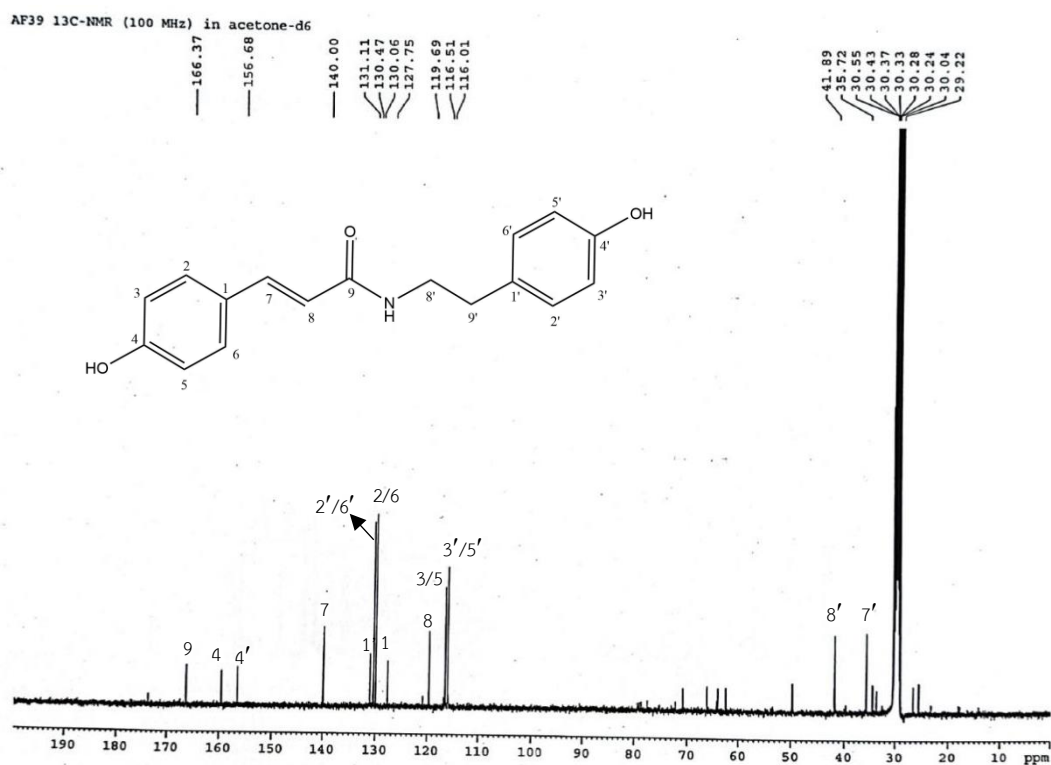


Figure 93 <sup>1</sup>H-NMR spectrum (400 MHz) of compound AF10 (1-10 ppm)





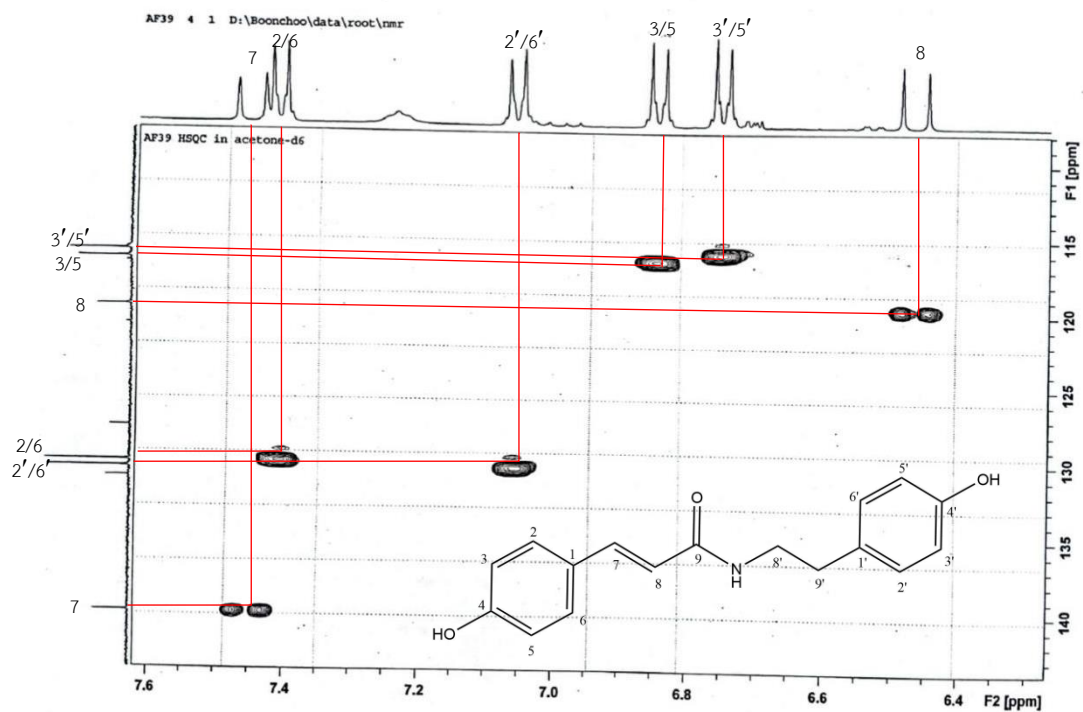


Figure 96 HSQC spectrum of compound AF10 (6.3-7.6 ppm and 108-143 ppm)

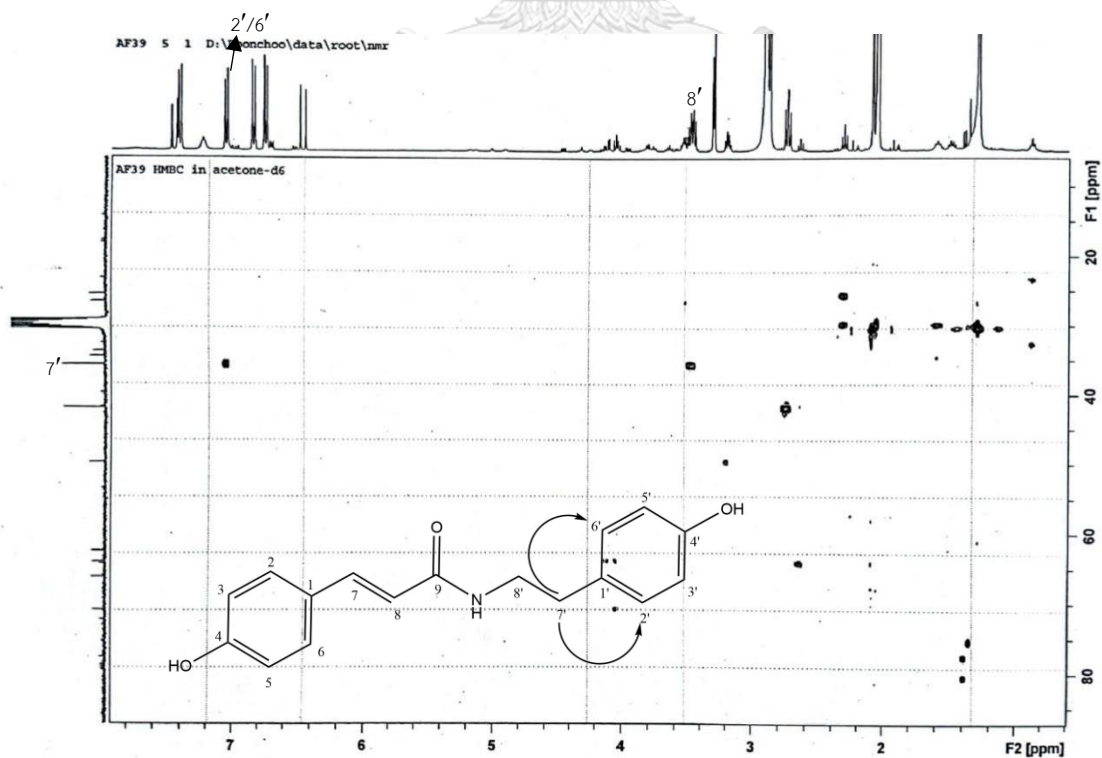


Figure 97 HMBC spectrum of compound AF10 (0.6-8 ppm and 5-85 ppm)

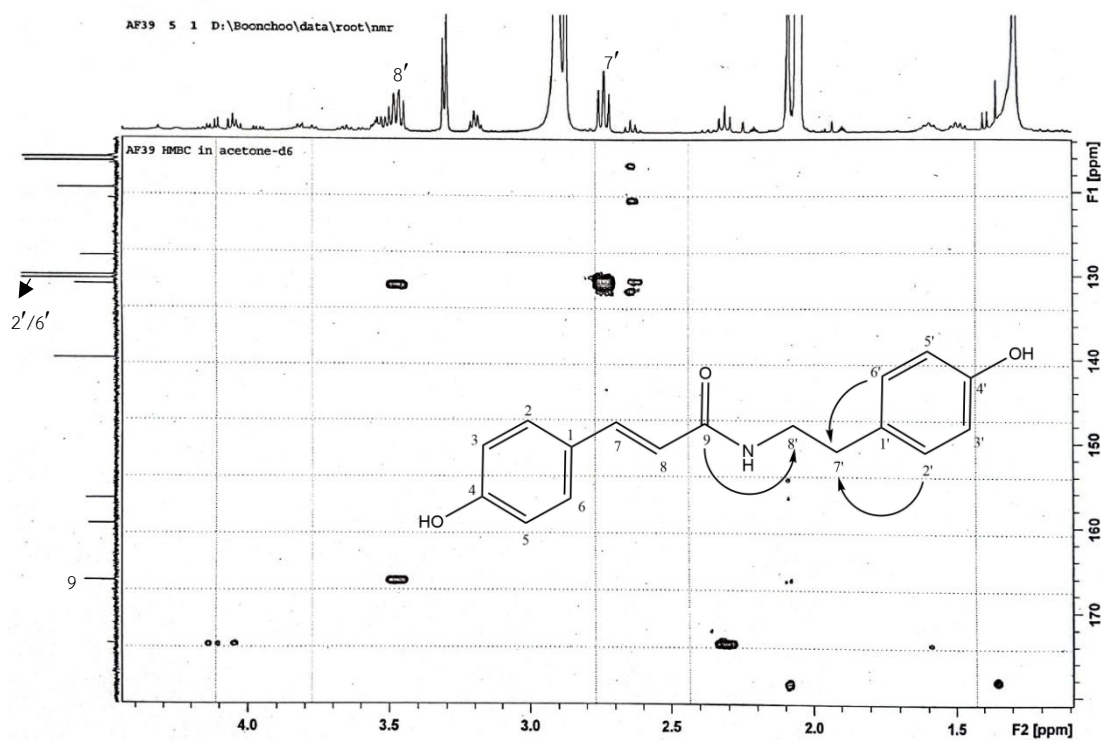


Figure 98 HMBC spectrum of compound AF10 (1.1-4.5 ppm and 114-180 ppm)

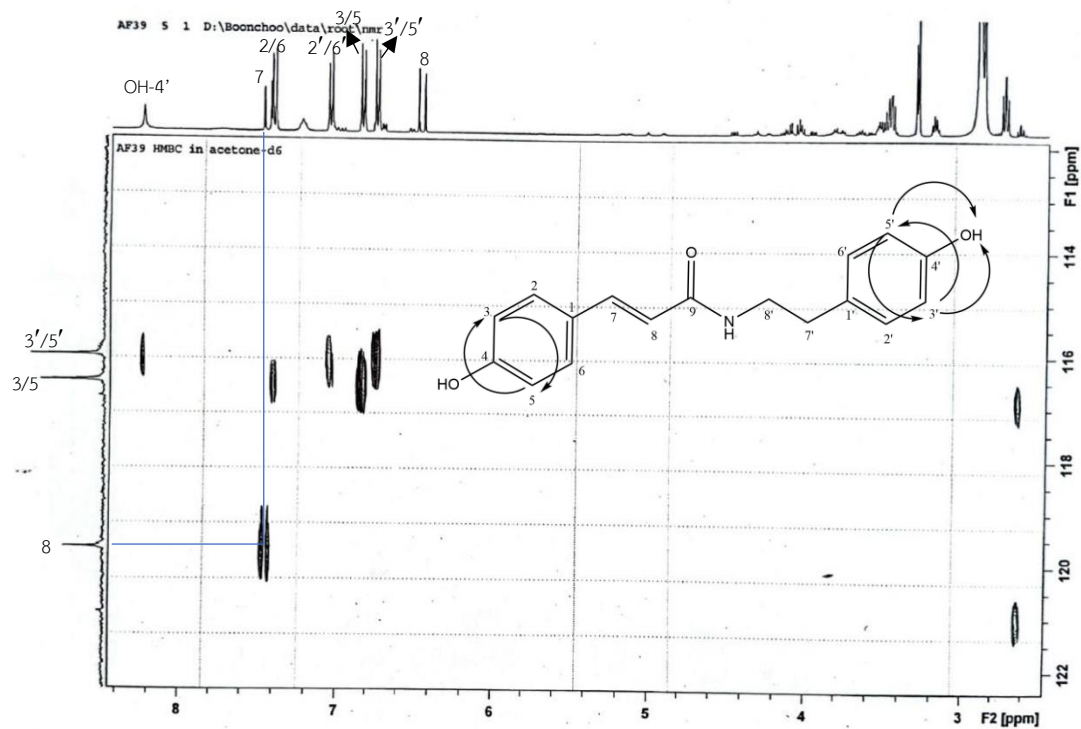


Figure 99 HMBC spectrum of compound AF10 (2.4-8.4 ppm and 112-122 ppm)



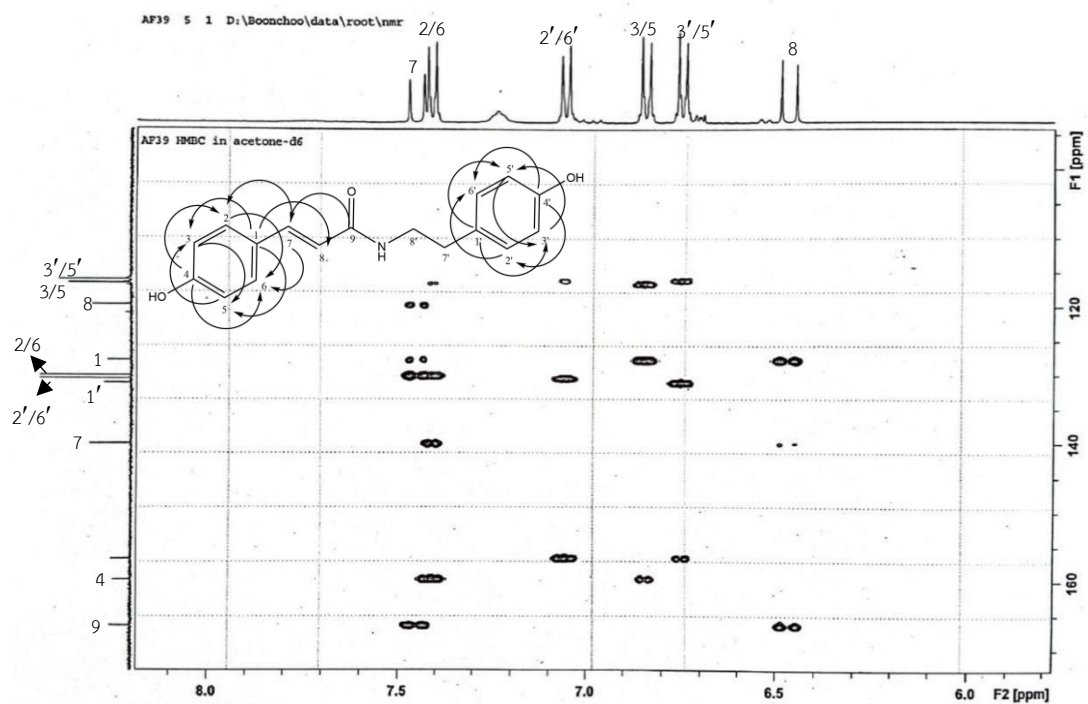


Figure 100 HMBC spectrum of compound AF10 (5.8-8.2 ppm and 95-170 ppm)

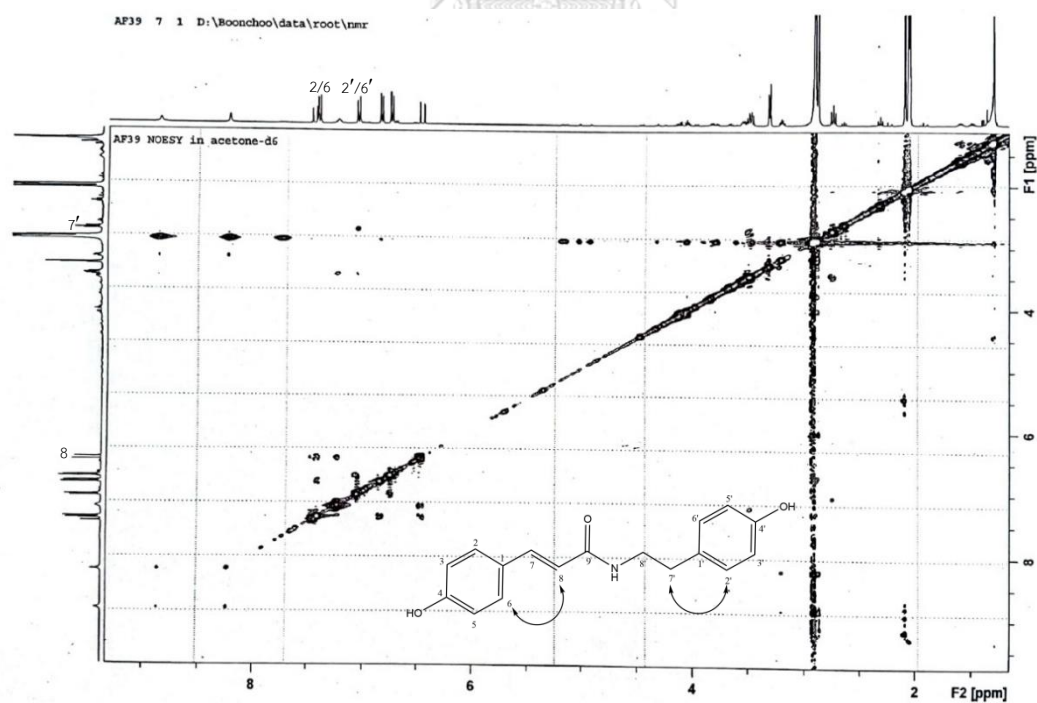


Figure 101 NOESY spectrum of compound AF10

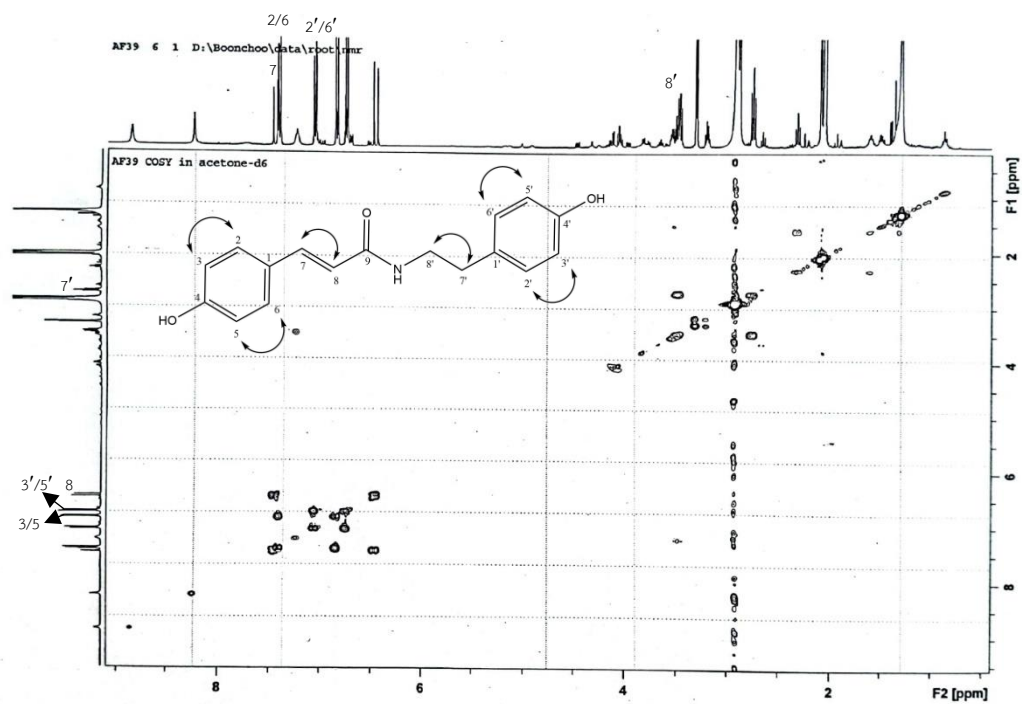


Figure 102 COSY spectrum of compound AF10

- Summary cell viability (MTT assay)

Conc.	Percentage cell viability			AVG	SD
	N1	N2	N3		
COMP.1					
80	14.069038	12.881367	13.118475	13.4	0.6
40	16.265691	14.364419	15.161144	15.3	1.0
20	23.012554	18.432219	18.157058	19.9	2.7
10	47.489542	53.813605	31.139355	44.1	11.7
5	106.27616	98.008558	102.40581	102.2	4.1
0	100	100	100	100.0	0.0

Conc.	Percentage cell viability			AVG	SD
	N1	N2	N3		
COMP.2					
80	103.19423	102.46741	103.61057	103.1	0.6
40	103.50335	98.417132	101.93424	101.3	2.6
20	101.95775	95.018622	101.41844	99.5	3.9
10	101.85471	98.836127	91.166989	97.3	5.5
5	100.82432	102.51397	98.774984	100.7	1.9
0	100	100	100	100.0	0.0

Conc.	Percentage cell viability			AVG	SD
	N1	N2	N3		
COMP.3					
80	70.189432	78.271729	84.469503	77.6	7.2
40	128.0658	120.77922	119.22091	122.7	4.7
20	113.06082	106.14386	108.50846	109.2	3.5
10	105.68295	96.303697	103.84418	101.9	5.0
5	100.1994	94.405595	98.974885	97.9	3.1
0	100	100	100	100.0	0.0

Conc.	Percentage cell viability			AVG	SD
	N1	N2	N3		
COMP.4					
80	69.684843	71.974522	68.421053	70.0	1.8
40	97.69885	88.535032	102.08442	96.1	6.9
20	92.696349	97.361238	105.26316	98.4	6.4
10	107.55378	102.00182	105.00261	104.9	2.8
5	109.2046	102.72975	95.049505	102.3	7.1
0	100	100	100	100.0	0.0

Conc.	Percentage cell viability			AVG	SD
	N1	N2	N3		
COMP.5					
80	83.977663	83.562293	83.801083	83.8	0.2
40	84.321306	86.972999	84.93353	85.4	1.4
20	98.152921	106.39507	102.26489	102.3	4.1
10	103.52234	103.22122	93.894633	100.2	5.5
5	102.27663	105.2108	99.162974	102.2	3.0
0	100	100	100	100.0	0.0

Conc.	Percentage cell viability			AVG	SD
	N1	N2	N3		
COMP.6					
80	85.253849	87.389356	82.04698	84.9	2.7
40	94.931313	105.10694	95.637584	98.6	5.7
20	97.051138	102.81407	97.818792	99.2	3.1
10	98.940548	105.78437	104.19463	103.0	3.6
5	96.728556	103.80417	101.67785	100.7	3.6
0	100	100	100	100.0	0.0

Conc.	Percentage cell viability			AVG	SD
	N1	N2	N3		
COMP.7					
80	33.77193	41.000026	23.778707	32.9	8.6
40	38.471178	43.250027	28.958228	36.9	7.3
20	64.912281	82.750052	70.865257	72.8	9.1
10	91.97995	96.31256	95.232546	94.5	2.3
5	102.25564	104.43757	95.526837	100.7	4.6
0	100	100	100	100.0	0.0

Conc.	Percentage cell viability			AVG	SD
	N1	N2	N3		
COMP.8					
80	48.4411	62.885111	62.900774	58.1	8.3
40	73.393678	76.58465	71.054578	73.7	2.8
20	82.750894	81.473032	74.782031	79.7	4.3
10	86.124585	90.525592	81.654523	86.1	4.4
5	98.155292	98.552194	97.612683	98.1	0.5
0	100	100	100	100.0	0.0

Conc.	Percentage cell viability			AVG	SD
	N1	N2	N3		
COMP.9					
80	86.245445	84.880088	75.903654	82.3	5.6
40	99.203504	102.39834	98.480932	100.0	2.1
20	95.698455	93.065698	106.75752	98.5	7.3
10	100.79671	93.534937	106.8099	100.4	6.6
5	100.05321	95.985406	101.10011	99.0	2.7
0	100	100	100	100.0	0.0

Conc.	Percentage cell viability			AVG	SD
	N1	N2	N3		
EXT. A					
80	134.2361	124.1677	117.30769	125.2	8.5
40	130.64154	132.70691	134.88248	132.7	2.1
20	126.10415	122.12688	122.91667	123.7	2.1
10	123.92384	116.7563	112.12607	117.6	5.9
5	115.55618	106.98185	97.596154	106.7	9.0
0	100	100	100	100.0	0.0

Conc.	Percentage cell viability			AVG	SD
	N1	N2	N3		
EXT. B					
80	121.16858	114.87983	114.87696	117.0	3.6
40	116.4751	116.74585	113.67214	115.6	1.7
20	109.09962	104.01864	105.867	106.3	2.6
10	106.84866	99.138282	101.15249	102.4	4.0
5	105.50766	104.11433	99.528601	103.1	3.1
0	100	100	100	100.0	0.0

**Table 15** Effects of compounds of *Aerides falcata* on the viability of BV-2 microglial cells.

Comp.	Percentage cell viability (mean $\pm$ SD) (%)					
	Vehicle	5 $\mu$ M	10 $\mu$ M	20 $\mu$ M	40 $\mu$ M	80 $\mu$ M
1	100.0 $\pm$ 0.0	102.2 $\pm$ 4.1	44.1 $\pm$ 11.7***	19.9 $\pm$ 2.7***	15.3 $\pm$ 1.0***	13.4 $\pm$ 0.6***
2	100.0 $\pm$ 0.0	100.7 $\pm$ 1.9	97.3 $\pm$ 5.5	99.5 $\pm$ 3.9	101.3 $\pm$ 2.6	103.1 $\pm$ 0.6
3	100.0 $\pm$ 0.0	97.9 $\pm$ 3.1	101.9 $\pm$ 5.0	109.2 $\pm$ 3.5	122.7 $\pm$ 4.7	77.6 $\pm$ 7.2***
4	100.0 $\pm$ 0.0	102.3 $\pm$ 7.	104.9 $\pm$ 2.8	98.4 $\pm$ 6.4	96.1 $\pm$ 6.9	70.0 $\pm$ 1.8***
5	100.0 $\pm$ 0.0	102.2 $\pm$ 3.0	100.2 $\pm$ 5.5	102.3 $\pm$ 4.1	85.4 $\pm$ 1.4***	83.8 $\pm$ 0.2***
6	100.0 $\pm$ 0.0	100.7 $\pm$ 3.6	103.0 $\pm$ 3.6	99.2 $\pm$ 3.1	98.6 $\pm$ 5.7	84.9 $\pm$ 2.7***
7	100.0 $\pm$ 0.0	100.7 $\pm$ 4.6	94.5 $\pm$ 2.3	72.8 $\pm$ 9.1***	36.9 $\pm$ 7.3***	32.9 $\pm$ 8.6***
9	100.0 $\pm$ 0.0	98.1 $\pm$ 0.5	86.1 $\pm$ 4.4**	79.7 $\pm$ 4.3***	73.7 $\pm$ 2.8***	58.1 $\pm$ 8.3***
10	100.0 $\pm$ 0.0	99.0 $\pm$ 2.7	100.4 $\pm$ 6.6	98.5 $\pm$ 7.3	100.0 $\pm$ 2.1	82.3 $\pm$ 5.6**

**Table 16** Effects of extracts of *Aerides falcata* on the viability of BV-2 microglial cells

Comp.	Percentage cell viability					
	0 $\mu$ g/mL	5 $\mu$ g/mL	10 $\mu$ g/mL	20 $\mu$ g/mL	40 $\mu$ g/mL	80 $\mu$ g/mL
Ext. EtOAc	100.0 $\pm$ 0.0	106.7 $\pm$ 9.0	117.6 $\pm$ 5.9	123.7 $\pm$ 2.1	132.7 $\pm$ 2.1	125.2 $\pm$ 8.5
Ext. MeOH	100.0 $\pm$ 0.0	103.1 $\pm$ 3.1	102.4 $\pm$ 4.0	106.3 $\pm$ 2.6	115.6 $\pm$ 1.7	117.0 $\pm$ 3.6

**Table 17** Effects of compounds of *Aerides falcata* on the NO inhibition

Comp	Percentage inhibition of NO (mean $\pm$ SD)									
	0.031 $\mu$ M	0.063 $\mu$ M	0.125 $\mu$ M	0.25 $\mu$ M	5 $\mu$ M	10 $\mu$ M	20 $\mu$ M	40 $\mu$ M		
1	16.9 $\pm$ 15.9	49.0 $\pm$ 15.6	60.6 $\pm$ 11.7	78.4 $\pm$ 8.5	90.1 $\pm$ 5.1	NA	NA	NA		
2	NA	NA	NA	5.9 $\pm$ 3.8	20.4 $\pm$ 10.2	40.1 $\pm$ 5.7	52.4 $\pm$ 4.3	60.3 $\pm$ 0.8		
3	NA	NA	NA	19.4 $\pm$ 10.4	27.8 $\pm$ 14.6	48.9 $\pm$ 2.3	75.6 $\pm$ 13.6	94.3 $\pm$ 2.3		
4	NA	NA	NA	14.4 $\pm$ 5.5	19.6 $\pm$ 6.9	45.2 $\pm$ 9.1	58.4 $\pm$ 2.3	91.2 $\pm$ 4.7		
5	NA	NA	31.6 $\pm$ 10.5	44.8 $\pm$ 6.4	71.8 $\pm$ 4.3	84.4 $\pm$ 6.6	94.7 $\pm$ 3.6	NA		
6	NA	NA	NA	4.1 $\pm$ 3.0	26.4 $\pm$ 7.1	35.6 $\pm$ 5.5	43.4 $\pm$ 5.4	63.6 $\pm$ 5.3		
7	NA	7.6 $\pm$ 5.0	20.6 $\pm$ 5.6	41.8 $\pm$ 4.3	83.7 $\pm$ 2.3	96.3 $\pm$ 2.4	NA	NA		
8	16.7 $\pm$ 4.0	26.3 $\pm$ 4.0	37.7 $\pm$ 5.1	70.8 $\pm$ 3.0	91.2 $\pm$ 4.9	NA	NA	NA		
9	NA	NA	NA	7.0 $\pm$ 7.7	23.3 $\pm$ 2.9	53.7 $\pm$ 15.5	50.2 $\pm$ 12.3	59.2 $\pm$ 8.2		
Mino	NA	NA	NA	37.7 $\pm$ 5.1	56.0 $\pm$ 3.3	76.0 $\pm$ 6.5	95.7 $\pm$ 2.1	98.9 $\pm$ 1.1		

**Table 18** Effects of extracts of *Aerides falcata* on the NO inhibition

Extracts	Percentage inhibition of NO (mean $\pm$ SD)				
	2.5 $\mu$ g/mL	5 $\mu$ g/mL	10 $\mu$ g/mL	20 $\mu$ g/mL	40 $\mu$ g/mL
EtOAc	22.9 $\pm$ 21.8	48.7 $\pm$ 7.7	78.0 $\pm$ 12.1	85.7 $\pm$ 6.3	98.2 $\pm$ 1.2
MeOH	25.4 $\pm$ 10.7	26.7 $\pm$ 4.5	56.9 $\pm$ 6.5	73.4 $\pm$ 1.6	79.0 $\pm$ 9.9

**Table 19** The IC<sub>50</sub> values of compounds on the NO inhibition.

NO.	Treatment	IC <sub>50</sub> ( $\mu$ M)			AVG	SD
		N1	N2	N3		
1	COMP. 1	0.7506	0.4948	1.368	0.87	0.45
2	COMP. 2	18.44	21.16	19.69	19.76	1.36
3	COMP. 3	8.932	8.114	9.933	8.99	0.91
4	COMP. 4	14.05	11.96	11.67	12.56	1.30
5	COMP. 5	1.856	2.266	3.275	2.47	0.73
6	COMP. 6	23.07	24.9	17.78	21.92	3.70
7	COMP. 7	2.199	2.645	2.818	2.55	0.32
8	COMP. 8	1.298	1.596	1.311	1.40	0.17
9	COMP. 9	14.49	11.83	29.55	18.62	9.56
10	MINO	3.15	3.332	3.734	3.41	0.30
11	EtOAc	4.417	5.484	3.898	4.60	0.81
12	MeOH	9.592	7.539	9.902	9.01	1.28



- ELISA Assay (determine IL6 levels)

Compound AF1

Treatment	OD			Conc. (pg/mL)			AVG	SD
	N1	N2	N3	N1	N2	N3		
C	0.096	0.102	0.100	7.67	17.67	14.33	13.222	5.0917508
LPS	0.210	0.200	0.235	197.67	181.00	239.33	206.000	30.046261
LW (+)	0.142	0.149	0.138	84.33	96.00	77.67	86.000	9.2796073
M (+)	0.140	0.121	0.128	81.00	49.33	61.00	63.778	16.015039
H (+)	0.129	0.128	0.123	62.67	61.00	52.67	58.778	5.3575838
H (-)	0.101	0.105	0.104	16.00	22.67	21.00	19.889	3.4694433

Compound AF5

Treatment	OD			Conc. (pg/mL)			AVG	SD
	N1	N2	N3	N1	N2	N3		
C	0.093	0.094	0.107	2.667	4.333	26.000	11.000	13.017083
LPS	0.222	0.215	0.245	217.667	206.000	256.000	226.556	26.15835
LW (+)	0.209	0.209	0.204	196.000	196.000	187.667	193.222	4.8112522
M (+)	0.173	0.171	0.168	136.000	132.667	127.667	132.111	4.1943525
H (+)	0.109	0.112	0.121	29.333	34.333	49.333	37.667	10.40833
H (-)	0.101	0.098	0.099	16.000	11.000	12.667	13.222	2.5458754

### Compound AF7

Treatment	OD			Conc. (pg/mL)			AVG	SD
	N1	N2	N3	N1	N2	N3		
C	0.106	0.107	0.109	6.500	9.000	14.000	9.833	3.8188131
LPS	0.178	0.18	0.185	186.500	191.500	204.000	194.000	9.0138782
LW (+)	0.133	0.15	0.157	74.000	116.500	134.000	108.167	30.855848
M (+)	0.124	0.13	0.133	51.500	66.500	74.000	64.000	11.456439
H (+)	0.122	0.121	0.128	46.500	44.000	61.500	50.667	9.4648472
H (-)	0.109	0.11	0.114	14.000	16.500	26.500	19.000	6.6143783

### Compound AF8

Treatment	OD			Conc. (pg/mL)			AVG	SD
	N1	N2	N3	N1	N2	N3		
C	0.114	0.116	0.106	26.500	31.500	6.500	21.500	13.228757
LPS	0.187	0.202	0.186	209.000	246.500	206.500	220.667	22.407216
LW (+)	0.161	0.172	0.166	144.000	171.500	156.500	157.333	13.768926
M (+)	0.164	0.15	0.156	151.500	116.500	131.500	133.167	17.559423
H (+)	0.158	0.149	0.151	136.500	114.000	119.000	123.167	11.814539
H (-)	0.116	0.108	0.115	31.500	11.500	29.000	24.000	10.897247

### EtOAc extract

Treatment	OD			Conc. (pg/mL)			AVG	SD
	N1	N2	N3	N1	N2	N3		
C	0.106	0.097	0.096	24.333	9.333	7.667	13.778	9.1792842
LPS	0.211	0.209	0.219	199.333	196.000	212.667	202.667	8.819171
LW (+)	0.145	0.127	0.129	89.333	59.333	62.667	70.444	16.442943
M (+)	0.12	0.115	0.144	47.667	39.333	87.667	58.222	25.837813
H (+)	0.115	0.132	0.117	39.333	67.667	42.667	49.889	15.485955
H (-)	0.097	0.096	0.098	9.333	7.667	11.000	9.333	1.6666667

### MeOH extract

Treatment	OD			Conc. (pg/mL)			AVG	SD
	N1	N2	N3	N1	N2	N3		
C	0.117	0.106	0.116	34.000	6.500	31.500	24.000	15.206906
LPS	0.185	0.188	0.199	204.000	211.500	239.000	218.167	18.427787
LW (+)	0.182	0.202	0.192	196.500	246.500	221.500	221.500	25
M (+)	0.177	0.16	0.178	184.000	141.500	186.500	170.667	25.289985
H (+)	0.157	0.161	0.167	134.000	144.000	159.000	145.667	12.583057
H (-)	0.113	0.107	0.109	24.000	9.000	14.000	15.667	7.6376262

- ELISA Assay (determine TNF- $\alpha$  levels)

## Compound AF1

Treatment	OD			Conc. (pg/mL)			AVG	SD
	N1	N2	N3	N1	N2	N3		
C	0.267	0.269	0.298	63.947	65	80.263	69.737	9.1312377
LPS	0.834	0.854	0.808	362.368	372.894	348.684	361.316	12.13954
LW (+)	0.584	0.567	0.578	230.789	221.842	227.631	226.754	4.5377253
M (+)	0.426	0.425	0.421	147.631	147.105	145	146.579	1.3925007
H (+)	0.385	0.365	0.359	126.052	115.526	112.368	117.982	7.165115
H (-)	0.268	0.247	0.242	64.473	53.421	50.789	56.228	7.2611235

## Compound AF5

Treatment	OD			Conc. (pg/mL)			AVG	SD
	N1	N2	N3	N1	N2	N3		
C	0.204	0.242	0.216	30.79	50.79	37.11	39.561	10.223721
LPS	0.848	0.85	0.87	369.74	370.79	381.32	373.947	6.4029079
LW (+)	0.719	0.824	0.819	301.84	357.11	354.47	337.807	31.174308
M (+)	0.65	0.687	0.667	265.53	285.00	274.47	275.000	9.7475048
H (+)	0.589	0.516	0.508	233.42	195.00	190.79	206.404	23.492401
H (-)	0.224	0.259	0.161	41.32	59.74	8.16	36.404	26.137996

## Compound AF7

Treatment	OD			Conc. (pg/mL)			AVG	SD
	N1	N2	N3	N1	N2	N3		
C	0.255	0.276	0.269	57.632	68.684	65.000	63.772	5.6277245
LPS	0.773	0.822	0.794	330.263	356.053	341.316	342.544	12.938522
LW (+)	0.767	0.826	0.798	327.105	358.158	343.421	342.895	15.533005
M (+)	0.725	0.636	0.635	305.000	258.158	257.632	273.596	27.19751
H (+)	0.475	0.489	0.404	173.421	180.789	136.053	163.421	23.986377
H (-)	0.214	0.29	0.223	36.053	76.053	40.789	50.965	21.855312

## Compound AF8

Treatment	OD			Conc. (pg/mL)			AVG	SD
	N1	N2	N3	N1	N2	N3		
C	0.294	0.293	0.406	78.157895	77.631579	137.10526	97.632	34.186226
LPS	0.841	0.836	0.815	366.05263	363.42105	352.36842	360.614	7.2611235
LW (+)	0.750	0.755	0.756	318.15789	320.78947	321.31579	320.088	1.6918686
M (+)	0.697	0.718	0.630	290.26316	301.31579	255	282.193	24.189541
H (+)	0.575	0.561	0.507	226.05263	218.68421	190.26316	211.667	18.898573
H (-)	0.295	0.295	0.339	78.684211	78.684211	101.84211	86.404	13.370217

## EtOAc extract

Treatment	OD			Conc. (pg/mL)			AVG	SD
	N1	N2	N3	N1	N2	N3		
C	0.249	0.222	0.227	54.473684	40.263158	42.894737	45.877	7.5601619
LPS	0.891	0.8	0.97	392.36842	344.47368	433.94737	390.263	44.773978
LW (+)	0.892	0.88	0.912	392.89474	386.57895	403.42105	394.298	8.5083198
M (+)	0.683	0.778	0.646	282.89474	332.89474	263.42105	293.070	35.837172
H (+)	0.576	0.527	0.544	226.57895	200.78947	209.73684	212.368	13.094585
H (-)	0.23	0.238	0.292	44.473684	48.684211	77.105263	56.754	17.74967

## MeOH extract

Treatment	OD			Conc. (pg/mL)			AVG	SD
	N1	N2	N3	N1	N2	N3		
C	0.196	0.233	0.265	26.578947	46.052632	62.894737	45.175	18.173779
LPS	0.746	0.793	0.742	316.05263	340.78947	313.94737	323.596	14.926722
LW (+)	0.74	0.744	0.722	312.89474	315	303.42105	310.439	6.1678582
M (+)	0.737	0.639	0.658	311.31579	259.73684	269.73684	280.263	27.353235
H (+)	0.58	0.612	0.582	228.68421	245.52632	229.73684	234.649	9.4346173
H (-)	0.219	0.248	0.294	38.684211	53.947368	78.157895	56.930	19.90513

● **Statistical data of IL-6 AF1**

Ordinary one-way ANOVA

F (DFn, DFd)	1.274 (5, 12)
P value	0.3368
P value summary	ns
Are SDs significantly different (P < 0.05)?	No

Bartlett's test

Bartlett's statistic (corrected)

P value

P value summary

Are SDs significantly different (P < 0.05)?

ANOVA table	SS	DF	MS	F (DFn, DFd)	P value
Treatment (between columns)	73571	5	14714	F (5, 12) = 67.29	P<0.0001
Residual (within columns)	2624	12	218.7		
Total	76195	17			

Data summary

Number of treatments (columns)

6

Number of values (total)

18

Multiple comparison test.

Number of families

1

Number of comparisons per family

15

Alpha

0.05

Bonferroni's multiple

comparisons test

	Mean Diff.	95.00% CI of diff.	Sig?	Summ Adjusted P Value	
C vs. LPS	-192.8	-236.8 to -148.7	Yes	****	<0.0001 A-B
C vs. LW	-72.78	-116.8 to -28.72	Yes	***	0.0009 A-C
C vs. MD	-50.55	-94.61 to -6.499	Yes	*	0.0189 A-D
C vs. H	-45.56	-89.61 to -1.502	Yes	*	0.0398 A-E
C vs. H(-)	-6.667	-50.72 to 37.39	No	ns	>0.9999 A-F
LPS vs. LW	120.0	75.95 to 164.1	Yes	****	<0.0001 B-C
LPS vs. MD	142.2	98.17 to 186.3	Yes	****	<0.0001 B-D
LPS vs. H	147.2	103.2 to 191.3	Yes	****	<0.0001 B-E

LPS vs. H(-)	186.1	142.1 to 230.2	Yes	****	<0.0001	B-F
LW vs. MD	22.22	-21.83 to 66.28	No	ns	>0.9999	C-D
LW vs. H	27.22	-16.83 to 71.27	No	ns	0.6546	C-E
LW vs. H(-)	66.11	22.06 to 110.2	Yes	**	0.0021	C-F
MD vs. H	4.997	-39.06 to 49.05	No	ns	>0.9999	D-E
MD vs. H(-)	43.89	-0.1681 to 87.94	No	ns	0.0513	D-F
H vs. H(-)	38.89	-5.165 to 82.94	No	ns	0.1101	E-F

Test details	Mean 1	Mean 2	Mean Diff.	SE of diff.	n1	n2	t	DF
C vs. LPS	13.22	206.0	-192.8	12.07	3	3	15.97	12
C vs. LW	13.22	86.00	-72.78	12.07	3	3	6.028	12
C vs. MD	13.22	63.78	-50.55	12.07	3	3	4.187	12
C vs. H	13.22	58.78	-45.56	12.07	3	3	3.773	12
C vs. H(-)	13.22	19.89	-6.667	12.07	3	3	0.5522	12
LPS vs. LW	206.0	86.00	120.0	12.07	3	3	9.939	12
LPS vs. MD	206.0	63.78	142.2	12.07	3	3	11.78	12
LPS vs. H	206.0	58.78	147.2	12.07	3	3	12.19	12
LPS vs. H(-)	206.0	19.89	186.1	12.07	3	3	15.41	12
LW vs. MD	86.00	63.78	22.22	12.07	3	3	1.841	12
LW vs. H	86.00	58.78	27.22	12.07	3	3	2.255	12
LW vs. H(-)	86.00	19.89	66.11	12.07	3	3	5.476	12
MD vs. H	63.78	58.78	4.997	12.07	3	3	0.4139	12
MD vs. H(-)	63.78	19.89	43.89	12.07	3	3	3.635	12
H vs. H(-)	58.78	19.89	38.89	12.07	3	3	3.221	12

● **Statistical data of IL-6 AF5**

Ordinary one-way ANOVA

Table Analyzed IL-6-COMP-5  
 Data sets analyzed A-F

ANOVA summary

F 160.7  
 P value <0.0001  
 P value summary \*\*\*\*  
 Significant diff. among means (P < 0.05)? Yes  
 R square 0.9853

Brown-Forsythe test

F (DFn, DFd) 0.9027 (5, 12)  
 P value 0.5103  
 P value summary ns  
 Are SDs significantly different (P < 0.05)? No

Bartlett's test

Bartlett's statistic (corrected)  
 P value  
 P value summary  
 Are SDs significantly different (P < 0.05)?

ANOVA table	SS	DF	MS	F (DFn, DFd)	P value
Treatment (between columns)	135129	5	27026	F (5, 12) = 160.7	P<0.0001
Residual (within columns)	2019	12	168.2		
Total	137148	17			

Data summary

Number of treatments (columns) 6  
 Number of values (total) 18

Multiple comparison test.

Number of families 1  
 Number of comparisons per family 15  
 Alpha 0.05

Bonferroni's multiple comparisons test	Mean	95.00% CI of diff.		Sig?	Summ	Adjusted P Value			
	Diff.								
C vs. LPS	-215.6	-254.2	-176.9	Yes	****	<0.0001			A-B
C vs. LW	-182.2	-220.9	-143.6	Yes	****	<0.0001			A-C
C vs. MD	-121.1	-159.8	-82.47	Yes	****	<0.0001			A-D
C vs. H	-26.67	-65.31	11.97	No	ns	0.4050			A-E
C vs. H(-)	-2.222	-40.86	36.42	No	ns	>0.9999			A-F
LPS vs. LW	33.33	-5.307	71.97	No	ns	0.1262			B-C
LPS vs. MD	94.44	55.80	133.1	Yes	****	<0.0001			B-D
LPS vs. H	188.9	150.2	227.5	Yes	****	<0.0001			B-E
LPS vs. H(-)	213.3	174.7	252.0	Yes	****	<0.0001			B-F
LW vs. MD	61.11	22.47	99.75	Yes	**	0.0013			C-D
LW vs. H	155.6	116.9	194.2	Yes	****	<0.0001			C-E
LW vs. H(-)	180.0	141.4	218.6	Yes	****	<0.0001			C-F
MD vs. H	94.45	55.80	133.1	Yes	****	<0.0001			D-E
MD vs. H(-)	118.9	80.25	157.5	Yes	****	<0.0001			D-F
H vs. H(-)	24.44	-14.20	63.08	No	ns	0.5940			E-F
Test details	Mean 1	Mean 2	Mean Diff.	SE of diff.	n1	n2	t	DF	
C vs. LPS	11.00	226.6	-215.6	10.59	3	3	20.36	12	
C vs. LW	11.00	193.2	-182.2	10.59	3	3	17.21	12	
C vs. MD	11.00	132.1	-121.1	10.59	3	3	11.44	12	
C vs. H	11.00	37.67	-26.67	10.59	3	3	2.518	12	
C vs. H(-)	11.00	13.22	-2.222	10.59	3	3	0.2099	12	
LPS vs. LW	226.6	193.2	33.33	10.59	3	3	3.148	12	
LPS vs. MD	226.6	132.1	94.44	10.59	3	3	8.919	12	
LPS vs. H	226.6	37.67	188.9	10.59	3	3	17.84	12	
LPS vs. H(-)	226.6	13.22	213.3	10.59	3	3	20.15	12	
LW vs. MD	193.2	132.1	61.11	10.59	3	3	5.771	12	
LW vs. H	193.2	37.67	155.6	10.59	3	3	14.69	12	
LW vs. H(-)	193.2	13.22	180.0	10.59	3	3	17.00	12	
MD vs. H	132.1	37.67	94.45	10.59	3	3	8.919	12	
MD vs. H(-)	132.1	13.22	118.9	10.59	3	3	11.23	12	
H vs. H(-)	37.67	13.22	24.44	10.59	3	3	2.308	12	



● **Statistical data of IL-6 AF7**

Ordinary one-way ANOVA

Table Analyzed IL-6-COMP-7  
Data sets analyzed A-F

ANOVA summary

F 64.06  
P value <0.0001  
P value summary \*\*\*\*  
Significant diff. among means (P < 0.05)? Yes  
R square 0.9639

Brown-Forsythe test

F (DFn, DFd) 1.096 (5, 12)  
P value 0.4117  
P value summary ns  
Are SDs significantly different (P < 0.05)? No

Bartlett's test

Bartlett's statistic (corrected)  
P value  
P value summary  
Are SDs significantly different (P < 0.05)?

ANOVA table	SS	DF	MS	F (DFn, DFd)	P value
Treatment (between columns)	70061	5	14012	F (5, 12) = 64.06	P<0.0001
Residual (within columns)	2625	12	218.8		
Total	72686	17			

Data summary

Number of treatments (columns) 6  
Number of values (total) 18

Multiple comparison test.

Number of families 1  
Number of comparisons per family 15  
Alpha 0.05

Bonferroni's multiple comparisons test	Mean		Sig?	Summ	Adjusted P			
	Diff.	95.00% CI of diff.			Value	Value		
C vs. LPS	-184.2	-228.2 to -140.1	Yes	****	<0.0001		A-B	
C vs. LW	-98.33	-142.4 to -54.27	Yes	****	<0.0001		A-C	
C vs. MD	-54.17	-98.23 to -10.10	Yes	*	0.0112		A-D	
C vs. H	-40.83	-84.90 to 3.231	No	ns	0.0818		A-E	
C vs. H(-)	-9.167	-53.23 to 34.90	No	ns	>0.9999		A-F	
LPS vs. LW	85.83	41.77 to 129.9	Yes	***	0.0002		B-C	
LPS vs. MD	130.0	85.94 to 174.1	Yes	****	<0.0001		B-D	
LPS vs. H	143.3	99.27 to 187.4	Yes	****	<0.0001		B-E	
LPS vs. H(-)	175.0	130.9 to 219.1	Yes	****	<0.0001		B-F	
LW vs. MD	44.17	0.1021 to 88.23	Yes	*	0.0492		C-D	
LW vs. H	57.50	13.44 to 101.6	Yes	**	0.0069		C-E	
LW vs. H(-)	89.17	45.10 to 133.2	Yes	***	0.0001		C-F	
MD vs. H	13.33	-30.73 to 57.40	No	ns	>0.9999		D-E	
MD vs. H(-)	45.00	0.9355 to 89.06	Yes	*	0.0434		D-F	
H vs. H(-)	31.67	-12.40 to 75.73	No	ns	0.3344		E-F	
Test details	Mean 1	Mean 2	Mean Diff.	SE of diff.	n1	n2	t	DF
C vs. LPS	9.833	194.0	-184.2	12.08	3	3	15.25	12
C vs. LW	9.833	108.2	-98.33	12.08	3	3	8.143	12
C vs. MD	9.833	64.00	-54.17	12.08	3	3	4.485	12
C vs. H	9.833	50.67	-40.83	12.08	3	3	3.381	12
C vs. H(-)	9.833	19.00	-9.167	12.08	3	3	0.7591	12
LPS vs. LW	194.0	108.2	85.83	12.08	3	3	7.108	12
LPS vs. MD	194.0	64.00	130.0	12.08	3	3	10.77	12
LPS vs. H	194.0	50.67	143.3	12.08	3	3	11.87	12
LPS vs. H(-)	194.0	19.00	175.0	12.08	3	3	14.49	12
LW vs. MD	108.2	64.00	44.17	12.08	3	3	3.657	12
LW vs. H	108.2	50.67	57.50	12.08	3	3	4.761	12
LW vs. H(-)	108.2	19.00	89.17	12.08	3	3	7.384	12
MD vs. H	64.00	50.67	13.33	12.08	3	3	1.104	12
MD vs. H(-)	64.00	19.00	45.00	12.08	3	3	3.726	12
H vs. H(-)	50.67	19.00	31.67	12.08	3	3	2.622	12

● **Statistical data of IL-6 AF8**

Ordinary one-way ANOVA

Table Analyzed IL-6-COMP-8  
Data sets analyzed A-F

ANOVA summary

F 76.25  
P value <0.0001  
P value summary \*\*\*\*  
Significant diff. among means (P < 0.05)? Yes  
R square 0.9695

Brown-Forsythe test

F (DFn, DFd) 0.1327 (5, 12)  
P value 0.9817  
P value summary ns  
Are SDs significantly different (P < 0.05)? No

Bartlett's test

Bartlett's statistic (corrected)  
P value  
P value summary  
Are SDs significantly different (P < 0.05)?

ANOVA table	SS	DF	MS	F (DFn, DFd)	P value
Treatment (between columns)	91081	5	18216	F (5, 12) = 76.25	P<0.0001
Residual (within columns)	2867	12	238.9		
Total	93948	17			

Data summary

Number of treatments (columns) 6  
Number of values (total) 18

Multiple comparison test.

Number of families 1  
Number of comparisons per family 15  
Alpha 0.05

Bonferroni's multiple comparisons test	Mean	95.00% CI of diff.	Sig?	Summ	Adjusted P	
	Diff.				Value	
C vs. LPS	-199.2	-245.2 to -153.1	Yes	****	<0.0001	A-B
C vs. LW	-135.8	-181.9 to -89.79	Yes	****	<0.0001	A-C
C vs. MD	-111.7	-157.7 to -65.62	Yes	****	<0.0001	A-D
C vs. H	-101.7	-147.7 to -55.62	Yes	****	<0.0001	A-E
C vs. H(-)	-2.500	-48.55 to 43.55	No	ns	>0.9999	A-F
LPS vs. LW	63.33	17.29 to 109.4	Yes	**	0.0045	B-C
LPS vs. MD	87.50	41.45 to 133.5	Yes	***	0.0002	B-D
LPS vs. H	97.50	51.45 to 143.5	Yes	****	<0.0001	B-E
LPS vs. H(-)	196.7	150.6 to 242.7	Yes	****	<0.0001	B-F
LW vs. MD	24.17	-21.88 to 70.21	No	ns	>0.9999	C-D
LW vs. H	34.17	-11.88 to 80.21	No	ns	0.2857	C-E
LW vs. H(-)	133.3	87.29 to 179.4	Yes	****	<0.0001	C-F
MD vs. H	10.00	-36.05 to 56.05	No	ns	>0.9999	D-E
MD vs. H(-)	109.2	63.12 to 155.2	Yes	****	<0.0001	D-F
H vs. H(-)	99.17	53.12 to 145.2	Yes	****	<0.0001	E-F

Test details	Mean 1	Mean 2	Mean Diff.	SE of diff.	n1	n2	t	DF
C vs. LPS	21.50	220.7	-199.2	12.62	3	3	15.78	12
C vs. LW	21.50	157.3	-135.8	12.62	3	3	10.76	12
C vs. MD	21.50	133.2	-111.7	12.62	3	3	8.849	12
C vs. H	21.50	123.2	-101.7	12.62	3	3	8.056	12
C vs. H(-)	21.50	24.00	-2.500	12.62	3	3	0.1981	12
LPS vs. LW	220.7	157.3	63.33	12.62	3	3	5.019	12
LPS vs. MD	220.7	133.2	87.50	12.62	3	3	6.934	12
LPS vs. H	220.7	123.2	97.50	12.62	3	3	7.726	12
LPS vs. H(-)	220.7	24.00	196.7	12.62	3	3	15.58	12
LW vs. MD	157.3	133.2	24.17	12.62	3	3	1.915	12
LW vs. H	157.3	123.2	34.17	12.62	3	3	2.707	12
LW vs. H(-)	157.3	24.00	133.3	12.62	3	3	10.57	12
MD vs. H	133.2	123.2	10.00	12.62	3	3	0.7924	12
MD vs. H(-)	133.2	24.00	109.2	12.62	3	3	8.650	12
H vs. H(-)	123.2	24.00	99.17	12.62	3	3	7.858	12

● **Statistical data of TNF- $\alpha$  AF1**

Ordinary one-way ANOVA

Table Analyzed TNF-COMP-1  
 Data sets analyzed A-F

ANOVA summary

F 662.8  
 P value <0.0001  
 P value summary \*\*\*\*  
 Significant diff. among means (P < 0.05)? Yes  
 R square 0.9964

Brown-Forsythe test

F (DFn, DFd) 0.5327 (5, 12)  
 P value 0.7480  
 P value summary ns  
 Are SDs significantly different (P < 0.05)? No

Bartlett's test

Bartlett's statistic (corrected)  
 P value  
 P value summary  
 Are SDs significantly different (P < 0.05)?

ANOVA table

	SS	DF	MS	F (DFn, DFd)	P value
Treatment (between columns)	197365	5	39473	F (5, 12) = 662.8	P<0.0001
Residual (within columns)	714.7	12	59.56		
Total	198079	17			

Data summary

Number of treatments (columns) 6  
 Number of values (total) 18

Multiple comparison test.

Number of families 1  
 Number of comparisons per family 15  
 Alpha 0.05

Bonferroni's multiple Mean Diff. 95.00% CI of diff. Sig? Summ Adjusted P

comparisons test					Value	
C vs. LPS	-291.6	-314.6 to -268.6	Yes	****	<0.0001	A-B
C vs. LW	-157.0	-180.0 to -134.0	Yes	****	<0.0001	A-C
C vs. MD	-76.84	-99.83 to -53.85	Yes	****	<0.0001	A-D
C vs. H	-48.25	-71.24 to -25.25	Yes	****	<0.0001	A-E
C vs. H(-)	13.51	-9.483 to 36.50	No	ns	0.7984	A-F
LPS vs. LW	134.6	111.6 to 157.6	Yes	****	<0.0001	B-C
LPS vs. MD	214.7	191.7 to 237.7	Yes	****	<0.0001	B-D
LPS vs. H	243.3	220.3 to 266.3	Yes	****	<0.0001	B-E
LPS vs. H(-)	305.1	282.1 to 328.1	Yes	****	<0.0001	B-F
LW vs. MD	80.18	57.18 to 103.2	Yes	****	<0.0001	C-D
LW vs. H	108.8	85.78 to 131.8	Yes	****	<0.0001	C-E
LW vs. H(-)	170.5	147.5 to 193.5	Yes	****	<0.0001	C-F
MD vs. H	28.60	5.604 to 51.59	Yes	*	0.0102	D-E
MD vs. H(-)	90.35	67.36 to 113.3	Yes	****	<0.0001	D-F
H vs. H(-)	61.75	38.76 to 84.75	Yes	****	<0.0001	E-F

Test details	Mean		Diff.	SE of diff.	n1	n2	t	DF
	Mean 1	Mean 2						
C vs. LPS	69.74	361.3	-291.6	6.301	3	3	46.27	12
C vs. LW	69.74	226.8	-157.0	6.301	3	3	24.92	12
C vs. MD	69.74	146.6	-76.84	6.301	3	3	12.19	12
C vs. H	69.74	118.0	-48.25	6.301	3	3	7.657	12
C vs. H(-)	69.74	56.23	13.51	6.301	3	3	2.144	12
LPS vs. LW	361.3	226.8	134.6	6.301	3	3	21.36	12
LPS vs. MD	361.3	146.6	214.7	6.301	3	3	34.08	12
LPS vs. H	361.3	118.0	243.3	6.301	3	3	38.62	12
LPS vs. H(-)	361.3	56.23	305.1	6.301	3	3	48.42	12
LW vs. MD	226.8	146.6	80.18	6.301	3	3	12.72	12
LW vs. H	226.8	118.0	108.8	6.301	3	3	17.26	12
LW vs. H(-)	226.8	56.23	170.5	6.301	3	3	27.06	12
MD vs. H	146.6	118.0	28.60	6.301	3	3	4.538	12
MD vs. H(-)	146.6	56.23	90.35	6.301	3	3	14.34	12
H vs. H(-)	118.0	56.23	61.75	6.301	3	3	9.800	12

● **Statistical data of TNF- $\alpha$  AF5**

Ordinary one-way ANOVA

Table Analyzed TNF-COMP--5  
Data sets analyzed A-F

ANOVA summary

F 156.8  
P value <0.0001  
P value summary \*\*\*\*  
Significant diff. among means (P < 0.05)? Yes  
R square 0.9849

Brown-Forsythe test

F (DFn, DFd) 0.4074 (5, 12)  
P value 0.8347  
P value summary ns  
Are SDs significantly different (P < 0.05)? No

Bartlett's test

Bartlett's statistic (corrected)  
P value  
P value summary  
Are SDs significantly different (P < 0.05)?

ANOVA table	SS	DF	MS	F (DFn, DFd)	P value
Treatment (between columns)	319864	5	63973	F (5, 12) = 156.8	P<0.0001
Residual (within columns)	4895	12	407.9		
Total	324760	17			

Data summary

Number of treatments (columns) 6  
Number of values (total) 18

Multiple comparison test.

Number of families 1  
Number of comparisons per family 15  
Alpha 0.05

Bonferroni's multiple comparisons test						Adjusted P Value		
	Mean Diff.	95.00% CI of diff.	Sig?	Summ	Value			
C vs. LPS	-334.4	-394.6 to -274.2	Yes	****	<0.0001	A-B		
C vs. LW	-298.2	-358.4 to -238.1	Yes	****	<0.0001	A-C		
C vs. MD	-235.4	-295.6 to -175.3	Yes	****	<0.0001	A-D		
C vs. H	-166.8	-227.0 to -106.7	Yes	****	<0.0001	A-E		
C vs. H(-)	3.157	-57.02 to 63.33	No	ns	>0.9999	A-F		
LPS vs. LW	36.14	-24.03 to 96.32	No	ns	0.7329	B-C		
LPS vs. MD	98.95	38.78 to 159.1	Yes	***	0.0009	B-D		
LPS vs. H	167.5	107.4 to 227.7	Yes	****	<0.0001	B-E		
LPS vs. H(-)	337.5	277.4 to 397.7	Yes	****	<0.0001	B-F		
LW vs. MD	62.81	2.633 to 123.0	Yes	*	0.0374	C-D		
LW vs. H	131.4	71.23 to 191.6	Yes	****	<0.0001	C-E		
LW vs. H(-)	301.4	241.2 to 361.6	Yes	****	<0.0001	C-F		
MD vs. H	68.60	8.423 to 128.8	Yes	*	0.0199	D-E		
MD vs. H(-)	238.6	178.4 to 298.8	Yes	****	<0.0001	D-F		
H vs. H(-)	170.0	109.8 to 230.2	Yes	****	<0.0001	E-F		
Test details	Mean 1	Mean 2	Mean Diff.	SE of diff.	n1	n2	t	DF
C vs. LPS	39.56	374.0	-334.4	16.49	3	3	20.28	12
C vs. LW	39.56	337.8	-298.2	16.49	3	3	18.09	12
C vs. MD	39.56	275.0	-235.4	16.49	3	3	14.28	12
C vs. H	39.56	206.4	-166.8	16.49	3	3	10.12	12
C vs. H(-)	39.56	36.41	3.157	16.49	3	3	0.1914	12
LPS vs. LW	374.0	337.8	36.14	16.49	3	3	2.192	12
LPS vs. MD	374.0	275.0	98.95	16.49	3	3	6.000	12
LPS vs. H	374.0	206.4	167.5	16.49	3	3	10.16	12
LPS vs. H(-)	374.0	36.41	337.5	16.49	3	3	20.47	12
LW vs. MD	337.8	275.0	62.81	16.49	3	3	3.809	12
LW vs. H	337.8	206.4	131.4	16.49	3	3	7.968	12
LW vs. H(-)	337.8	36.41	301.4	16.49	3	3	18.28	12
MD vs. H	275.0	206.4	68.60	16.49	3	3	4.160	12
MD vs. H(-)	275.0	36.41	238.6	16.49	3	3	14.47	12
H vs. H(-)	206.4	36.41	170.0	16.49	3	3	10.31	12



● **Statistical data of TNF- $\alpha$  AF7**

Ordinary one-way ANOVA

Table Analyzed TNF-COMP-7  
Data sets analyzed A-F

ANOVA summary

F 141.9  
P value <0.0001  
P value summary \*\*\*\*  
Significant diff. among means (P < 0.05)? Yes  
R square 0.9834

Brown-Forsythe test

F (DFn, DFd) 0.2276 (5, 12)  
P value 0.9433  
P value summary ns  
Are SDs significantly different (P < 0.05)? No

Bartlett's test

Bartlett's statistic (corrected)  
P value  
P value summary  
Are SDs significantly different (P < 0.05)?



ANOVA table	SS	DF	MS	F (DFn, DFd)	P value
Treatment (between columns)	264093	5	52819	F (5, 12) = 141.9	P<0.0001
Residual (within columns)	4466	12	372.2		
Total	268559	17			

Data summary

Number of treatments (columns) 6  
Number of values (total) 18

Multiple comparison test.

Number of families 1

Number of comparisons per family

15

Alpha

0.05

Bonferroni's multiple comparisons test	Mean				Adjusted P		
	Diff.	95.00% CI of diff.	Sig?	Summ	Value		
C vs. LPS	-278.8	-336.2 to -221.3	Yes	****	<0.0001	A-B	
C vs. LW	-279.1	-336.6 to -221.6	Yes	****	<0.0001	A-C	
C vs. MD	-209.8	-267.3 to -152.3	Yes	****	<0.0001	A-D	
C vs. H	-99.65	-157.1 to -42.17	Yes	***	0.0006	A-E	
C vs. H(-)	12.81	-44.67 to 70.28	No	ns	>0.9999	A-F	
LPS vs. LW	-0.3507	-57.83 to 57.13	No	ns	>0.9999	B-C	
LPS vs. MD	68.95	11.47 to 126.4	Yes	*	0.0135	B-D	
LPS vs. H	179.1	121.6 to 236.6	Yes	****	<0.0001	B-E	
LPS vs. H(-)	291.6	234.1 to 349.1	Yes	****	<0.0001	B-F	
LW vs. MD	69.30	11.82 to 126.8	Yes	*	0.0130	C-D	
LW vs. H	179.5	122.0 to 236.9	Yes	****	<0.0001	C-E	
LW vs. H(-)	291.9	234.5 to 349.4	Yes	****	<0.0001	C-F	
MD vs. H	110.2	52.70 to 167.7	Yes	***	0.0002	D-E	
MD vs. H(-)	222.6	165.2 to 280.1	Yes	****	<0.0001	D-F	
H vs. H(-)	112.5	54.98 to 169.9	Yes	***	0.0002	E-F	

Test details	Mean		Diff.	SE of diff.	n1	n2	t	DF
	Mean 1	Mean 2						
C vs. LPS	63.77	342.5	-278.8	15.75	3	3	17.70	12
C vs. LW	63.77	342.9	-279.1	15.75	3	3	17.72	12
C vs. MD	63.77	273.6	-209.8	15.75	3	3	13.32	12
C vs. H	63.77	163.4	-99.65	15.75	3	3	6.326	12
C vs. H(-)	63.77	50.97	12.81	15.75	3	3	0.8131	12
LPS vs. LW	342.5	342.9	-0.3507	15.75	3	3	0.02226	12
LPS vs. MD	342.5	273.6	68.95	15.75	3	3	4.377	12
LPS vs. H	342.5	163.4	179.1	15.75	3	3	11.37	12
LPS vs. H(-)	342.5	50.97	291.6	15.75	3	3	18.51	12
LW vs. MD	342.9	273.6	69.30	15.75	3	3	4.399	12
LW vs. H	342.9	163.4	179.5	15.75	3	3	11.39	12
LW vs. H(-)	342.9	50.97	291.9	15.75	3	3	18.53	12
MD vs. H	273.6	163.4	110.2	15.75	3	3	6.995	12
MD vs. H(-)	273.6	50.97	222.6	15.75	3	3	14.13	12
H vs. H(-)	163.4	50.97	112.5	15.75	3	3	7.139	12

● **Statistical data of TNF- $\alpha$  AF8**

Ordinary one-way ANOVA

Table Analyzed TNF-COMP-8  
 Data sets analyzed A-F

ANOVA summary

F 101.8  
 P value <0.0001  
 P value summary \*\*\*\*  
 Significant diff. among means (P < 0.05)? Yes  
 R square 0.9770

Brown-Forsythe test

F (DFn, DFd) 0.4623 (5, 12)  
 P value 0.7970  
 P value summary ns  
 Are SDs significantly different (P < 0.05)? No

Bartlett's test

Bartlett's statistic (corrected)  
 P value  
 P value summary  
 Are SDs significantly different (P < 0.05)?

ANOVA table	SS	DF	MS	F (DFn, DFd)	P value
Treatment (between columns)	198903	5	39781	F (5, 12) = 101.8	P<0.0001
Residual (within columns)	4691	12	390.9		
Total	203594	17			

Data summary

Number of treatments (columns) 6  
 Number of values (total) 18

Multiple comparison test.

Number of families 1  
 Number of comparisons per family 15  
 Alpha 0.05

Bonferroni's multiple comparisons test	Mean Diff.	95.00% CI of diff.	Sig?	Summ	Adjusted P Value				
C vs. LPS	-263.0	-321.9 to -204.1	Yes	****	<0.0001	A-B			
C vs. LW	-222.5	-281.4 to -163.6	Yes	****	<0.0001	A-C			
C vs. MD	-184.6	-243.5 to -125.7	Yes	****	<0.0001	A-D			
C vs. H	-114.0	-172.9 to -55.13	Yes	***	0.0002	A-E			
C vs. H(-)	11.23	-47.68 to 70.13	No	ns	>0.9999	A-F			
LPS vs. LW	40.53	-18.38 to 99.43	No	ns	0.4108	B-C			
LPS vs. MD	78.42	19.52 to 137.3	Yes	**	0.0059	B-D			
LPS vs. H	148.9	90.04 to 207.9	Yes	****	<0.0001	B-E			
LPS vs. H(-)	274.2	215.3 to 333.1	Yes	****	<0.0001	B-F			
LW vs. MD	37.89	-21.01 to 96.80	No	ns	0.5532	C-D			
LW vs. H	108.4	49.52 to 167.3	Yes	***	0.0003	C-E			
LW vs. H(-)	233.7	174.8 to 292.6	Yes	****	<0.0001	C-F			
MD vs. H	70.53	11.62 to 129.4	Yes	*	0.0137	D-E			
MD vs. H(-)	195.8	136.9 to 254.7	Yes	****	<0.0001	D-F			
H vs. H(-)	125.3	66.36 to 184.2	Yes	****	<0.0001	E-F			

Test details	Mean		Diff.	SE of diff.	n1	n2	t	DF
	Mean 1	Mean 2						
C vs. LPS	97.63	360.6	-263.0	16.14	3	3	16.29	12
C vs. LW	97.63	320.1	-222.5	16.14	3	3	13.78	12
C vs. MD	97.63	282.2	-184.6	16.14	3	3	11.43	12
C vs. H	97.63	211.7	-114.0	16.14	3	3	7.064	12
C vs. H(-)	97.63	86.40	11.23	16.14	3	3	0.6955	12
LPS vs. LW	360.6	320.1	40.53	16.14	3	3	2.510	12
LPS vs. MD	360.6	282.2	78.42	16.14	3	3	4.858	12
LPS vs. H	360.6	211.7	148.9	16.14	3	3	9.227	12
LPS vs. H(-)	360.6	86.40	274.2	16.14	3	3	16.99	12
LW vs. MD	320.1	282.2	37.89	16.14	3	3	2.347	12
LW vs. H	320.1	211.7	108.4	16.14	3	3	6.716	12
LW vs. H(-)	320.1	86.40	233.7	16.14	3	3	14.48	12
MD vs. H	282.2	211.7	70.53	16.14	3	3	4.369	12
MD vs. H(-)	282.2	86.40	195.8	16.14	3	3	12.13	12
H vs. H(-)	211.7	86.40	125.3	16.14	3	3	7.760	12

## VITA

**NAME** Bachtiar Rivai

**DATE OF BIRTH** 14 Jun 1995

**PLACE OF BIRTH** Medan

**INSTITUTIONS ATTENDED** Brawijaya University

**HOME ADDRESS** Jalan Kayu Manis Timur, Matraman, Jakarta Timur,  
Indonesia

**PUBLICATION** Rivai B, Hasriadi, Dasuni Wasana PW, Chansriniyom C,  
Towiwat P, Punpreuk Y, Likhitwitayawuid K, Rojsitthisak P,  
and Sritularak B. Potential role of a novel biphenanthrene  
derivative isolated from *Aerides falcata* in central nervous  
system diseases. *RSC Adv.* 2023;13(16):10757–67.